



HAL
open science

Development of polyamide composites with natural fibers for automotive applications

Renato Pereira de Melo

► **To cite this version:**

Renato Pereira de Melo. Development of polyamide composites with natural fibers for automotive applications. Materials. Ecole Nationale Supérieure des Mines de Paris; Universidade federal do Rio de Janeiro, 2015. English. NNT: 2015ENMP0062 . tel-02892103

HAL Id: tel-02892103

<https://pastel.hal.science/tel-02892103>

Submitted on 7 Jul 2020

HAL is a multi-disciplinary open access archive for the deposit and dissemination of scientific research documents, whether they are published or not. The documents may come from teaching and research institutions in France or abroad, or from public or private research centers.

L'archive ouverte pluridisciplinaire **HAL**, est destinée au dépôt et à la diffusion de documents scientifiques de niveau recherche, publiés ou non, émanant des établissements d'enseignement et de recherche français ou étrangers, des laboratoires publics ou privés.

École doctorale n°364 : Sciences Fondamentales et Appliquées

Doctorat ParisTech

THÈSE

pour obtenir le grade de docteur préparée dans le cadre d'une
cotutelle

**l'École nationale supérieure des mines de Paris et IMA –
Université de Rio de Janeiro
Spécialité "Sciences et Génie des Matériaux"**

présentée et soutenue publiquement par

Renato PEREIRA DE MELO

le 30 Mars 2015

**Thèse confidentielle
(29 mars 2020)**

**Développement de composites en polyamide à partir de fibres naturelles pour des applications
automobiles**

Development of polyamide composites with natural fibers for automotive applications

Directeurs de thèse : **Patrick NAVARD / Maria de Fátima VIEIRA MARQUES**

Jury

| | | |
|-------------------------------------|--|----------------------|
| M. Edvani CURTI MUNIZ | Professeur, University of Maringá | Rapporteur |
| Mme. Lúcia HELENA INNOCENTINI MEI | Professeur, University of Campinas | Rapporteur |
| M. Marcos LOPES DIAS | Professeur, University of Rio de Janeiro | Examineur |
| M. Norman PENEDO DUQUE | Docteur, PSA – Peugeot Citroën | Examineur |
| M. Patrick NAVARD | Directeur de Recherche, CEMEF-CNRS | Président, Examineur |
| Mme. Maria de Fátima VIEIRA MARQUES | Professeur, University of Rio de Janeiro | Président, Examineur |

MINES ParisTech
Centre de Mise en Forme des Matériaux
Rue Claude Daunesse, BP 207
06904 Sophia Antipolis

DEVELOPMENT OF POLYAMIDE COMPOSITES WITH NATURAL FIBERS FOR AUTOMOTIVE APPLICATIONS

PhD Thesis in Polymer Science and Technology, submitted to Instituto de Macromoléculas Professora Eloisa Mano of University of Rio de Janeiro and CEMEF – Centre de Mise En Forme Des Materiaux, Ecole des Mines de Paris, as partial fulfillment of the requirement for the PhD degree in Science, in Polymer Science and Technology.

Advisors: Prof. Maria de Fátima Vieira Marques
Prof. Patrick Navard

Rio de Janeiro
2015

PhD Thesis:

Development of Polyamide Composites with Natural Fibers for Automotive Applications

Author: Renato Pereira de Melo

Supervisors: Maria de Fátima Vieira Marques/Patrick Navard

Date: 30 march 2015

Approved by:

Professor Maria de Fátima Vieira Marques, PhD
University of Rio de Janeiro – IMA/UFRJ
Supervisor Thesis / President of Committee

Professor Patrick Navard, PhD
Ecole des Mines de Paris/Mines ParisTech
Supervisor Thesis / President of Committee

Professor Edvani Curti Muniz, PhD
University of Maringá - UEM

Professor Lúcia Helena Innocentini Mei, PhD
University of Campinas – UNICAMP

Professor Marcos Lopes Dias, PhD
University of Rio de Janeiro – IMA/UFRJ

Dr. Norman Penedo Duque, PhD
PSA – Peugeot Citroën

Dedicated to my family and my loyal friends.

ACKNOWLEDGMENTS

To God, for giving me strength and sustained me during the preparation of this work;

To my family. You were my strength source while I was so far from Brazil and all of you for one and a half year.

To my Brazilian advisor, Maria de Fátima, for help me to grow professionally since my beginning as a Master student, 7 years ago. Thank you for your precious advices and friendship.

To my French advisor, Patrick Navard. Thank you for all supporting and kindness since I left Brazil for the first time in the beginning of 2012. Particularly, I will never forget your advices in our last meeting at CEMEF that, certainly, I will take with me for my entire career.

To my PSA tutors, Norman Penedo, Didier Fromonteil and Laurent Bechu. I have learnt a lot with you during the preparation of this work.

To my friends from IMA-UFRJ. I have no words to describe all of you. You are awesome.

To the friends that I have met in CEMEF (Jose Antonio, Jordi, Mindas, Carlos, Jose, Yukio, Loan, Gabriel, George, Yang Fu, Carole and Ana Laura. It was a huge pleasure met and stay with you all the time that I have lived in Nice, France).

To the laboratories of CETEM – UFRJ and University of Nice, for helping me in TGA and SEM measurements.

“Because given mission is accomplished mission”

“Elite Squad” movie

ABBREVIATIONS LIST

- APTES – Amino-propyl tri-methoxy silane
- DMTA – Thermo dynamic mechanical analysis
- DSC – Differential Scanning calorimetry
- DTA – Differential thermal analysis
- DTG - Derivative thermogravimetric
- E' – Storage modulus / Elastic modulus
- E'' – Loss modulus
- FTIR – Infra-red spectroscopy
- HP – high pressure
- I_c – Crystallinity index
- NBBSA – N-butyl-benzene sulfonamide
- PA 6 – Polyamide 6
- PA 6.6 – Polyamide 6.6
- PP – Polypropylene
- RP – room pressure
- SEM – Scanning electronic microscopy
- TGA – Thermogravimetric analysis
- T_c – Crystallization temperature
- T_g – Glass transition temperature
- T_i – Initial weight loss temperature
- T_m – Melting temperature
- T_{max} – Maximum degradation temperature rate
- T_{0,05} – Temperature at 5.0 wt. % degradation
- tanδ – Tangent delta
- VTMS – Vinyl tri-methoxy silane
- XRD – X-ray diffraction
- wt. % - weight percent
- ΔH_m^a - Melt heating of sample
- ΔH_m^{100} - Melt heating of 100% crystalline polyamide

SUMMARY

| | | |
|--------------|--|-----------|
| 1 | INTRODUCTION | 15 |
| 2 | OBJECTIVES OF THE WORK | 18 |
| 3 | STATE OF THE ART | 19 |
| 3.1 | STRUCTURE AND COMPOSITION OF NATURAL FIBERS | 19 |
| 3.2 | BIOSYNTHESIS OF CELL WALL STRUCTURES | 22 |
| 3.3 | MAIN NATURAL FIBERS | 26 |
| 3.4 | THERMAL DEGRADATION OF NATURAL FIBERS | 30 |
| 3.5 | CHEMICAL TREATMENTS ON NATURAL FIBERS | 34 |
| 3.5.1 | Alkaline treatment | 35 |
| 3.5.2 | Silane treatment | 38 |
| 3.5.3 | Acetylation | 40 |
| 3.6 | NATURAL FIBERS / POLYAMIDE COMPOSITES | 41 |
| 3.7 | APPLICATION OF NATURAL FIBERS ON AUTOMOTIVE INDUSTRY | 49 |
| 4 | MATERIALS AND METHODS | 53 |
| 4.1 | MATERIALS | 53 |
| 4.2 | EQUIPMENTS | 54 |
| 4.3 | ALKALINE TREATMENT OF NATURAL FIBERS | 55 |
| 4.3.1 | Alkaline treatment of natural fibers at room pressure (RP-alkaline treatment) | 55 |
| 4.3.2 | Alkaline treatment of natural fibers at high pressure (HP-alkaline treatment) | 55 |
| 4.4 | SURFACE MODIFICATION OF NATURAL FIBERS | 56 |
| 4.4.1 | Acetylation and Treatment with Silane | 56 |
| 4.5 | PROCESSING OF COMPOSITES PP, PA 6 AND 6.6/ NATURAL FIBERS BY MIXING IN MELT STATE | 56 |
| 4.5.1 | Composites PP/Natural Fibers | 56 |
| 4.5.2 | Composites PA 6/Natural Fibers | 57 |
| 4.5.3 | Composites PA 6.6/Natural Fibers | 58 |
| 4.5.3.1 | Effect of plasticizers on PA 6.6: experimental design | 60 |
| 4.5.3.2 | Experimental design of compounding PA 6.6 / natural fibers composites | 60 |

| | | |
|-----------|---|----|
| 4.6 | CHARACTERIZATION | 60 |
| 4.6.1 | Characterization of Chemically Modified Fibers | 60 |
| 4.6.2 | Characterization of Composites | 61 |
| 4.6.2.1 | Mechanical properties of PP / natural fibers composites by dynamic mechanical analysis (DMA) | 61 |
| 4.6.2.2 | Establishment of methods for estimating degradation of pure cellulose and treated curauá fibers after processing with PA 6 | 62 |
| 4.6.2.2.1 | <i>Colorimetry</i> | 62 |
| 4.6.2.2.2 | <i>Infrared spectroscopy</i> | 62 |
| 4.6.2.2.3 | <i>Viscosimetry</i> | 63 |
| 4.6.2.3 | Mechanical properties | 63 |
| 4.6.2.4 | Characterization of PA 6.6 / natural fibers composites | 63 |
| 5 | RESULTS AND DISCUSSION | 65 |
| 5.1 | INFLUENCE OF SUCCESSIVE ROOM PRESSURE ALKALINE TREATMENTS ON NATURAL FIBERS AND ON MECHANICAL PROPERTIES OF COMPOSITES WITH POLYPROPYLENE | 65 |
| 5.1.1 | Thermogravimetric analysis of of room pressure alkaline treated natural fibers | 65 |
| 5.1.2 | Infra-red spectroscopy of room-pressure alkaline treated natural fibers | 69 |
| 5.1.3 | Degree of crystallinity of room-pressure alkaline treated natural fibers | 71 |
| 5.1.4 | Analysis of mechanical properties of PP/Natural fibers composites by DMTA | 73 |
| 5.1.5 | Analysis of morphology of PP/Natural fibers composites by SEM | 79 |
| 5.2 | EFFECT OF ACETYLATION AND SILANIZATION ON RP-ALKALINE TREATED FIBERS | 81 |
| 5.2.1 | Infra-red spectroscopy of RP – alkaline treated + acetylated fibers | 81 |
| 5.2.2 | Infra-red spectroscopy of RP – alkaline treated + silanized fibers | 84 |
| 5.2.3 | XRD of RP alkaline-treated, acetylated and silanized fibers | 86 |
| 5.2.4 | TGA of RP alkaline-treated, acetylated and silanized fibers | 88 |

| | | |
|---------|---|------------|
| 5.3 | CHARACTERIZATION OF HIGH-PRESSURE ALKALINE TREATED FIBERS | 94 |
| 5.3.1 | X-Ray diffraction: analysis of crystallinity | 94 |
| 5.3.2 | Thermal stability of high-pressure alkaline treated fibers | 96 |
| 5.4 | INFLUENCE OF GASEOUS ENVIRONMENT ON DEGRADATION AND PROPERTIES OF NATURAL FIBER FILLED POLYMER COMPOSITES | 102 |
| 5.4.1 | Thermostability of fibers in air and nitrogen studied by TGA | 102 |
| 5.4.2 | Isothermal of treated fibers under air and under nitrogen | 102 |
| 5.4.3 | IR spectroscopy of degraded fibers in air and nitrogen | 101 |
| 5.4.4 | Surface morphology of degraded fibers in air and nitrogen | 104 |
| 5.5 | STUDY OF PROCESSING CONDITIONS ON THE NATURAL FIBER FILLED POLYAMIDE 6 COMPOSITES | 121 |
| 5.5.1 | Evaluation of degradation risks of composites | 121 |
| 5.5.1.1 | Analysis of composites color | 121 |
| 5.5.1.2 | Analysis of molar mass of pure cellulose - viscosimetry | 123 |
| 5.5.1.3 | Identification of degradation products - IR spectra | 124 |
| 5.5.2 | Mechanical properties of composites – tension testings | 127 |
| 5.5.3 | Mechanical properties of PA6 / alkaline-treated curauá composites – influence of compounding time | 131 |
| 5.5.4 | Mechanical properties of PA 6/ alkaline-treated curauá and PA 6 / Avicel composites – influence of fiber content | 135 |
| 5.6 | COMPOUNDING PA 6.6 – NATURAL FIBERS | 140 |
| 5.6.1 | TGA of alkaline-treated curauá with different silanes | 140 |
| 5.6.2 | Mechanical properties of PA 6/ fibers – influence of fiber silanization | 142 |
| 5.6.3 | Decreasing melting temperature of PA 6.6 – influence of plasticizers | 144 |
| 5.6.3.1 | DSC of different extruded formulations of PA 6.6 | 144 |
| 5.6.3.2 | DMTA of different extruded formulations of PA 6.6 | 148 |
| 5.6.3.3 | Experimental Design | 149 |
| 5.6.4 | FTIR and DSC of compounded PA 6.6/ silanized curauá composites | 151 |

| | | |
|--------------|---|------------|
| 5.6.5 | Mechanical properties: tension testings of PA 6.6 / natural fibers | 154 |
| 5.6.6 | Mechanical properties: impact testings of PA 6.6 / natural fibers | 157 |
| 5.6.7 | Mechanical properties: tension testings of plasticized PA 6.6 / curauá fibers - influence of fiber content | 159 |
| 5.6.8 | SEM analysis of PA 6.6 / curauá fibers composites | 161 |
| 5.6.9 | Thermal behaviour of PA 6.6 / curauá fibers composites | 167 |
| 6 | CONCLUSIONS | 171 |
| 7 | PERSPECTIVES | 173 |
| | REFERENCES | 174 |
| | APPENDIX A – TGA CURVES OF NATURAL FIBERS | 184 |
| | APPENDIX B – DMA CURVES OF NEAT PA 66 AND WITH DIFFERENT FORMULATIONS | 193 |
| | APPENDIX C – DSC CURVES OF PA 66 WITH DIFFERENT FORMULATIONS | 196 |
| | APPENDIX D – PUBLICATIONS GENERATED FROM THIS WORK | 198 |

1 INTRODUCTION

Present-day research in the field of polymer science and technology is focused on developing plastics, papers, adhesives, textile fibers, composites, blends and many other industrial products from renewable resources, mostly from the abundantly available agro-waste and lignocellulosic materials. Newer materials and composites that have both economic and environmental benefits have been considered for applications in the automotive, building, furniture, and packaging industries. Growing environmental awareness, new rules and regulations throughout the world for the creation of a bio-based economy are challenging industry, academia, government, and agriculture. Within the past few years, there has been a dramatic increase in the use of natural fibers for composites. Recent advances in natural fiber development, genetic engineering, and composite science offer significant opportunities for improved materials from renewable resources with enhanced support for global sustainability (MISHRA et al., 2004).

The use of lignocellulosic fibers derived from annually renewable resources as a reinforcing phase in polymeric matrix composites provides positive environmental benefits with respect to ultimate disposability and raw material use. Compared to inorganic fillers, the main advantages of lignocellulosics are listed below:

- renewable nature;
- wide variety of fillers available throughout the world;
- nonfood agricultural based economy;
- low energy consumption, cost and density;
- high specific strength and modulus;
- comparatively easy processability due to their nonabrasive nature, which allows high filling levels, resulting in significant cost savings;
- reactive surfaces which can be used for grafting specific groups.

About 2.5 billion tons of lignocellulosic materials are available worldwide. Their use is very ancient, probably since 6000 BC. Fibers are available from many of

these materials, and they are also called 'plant', 'natural' or 'vegetable' fibers. Brazil, which produces many of them, is in a unique position amongst South American countries, having an area of approximately 8.5 million km² of which about 5–6% are arable lands, 22% permanent pastures and 58% forest and woodland. The country is also privileged geographically in possessing exceptional climate conditions and fertile soil for the cultivation of a large variety of plant species.

International trends in the study of lignocellulosic fibers reveal that these fibers have the potential to be used in automotive applications where they can be competitive with glass fibers (MARSH, 2003; NETRAVALI; CHABBA, 2003; NICKEL; RIEDEL, 2003) . Many countries are becoming aware of ecological concerns and in particular European countries which are passing laws that will require, by 2015, the use of up to 95% recyclable materials in vehicles (PEIJS, 2003). Moreover, it is possible to produce quality fibers, suitable for different applications, through better cultivation, including genetic engineering and treatment methods to develop uniform properties (RAJESH; KOZLOWSKI, 2005).

Despite these attractive properties, lignocellulosic fillers are used only to a limited extent in industrial practice due to difficulties associated with surface compatibilisation and low thermal stability. The inherent polar and hydrophilic nature of polysaccharides and the nonpolar characteristics of most of the thermoplastics result in difficulties in compounding the filler and the matrix and in interface adhesion, therefore giving poor dispersion levels, which results in inefficient composites. Moreover, the processing temperature of composites is restricted to about 200 °C because lignocellulosic materials start to degrade near 230 °C. This limits the type of thermoplastics that can be used in association with polysaccharide fillers. Another drawback of lignocellulosic fillers is their high moisture absorption and the resulting swelling and decrease in mechanical properties. Moisture absorbance and corresponding dimensional changes can be largely prevented if hydrophilic fillers are thoroughly wet hydrophobic polymer matrices giving a good adhesion between both components (EICHHORN et al., 2001; SAMIR; ALOIN; DUFRESNE, 2004).

Treatment of cellulosic fibers such as extraction of some of their compounds or by adding coupling agents allow obtaining new materials with natural fibers. In automotive applications, composites based in polypropylene matrices are mostly used, specifically in non-structural components. However, several thermoplastics has been employed in vehicles, as polyamide (PA 6 and PA 6.6). Polyamides are semi-crystalline thermoplastics with good mechanical and chemical resistance, and are differentiated by numbers that indicate the amount of carbon atoms in the original monomer units. They also have good ability to bear loads, with good mechanical performance at elevated temperatures (mainly PA 6.6), good toughness and good chemical resistance.

The preparation of composites of polyamide/cellulosic-based fibers for automotive applications is the subject of this PhD thesis. The selection and treatment of the fibers, the preparation and processing of composites and evaluation of the best compositions for automotive applications are the parameters on which this project is based.

2 OBJECTIVES OF THE WORK

The European automotive industry has sought technical solutions to replace the usual glass fibers for materials benign to the environment with the highest level possible biocomponents. In this context, it is necessary to develop polymer composites with natural fibers that can withstand high temperatures, which are common inside cars.

- ***Global objective***

The objective of this work is to prepare composites of polyamides with natural fibers, as curauá, jute and flax, able to withstand high temperatures. The polymeric matrix and treated fibers should be resistant to temperature separately, and suitable coupling agents are needed. In fact, the modification of fibers is a key point to obtain optimum adhesion matrix-load, thus improving the thermal and mechanical properties of composites.

- ***Specific objectives***

1. Propose appropriate physical and chemical treatments to natural fibers selected so as to remove components of low melting points;
2. Perform and characterize surface treatments on fibers for improving their thermal stability and allow processing with polyamide;
3. Prepare composites of polyamide with natural fibers materials by processing in a twin-screw extruder or internal mixer;
4. Evaluate the best compositions of the composites for applications in automotive industry.

3 STATE OF THE ART

3.1 STRUCTURE AND COMPOSITION OF NATURAL FIBERS

Natural fibers are complex composites with different structural levels. Cellulose chains, arranged in a complex, spatially varying manner, are held together by a lignin and hemicelluloses matrix. The basic unit is a plant cell which walls contain mainly cellulose. Cell walls are themselves a complex structure which structural arrangement and composition strongly depends on the type of plant, its genotype, the role the cell has in the plant and is submitted to variations linked to soil quality and climate. An example of the arrangement of cellulose in the wall of a plant cell is given in Figure 1. Each cell has a complex, layered structure of its wall consisting

of a thin primary wall, which is the first layer deposited during cell growth encircling a secondary wall. The secondary wall is made up of three layers depending on the plant and the

thick middle layer determines the mechanical properties of the fiber. The middle layer consists of a series of helically

wound microfibrils formed from long chain cellulose molecules. The angle between the plant cell axis and the microfibrils is called the microfibrillar angle. The characteristic value of microfibrillar angle varies from one fiber botanic origin to another. As can be understood, the word “fiber” refers to different entities depending on the scale at which we consider the structure. We will use the word “fiber” in this thesis to describe the macroscopic entity of the plant, in the range of tens of microns to centimeter.

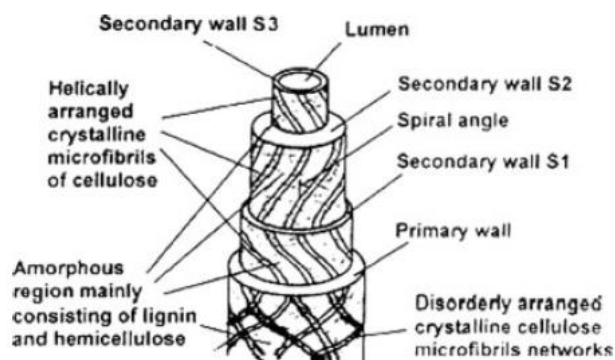


Figure 1: Structure of natural fiber

Source: JOHN, M.J.; ANANDJIWALA, R.D.
(2008)

To come back to the cell wall, the smallest cellulose organized entity is a group of 24 to 36 chains formed at the outside of the plasma membrane. They

assemble into what is often called microfibril, having typically diameters of about 10-30 nm and made up of 30-100 cellulose molecules in extended chain conformation. This is providing mechanical strength to the fiber. The amorphous matrix phase in a cell wall is very complex and consists of hemicelluloses, lignin and in some cases pectin. The hemicelluloses molecules are hydrogen bonded to cellulose and act as a cementing matrix between the cellulose microfibrils, forming the cellulose-hemicellulose network, which is thought to be the main structural component of the fiber cell. The hydrophobic lignin network, mainly glueing different cells together acts as a coupling agent and increases the stiffness of the cellulose/hemicellulose composite.

The reinforcing efficiency of natural fiber is related to the nature of cellulose and its crystallinity. The main components of natural fibers are thus cellulose (called in previously α -cellulose), hemicelluloses, lignin and pectins.

Cellulose is a natural polymer consisting of D-anhydroglucose ($C_6H_{11}O_5$) repeating units joined by β -1,4-glycosidic linkages at C_1 and C_4 position. The degree of polymerization (DP) is above 10 000 in plants. Each repeating unit contains three hydroxyl groups. These hydroxyl groups and their ability to form hydrogen bond play a major role in directing the crystalline packing and also govern the physical properties of cellulose. Solid cellulose forms a microcrystalline structure with regions of high order, i.e., crystalline regions, and regions of low order, called amorphous regions. The crystal structure of naturally occurring cellulose is called cellulose I. Cellulose is resistant to strong alkali but is easily hydrolyzed by acid to water-soluble sugars and is relatively resistant to oxidizing agents.

Cellulose displays six crystalline polymorphs: I, II, III_I, III_{II}, IV_I and IV_{II} with the possibility of conversion from one form to another. For a long time, the native cellulose (cellulose I) attracted the interest of a large scientific community in attempt to elucidate its crystal structure. It is now known that there are two crystalline forms of natural cellulose: cellulose I α and cellulose I β . Cellulose I α is a rare form, and only exists in some green algae along with cellulose I β in a ratio of I α :I β of 7:3. The exact unit cells of these two crystalline allomorphs are

still a matter of research. Cellulose I β is the major form, and occurs in an almost pure in various species from higher plants to algae, and also in animal tunicates. Cellulose I α can be transformed fully into cellulose I β without losing its crystallinity using a hydrothermal treatment in a dilute alkaline solution. This means that cellulose I β is a more thermodynamically stable structure than cellulose I α .

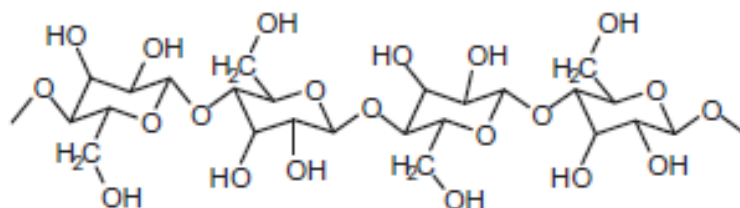


Figure 2: Chemical structure of cellulose

Source: PARK, J.M. et al. (2008)

Hemicellulose comprises a group of polysaccharides composed of 5 and/or 6 carbon ring sugars. Hemicellulose differs from cellulose in three aspects. Firstly, it contains several different sugar units whereas cellulose contains only 1,4 β -D-glucopyranose units. Secondly, it exhibits a considerable degree of chain branching containing pendant side groups at the origin to its non-crystalline nature. Thirdly, the degree of polymerisation of hemicellulose is around 50-300, whereas that of native cellulose is 10-100 times higher. Hemicellulose forms the supportive matrix for cellulose microfibrils and is very hydrophilic, soluble in alkali and easily hydrolyzed in acids.

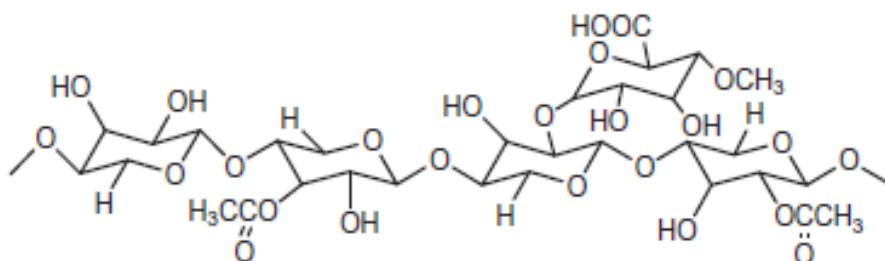


Figure 3: Chemical structure of one hemicellulose

Source: PARK, J.M. et al. (2008)

Lignin is a complex hydrocarbon polymer with both aliphatic and aromatic constituents. It is totally insoluble in most solvents and cannot be broken down to monomeric units. Lignin is totally amorphous and hydrophobic in nature. It is the compound that gives rigidity to the plants by gluing the various cells together. It is thought to be a complex three-dimensional copolymer of aliphatic and aromatic constituents with very high molecular weight. Hydroxyl, methoxyl and carbonyl groups have been identified in lignin. Lignin has been found to contain five hydroxyl and five methoxyl groups per building unit. It is believed that the structural units of lignin molecule are derivatives of 4-hydroxy-3-methoxy phenyl-propane. The main problem in lignin chemistry is that no method has been established by which it is possible to isolate lignin in its native state. Lignin is considered to be a thermoplastic polymer exhibiting a glass transition temperature of around 90 °C and melting temperature of around 170 °C. It is not hydrolyzed by acids, but soluble in hot alkali, readily oxidized, and easily condensable with phenol (JOHN; ANANDJIWALA, 2008; PARK et al., 2008; WADA et al., 2010)

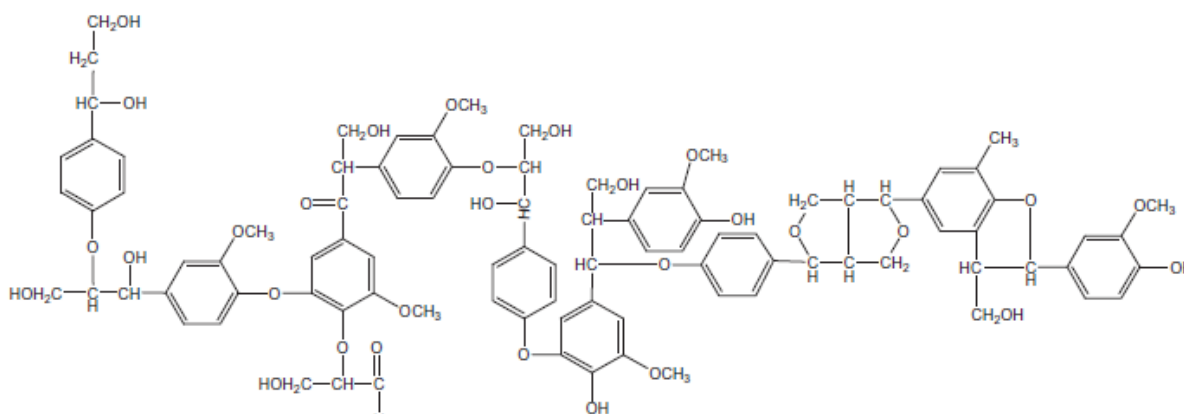


Figure 4: Chemical structure of lignin

Source: PARK, J.M. et al. (2008)

3.2 BIOSYNTHESIS OF CELL WALL STRUCTURES

The synthesis of the different constituents of cell wall (cellulose, hemicelluloses, pectins, proteins and lignin) occurs in the cell and is mainly governed by two

apparatus: the Cellulose Synthase Complex, which produces cellulose, and the Golgi, which products the matrix polysaccharides.

A plant cell is composed of the following main entities the cell wall (the cytoplasm) delimited by the plasma membrane, the nucleus which contains the DNA and the organelles as the mitochondria, the Golgi apparatus or the chloroplasts (Figure 5). The chlorophyll molecules present in the chloroplasts are able to convert solar energy (photons), CO_2 and water (present in vacuole) into glucose molecules, O_2 and water through the photosynthesis mechanism. One part of these glucose molecules is then stored in the cell wall in the form of macromolecules as cellulose, hemicelluloses and pectins while the other part is used in mitochondria to produce useable energy, called ATP.

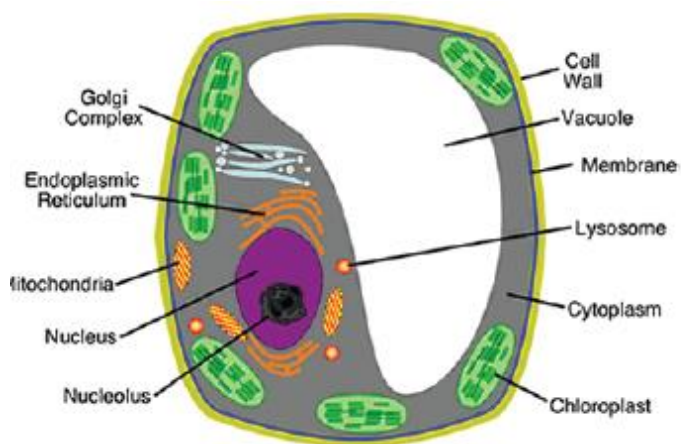


Figure 5: Schematic representation of the plant cell with the main entities involved in the biosynthesis

Source: LE MOIGNE, M.L. (2009)

The ATP molecules are consumed by many enzymes and cellular processes including

biosynthetic reactions, mobility and cell division. A constant amount of about 8000 available ATP molecules is present in each cell.

The glucose macromolecules made for storage are used by the cell in an activated form called UDP-glucose (Uridini diphosphate glucose). The UDP-glucose is the substrate for the cellulose synthesis by the Cellulose Synthase Complex present in the plasma membrane. Other sugars as NDP-sugars are used in the Golgi apparatus to produce the others matrix components as hemicelluloses and pectins (LE MOIGNE, 2009).

Cellulose is at the core of plant cell walls, where it serves as scaffold for the binding of other wall components. In the primary wall of cell plants, cellulose

microfibrils are about 3 nm in diameter and generally consist of parallel arrangements of 36 β -1,4-glucan chains. Membrane-bound cellulose synthase enzyme complexes are required for cellulose biosynthesis. These complexes are visible as hexameric rosettes of approximately 25-30 nm in diameter when plant cells are examined using freeze-fracture electron microscopy. When cytosolic uridine-diphosphoglucose (UDP-glucose) is used as substrate, each rosette subunit is thought to extrude multiple β -1,4-glucan chains that coalesce as microfibrils outside of the plasma membrane.

Hemicelluloses can be divided into four main classes: xyloglucans (XyG), which contain a heavily substituted β -1,4-glucan backbone; (gluco)mannans, containing a variably substituted backbone that includes β -1,4-linked mannose (glucose and mannose) residues; glucuronarabinoxylans (GAX), containing a substituted β -1,4-linked xylan backbone; and mixed-linkage glucans (MLG), which involve an unsubstituted backbone of glucosyl residues containing both β -1,3 and β -1,4 linkages. The main building blocks of lignin are the hydroxycinnamyl alcohols (or monolignols) coniferyl alcohol and sinapyl alcohol, with typically minor amounts of *p*-coumaryl alcohol (Figure 6).

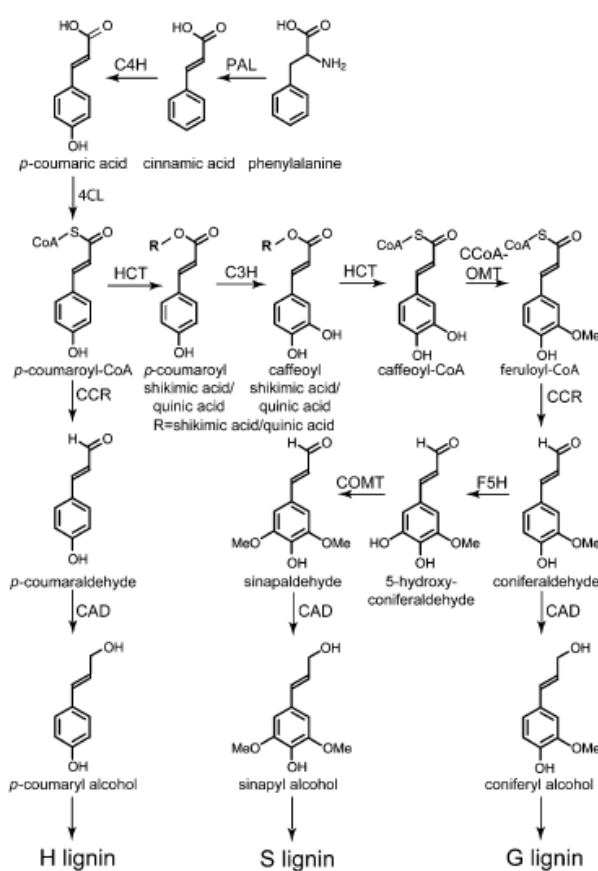


Figure 6: Biosynthesis of lignin: the main biosynthetic route towards the monolignols *p*-coumaryl, coniferyl and sinapyl alcohol

Source: RIPPERT, P. et al. (2009)

A schematic representation of possible wall polysaccharide biosynthesis is presented in Figure 7 (a-e). Wall polysaccharides are made in two cellular

compartments. Cellulose and callose (not shown) are made at the plasma membrane. Rosettes move in the plane of the membrane, guided by cortical microtubules, producing cellulose microfibrils in the wall that have the same orientation as the microtubules in the cytosol (Figure 7a). It is thought that each hexameric rosette comprises six rosette subunits, and that each one rosette subunit contains six CESA proteins, providing a total of thirty-six CESA proteins per rosette. Matrix polysaccharides are synthesized in the Golgi before deposition into secretory vesicles that deliver them to the cell surface. The backbones of at least some hemicellulosic polysaccharides are synthesized by CSL proteins that show sequence similarity to the CESA proteins (Figure 7c). The topology of the CSL proteins is not known, but two possibilities are shown. If the CSL proteins use sugar nucleotides present in the Golgi lumen, then the model shown in Figure 7d would apply. If the CSL proteins operate in the same way as the CESA proteins, then the model shown in the lower part (Figure 7d) and in expanded view (Figure 7e), would be favored. The glycan synthases are thought to form complexes with glycosyltransferases that add side chains to the polymer (bottom part of Figure 7d). Such organization in a complex might be especially important for the synthesis of polysaccharides such as XyG, which has a regular pattern of side chain substitution (LEROUXEL et al., 2006).

In recent years, significant insight into the molecular details of cellulose biosynthesis has been gained using forward and reverse genetic analysis coupled with advances in plant genomics. The plasma membrane rosettes contain the cellulose synthase catalytic subunit (CESA), proteins that are encoded by the CESA genes. Plant genomes typically contain multiple CESA genes as a part of gene family. For example, ten CESA genes are present in *Arabidopsis*, rice has at least nine and poplar has 18. It is thought that each hexameric rosette comprises six rosette subunits and that each rosette subunit contains six CESA proteins, providing a total of thirty six CESA proteins per rosette (LEROUXEL et al., 2006).

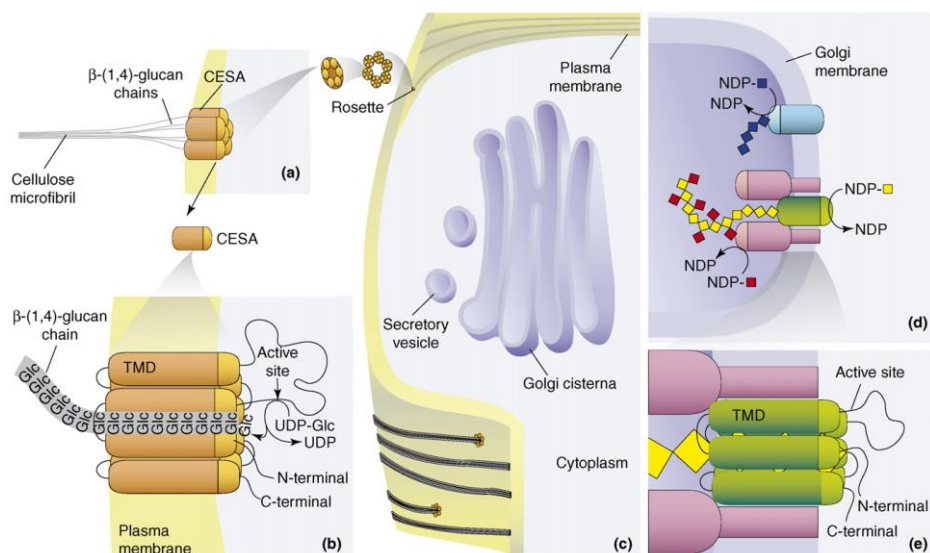


Figure 7: Schematic representation of possible wall polysaccharide biosynthesis

Source: LEROUXEL, O. et al. (2006)

The idea that there are at least three different CESA proteins in a rosette comes from genetic evidence, which also supports the conclusion that the cellulose in primary cell walls is synthesized by a different set of CESA proteins than that in secondary cell walls. In *Arabidopsis*, CESA1, CESA3 and CESA6 are required for cellulose biosynthesis in primary cell walls, whereas CESA4, CESA7 and CESA8 are required for cellulose biosynthesis during second wall deposition. Similar conclusions have been reached in other plants, although the numbering system for CESA proteins varies among plant species (LEROUXEL et al., 2006).

3.3 MAIN NATURAL FIBERS

There is a wide variety of different natural fibers, which can be used as reinforcers or fillers. Figure 8 presents a diagram with a classification of the various fibers. The most usual natural fibers used in composite materials are flax, hemp, jute, kenaf and sisal, due to their good properties and availability. Flax, hemp, jute and kenaf are bast fibers, which develop in the bast of the plant. Flax, hemp and jute have more or less similar morphologies and can

have similar roles in a composite (VANHOLME et al., 2010). Species derived from natural fibers as well as their annual production are listed on Table 1.

Among the purpose-grown plants, bast fibers represent the vast majority of natural fibers with potential for composites usage. Bast plant stems are characterized by long fibers surrounding a core of pulp or short fibers and covered with a protective bark layer. Separation of the useful fibers from the bark and core starts with a process called "retting," in which the cut stalks are soaked in water or left in the field in a humid environment for up to several weeks to degrade the natural binders. This makes the fiber bundles easier to process by mechanical means. As of the mid-1990s, flax and jute were the principal fibers used in biocomposites, but have been joined by higher strength industrial hemp and kenaf, at least in automotive applications (BOS, 2004).

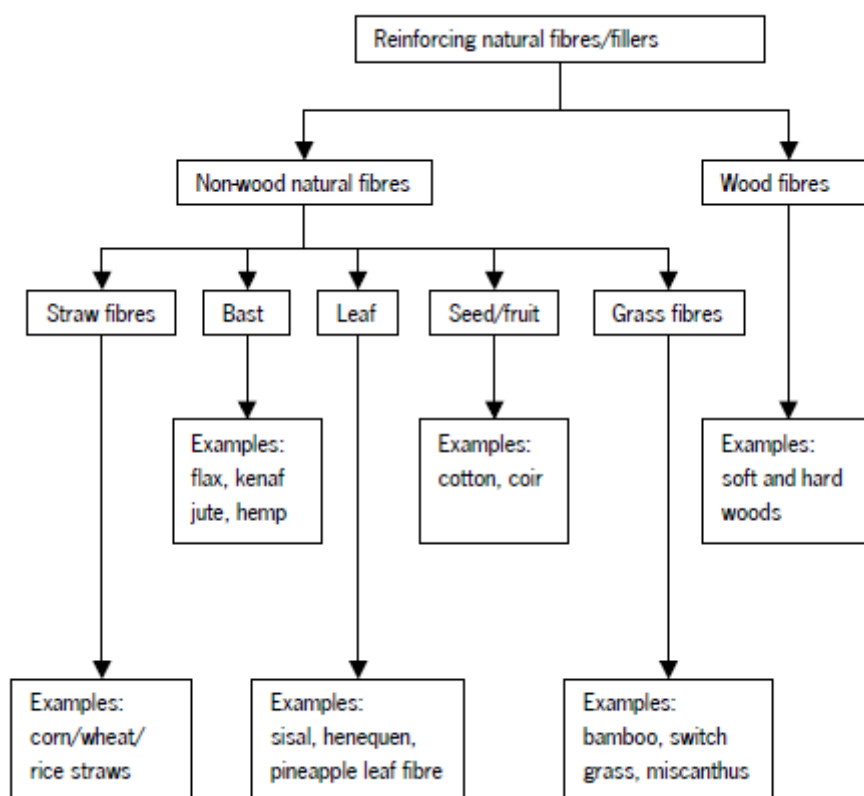


Figure 8: Classification of main natural fibers

Source: VANHOLME, R. et al. (2010)

Table 1: Species derived from natural fibers and annual production

| Natural Fiber | Main species | Annual Worldwide Production (x 10 ³ ton) |
|---------------|-----------------------------|---|
| Cotton | <i>Gossypium</i> sp. | 18500 |
| Hemp | <i>Cannabis sativa</i> | 215 |
| Jute | <i>Corchorus capsularis</i> | 2500 |
| Kenaf | <i>Hibiscus cannabinus</i> | 770 |
| Flax | <i>Linum usitatissimum</i> | 810 |
| Sisal | <i>Agave sisilana</i> | 380 |

Source: BOS, H. (2004); JOHN, M.J.; ANANDJIWALA, R.D. (2008)

Flax fibers are grown in two common forms. In North America, almost all flax being of the oil seed variety, predominantly grown in central Canada, but also cultivated in North Dakota and Minnesota. Its primary use is for linseed oil and food products. Attempts to commercialize the stalk fibers for composites were only marginally successful and have been largely abandoned. However, textile flax, a much taller plant and the source of commercial linen fiber used in clothing, is now the source for almost all flax-based natural fiber composites. It is grown widely in Russia, China and, to a lesser extent, Northern Ireland, Belgium and France (TAJ et al., 2007)

The jute plant is native from Southeast Asia, with India and Bangladesh responsible for more than 90 percent of worldwide production. Popular for the production of carpet backing, tote bags, sackcloth (burlap) and rope, jute is cut, retted, separated and cleaned in largely manual processes. Although jute has been partially replaced by other bast fibers in some of its earliest composite applications, it continues to be popular in interior automotive components (BROSIUS, 2010).

Curaua (*Ananas erectifolius*) is an Amazonian plant known since pre-Columbian times by the quality of its fibers extracted from plant leaves. It is a plant of the *bromeliaceae* family that has attracted much attention, particularly since 1993, when this fiber was commercially recognized by the Brazilian automotive industry. The curauá fiber is the third in economic analysis in Brazil, after sisal, jute, and is among the lignocellulosic material with the greatest rigidity. Sometimes cited as the most competitive among Brazilian fibers, attention to it

has been growing and somewhat offsetting the decrease in the cultivation of jute, being cultivated on a large scale in the Amazon region (SILVA, 2010).

The flax fiber has great potential for the production of polymeric composites according to their properties, which can be observed in Tables 2 and 3. In Table 2, minimum and maximum values of average diameter are presented for the total number of fibers tested. The results of tensile test data and other fibers are also shown for comparison (BOGOEVA-GACEVA et al., 2007; SILVA; AQUINO, 2007).

Table 2: Diameter, tensile strength and elastic modulus of purple and white in comparison with other natural fibers and glass fibers

| Fiber | Diameter (μm) | Tensile Strength (MPa) | Young's Modulus (GPa) |
|---------------|--|-----------------------------------|----------------------------------|
| Purple curauá | 43-93 | 665-1300 | 20-33 |
| White curauá | 60-100 | 859-1404 | 20-36 |
| Jute | 200 | 393-773 | 26,5 |
| Sisal | 50-300 | 511-635 | 9,4-22 |
| Coconut | 100-450 | 131-175 | 4-13 |
| Flax | 22-27 | 345-1500 | 10-80 |
| Glass | 8-14 | 1800-3000 | 72-83 |

Source: BOGOEVA-GACEVA, G. et al., 2007; SILVA, R.V.; AQUINO, E.M.F., 2007)

It was found that flax fibers showed a smaller diameter and greater tensile strength and Young's modulus when compared to sisal, jute, coconut and curauá. Flax fibers have properties close to glass fibers. The mechanical strength of lignocellulosic fibers is mainly determined by the content of cellulose. The chemical compositions of some natural fibers, including hemp fiber, are reported in Table 3 (GOWDA, 1999; BLEDSKI; GASSAN, 1999; MOHANTY, 2000.; LEÃO, 2001; BOGOEVA-GACEVA et al., 2007; MOTHÉ; ARAÚJO, 2007; SILVA; AQUINO, 2007).

Table 3: Chemical composition of some plant fibers (wt. %)

| Fiber | Curaua | Jute | Sisal | Coconut | Flax |
|-------------------------|-----------|-----------|---------|-----------|-----------|
| Cellulose | 70,7-73,6 | 61-71,5 | 67-78 | 36-43 | 71-78 |
| Hemicellulose | 9,9 | 13,6-20,4 | 10-14,2 | 0,15-0,25 | 18,6-20,6 |
| Lignin | 7,5-11,1 | 12-15 | 8-11 | 41-45 | 2,2 |
| Pectin | - | 0,2 | 10 | 3-4 | 2,2 |
| Water Solubility | - | 1,1 | 16,2 | - | - |
| Waxes | - | 0,5 | 2 | - | 1,7 |
| Microfibrilar Angle (°) | - | 8,0 | 20 | 41-45 | 10 |
| Moisture | 7,9 | 12,6 | 11,0 | - | 10 |

Source: BOGOEVA-GACEVA, G. et al., 2007; SILVA, R.V.; AQUINO, E.M.F., 2007)

3.4 THERMAL DEGRADATION OF NATURAL FIBERS

The understanding of pyrolytic behavior of cellulose is fundamental to biomass thermochemical conversions. Early work for cellulose pyrolysis outlines the classical kinetic schemes of three main chemical pathways. It is found that low-temperature delays the initial process, corresponding to a reduction in the degree of polymerization and the formation of so-called “anhydrocellulose” or “active cellulose”. High temperature pyrolysis of cellulose is expressed by two competitive degradation reactions, the first essentially leading to char and gas, the second to tars (mainly levoglucosan). The notion of “anhydrocellulose” is excluded in the work of Capart, Khezami and Burnham (2004), which explains cellulose decomposition solely by two competitive reaction channels, one ascribed to the formation of tars (mainly levoglucosan) and char, the other to the formation of the light gases. The formation of “anhydrocellulose” has been confirmed, but the formation of light gases is not considered to be related to the low-temperature step of “anhydrocellulose” (CAPART; KHEZAMI; BURNHAM, 2004; SHEN; GU, 2009).

Studies show that the thermal decomposition of lignocellulosic fibers is not necessarily an additive function resulting from the contribution of each fraction of its components, that is, cellulose, hemicelluloses and lignin, because of interactions between these fractions. In general, the thermolysis reaction of polysaccharides (cellulose and hemicelluloses) occurs by the cleavage of glycoside bonds, C – H, C – O and C – C bonds, as well as by dehydration, decarboxylation and decarbonylation. Considering the mixture arising from the

degradation of cellulose, levoglucosan, produced by transglycosylation intramolecular reactions, is the most abundant product. At around 600 °C, there can be carbonization of levoglucosan with the release of water.

One of the degradation mechanisms of lignin to be considered occurs through dehydration, yielding derivatives with lateral unsaturated chains and the release of water. Yet, carbon monoxide, carbon dioxide and methane are also formed. The decomposition of aromatic rings occurs above 400 °C. Continued burning leads to the saturation of the aromatic rings, the rupture of C – C bonds present in lignin, the release of water, CO₂ and CO, and structural rearrangements. Considering the three main components of the lignocellulosic material, lignin is the component that presents thermal degradation over the larger temperature range (TRINDADE et al., 2005).

Polletto et al. (2011) investigated thermal degradation of four species of wood fibers (*Pinus elliottii*, *Eucalyptus grandis*, *Mezilaurus itauba* and *Dipteryx odorata*), with particle size between 200 and 300 µm. Figure 9 shows the results of thermogravimetric analysis performed on the different wood species. Figure 9a gives the percentage of weight loss as a function of temperature, while Figure 9b presents the derivative thermogravimetric curves. According to this study, water loss is observed at around 100 °C, and further thermal degradation takes place as a two-step process. In the first step, the degradation of hemicelluloses takes place at around 300 °C and a slight shoulder in the DTG curve can be seen in Figure 9b for all wood species studied. At around 350 °C, the main degradation of cellulose occurs and a prominent peak appears at the temperature corresponding to the maximum decomposition rate. According to Kim et al. (2006), the depolymerization of hemicellulose occurs between 180 and 350 °C, the random cleavage of the glycosidic linkage of cellulose between 275 and 350 °C and the degradation of lignin between 250 and 500 °C. The higher activity of hemicellulose in thermal decomposition may be attributed to its chemical structure. Hemicellulose has a random amorphous structure and it is easily hydrolyzed. In contrast, the cellulose molecule is a very long polymer of glucose units, and its crystalline regions improve the thermal stability of wood. Lignin is different from hemicelluloses and cellulose because it is composed of

three kinds of benzene-propane units, being highly crosslinked and having very high molecular weight. Therefore, the thermal stability of lignin is very high and it is difficult to decompose it.

The initial weight loss temperature, T_i , of all samples is defined as the temperature at which the sample loses 3% of its weight, as showed in Table 4. The lowest T_i value was attributed to *Mezilaurus itauba* (ITA), as can be seen in detail in Figure 9a. According to the authors, this might be associated with higher volatility of extractives and hemicellulose in this wood. The highest T_i values were observed for the EUG, PIE and DIP wood species. On the other hand, EUG, ITA and DIP had a significant amount of residue at 800 °C probably due to higher inorganic contents in these three wood species.

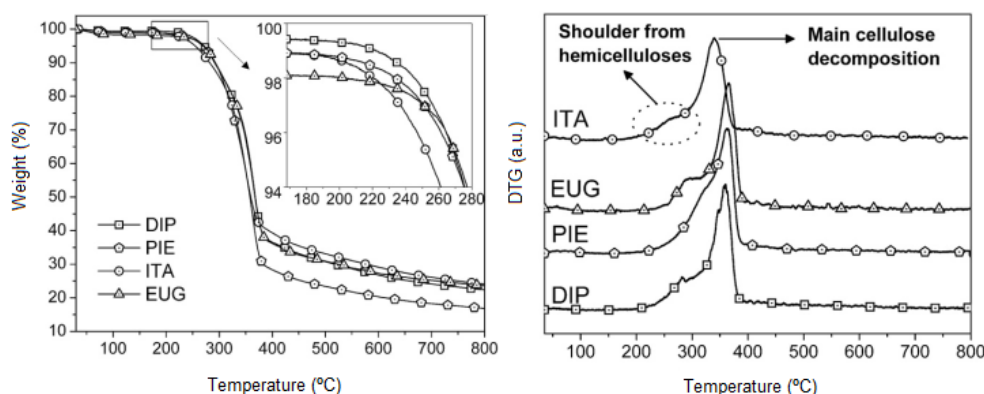


Figure 9: TGA (a) and DTG (b) curves for the different wood species studied

Source: POLETTO, M. et al., 2011

Table 4: Thermal degradation temperature, T_i shoulder, DTG peak and residue at 800 °C for the wood species under study

| Wood species | T_i (°C) | T shoulder (°C) | DTG peak (°C) | Residue at 800 °C (%) |
|------------------------------------|---------------|--------------------|------------------|--------------------------|
| <i>Eucalyptus grandis</i> (EUG) | 250 | 291 | 364 | 23.6 |
| <i>Pinus elliottii</i> (PIE) | 251 | 322 | 367 | 16.8 |
| <i>Dipteryx odorata</i> (DIP) | 257 | 289 | 368 | 22.4 |
| <i>Mezilaurus itauba</i> (ITA) | 237 | 275 | 350 | 24.1 |

Source: POLETTO, M. et al., 2011

Kim et al. (2010) correlated the thermal behavior and crystallite size of cellulose of three sample sources: *Halocynthia* (a sea animal giving highly crystalline

form of cellulose), cotton and microcrystalline cellulose Funacel. Figure 10 shows the TG, DTA and derivative thermogravimetric curves (DTG) of the cellulose samples. According to the study, decomposition of Funacel, cotton and *Halocynthia* began at 285, 305 and 325 °C, respectively, and a rapid weight loss occurred in the ranges of 315 – 360, 340 – 380 and 370 – 410 °C, respectively. DTA curves also showed a characteristic change in the thermal decomposition. A large endothermic peak of cellulose appeared in the temperature range corresponding to the rapid weight loss. The DTA peaks were centered at 341, 366 and 389 °C for Funacel, cotton and *Halocynthia*, respectively.

The peak positions in the DTG curves were nearly the same of those in the DTA curves. The initial temperature of thermal decomposition and the peak temperature in the DTA and DTG curves shifted to higher temperatures with increasing crystallite size, crystallinity index and degree of polymerization (Table 5). Several models of the thermal decomposition of cellulose in wood have been suggested: (a) where decomposition preferentially proceeds along the fiber axis, (b) where a crystallite that once starts to decompose undergoes rapid decomposition while the other crystallites remain largely intact, and (c) a combination of (a) and (b). It has also been reported that the thermal expansion of cellulose is related to the crystallite size and crystallinity index. Less crystalline cellulose with small crystallites, such as wood cellulose, expands when subjected to a small amount of heat. Although the mechanism of this process is not well understood, the crystallite size, crystallinity index, and degree of polymerization may be important factors for the transfer of heat in the decomposition of cellulose.

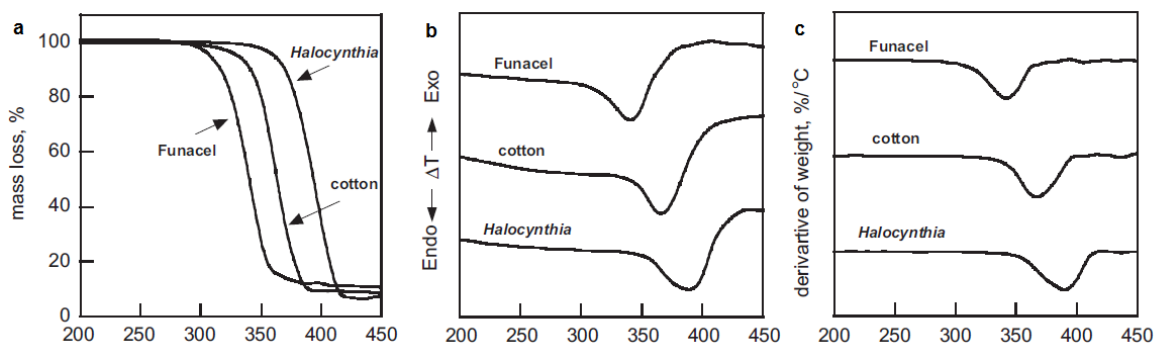


Figure 10: TGA (a), DTA (b) and DTG (c) curves of native cellulose samples

Source: KIM, S.H. et al. (2010)

Table 5: The degree of polymerization, d-spacing, crystallite size and crystallinity indice of native cellulose samples

| Samples | DP ^a | d-spacing (nm) ^b | | | L (nm) ^c | | | CI ^d |
|--------------------|-----------------|-----------------------------|-------|-------|-----------------------|-------|-------|-----------------|
| | | ($\bar{1}\bar{1}0$) | (110) | (200) | ($\bar{1}\bar{1}0$) | (110) | (200) | |
| Funacel | 520 | 0.597 | 0.536 | 0.395 | 3.9 | 5.5 | 4.5 | 0.54 |
| Cotton | 4300 | 0.623 | 0.539 | 0.394 | 4.9 | 6.5 | 5.8 | 0.58 |
| <i>Halocynthia</i> | 19000 | 0.603 | 0.536 | 0.390 | 8.7 | 11.7 | 10.6 | 0.74 |

^a Degree of polymerization.

^b d-Spacing of typical three equatorial peaks on cellulose.

^c Crystallite size perpendicular to each plane.

^d Crystallinity index.

Source: KIM, S.H. et al. (2010)

3.5 CHEMICAL TREATMENTS ON NATURAL FIBERS

Fiber-matrix interface plays an important role on the physical and mechanical properties of composites. To improve the interface properties, natural fibers are subjected to chemical treatments such as mercerization, bleaching, silane treatment, peroxide treatment, benzoylation, treatment with isocyanates acrylation, acetylation, latex coating, steam explosion etc. Surface modification of natural fibers before their use in composites is necessary in order to achieve two objectives: the first is to increase the crystallinity of the fiber by extraction of the amorphous fractions of lignin and especially hemicellulose of low molar

mass. These light fractions of the fibers are responsible for the low temperature degradation and poor mechanical properties; and the second is to increase fiber dispersion and induce the formation of bonds between the fiber and polymer matrix. On the other hand, treatment of the fibers represents an increase in the cost of the final product (MISHRA et al., 2002; BOGOEVA-GACEVA et al., 2007).

Chemical modification can be defined as the reaction between some reactive groups of natural fiber and the chemical reagent, with or without presence of a catalyst to form a covalent bond between both. As the properties of natural fibers are due to cell wall components, the chemical modification of these can change several basic properties of a fiber. The reagents to be used in the modification process must be capable of reacting with the hydroxyl lignocellulosic under acidic, neutral or alkaline conditions at a temperature below 150 °C. The system must be simple and able to swell the cell wall structure to facilitate penetration of reactants. The molecule must react quickly with the lignocellulosic components to form stable chemical bonds and then the treated fibers must possess the desired properties (BOGOEVA-GACEVA et al., 2007).

3.5.1 Alkaline Treatment

Also known as mercerization, it is one of the most widely used chemical methods for the treatment of natural fibers when they are used to reinforce thermoplastic and thermoset polymers. The major modification provided by the alkali treatment is the disruption of hydrogen bonds in the structure, thus increasing its roughness. This treatment is capable of removing hemicelluloses, some lignin, waxes and oils that cover the outer surface of the cell wall of the fibers (MOHANTY; MISHA; DRZAL, 2001). The addition of aqueous sodium hydroxide to natural fibers promotes the ionization of the hydroxyl groups to alkoxide, as shown in Scheme 1 (AGRAWAL et al., 2000) Thus, this process directly influences the cellulose fibrils and may reduce the degree of polymerization and especially hemicellulose and lignin extract (JÄHN et al., 2002).

Scheme 1:

The type of alkali (KOH, NaOH or LiOH) and its concentration influence the degree of swelling of the fiber, and thus the degree of conversion of crystal structure from cellulose I to II (JOHN; ANANDJIWALA, 2008). Studies have shown that the Na⁺ hydrates may a diameter able to fill the smaller pores between the crystalline parts and penetrate them. Consequently, the NaOH treatment results in a better yield. At suitable (in the range of 20%) concentrations of NaOH, this leads to the formation of a new lattice Na - cellulose I with large distances between cellulose molecules, and these spaces are filled with water molecules. Thus, the OH groups of the cellulose are converted to O-Na groups, expanding the size of the molecules. Subsequent rinsing with water removes the sodium ion and convert the pulp to a new crystal structure, that is cellulose II, which is thermodynamically more stable than cellulose I. NaOH can provide a complete conversion of cellulose I to cellulose II, unlike other alkalis which are leading to partial conversion. The alkaline solution employed influences the cellulosic components within the natural fiber and remove non-cellulosic components (hemicellulose, lignin and pectin) (WEYENBERG et al., 2006).

In general, in the alkali treatment, the fibers are immersed in low concentrated NaOH solution for a certain time. Ray et al. (2001) and Mishra et al. (2001) treated sisal and jute fibers with 5.0% NaOH for 2 hours, leaving them immersed in this alkaline solution for a period of 72 h at room temperature. A similar treatment was conducted by Morrison et al. (2000) for flax fibers. Garcia-Jaldon, Dupeyre and Vignon (1998) reported that using alkaline solution at 2.0% for 90 s at 200 °C under pressure of 1.5 MPa, achieved satisfactory defibrillation for hemp fiber.

Alkaline treatment brings two effects on the natural fiber. One is the increased roughness on the surface, resulting in better adhesion of the matrix to the fiber. Another effect is the increase of the exposed surface of the cellulose fiber, thereby increasing the number of probable sites of reaction (VALADEZ-

GONZALEZ et al., 1999). The alkaline treatment has a lasting effect on the mechanical behavior, increasing properties such as rigidity and tension of flax fibers (JÄHN, 2002). Van der Weyenberg et al. (2003) reported that the alkaline treatment increases by an order of 30%, the mechanical properties (stress and modulus) for epoxy resin composites / flax fiber. This coincided, according to the authors, with the removal of pectin. Jacob et al. (2004) examined different NaOH concentrations (0.5, 1.0, 2.0, 4.0 and 10.0%) for composites reinforced with sisal fiber and concluded that with 4.0% of alkali, composite showed better tensile properties.

3.5.2 Silane treatment

Silanes are recognized as efficient coupling agents extensively used in polymer composites and adhesive formulations. They have been successfully applied on the surface of inorganic fillers such as glass fiber and silica for reinforcing polymer composites. Silanes are also adhesion promoters in many adhesive formulations or are used as substrate primers, giving stronger adhesion. The bifunctional structures of silanes have also been of interest in applying them for natural fiber/polymer composites, since both glass fibers and natural fibers bear reactive hydroxyl groups, and extensive researches have accordingly been carried out to screen the varied silane structures for natural fiber/polymer composite production (KALIA; KAITH; KAUR, 2009).

These agents are able to reduce the number of hydroxyl groups on the interface. In the presence of moisture, the hydrolyzable alkoxy groups of alkoxy silanes lead to the formation of silanols. Some silanes used for the natural fiber/polymer composites are shown in Table 6. Aminosilanes have been extensively reported in the literature as coupling agents between natural fibers and thermoplastics or thermosets. Vinyl- and acryl-silanes are coupling agents that are able to establish covalent bonds with polymeric matrices in the presence of peroxide initiators. Methacrylate-functional silanes can display high levels of reactivity with unsaturated polyester matrices, while azidosilanes can efficiently couple inorganic fillers with thermoplastic matrices (XIE et al., 2010).

Table 6: Silanes used for the natural fiber/polymer composites: chemical structures, organofunctionalities and target polymer matrices

| Structure | Functionality | Abbreviation | Target matrix |
|-------------------------------------|---------------|--------------|--|
| $(RO)_3Si-(CH_2)_3-NH_2^a$ | Amino | APS | Epoxy Polyethylene Butyl rubber Polyacrylate PVC |
| $(RO)_3Si-CH=CH_2$ | Vinyl | VTS | Polyethylene Polypropylene Polyacrylate |
| $(RO)_3Si-(CH_2)_3-OOC(CH_3)C=CH_2$ | Methacryl | MPS | Polyethylene Polyester |
| $(RO)_3Si-(CH_2)_3-SH$ | Mercapto | MRPS | Natural rubber PVC |
| $(RO)_3Si-(CH_2)_3-O-CH_2CHCH_2O$ | Glycidoxy | GPS | Epoxy Butyl rubber Polysulfide |
| $R_2-Si-Cl_2$ | Chlorine | DCS | Polyethylene PVC |
| VTS grafted plastics | Vinyl | VSPP VSPE | Polypropylene Polyethylene |
| $(RO)_3-Si-R''-N_3^b$ | Azide | ATS | Polypropylene Polyethylene Polystyrene |
| $(RO)_3Si-(CH_2)_{15}CH_3$ | Alkyl | HDS | Polyethylene Natural rubber |

^a R = -methyl or ethyl.

^b R'' = -C₆H₄-SO₂-.

Source: XIE, Y. et al. (2010)

In Figure 11 the four steps of interaction between silane coupling agents and natural fibers are presented (XIE et al., 2010):

1 - Hydrolysis (Figure 11a): The silane monomers are hydrolyzed in the presence of water and catalyst (normally acid or base) releasing alcohol and yielding reactive silanol groups.

2 - Self-condensation (Figure 11b): During the hydrolysis process, the concomitant condensation of silanols (aging) also takes place. The condensation should be minimized at this stage to leave the silanols free for being absorbed to the hydroxyl groups in the natural fibers. For the treatment of bulk fibers, the condensation should also be controlled in order to retain a small molecular size of monomers or oligomers to diffuse into the cell walls. The condensation rate of silanols is controllable by adjusting the pH of the hydrolysis system. An acid pH environment is usually preferable to accelerate the hydrolysis rate of silanes but slows down the condensation rate of silanols.

3 - Adsorption (Figure 11c): The reactive silanol monomers or oligomers are physically adsorbed to hydroxyl groups of natural fibers by hydrogen bonds on the fiber surfaces (surface coating) and/or in the cell walls (cell wall bulking), which depends on the molecular size of silanol monomers/oligomers formed. The free silanols also adsorb and react with each other thereby forming a rigid polysiloxane structures linked with a stable – Si – O – Si – bond.

4 - Grafting (Figure 11d): Under heating conditions, the hydrogen bonds between the silanols and the hydroxyl groups of fibers can be converted into the covalent – Si – O – C – bonds and liberating water. The residual silanol groups in the fibers will further condense with each other. The bonds of – Si – O – C – may not be stable towards hydrolysis; however, this bond is reversible when the water is removed when raising temperature.

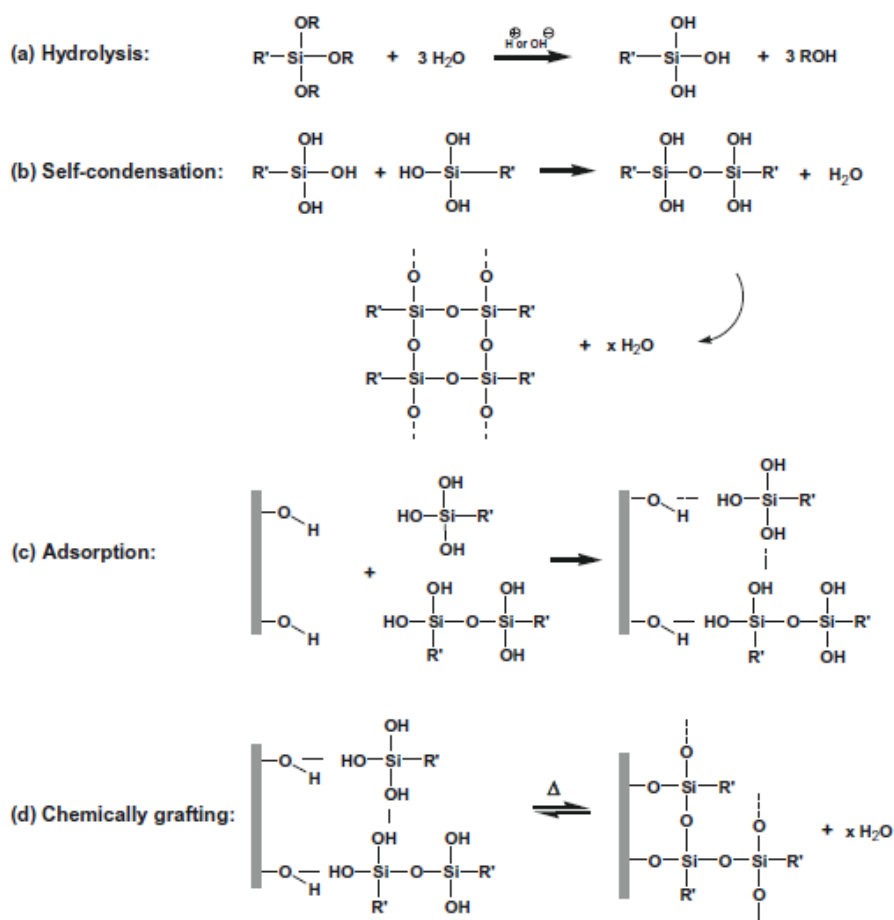


Figure 11 – Interaction of silane with natural fibers by hydrolysis process

Source: XIE, Y. et al. (2010)

Silanes have been shown to be effective in improving the interfacial properties of polymer composites with natural fibers (CULLER; ISHIDA; KOENIG, 1986; GHATGE; KHISTI, 1989; COUTINHO et al., 1997; GONZALEZ et al., 1997). An example is the treatment of the fiber with toluene diisocyanate (TDI) and vinyl triethoxy silane (SREEKALA et al., 2000) It has been reported in the literature (WEYENBERG et al., 2003) that treatment with 1.0% solution of 3-amino propyl trimethoxy silane in a 50/50 by volume of water for 2 h and acetone was responsible for modifying the surface of flax. Rong et al. (2001) soaked sisal fibers in a 2.0% solution of aminosilane in 95% ethanol for 5 minutes in a pH range of 4.5 to 5.5, followed by drying for 30 minutes with air for, according to the authors, hydrolyzing the coupling agent.

3.5.3 Acetylation

This process is characterized by the insertion of a functional acetyl (CH_3COO^-) grouping in an organic compound. Acetylation of natural fibers is a well-known esterification method that causes plasticization thereof. The reaction with acetic anhydride involves the formation of acetic acid (CH_3COOH), which needs to be removed from the lignocellulosic material before the fiber is employed (Scheme 2). The chemical modification with acetic anhydride replaces the hydroxyl groups of the cell wall by acetyl groups of the polymer, modifying their properties and making them hydrophobic.

This treatment is able to reduce the hygroscopic nature of natural fibers and increase the dimensional stability of the composites. Moreover, it has already been used for surface treatment of cellulosic fibers (PAUL; JOSEPH; THOMAS, 1997; HILL et al., 1998; SREEKALA; THOMAS, 2003). Acetylation of sisal fibers by immersion in 5.0 and 10.0% wt. NaOH solution in 1 hour at 30 °C was reported (MISHRA et al., 2003). Then, the fiber was soaked in glacial acetic acid under the same conditions of time and temperature, decanted and immersed in acetic anhydride containing one drop of concentrated H_2SO_4 for 5 minutes. In another study (NAIR; THOMAS; GROENINCKX, 2001), sisal fibers were treated in 18.0% wt. NaOH solution, followed by immersion in acetic acid and finally acetic anhydride, containing two drops of concentrated H_2SO_4 for 1

h. The treated surface became rougher, with a number of voids that allow better mechanical interaction with a matrix of polystyrene (PS).

Scheme 2:



3.6 NATURAL FIBERS / POLYAMIDE COMPOSITES

The shortcomings associated with lignocellulosic natural fibers must be solved to be applied in polymer composites. The biggest concern is their hydrophilic nature caused by strongly polarized hydroxyl groups, which provides its swelling and, ultimately, rotting by microbiological agents such as fungi. This hydrophilicity confers incompatibility with hydrophobic thermoplastic polymers such as polyolefins, causing poor miscibility (JOHN; ANANDJIWALA, 2008). A possible solution to improve interaction polymer-fiber is the use of coupling agents and adhesion promoters (KALIA; KAITH; KAUR, 2009).

In the case of polyamides, the compatibility is not a significant problem due to its low hydrophobicity. The biggest challenge in these composites is to use polyamide 6.6 as the polymer matrix in composites with treated vegetable fibers, while maintaining the thermal stability of cellulosic filler. The processing temperature in this case is around 280-300 °C, so the physical-chemical treatments performed on the fiber aim at maximizing their thermal stability. In fact, untreated cellulosic fibers do not support such temperatures and are susceptible to weight loss and, consequently, lead to the deterioration of the mechanical and thermal properties of the manufactured composite.

In one of the few studies described in the literature (ARCAYA et al., 2009), it was possible to obtain PA 6.6 composites with different types of cellulosic fibers, including wood fiber and jute. The thermal stability properties of the fibers after treatment were analyzed by thermogravimetry, indicating that after proper treatments, the fibers had very little weight loss temperature up to 300 °C. The results of the mechanical properties of the composite PA 6.6 / cellulosic fiber

also showed that the tensile and flexural modulus have increased significantly, which can be seen in Figures 12 and 13.

As shown in Figure 12, below T_g , flexural modulus increased with increasing content of wood fiber. According to the study, this is a consequence of the high polarity of the polyamide matrix when compared to other matrices, especially polyolefin. Still analyzing Figure 11, it can be seen an increase in modulus at 23 °C, while a decrease in flexural stiffness that can be observed with 25 to 35% of wood fiber incorporated. This can be explained due to insufficient coating of the fiber by the matrix. Other effects such as poor fiber dispersion in the matrix may also be responsible for the decrease in property.

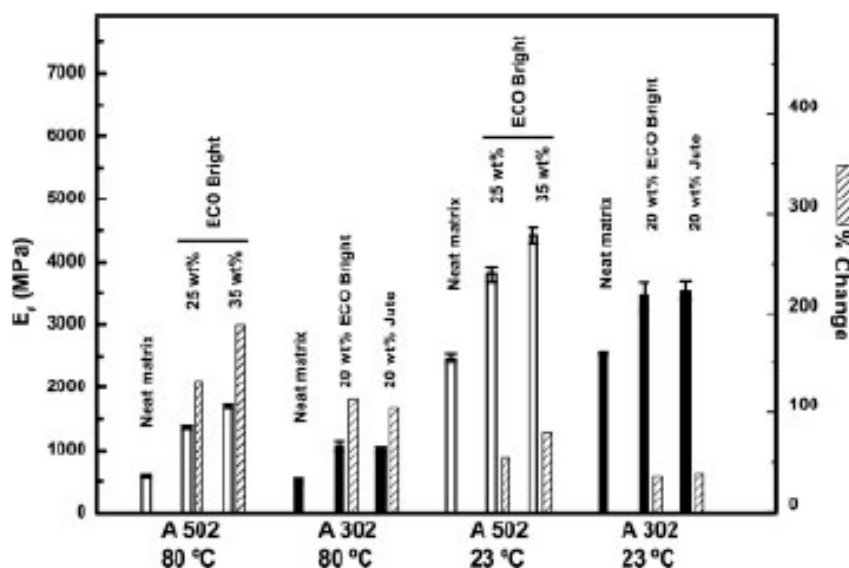


Figure 12: Flexural modulus above and below the T_g of PA 6.6 composites with natural fibers (A502 - suitable polymer for extrusion; A302 - suitable polymer for injection and extrusion)

Source: ARCAYA, P.A. et al. (2009)

Figures 12 and 13 show similar results for modulus and flexural strength at 20% of jute or wood fiber in the composite. Mechanically, no significant differences were found between the reinforcing effect of the two fibers, which can be explained by the reduction in aspect ratio (ratio length / diameter) induced by high shear forces during the mixing process fibers. When these tests were performed at 80 °C (above T_g) both the resistance and the flexural modulus

decreased by about 1/4. In this case, the reinforcing effect in terms of resistance becomes more pronounced than below T_g . The strength and modulus of the composites PA 6.6 with wood fiber (25%) almost doubled compared to the same properties tested at temperatures below T_g .

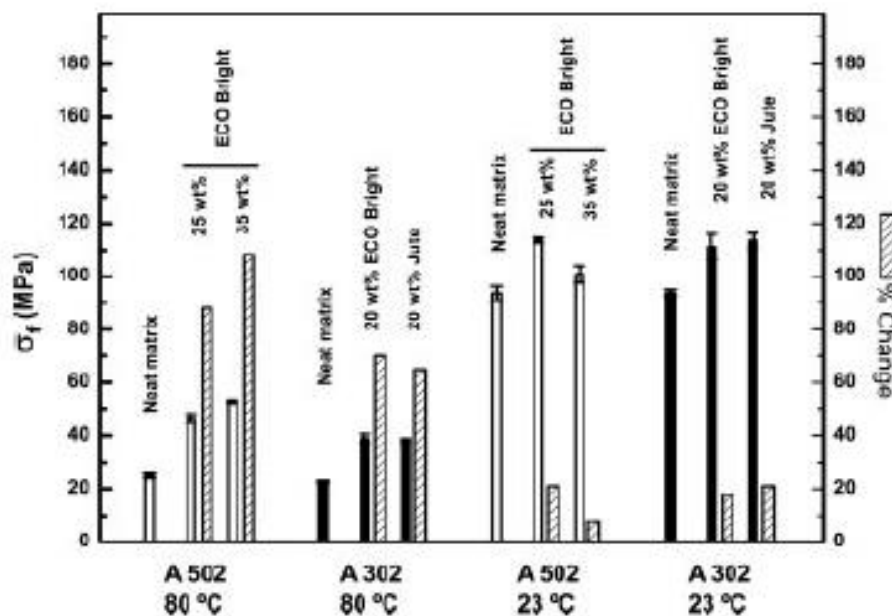


Figure 13: Flexural strength above and below the T_g of PA 6.6 composites with natural fibers (A502 - suitable polymer for extrusion; A302 - suitable polymer for injection and extrusion)

Source: ARCAYA, P.A. et al. (2009)

In another study (SANTOS et al., 2007), PA 6 composites with curauá fibers were processed in a twin-screw extruder and their mechanical properties (tension and bending) were evaluated. Table 7 shows the samples regarding the content of PA 6, (short and long) fibers and treatment to which the fibers were subjected.

Table 7: Composition of processed composites in double-screw extruder

| Sample | PA6 (%) | Short fiber | Long fiber | Treatment |
|--------|---------|-------------|------------|-----------------------|
| APV1 | 100 | 0 | 0 | - |
| APV2* | 80 | 20 | 0 | - |
| APV3 | 80 | 20 | 0 | - |
| APV4 | 80 | 20 | 0 | Plasma N ₂ |
| APV5 | 80 | 20 | 0 | NaOH ½ h |
| APV6 | 80 | 0 | 20 | - |

Source: SANTOS, P.A. et al. (2007)

Analyzing the results of Tables 7 and 8, it can be seen that composites processed with and without drying of the pure materials (APV2 and APV3) show similar results in terms of tensile and impact. According to the authors, this means that, contrary to what is expected for pure polyamides, drying the material before extrusion has no influence on the mechanical properties of the composite. In comparison with the material without load (APV1), the samples showed a large increase in tension and flexural modules while, on the other hand, the elongation decreased greatly, which is a classical feature due to the high rigidity of the fibers and their low elongation at break. The samples treated with N₂ plasma or soda (APV4 and APV5) showed better mechanical properties, or at least similar to those samples containing untreated fibers, probably due to a better fiber-matrix adhesion. However, chemical treatment produces waste that must be neutralized before disposal.

Table 8: Composition of processed composites in double-screw extruder

| Sample | Tensile Tests | | | Flexural Tests | |
|--------|-----------------------|-----------|------------------|-----------------------|-----------|
| | σ^{\max} (MPa) | E (Gpa) | ϵ_b (%) | σ^{\max} (Mpa) | E (Gpa) |
| APV1 | 68 ± 1 | 1.4 ± 0.1 | 30 ± 12 | 100 ± 1 | 2.4 ± 0.1 |
| APV2 | 63 ± 9 | 3.6 ± 0.4 | 2.7 ± 0.8 | 113 ± 6 | 3.1 ± 0.2 |
| APV3 | 67 ± 1 | 3.8 ± 0.7 | 2.9 ± 0.1 | 109 ± 4 | 3.4 ± 0.1 |
| APV4 | 71 ± 2 | 4.6 ± 0.5 | 3.2 ± 0.5 | 110 ± 6 | 3.5 ± 0.2 |
| APV5 | 87 ± 5 | 5.4 ± 0.4 | 2.9 ± 0.5 | 121 ± 5 | 4.3 ± 0.3 |
| APV6 | 73 ± 3 | 4.3 ± 0.4 | 2.6 ± 0.2 | 108 ± 4 | 3.7 ± 0.3 |

Source: SANTOS, P.A. et al. (2007)

On the sample APV6, the presence of long fibers gives an increase in both mechanical properties compared with the pure samples (APV1), which can be explained by the high aspect ratio. According to the authors, it can be concluded that the addition of curauá to PA 6 causes a significant reinforcing effect, which is also mentioned in the literature for other polymers (FRISK; SCHWENDEMANN, 2004; SPINACÉ; FERMOSELLI; DE PAOLI, 2004).

SEM micrographs of the samples APV2 and APV3 after cryogenic fracture parallel and perpendicular to the flow direction were analyzed to study the adhesion between the fibers and the polymeric matrix (Figure 14). In both cases, there are no empty space between the fibers and the polymer (highlighted in circle), which is an evidence of good adhesion. This clearly

indicates that the drying of the fibers is not required and the moisture ends up aiding adherence in these composites. The moisture present in the fibers can cause partial hydrolysis in PA 6 at high temperatures, as shown in Scheme 3 to form terminal carboxylic acid. These terminals can react with OH groups of cellulose to form ester bridges.

Scheme 3

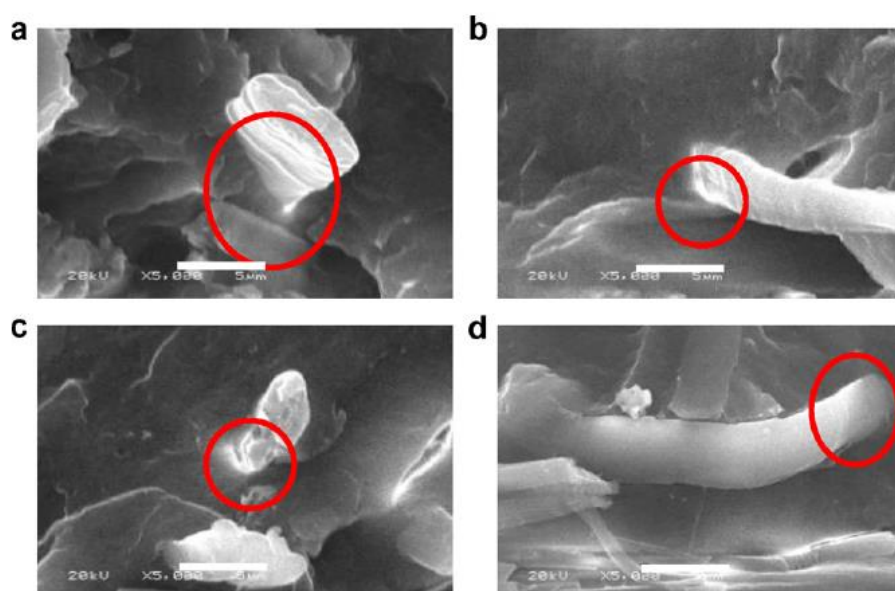


Figure 14: SEM micrographs: (a) APV2 across flow, (b) APV2 along flow, (c) APV3 across flow, and (d) APV3 along flow direction.

Source: SANTOS, P.A. et al. (2007)

In another study (TAJVIDI; FEIZMAND, 2009), composites of PA 6 with cellulosic fibers from wood were prepared by injection molding. The effect of temperature on the mechanical properties of the composite fiber with 25 wt. % was compared to pure polyamide. The curves relating the deflection with the applied load are shown in Figure 15. The slopes of the curves become smaller at higher temperatures, indicating less stiffness at higher temperatures. At all

the temperatures studied, the composite presents a higher slope, indicating improvement of mechanical properties of polyamide.

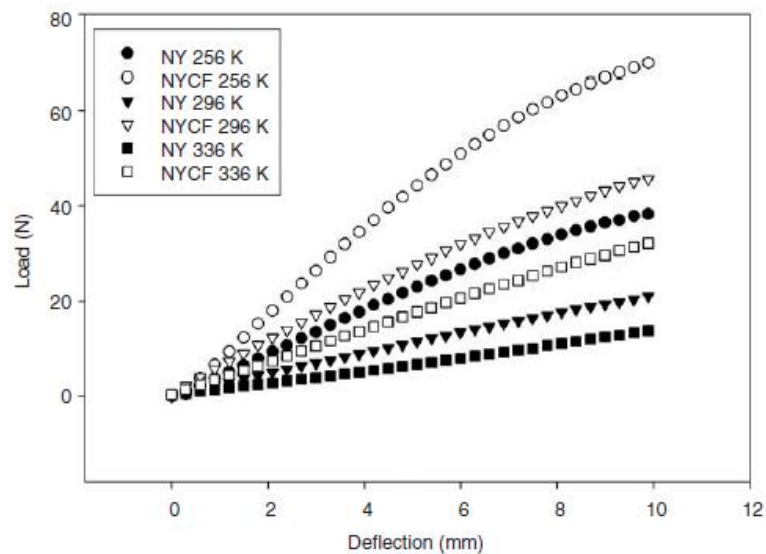


Figure 15: Flexural load–deflection curves of pure nylon and their composites at various temperatures

Source: TAJVIDI, M.; FEIZMAND, M. (2009)

The thermo-dynamic-mechanical behavior of these samples was also studied. Figure 16 shows that the loss factor, or damping factor, ($\tan\delta$) is about the same for both samples at temperatures below the T_g . However, the values of $\tan\delta$ of the composite are markedly inferior above the T_g when the material is in the rubbery state. In case of the behavior of viscoelastic materials, $\tan\delta$ is a better indicator to be considered in relation to the storage and loss moduli, since its value is independent of the sample geometry. The presence of 25% cellulose reduced considerably the damping, indicating that the composite is more elastic than pure polyamide at elevated temperatures.

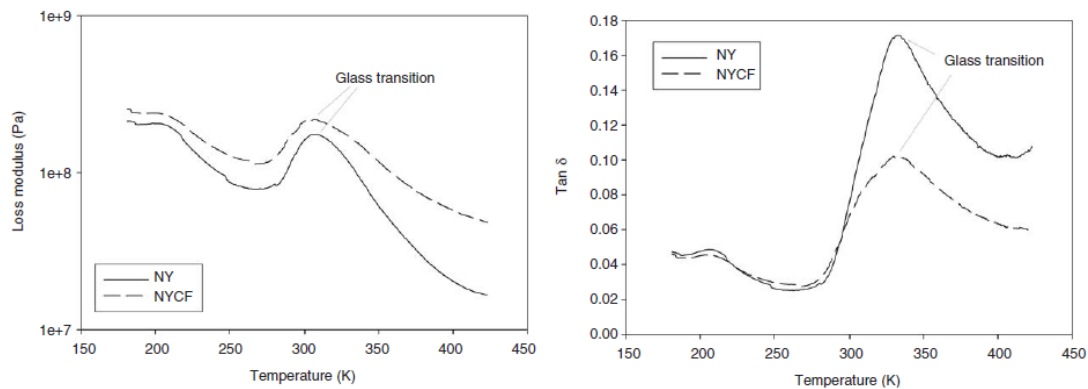


Figure 16: Loss modulus spectra of the formulations (top) and the mechanical loss factor ($\tan\delta$) (bottom)

Source: TAJVIDI, M.; FEIZMAND, M. (2009)

In another study (ARAÚJO; ADAMO; DE PAOLI, 2011), the dispersion of curauá fibers coated with polyaniline in polyamide-6 by extrusion was studied, to produce a material with a simultaneous improvement in mechanical and electrical properties. The aim was to use this material as an anti-static engineering plastic.

Conductivity measurements were made to find the percolation threshold of PANi in the surface of fibers. The average values obtained are shown in Table 9. The conductivity of the curauá fibers increase two orders of magnitude with only 1% wt. of PANi and with 12% reaches values very close to the conductivity of pure PANi. Above 17% the conductivity decreases due to the agglomeration of PANi particles, precluding the formation of a percolation path and hindering charge transport. A plot of the log conductivity vs. PANi content, Figure 17, shows that the percolation threshold of the modified curauá fibers was reached with 1% wt. of PANi.

Table 9: Conductivity values for different PANi contents in the fibers

| Sample | σ (S cm ⁻¹) | $\Delta\sigma^a$ (S cm ⁻¹) |
|------------|--------------------------------|--|
| Pure CF | 6.4×10^{-9} | 5.9×10^{-9} |
| CF-1%PANi | 2.1×10^{-7} | 0.7×10^{-7} |
| CF-2%PANi | 5.2×10^{-3} | 4.0×10^{-3} |
| CF-4%PANi | 2.2×10^{-1} | 0.7×10^{-1} |
| CF-12%PANi | 1.6 | 1.7 |
| CF-17%PANi | 4.2 | 4.6 |
| CF-30%PANi | 1.2 | 0.9 |
| CF-40%PANi | 0.4 | 0.1 |

^a Standard deviation.

Source: ARAÚJO, J.R.; ADAMO, C.B.; DE PAOLI, M.A. (2011)

The mechanical properties of the composites are compared in Figure 18. Dispersion of fibers in PA 6 is highly dependent on the processing method, as evidenced by the deviation bars in the figures. Results show that the composite of PA 6 reinforced with curauá fiber coated with PANi, PA 6/CF-PANi, presented a better capacity of matrix-fiber tension transference (reinforcement effect) than the composite with pure curauá fiber. This is probably due to the hydrophobicity of the three components of the composite; PA 6, curauá fiber and polyaniline.

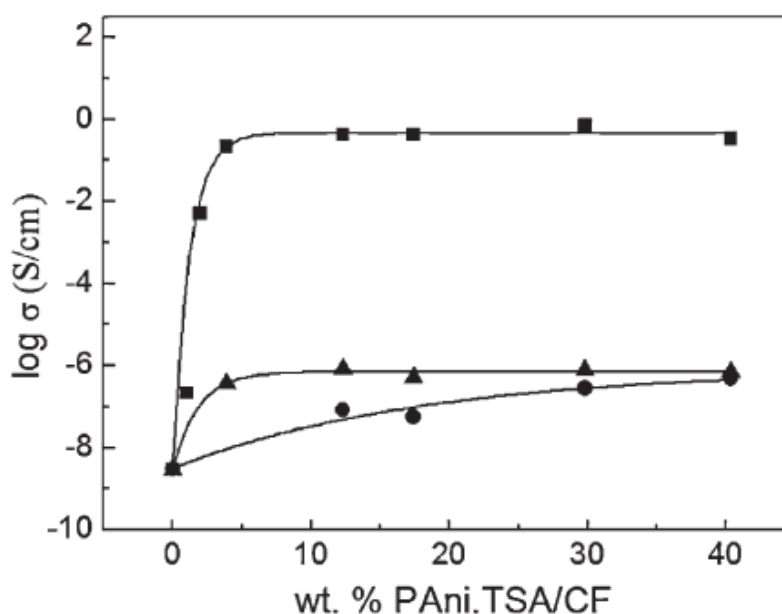


Figure 17: Variation of the log of conductivity with PANi content in the composites, where (▲) 85PA6/15CFPANi, (●) 90PA6/10CFPANi and (■) CFPANi [67]

Source: ARAÚJO, J.R.; ADAMO, C.B.; DE PAOLI, M.A. (2011)

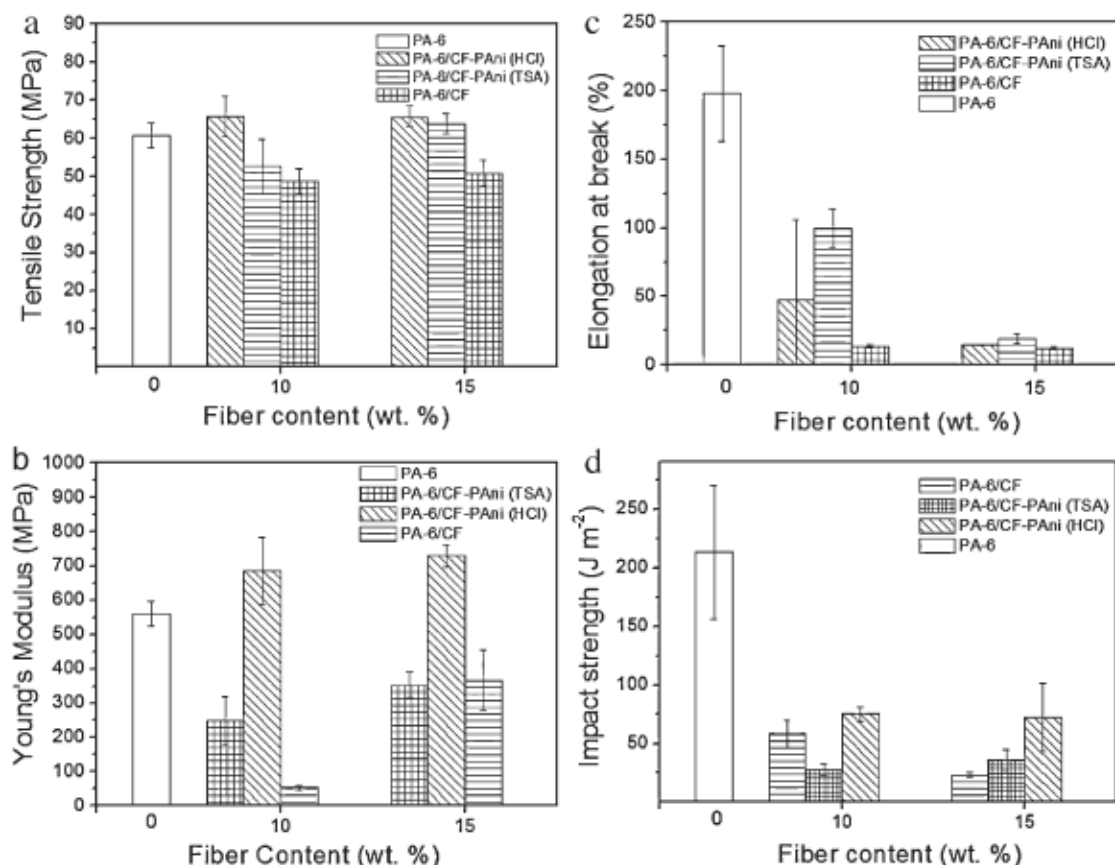


Figure 18: Mechanical properties of PA 6/CF and composites PA 6/CF and PA 6/CF-PAni with various fiber contents and two dopants (TSA – p-toluene sulfonic acid and HCl – hydrochloric acid): (a) tensile strength; (b) Young's modulus; (c) elongation at break; and (d) impact strength

Source: ARAÚJO, J.R.; ADAMO, C.B.; DE PAOLI, M.A. (2011)

3.7 APPLICATION OF NATURAL FIBERS ON AUTOMOTIVE INDUSTRY

Currently, about 50% of the vehicles by volume are made of polymeric materials. According to the American Plastics Council, vehicles contain approximately 110 kg of plastics, *ie*, somewhere around 12% of their weight (GEHM, 2010). As the use of plastics in cars is now well established, the use of sustainable plastics has become a very important target. Automakers are turning their efforts to manufacture automobiles from renewable materials, safe for its occupants, passersby and the environment. Furthermore, it has been suggested that bio-derived plastics could represent a reduction in oil consumption while increasing recycling capacity (HOUBERY; HOUSTON, 2006).

The use of natural fibers as reinforcing materials in the automobile industry is not new. In the 60s, coconut fibers were already used for the manufacture of seats and composites of polypropylene with wood dust, compression molded, were applied as substrates for the interior of automobiles (CLEMONS, 2002). Plant fibers are often used inside cars and truck cabs. They are also used extensively in thermo-acoustic insulation. Such insulating materials, especially cotton recycled fibers, have a high content of approximately 80% by weight. To manufacture some parts of trucks, jute fibers from waste coffee sacks are employed in composites with polypropylene. Another well-established field is the use of coconut fibers with natural latex in seat cushions. For this, the ability of the fiber to absorb large amounts of moisture leads to greater comfort, which does not happen with synthetic materials (SCHUH, 2010).

However, there has been a preference for traditional materials such as glass fibers and mineral fillers as vegetable fibers are characterized by having a high void volume (low density), low thermal stability and high moisture absorption. The processing temperatures, even for plastics with low melting temperature, are very high in order to integrate natural fibers without degrading them (CLEMONS, 2002). However, the natural fibers have the potential to lighten the vehicle by about 40% compared with the glass fiber. The energy used to cultivate, harvest, and prepare natural fibers has been estimated at 4 GJ / ton, compared to 30 GJ / ton to prepare fiberglass. Another relevant aspect is the release of gases into the atmosphere in the manufacturing process of the glass fibers. CO₂, along with NO_x and SO_x, represent high health hazard when released (MARSH, 2003).

Generally, the processing of composites based on natural fibers is similar to the production of composites with glass fibers, which are widely used in the automotive industry. During processing, the temperature should generally not exceed 200 °C and the exposure time of the material to high temperatures should not be too long, in order to prevent the destruction of the fibers. The most common processing technologies of composite with natural fibers are the resin transfer molding, vacuum injection molding, structural reaction injection

molding and compression. During these various procedures are formed materials with varied properties as a result of different levels of distribution and deterioration of fibers. Influence of fiber length on the mechanical properties of the composites can be explained by the fact that the long fibers tend to bend and become entangled during processing. This reduction of effective fiber length below a certain critical length results in loss of mechanical properties (BOGOEVA-GACEVA et al., 2007).

In 1996 the total fiber consumption in automotive industry did not exceed 4 Kt while in 1999, this number became five times greater according to the European automotive industry. This value includes flax, jute, hemp and kenaf, which are employed in the production of composites. Approximately 1.6 Kt of linen were also used in 1999, as reported by suppliers. Moreover, at that time, they projected that in the near future, 15-20 Kton linen would be used. German and Austrian automotive industries employed 8.5 to 9 Kt of flax fibers in the years 2000 and 2001. The introduction of each new car model increases demand in a range from 0.5 to 3 Kt per year.

The automotive industry provides a list of benefits in the application of natural fibers, which have justified the application in this segment:

- Low density, which can lighten the car in about 10 - 30%;
- Satisfactory mechanical and acoustic properties;
- High stability and low fragmentation in case of accidents;
- Favorable ecological balance for the production of parts;
- Favorable ecological balance during operation of the vehicle due to weight reduction;
- No release of toxic components.

Table 8 lists the manufacturers that use natural fibers in its production line with parts manufactured and their models (BOS, 2004).

Table 8: Applications of natural fibers in automakers and their models

| Manufacturer | Model | Main Applications |
|---------------------|---|---------------------------------------|
| Audi | A3, A4, A4 Avant, A6, A8, Roadster, Coupe | Rear seats, side panels and rear door |
| BMW | 3, 5, 7 series and others | Door panels, rear seat |
| Daimler/Crysler | A, C, E and S series | Door panels, windshield, dashboard |
| Ford | Mondeo CD 162, Focus | Door panels |
| Opel | Astra, Vectra, Zafira | Door panels and instrument |
| Rover | 2000 and others | Rear panel |
| SEAT | All | Door panels and rear seats |
| Volkswagen | Golf A4, Passat, Variant, Bora | Door panels and rear seats |

Source: BOS, H. (2004)

4 MATERIALS AND METHODS

4.1 MATERIALS

- Polymers: **Polypropylene, Polyamides 6 and 6.6**;

The polymers used to prepare composites with the fibers were:

- Polypropylene – grade 550, provided by Braskem S.A.
- Polyamide 6 – grade Technyl C 206 (melting temperature: 222 °C, density: 1.14 g/cm³, provided by Rhodia S.A.
- Polyamide 6.6 - grade Technyl A 218 (melting temperature: 255-265 °C, density: 1.14 g/cm³, provided by Rhodia S.A.
- Natural Fibers: **Curauá, jute and flax**;

The fibers and cellulose used in this work were:

Jute and Curauá: provided by Pematec Triangel do Brasil – Brazilian industry; milled in knife mills before chemical treatments. Cellulose I-type of crystal

Flax: provided by Vivabras Industria e Comercio LTDA. – Brazilian industry; milled in knife mills before chemical treatments. Cellulose I-type of crystal

Avicel: commercial microcrystalline cellulose, obtained after an acid hydrolysis of native cellulose. It is highly crystalline, with a low molar mass. Cellulose crystalline structure as for native cellulose (cellulose I).

Lyocell: commercial cellulose fiber obtained after dissolution in *N*-methylmorpholine *N*-oxide/water and regenerated. Highly crystalline and oriented with cellulose II type crystals.

Viscose: commercial cellulose fiber obtained after derivatisation, dissolution in NaOH and regeneration. Moderately crystalline with cellulose II type crystals.

Cotton: commercial native, moderately crystalline, high molar mass, cellulose I-type of crystal.

- Reagents:

3-Aminopropyl-trimethoxy silane; Glycidyloxipropyl-trimethoxy silane; Silicon tetrachloride; Vinyl-trimethoxy silane – Purchased from Vetec Quimica S.A. – used after dissolution in methanol.

Sodium Hydroxide – Proceeding: Vetec Quimica S.A. – used for preparation of alkaline solution in water.

Acetic anhydride; Glacial acetic acid; Methanol; Lithium chloride – Purchased from Vetec Quimica S.A. – used as received.

N-butylbenzenesulfonamide (Ketjenflex 8®) – Purchased from Chlarus Comercio, Imp e Exp Ltda – used as received.

4.2 EQUIPMENTS

- ◆ **Dynamic Mechanical Thermal Analyzer** - DMA Q800, TA Instruments (USA);
- ◆ **Thermogravimetric Analyzer** - Q500, TA Instruments (USA);
- ◆ **Vacuum bomb** - ATB-Loher ABF/48-7RΩ, Flender;
- ◆ **Differential Scanning Calorimeter** - DSC Q1000, TA Instruments (USA);
- ◆ **X-Ray Diffractometer** - Rigaku, Miniflex model;
- ◆ **FTIR Spectra Analysis** - Excalibur 3100 FT-IR;
- ◆ **Extruder** - MiniLab II Micro Compounder, Haake;
- ◆ **Mechanical Analysis** – Instron, model 5569;
- ◆ **Scanning Electron Microscope (SEM)** - JEOL JSM, model 5610LV and sputter DENTON VACUUM DESK II;
- ◆ **Optical Microscope (OM)** - Olympus, model 5210, coupled to camera;
- ◆ **Carver Press with heating** - Carver model B & C, NS 34000-623, Carver Laboratory Press;
- ◆ **Rheometer** - AR (Advanced Rheometer) 2000 – TA Instruments.

4.3 ALKALINE TREATMENT OF NATURAL FIBERS

At first, fibers were treated in a grinding mill with knives. The aim of this procedure is to reduce the particle size of the fibers. Subsequently, the size separation was carried out through a sieve with of 200 mesh (inch or 75 micron). Two types of alkaline treatments were employed:

4.3.1 Alkaline treatment of natural fibers at room pressure (RP-alkaline treatment)

Hemicellulose and part of lignin were separated of cellulose by three successive alkali treatments. For each treatment, a 5.0 wt. % sodium hydroxide solution was put in contact with the fibers at 80 °C during 1 h, at room pressure. These conditions were employed to avoid loss of molar mass due the possibility of cellulose be modified by soda in higher concentrations. Then, the fibers were washed with deionized water to remove the excess of NaOH. Finally, fibers were dried in vacuum at 80 °C overnight to constant weight for moisture removal (GRAFOVA et al., 2011).

4.3.2 Alkaline treatment of natural fibers at high pressure (HP-alkaline treatment)

The treatment with alkaline solution carried out for the fibers is time consuming and it should be optimized. Therefore, it was decided to perform the alkaline treatment in an autoclave to shorten this procedure.

Experiment conditions: autoclave works at temperature close to 120 °C and pressure of 1.5 MPa. Fibers were soaked in 5.0% wt. of NaOH solution. Each 15 min, a sample of fibers was separated, neutralized with 10.0% wt. of HCl until pH = 7.0, filtered, washed with distilled water and dried to process the characterizations. Moreover, in this time interval, the alkaline solution was substituted with a new amount of NaOH 5.0%. The intervals of time studied were 15, 30, 45 and 60 min.

After comparison of both techniques, according to results, it was decided to perform high-pressure alkaline treatments by 30 minutes (for surface modifications, followed by acetylation/silanization) in composites with polyamide 6 and 6.6. To perform preliminary compoundings with polypropylene, fibers were alkaline-treated at room pressure, since the processing temperature is lower (200 °C).

4.4 SURFACE MODIFICATION OF NATURAL FIBERS

4.4.1 Acetylation and Treatment with Silane

In acetylation treatments, the mercerized fibers were dried for at 100 °C during 6 h. Subsequently, each fiber was placed in 100 ml of round flask and the appropriate amount of acetic anhydride was added, so as to ensure that all fibers were totally covered with the reagent. Afterwards, the fibers were placed at 120 °C for 120 min. The treated fibers were then extracted using acetone as a solvent, in order to remove any remaining unreacted reagent and acid by-products. Finally, fibers were dried in vacuum at 80 °C overnight to constant weight for moisture removal (TSERKI et al., 2005).

Regarding the silanization process, this was done as follows: in a round flask, fibers were soaked in a methanol solution with 2.0% of coupling agents, over a period of 5 minutes, at room temperature. The pH was maintained in a range between 4.5 and 5.5 and then the fibers were filtered and washed with distilled water and dried under vacuum at 80 °C to constant weight (RONG et al., 2001).

4.5 PROCESSING OF COMPOSITES PP, PA 6 AND 6.6/ NATURAL FIBERS BY MIXING IN MELT STATE

4.5.1 PP/Natural Fibers Composites

Polypropylene homopolymer HP 550K, supplied by Braskem, with a melt flow index of 3.5 g/10 min (230 °C / 2.16 kg), was used as matrix. Chemical

treatments on vegetal fibers were performed using a liquor ratio of 1:30. For the compounding of composites with commercial PP, fibers were dried in an oven (treated and untreated) at 80 °C overnight and mixed with the polymer in the proportion 90/10 wt. % in a mini-extruder twin-screw counter-rotating Haake Minilab at 180 °C for 15 minutes and speed rotation of 60 rpm.

4.5.2 PA 6/Natural Fibers Composites

Treated fibers (curauá, jute and flax), as well as different types of commercial cellulose were mixed to neat polyamide in a twin-screw microextruder in the counter-rotating mode at 230 or 240 °C and 50 rpm for 8 minutes, in order to investigate if the difference of processing temperature and, consequently, a possible degradation of the fibers, influences properties of composites prepared. Moreover, the fibers content of the composite were 10 %.

In order to establish the influence of other cellulose components of curauá, different types of cellulose were used to prepare composites with polyamide 6: avicel, lyocell, cotton and viscose.

Before processing experiments, fibers and polyamide 6 were put in an oven at 80 °C, overnight. The alkaline treated, acetylated and silanized fibers were mixed to neat polyamide in a Haake Internal mixer at 240 °C and 50 rpm for 8 minutes. The fiber content of the composite was 10% wt.

After processing, composites (with natural fibers and pure cellulose) were grinded and molded by compression using a Carver press (10 minutes, 240 °C). Some test bars can be seen in Figure 19:

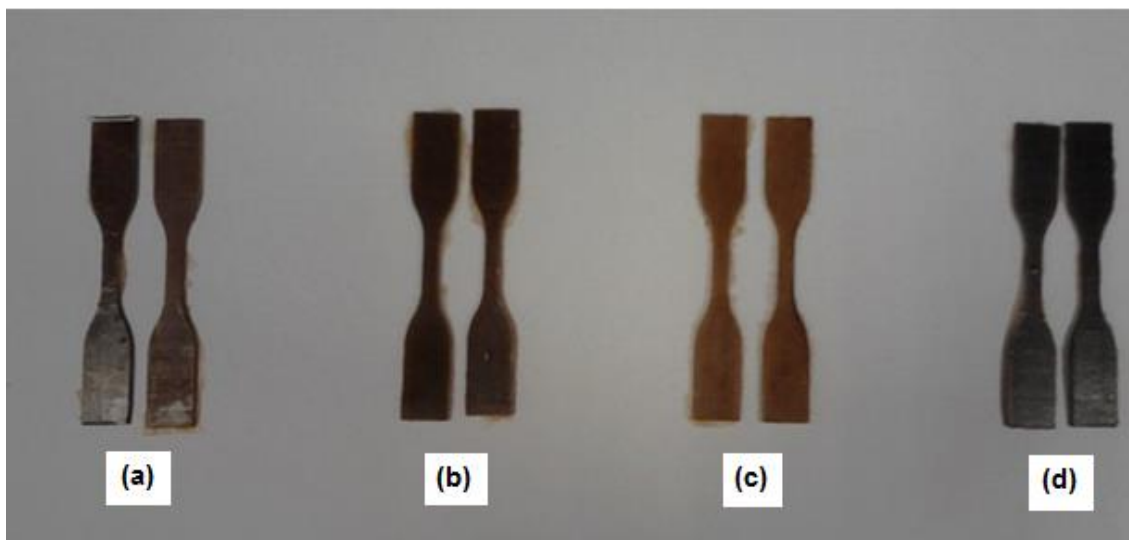


Figure 19: Test bars of processed composites: (a) PA 6/Avicel; (b) PA 6/Pretreated Curaua; (c) PA 6/Acetylated Curaua ; (d) PA 6/Silanized Curaua

4.5.3 PA 6.6/Natural Fibers Composites

4.5.3.1 Effect of plasticizers on PA 6.6: experimental design

Plasticizers can be used to decrease the melting temperature of polyamides. For polyamide, they are usually employed to modify some properties, as low temperature impact strength, toughness, fatigue life or decrease the glass transition temperature.

There is no plasticizer specifically used to decrease the melting temperature of PA 6 or PA 6.6. On the other hand, chloride metal salts are known to decrease the melting temperature of polyamide. For example, 4 wt. % LiCl can decrease the melting temperature of nylon 6.6 from 262 °C to 247 °C, while 10 wt. % LiCl can decrease the melting temperature of the same polymer to 227 °C, however, in both cases, decreasing also the mechanical properties (XU, 2008).

With the addition of LiCl, the torque increases significantly. With such high torque of matrix (3 wt. % LiCl/nylon 6.6), it is very difficult to add cellulose fibers because the addition of cellulose fibers can further increase the torque by 30%.

No more than 10% cellulose fibers can be added because of torque limitation of the extruder (XU, 2008).

So, according to a previous work (XU, 2008), N- butylbenzenesulfonamide (NBBSA), the most usually employed plasticizer, were used in combination with LiCl, looking for decreasing the melting temperature without loss of mechanical properties. It is known that the melting temperature of 3% LiCl / 3% NBBSA / nylon 6.6 is 251 °C.

Thus, about the experimental design proposed, the step of choosing the experimental plan involves considerations about the selection of the number of experiments and the number of samples or replicates. It is still questionable if there will be only first order effects or interactions and second-order effects may also occur. To determine the number of experiments, the equation below was used:

$$NE = L^{NV} + R \quad \text{Equation 1}$$

Where: L - number of levels (we chose 2 levels, - and +); NV - number of variables (LiCl and NBBSA concentrations) and R - replications on central point.

So, it was used 3 different concentrations of LiCl and NBBSA: 0 (-) ; 2.5 wt. % (0) and 5.0% (+) and 7 experiments were conducted with Minilab (Table 9). The response parameters chosen were melting temperature (measured by DSC), viscosity (directly detected by Haake Minilab) and elastic modulus (measured by DMA).

Table 9: Experimental Design of Experiments

| Experiment | % LiCl | % NBBSA |
|------------|--------|---------|
| 1 | - | - |
| 2 | - | + |
| 3 | + | - |
| 4 | + | + |
| 5 | 0 | 0 |
| 6 | 0 | 0 |
| 7 | 0 | 0 |

4.5.3.2 Experimental design of compounding PA 6.6 / natural fibers composites

With the best result of experimental design, 10 wt.% of treated fibers (alkaline treated + silanized with glycidyloxypropyl silane) were added into the plasticized polymer and unplasticized ones, in Haake Internal Mixer at 260 and 280 °C and 60 rpm for 2 minutes.

4.6 CHARACTERIZATION

4.6.1 Characterization of Chemically Modified Fibers

The fibers were characterized by X-ray diffraction (WAXS) to evaluate their crystallinity index. Samples were analyzed in powder form, where the diffractometer worked with a potential difference in the tube of 30 kV and electric current of 15 mA. The scan was in the range of 2θ from 2 to 40 °, with goniometer speed of 0.05 ° / min. The radiation used was $\text{CuK}\alpha$ with $\lambda = 1.5418 \text{ \AA}$. The crystallinity index was calculated according to Equation 2 (MORÁN et al., 2008):

$$I_c = \frac{(I_{(002)} - I_{(am)})}{(I_{(002)})} \times 100 \quad \text{Equation 2}$$

In which:

I_c – crystallinity index

$I_{(002)}$ – counter reading at peak intensity at 2θ angle close to 26° , representing crystalline material

$I_{(am)}$ – counter reading at peak intensity at 2θ angle close to 26° , representing amorphous material in cellulosic fibers

For thermal behavior of natural fibers, thermogravimetric analysis (TGA) was employed. This technique provides data on the thermal stability of materials. Using Q500, TA Instruments (USA), samples were heated by two ways:

- From room temperature to 700 °C under air and under nitrogen atmosphere at a heating rate of 10 °C/min to determine the temperatures of degradation $T_{0.05}$ (temperature with 5 % mass loss after the initial loss of moisture) and T_{max} (peak in DTG of maximum intensity) as well as ash content.
- In isothermal mode, which all treated fibers with the same amount (5.0 mg) were heated at 100 °C/min until reaching two temperatures desired in each case (270 and 290 °C). The isothermal time under each temperature was fixed at 15 minutes. These measurements were performed under two different atmospheres (air and nitrogen). Time before degradation, as well as residues after isothermal time, was measured.

The Fourier transform infrared spectroscopy (FTIR-ATR) was employed to analyze qualitatively the absorption bands related to the characteristic groups of chemical bonds, using Excalibur 3100 FT-IR equipment. The fibers (treated and untreated) spectra were obtained in the range of 4000 - 600 cm^{-1} at a resolution of 4 cm^{-1} .

4.6.2 Characterization of Composites

4.6.2.1 Mechanical properties of PP / natural fibers composites by dynamic mechanical analysis (DMA)

After processing, films of the composites were prepared by compression molding at 200 °C for 15 minutes and characterized by DMA analysis in order to evaluate the mechanical properties such as storage modulus (E') and loss (E'') as well as the glass transition temperature (T_g) and damping factor ($\tan \delta$).

The thermal dynamic mechanical analysis (DMA) was performed using TA Q800 with a heating rate of 3 °C/min., with a frequency of 1 Hz and strain of 0.1% in the range of -40 to 150 °C.

4.6.2.2 Establishment of methods for estimating degradation of commercial cellulose and treated curauá fibers after processing with PA 6

The objective was to quantitatively assess degradation by three complementary methods:

- intensity of colour
- change of molar mass of the cellulose chains
- By identification of degradation products

4.6.2.2.1 *Colorimetry*

Two techniques were used:

- a fast method by eye where darkness is estimated from a scale from zero to five
- a slower method where colour is measured by a colorimeter

Colorimeter – Separates components RGB (red, green and blue) of light and uses filters that simulates response of eyes giving numerical results in a standard model of colors L^*a^*b , which:

- L – can vary from 0 (black) to 100 (white); For degradation analysis, it is the most relevant parameter;
- a – can vary from -128 (green) to 128 (red);
- b – can vary from -128 (blue) to 128 (yellow);

4.6.2.2.2 *Infrared spectroscopy*

Identification and quantification of degradation products by analysis of absorption bands of polyamide and their composites with fibers. Spectra of composites were obtained in the range of $4000 - 600 \text{ cm}^{-1}$ at a resolution of 4 cm^{-1} .

4.6.2.2.3 Viscosimetry

Measurement of degree of polymerization by viscosimetry. It was only applied to commercial cellulose samples.

Methodology:

Cellulose is separated from polyamide by dissolution of PA in formic acid 90 %. Cellulose is dissolved in cuen (copper-ethylenodiamine solution) and the molar mass is estimated from the measurement of the flow time of a solution with known concentration in a tube (DIN 54270-2 standard).

4.6.2.3 Mechanical Properties

Tests were performed following the ASTM D638-5 standard. Deformation of the specimens was fixed at 1.0 mm/min. Dimensions of test bars for tension analysis were 6.0 x 3.0 x 1.2 mm (length x width x thickness). For each sample, seven specimens were evaluated for reproducibility of the results and standard deviations were calculated. The tensile strength, modulus and tensile strength were measured using an Instron testing machine.

For composites with PA 6.6, impact tests were also performed. They were carried out on in a Charpy-type impact machine. The specimens were tested under notched condition at room temperature. At least five impact specimens were used in the tests, and the average value was taken for each composite.

4.6.2.4 Characterization of PA 6.6 – natural fibers composites

Using differential scanning calorimetry (DSC), melting temperature (T_m), crystallization temperature (T_c) and enthalpy of fusion (ΔH_m) of the composites were measured. Using the melting enthalpy, the calculation is performed to obtain the degree of crystallinity (X_c) of polymers (Equation 3) (KLATA et al., 2004).

$$X_c = (\Delta H_m^a / \Delta H_m^{100}) \times 100 \quad \text{Equation 3}$$

Where:

X_c : degree of crystallinity (%);

ΔH_m^a : melt heating of sample (J/g);

ΔH_m^{100} : melt heating of 100% crystalline polyamide (301 J/g) [77].

Samples were analyzed in powder form, which will be heated to 30 °C to 300 °C with a heating rate of 10 °C/min and then cooled to 30 °C at a rate of 10 °C/min under nitrogen flow to then be heated again. Another technique that evaluates the thermal properties, and is also used in the characterization of polypropylenes, is the thermogravimetric analysis (TGA). This technique provides data on the thermal stability of materials. Samples are also analyzed as a powder and heated from ambient temperature to 700 °C in inert atmosphere at a heating rate of 10 °C/min to determine the temperatures of degradation $T_{0,05}$ (5.0 wt. % of degradation) and T_{max} and ash content (GRAFOVA et al., 2011).

Scanning electron microscopy (SEM) was used to observe the incorporation of the polyamide fiber and its interface by look at the morphology of the cross section of the sample obtained after extrusion. Samples were cryofractured using liquid nitrogen and then coated with a thin layer of gold prior to analysis. Infra-red spectroscopy of composites was also performed, in the same way as described in section 4.6.2.2.2.

5 - RESULTS AND DISCUSSION

5.1 INFLUENCE OF SUCCESSIVE ROOM PRESSURE ALKALINE TREATMENTS ON NATURAL FIBERS AND ON MECHANICAL PROPERTIES OF COMPOSITES WITH POLYPROPYLENE

5.1.1 Thermogravimetric analysis of of room pressure alkaline treated natural fibers

Results of thermogravimetric analysis of the fibers before and after the chemical treatments are presented in Tables 10 – 12 and Figures 20 – 22. It is observed that for the curauá fibers the thermal resistance is greatly improved after the first treatment, with an increase of 45 °C in degradation temperature between the untreated and treated fibers, which can be attributed to the removal of hemicellulose and other components of low molecular weight, such as pectin and waxes, as evidenced by the disappearance of the characteristic shoulder at 275 °C in DTG curve (Figure 1b) (POLETTTO et al., 2011) Similar behavior was observed for flax fibers. However, the increasing of thermal resistance only can be noted after the second alkaline treatment. No thermal improvement was detected in jute fibers and can be explained in terms of larger amount of lignin, which works as a strong adhesion component between the fibers, which difficults the penetration of alkaline solution (BOGOEVA-GACEVA et al., 2007; SILVA; AQUINO, 2007).

Furthermore, events can be observed in each curve in Figure 20a. The first, up to about 150 °C, can be attributed to evaporation of adsorbed water, whereas the curauá fiber is very hydrophilic. The second, in the range from 180 to 350 °C, is attributed to the depolymerization of hemicellulose (untreated fiber), and the breaking of cellulose glycosidic bond (for all the fibers). And finally, the third event, between 250 and 500 °C, is related to the degradation of lignin (for all the fibers). These results are in agreement with the work of Kim et al. (2006). An increase in the number of T_{max} peaks (Figure 20b) when increasing the number of treatments is observed by DTG curves.

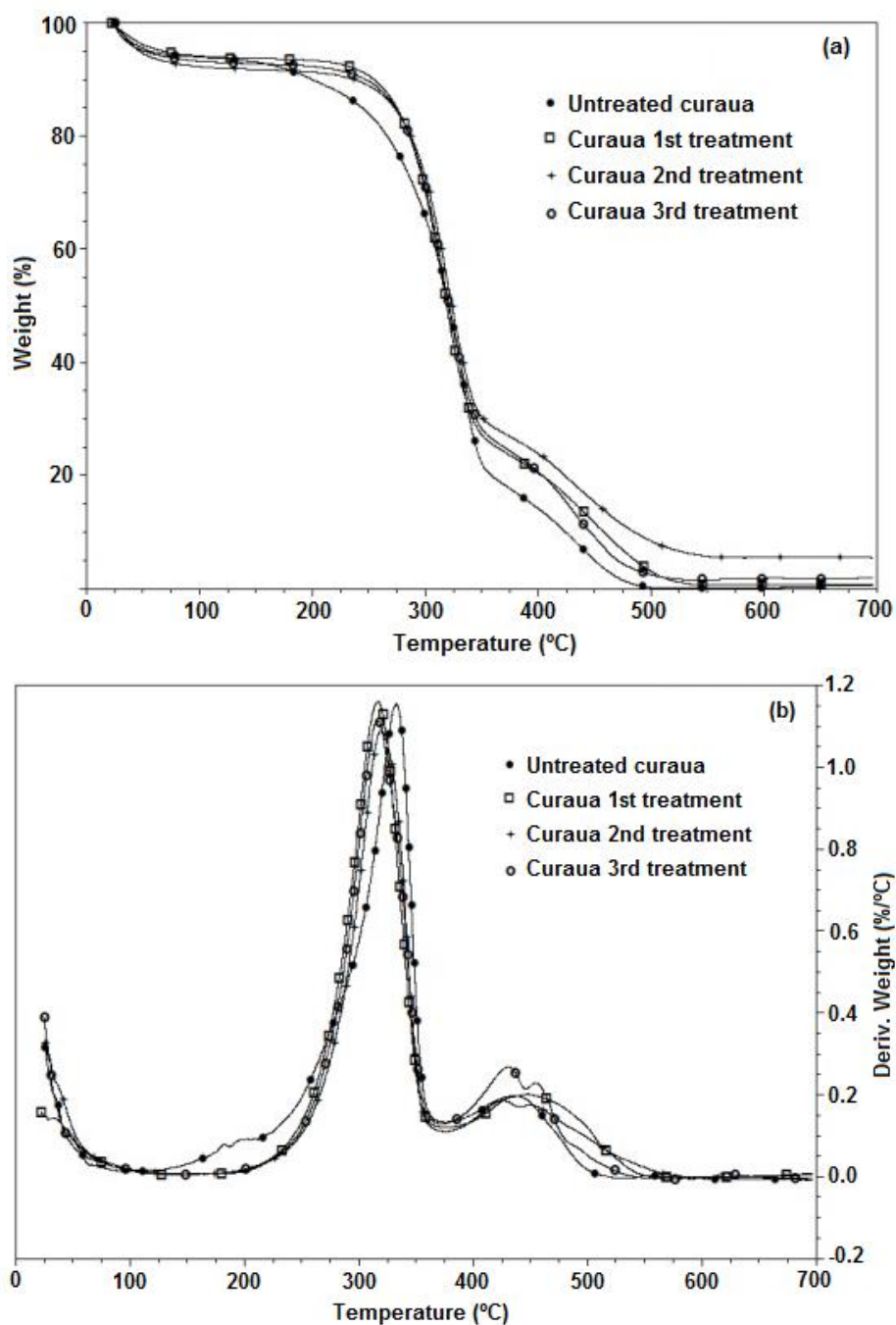


Figure 20: (a) TGA e (b) DTG curves of untreated and alkaline-treated curauá fibers

Table 10: Thermal properties of untreated and alkaline-treated curauá fibers

| Curauá | $T_{0.05}$ (°C) | T_{max} (°C) | Total loss (%) |
|---------------|-----------------|-------------------|----------------|
| Untreated | 217 | 333 // 439 | 99.2 |
| 1st treatment | 262 | 316 // 449 | 99.3 |
| 2nd treatment | 265 | 319 // 427 // 455 | 94.5 |
| 3rd treatment | 263 | 316 // 430 // 458 | 98.1 |

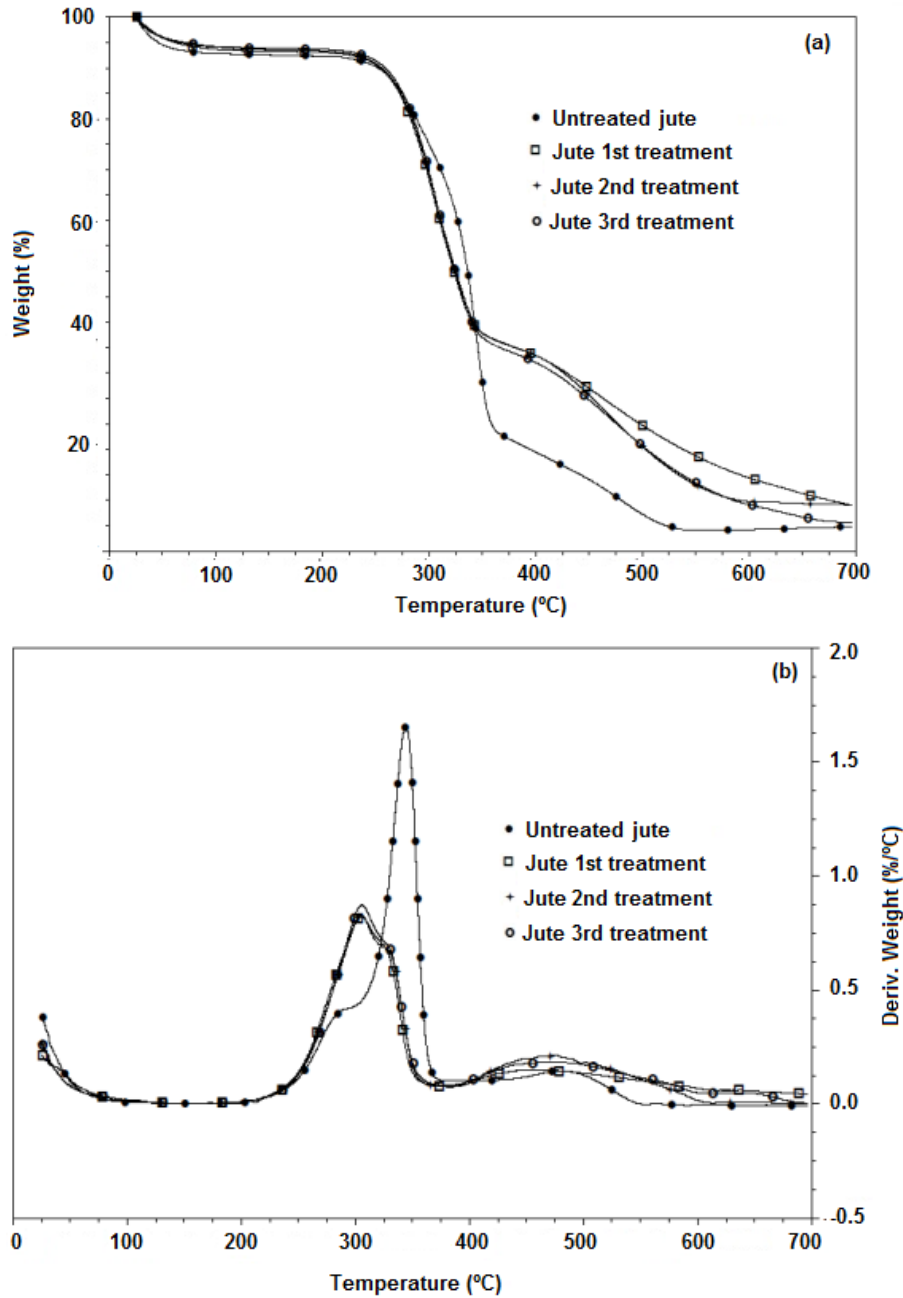


Figure 21: (a) TGA e (b) DTG curves of untreated and alkaline-treated jute fibers

Table 11: Thermal properties of untreated and alkaline-treated jute fibers

| Jute | $T_{0.05}$ (°C) | T_{max} (°C) | Total loss (%) |
|---------------|-----------------|----------------|----------------|
| Untreated | 267 | 344 | 100 |
| 1st treatment | 263 | 305 | 95.5 |
| 2nd treatment | 263 | 305 | 95.6 |
| 3rd treatment | 263 | 306 | 99.0 |

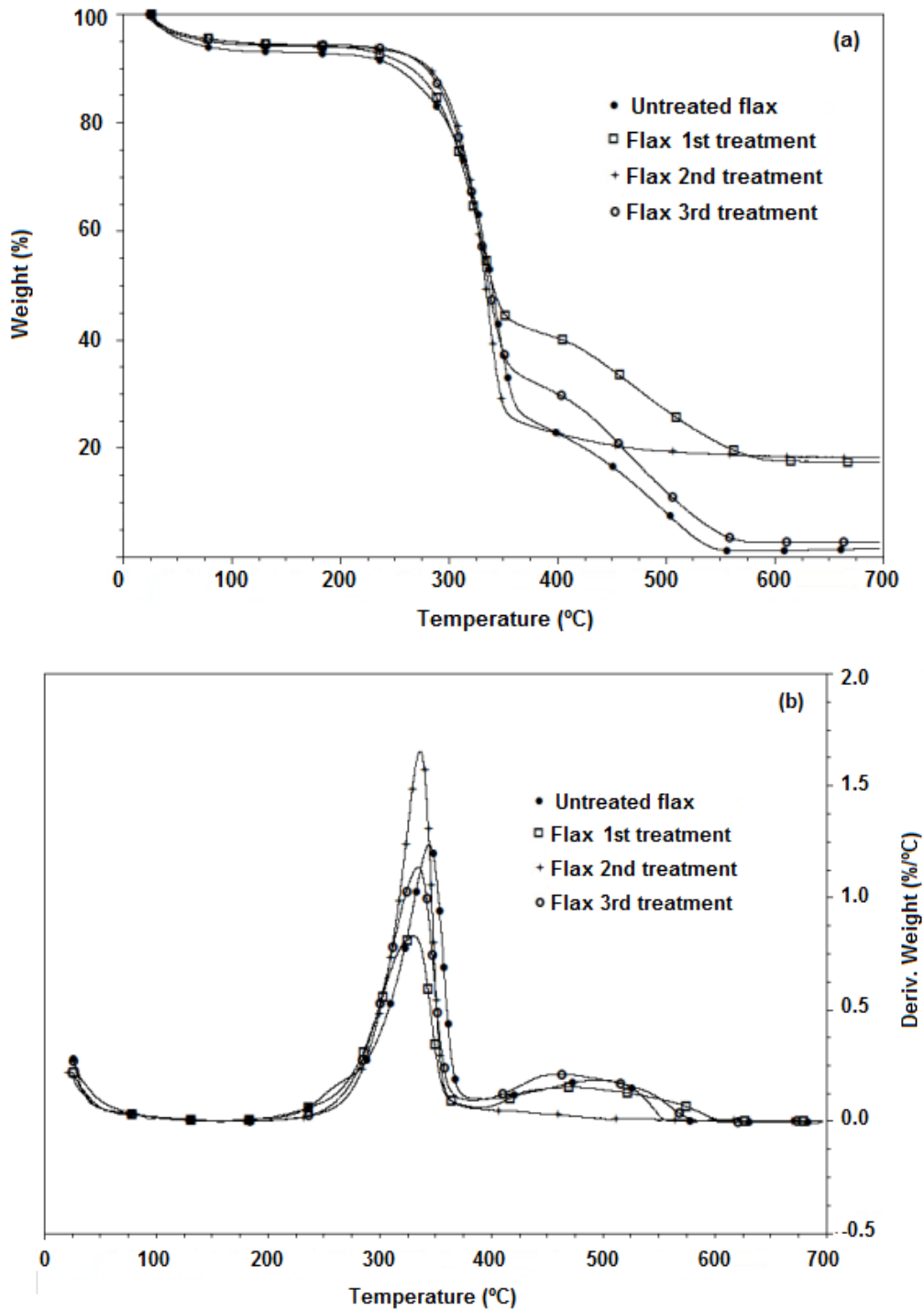


Figure 22: (a) TGA e (b) DTG curves of untreated and alkaline-treated flax fibers

Table 12: Thermal properties of untreated and alkaline-treated flax fibers

| Flax | $T_{0.05}$ (°C) | T_{max} (°C) | Total loss (%) |
|---------------|-----------------|----------------|----------------|
| Untreated | 266 | 344 // 506 | 98.1 |
| 1st treatment | 271 | 331 // 475 | 82.3 |
| 2nd treatment | 286 | 336 | 81.7 |
| 3rd treatment | 281 | 334 // 469 | 97.3 |

5.1.2 Infra-red spectroscopy of room-pressure alkaline treated natural fibers

Spectra of the pure and alkaline-treated fibers (Figure 23 – 25) reveal some important information about their characteristics absorption bands. The main peaks are located at: 3413 cm^{-1} (stretching of the O-H bond), 2900 cm^{-1} (stretch C-H bond), 897 cm^{-1} (stretch ring of glucose). This latter peak, directly connected to the structure of the cellulose, remains unchanged even after the third chemical treatments, which shows that the cellulose is not degraded by the alkaline treatment.

In alkaline treated jute fiber, it can also be noticed the disappearance of the absorption peak at 1030 cm^{-1} , corresponding to C – O stretching of hemicellulose and lignin. On the other hand, in alkaline treated curauá, the disappearance of the peak at 1270 cm^{-1} occurs, corresponding to C – O stretching of hemicellulose and lignin, indicating that most of the hemicellulose and lignin has been removed by those treatments (ROSA et al., 2010)

For all untreated fibers, an absorption band at about 1720 cm^{-1} was vanished in the alkaline-treated fibers. The first alkaline treatment was enough to remove a substantial portion of uronic acid, a constituent of hemicellulose xylan, which resulted in the disappearance of the corresponding peak. Hemicellulose contained groups that absorbed in the carbonyl region, which are soluble in aqueous alkaline solutions (HUJURI et al., 2008).

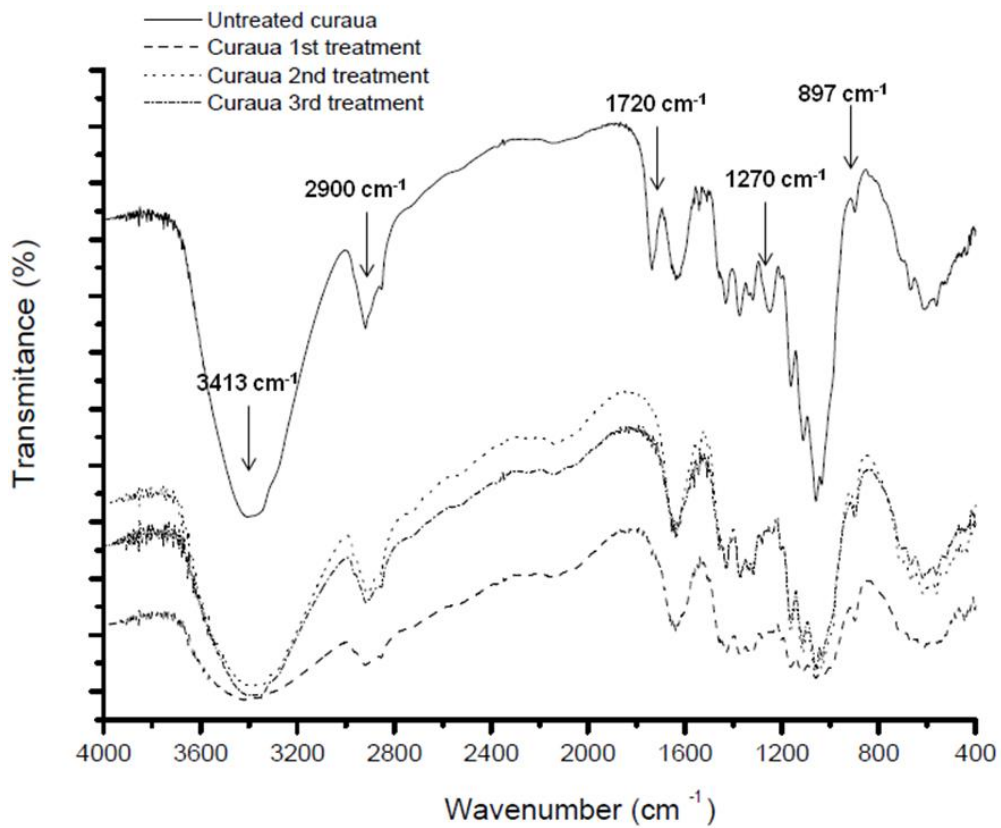


Figure 23: FTIR spectra of untreated and alkaline-treated curauá fibers

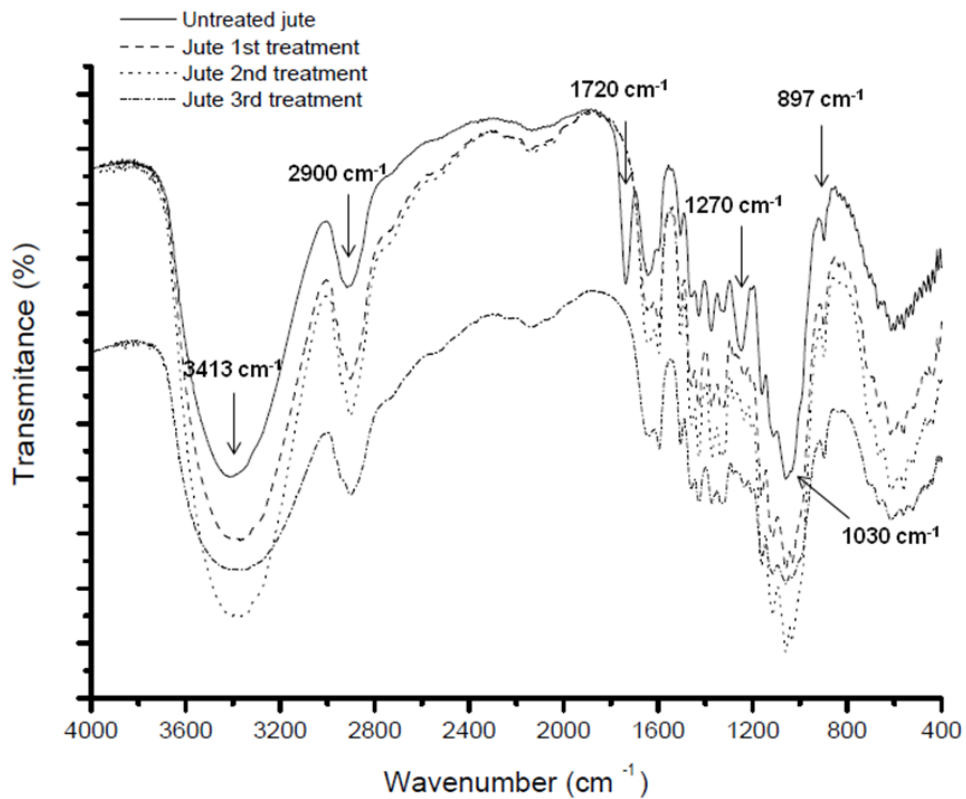


Figure 24: FTIR spectra of untreated and alkaline-treated jute fibers

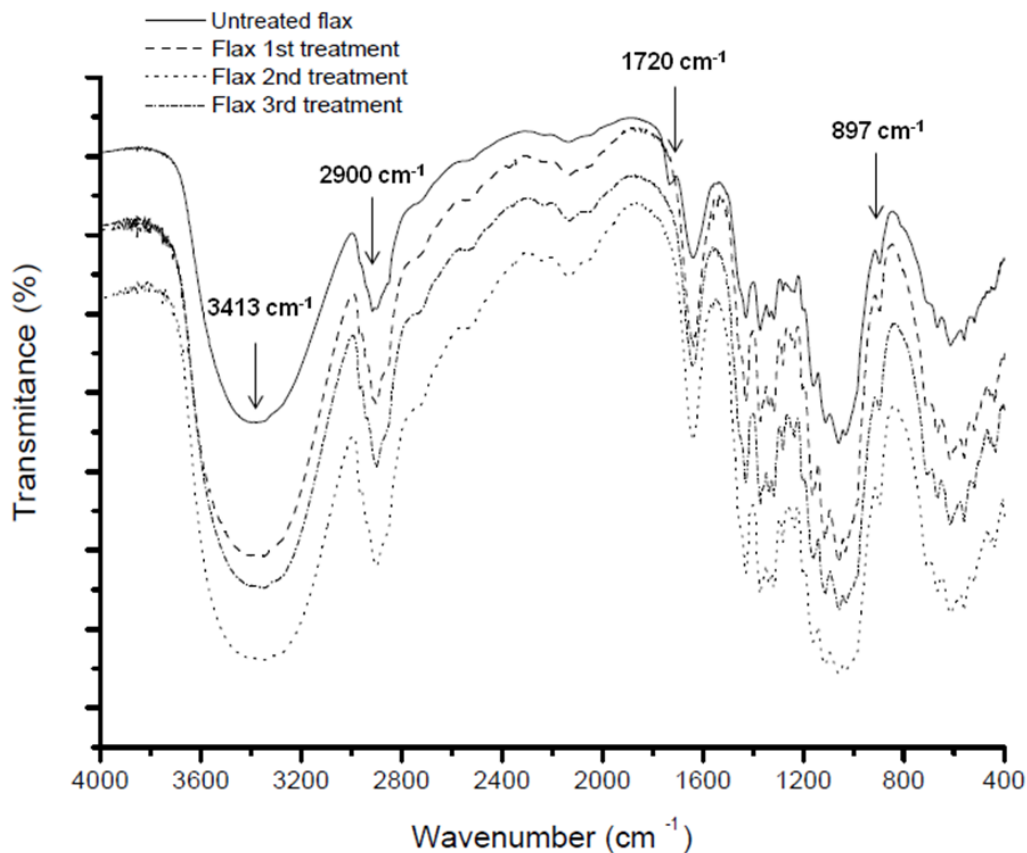


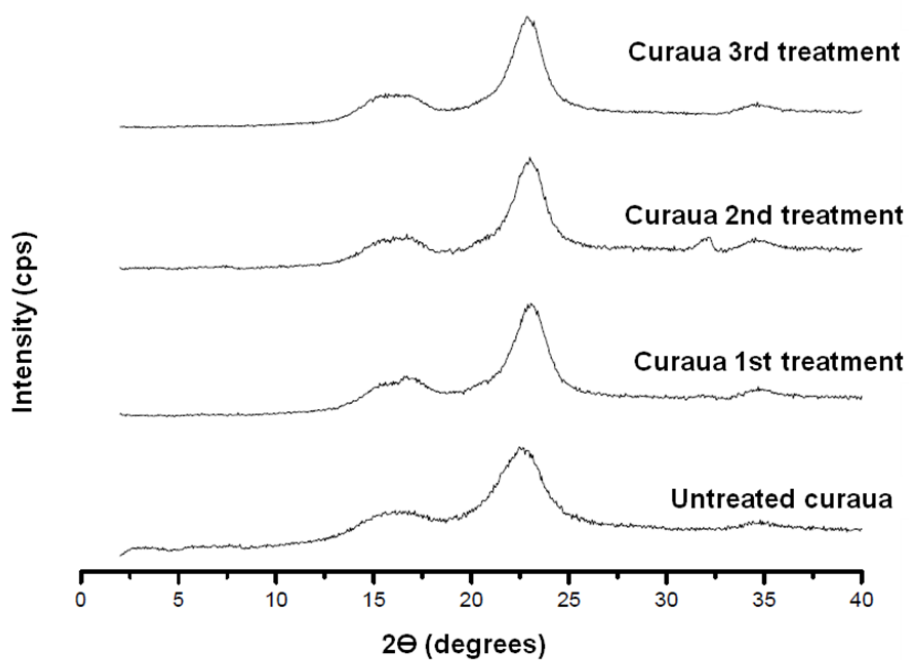
Figure 25: FTIR spectra of untreated and alkaline-treated flax fibers

5.1.3 Degree of crystallinity of room-pressure alkaline treated natural fibers

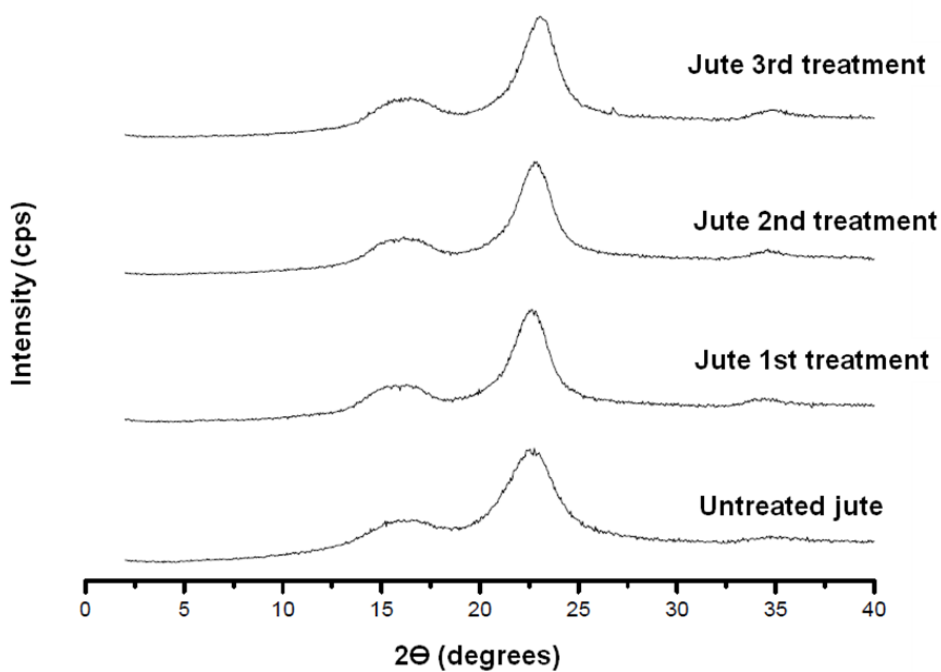
X-ray diffraction patterns of untreated natural fibers and those submitted to different treatments are presented in Figure 26 and Table 13, as well as the crystallinity index, measured from equation 2. Treated and untreated fibers showed three main reflection peaks at $2\theta = 15.6^\circ$, 22.7° and 34.6° relative to the cellulose crystalline structure. As a result of alkaline treatment, narrower and more intense crystalline peaks were observed for the treated fibers, mainly for curauá, increasing slightly the crystallinity index (ROSA et al., 2010).

Table 13: Degree of crystallinity of untreated and alkaline-treated natural fibers

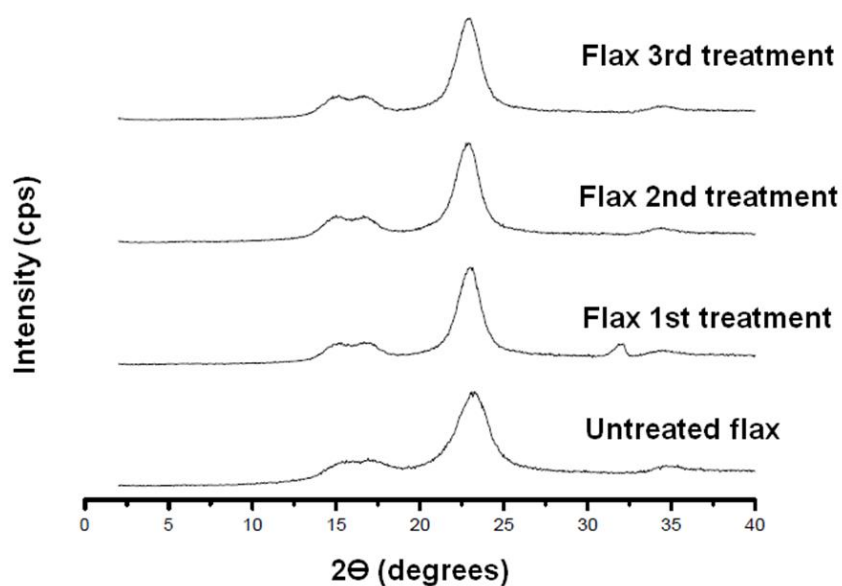
| Sample/Fiber | Crystallinity index (%) | | |
|---------------------------|-------------------------|------|------|
| | Curauá | Jute | Flax |
| Untreated | 62 | 64 | 75 |
| 1 st treatment | 70 | 67 | 79 |
| 2 nd treatment | 70 | 68 | 75 |
| 3 rd treatment | 73 | 68 | 77 |



(a)



(b)



(c)

Figure 26: X-ray diffractograms of untreated and alkaline-treated natural fibers. (a) Curauá, (b) Jute, (c) Flax

Regarding the diffractogram, it is clear that the amorphous halo due to the presence of lignin and the various hemicelluloses present in the untreated fiber is decreasing as soon as the alkaline treatment has been performed. In any case, crystallinity is not strongly affected by all these treatments. Except for curauá, the other fibers did not increase very strongly I_c .

5.1.4 Analysis of mechanical properties of PP/Natural Fibers composites by DMTA

Mechanical properties of the natural fibers/PP composites were analysed by DMTA. During the DMTA analysis, a sample is subjected to a sinusoidal deformation force at small amplitudes, over a wide temperature range, measuring both the elastic (E') and the loss (E'') moduli. The ratio between these parameters, $\tan \delta$ (or damping factor), characterizes the viscoelasticity of the material, indicating a relaxation process. In the proximity of the glass transition temperature (T_g), the modulus E' decreases and both E'' and $\tan \delta$ curves reach a maximum.

Experimental results of storage modulus are presented in Table 14 and Figures 27a, 28a and 29a. Addition of 10 wt. % of treated curauá fibers increases E' and E'' up to 50% respect to the values of neat polypropylene. On the other hand, treated jute and flax seem not to have any influence in the mechanical behavior of the composites, when compared to composites prepared with untreated fibers. The modulus of polypropylene is determined by two factors: strength of intermolecular forces and, ultimately, by packing polymer chains. When fibers are inserted to the resin, an increase of the modulus is observed due to the stiffness of fibers (ROMANZINI et al., 2012; ETAATI et al., 2014).

Table 14: DMTA results of composites of PP/natural fibers (10% w/w)

| Sample | Fiber | Description | E' (GPa) (-40°C) | E' (GPa) (25°C) | E'' (GPa) (25°C) | T_g (°C) (Tan δ) | Tan δ (damping factor) |
|------------|--------|--|--------------------|-------------------|--------------------|----------------------------|-------------------------------|
| PP-550P | - | Processed pure polypropylene | 1.94 | 0.81 | 0.04 | 8.7 | 0.073 |
| PP-550P-C1 | Curauá | PP550 + Untreated curauá | 2.33 | 1.08 | 0.05 | 7.1 | 0.067 |
| PP-550P-C2 | | PP 550 + Alkaline treated curauá (3 rd treatment) | 3.02 | 1.39 | 0.06 | 5.9 | 0.064 |
| PP-550P-J1 | Jute | PP550 + Untreated jute | 1.91 | 1.04 | 0.04 | 10.9 | 0.056 |
| PP-550P-J2 | | PP 550 + Alkaline treated jute (3 rd treatment) | 1.99 | 1.07 | 0.05 | 10.9 | 0.059 |
| PP-550P-F1 | Flax | PP550 + Untreated flax | 1.83 | 1.03 | 0.04 | 10.4 | 0.054 |
| PP-550P-F2 | | PP 550 + Alkaline treated flax (3 rd treatment) | 1.89 | 1.08 | 0.05 | 10.8 | 0.059 |

Tan delta values and curves are presented in Table 14 and Figures 27b, 28b and 29b, respectively. In a composite, damping factor takes place due to the nature of the matrix and fiber materials; friction generated from the slip in interface resin/fiber; energy dissipation at cracks and delaminations produced at

damaged locations; and viscoplastic and thermoelastic damping (JOHN; ANANDJIWALA, 2009). For pure PP, with increasing of temperature, tan delta initially increases until α -transition peak temperature and then decrease. The position of peak can represent the α -relaxation temperature of 82 °C for PP. Addition of fibers onto PP, treated or untreated in any case, did not cause significant changes in α -relaxation temperatures of the composites. This is in correlation with the literature (CHAUAN; KHARMARKAR; AGGARWAL, 2009; JOHN; ANANDJIWALA, 2009; JAWAID et al., 2013), in which the position of α -relaxation was not significantly altered upon incorporation of natural short fibers.

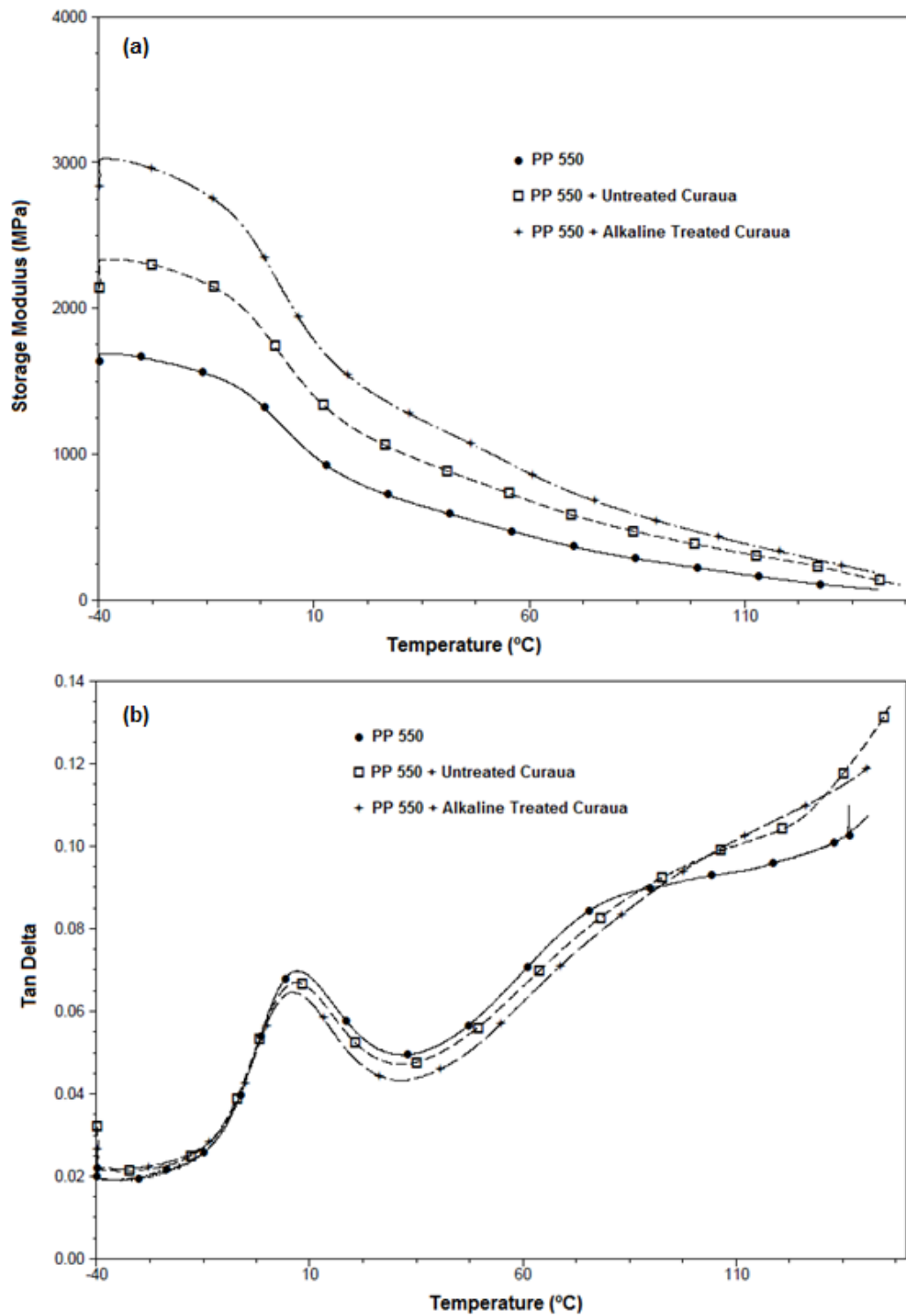


Figure 27: Storage modulus (a) and tan delta (b) curves of PP 550 and their composites with curauá fibers

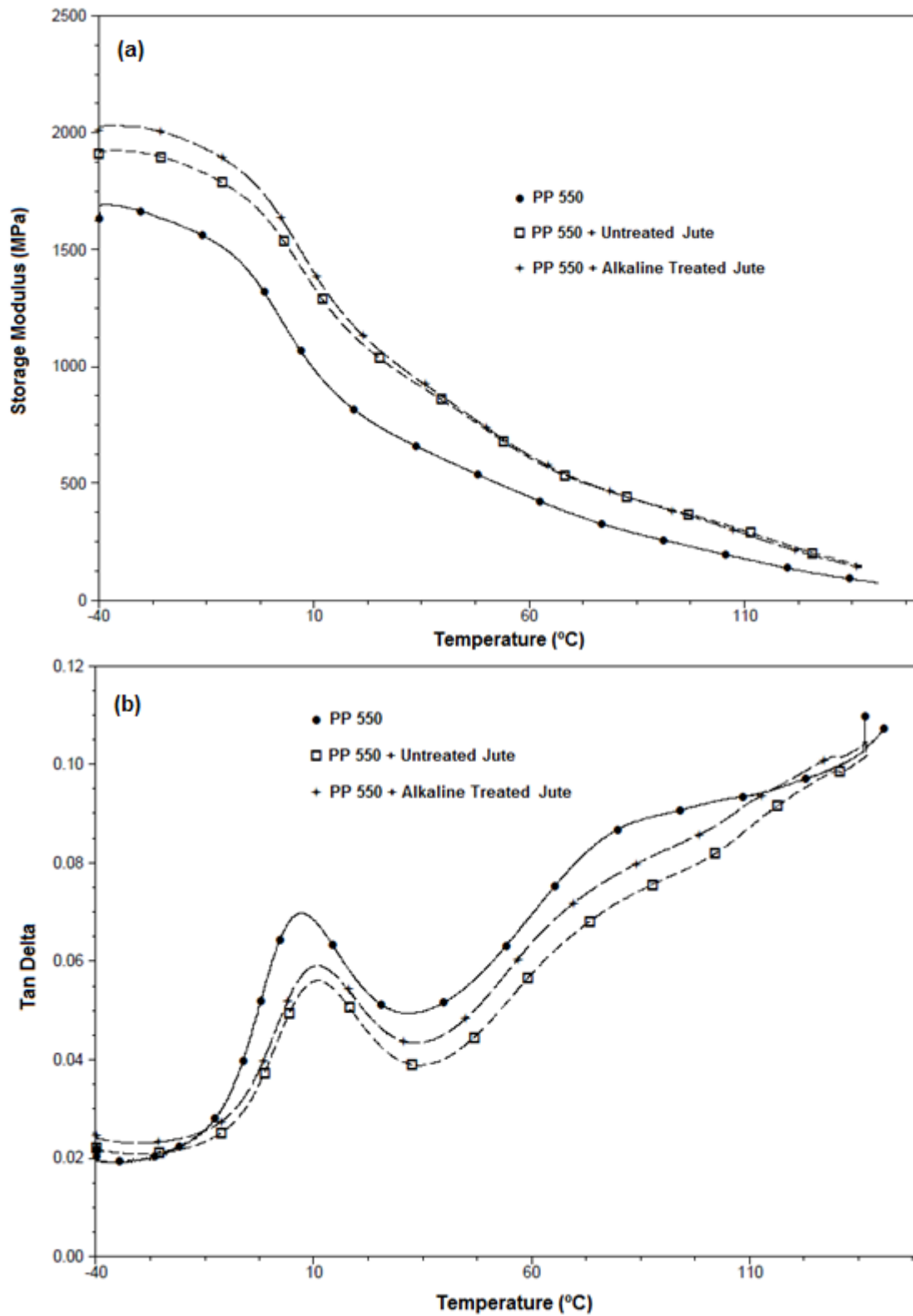


Figure 28: Storage modulus (a) and tan delta (b) curves of PP 550 and their composites with jute fibers

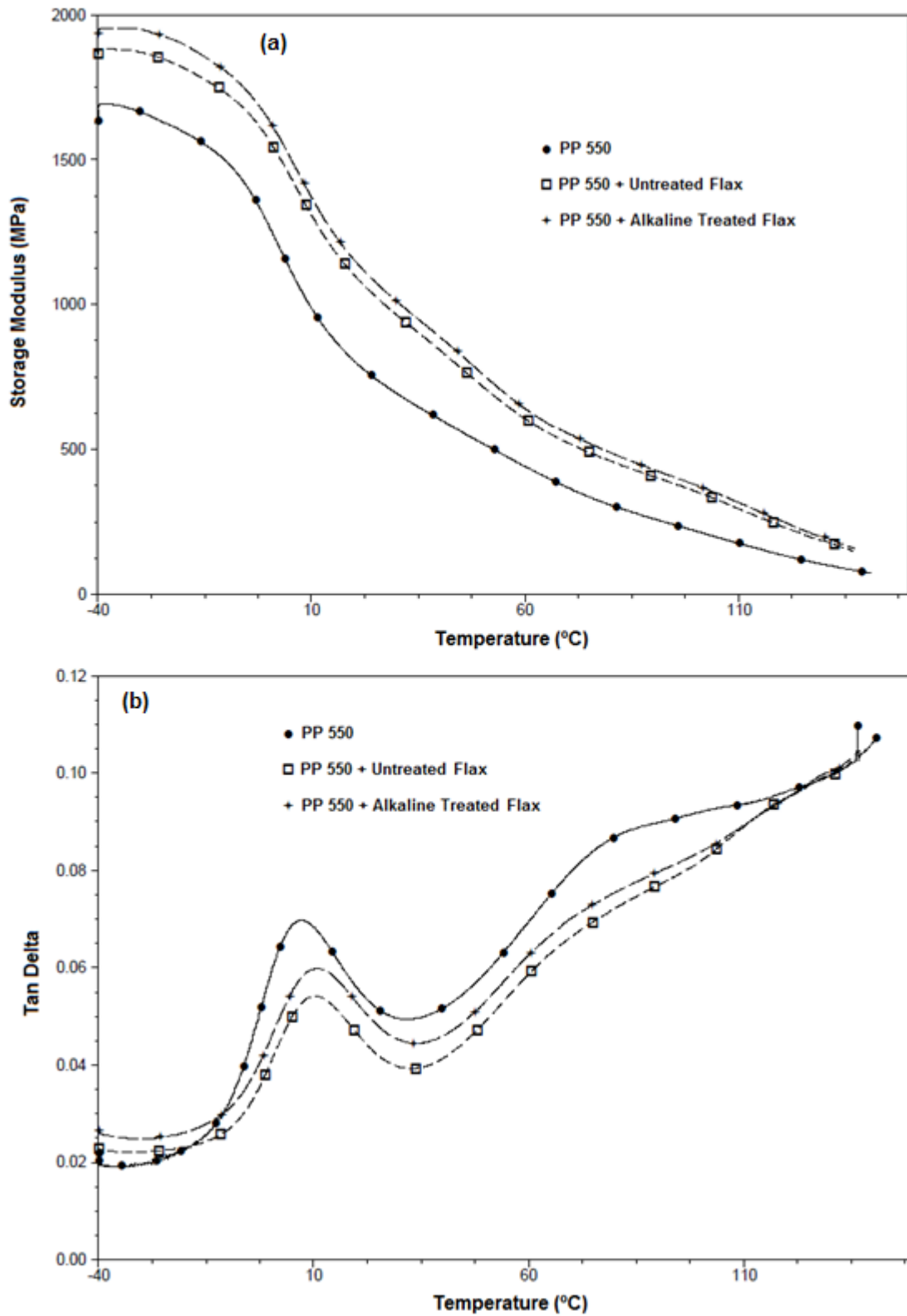


Figure 29: Storage modulus (a) and tan delta (b) curves of PP 550 and their composites with flax fibers

5.1.5 Analysis of morphology of PP/Natural Fibers composites by SEM

Morphology of natural fibers / polypropylene composites was observed by SEM (Figures 30 – 32). The SEM evidences why composites with treated curauá fibers show better results in terms of elastic modulus than other fibers. It can be observed a large number of voids in cross-section fractures in composites of PP 550 with untreated curauá fibers (Figure 30a), resulting in a poor interaction adhesion with resin. This leads to a poor mechanical behavior compared with a composite prepared with treated curauá (Figure 30c). In this case, the number of voids is drastically reduced and, consequently, there is a better fiber distribution into PP matrix, leading to less fiber agglomerations. Therefore, in this case, successive chemical treatments were able to improve adhesion between short curauá fibers and polypropylene matrix. However, it is important to notice a presence of fiber pullouts in both cases (Figures 30b and 30d), mainly for composites with untreated curauá fibers, with higher diameter and less distributed than treated ones.

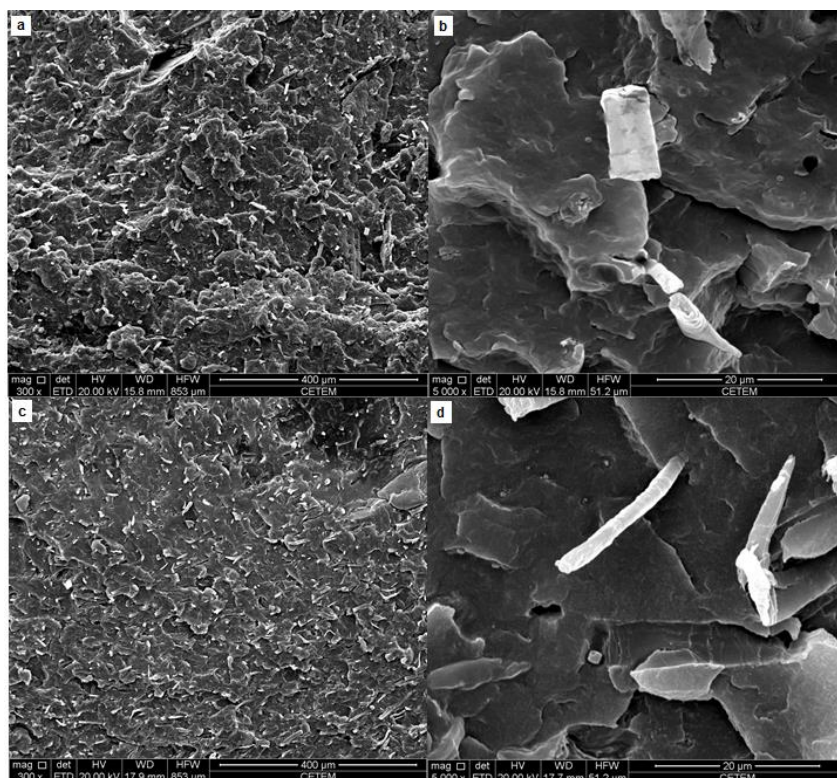


Figure 30: SEM micrographs of PP 550 composites with (a) untreated curauá fibers (300x), (b) untreated curauá fibers (5000x), (c) treated curauá fibers (300x), (b) treated curauá fibers (5000x)

In the case of the composites prepared with jute and flax (Figures 31 and 32), micrographies show a similar behavior, with a large number of gaps and voids, as well as fiber pullouts, mainly for composites prepared with treated flax fibers (Figures 32c and 32d). It can be also observed, in Figure 32d, presence of fractures onto the surface of treated flax fiber, which certainly contributes to poor adhesion between treated fiber and PP matrix, resulting in decrease of mechanical properties. Moreover, a factor that can contribute also to bad of mechanical properties is the different fiber lengths and diameters across the surface of composites, resulting in a non-uniform distribution of fibers in resin, avoiding an increase of mechanical properties of treated fibers compared with untreated ones. Therefore, it can be concluded that successive chemical treatments were not enough to improve elastic modulus of composites.

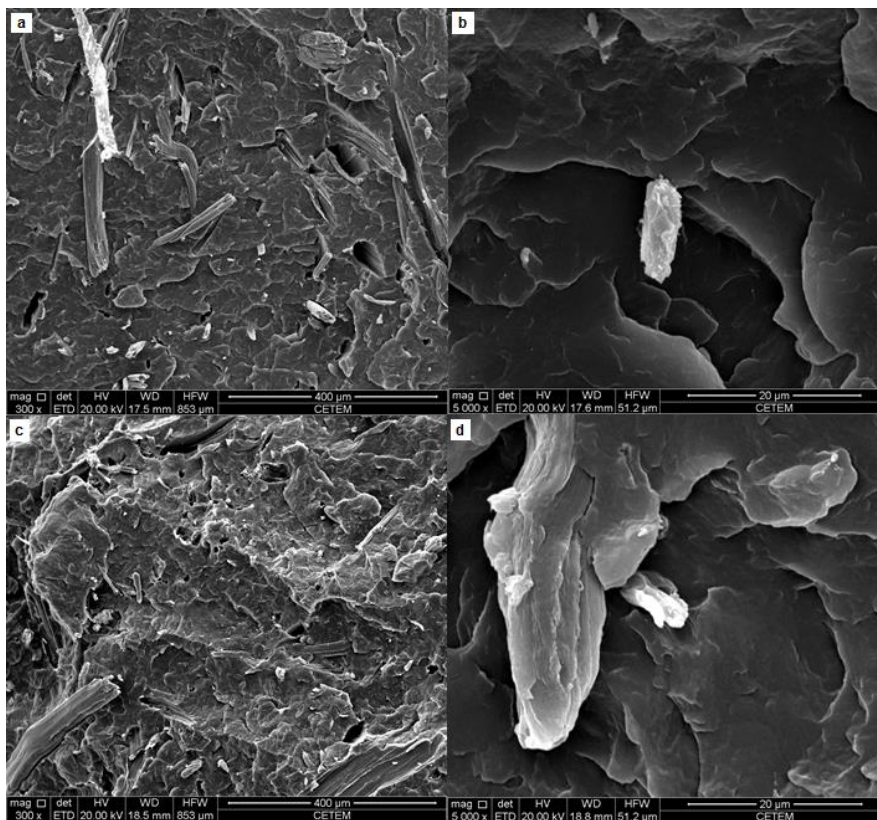


Figure 31: SEM micrographs of PP 550 composites with (a) untreated jute fibers (300x), (b) untreated jute fibers (5000x), (c) treated jute fibers (300x), (d) treated jute fibers (5000x)

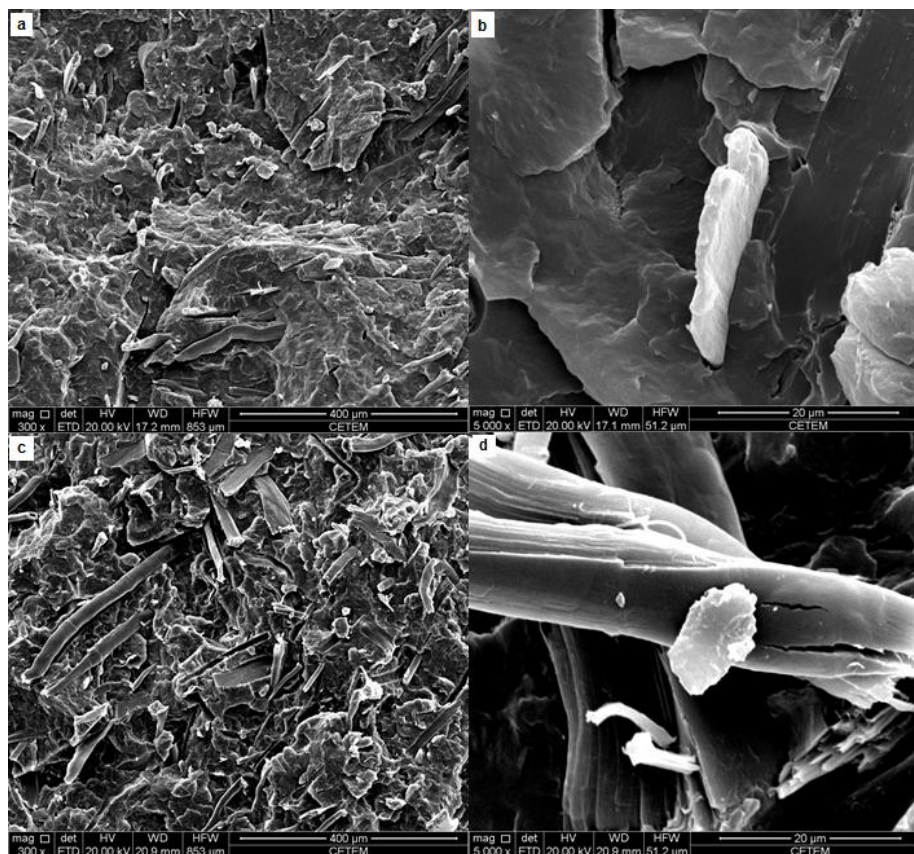


Figure 32: SEM micrographs of PP 550 composites with (a) untreated flax fibers (300x), (b) untreated flax fibers (5000x), (c) treated flax fibers (300x), (d) treated flax fibers (5000x)

5.2 EFFECT OF ACETYLATION AND SILANIZATION ON RP- ALKALINE TREATED FIBERS

5.2.1 Infra-red spectroscopy of RP – alkaline treated + acetylated fibers

Results of FTIR spectra of room-pressure alkaline treated fibers (RP - alkaline treated , i.e., after 3rd treatment) and treated fibers with subsequent acetylation can be observed in Figures 33 – 35. Efficiency of acetylation can be strongly noted in curauá and jute fibers with appearance of strong intensity peak at 1740 cm^{-1} , attributed to C=O carbonyl stretching from acetyl group.

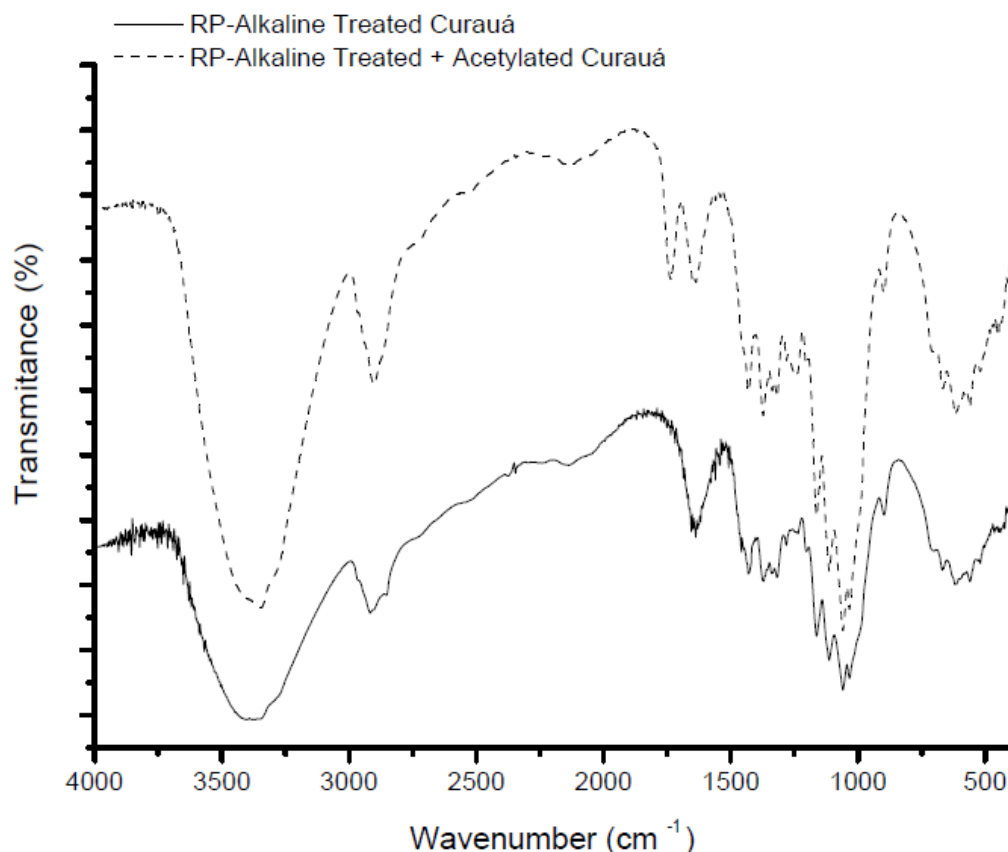


Figure 33: Spectra of curauá fibers treated with RP alkaline solutions and acetic anhydride

Moreover, it can be noted also a displacement of bands of at 1375 cm^{-1} (C-H bond bending in $-\text{O}(\text{C}=\text{O})-\text{CH}_3$) and 1241 cm^{-1} (attributed to C – O stretching of acetyl group) (MWAIKAMBO; ANSELL, 1999; OLARU et al., 2011) to higher values, as well as intensity of the same bands increases. According to previous results found in literature, these events can provide evidence of a well-performed acetylation treatment on natural fibers (RANA et al., 1997). The fact of all these events takes place in a more evident way in curauá and jute than flax fibers may be explained in terms of higher cellulose content of this last one and, therefore, more crystalline fiber (as seen previously in Table 13), becoming less accessible for the conversion of acetyl groups on the surface of flax.

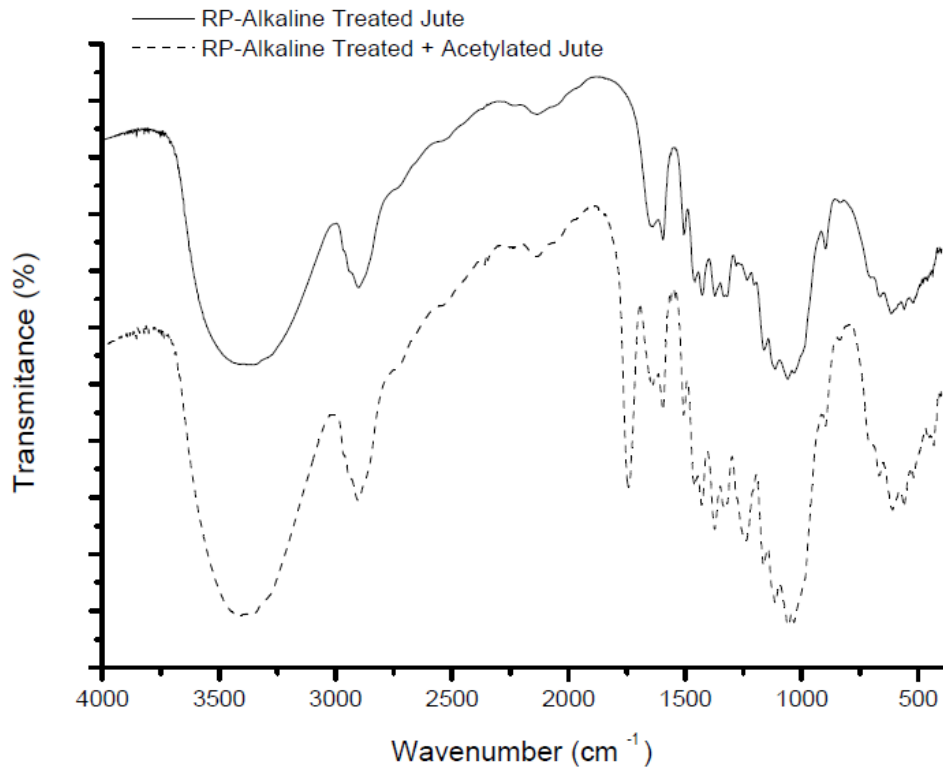


Figure 34: Spectra of jute fibers treated with RP alkaline solutions and acetic anhydride

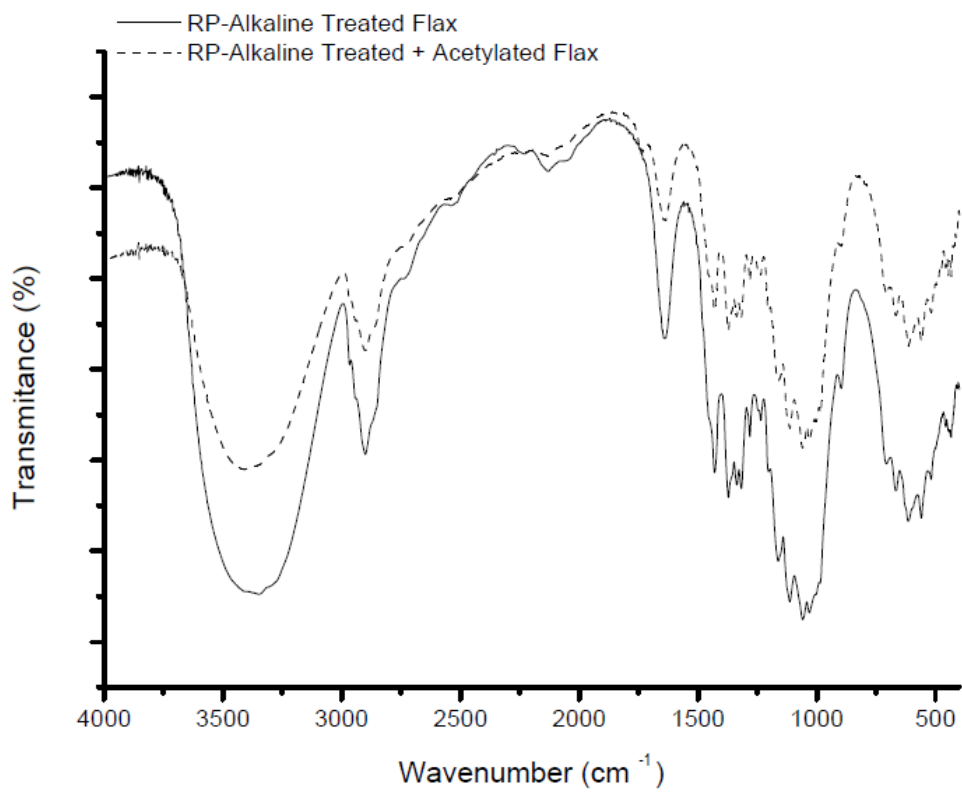


Figure 35: Spectra of flax fibers treated with RP alkaline solutions and acetic anhydride

5.2.2 Infra-red spectroscopy of RP – alkaline treated + silanized fibers

According to Figure 36, it is observed bands at 3371 and 3301 cm^{-1} , mainly in silanized curauá and flax, and they are related to the asymmetric and symmetric stretching of the NH_2 group of absorbed silane, respectively. The corresponding bands for the fully hydrolysed silane (SiOH) are 3352 and 3272 cm^{-1} . Hydrogen bonding shifts these stretching vibration bands to 3370 and 3310 cm^{-1} , respectively. This indicates that there is a chemical bonding between aminopropylsiloxane and the cellulose surface. For adsorbed silane, there is also a possibility of some interaction between C-OH groups of cellulose and NH_2 from silane through hydrogen bonding (EKLUND et al., 1999).

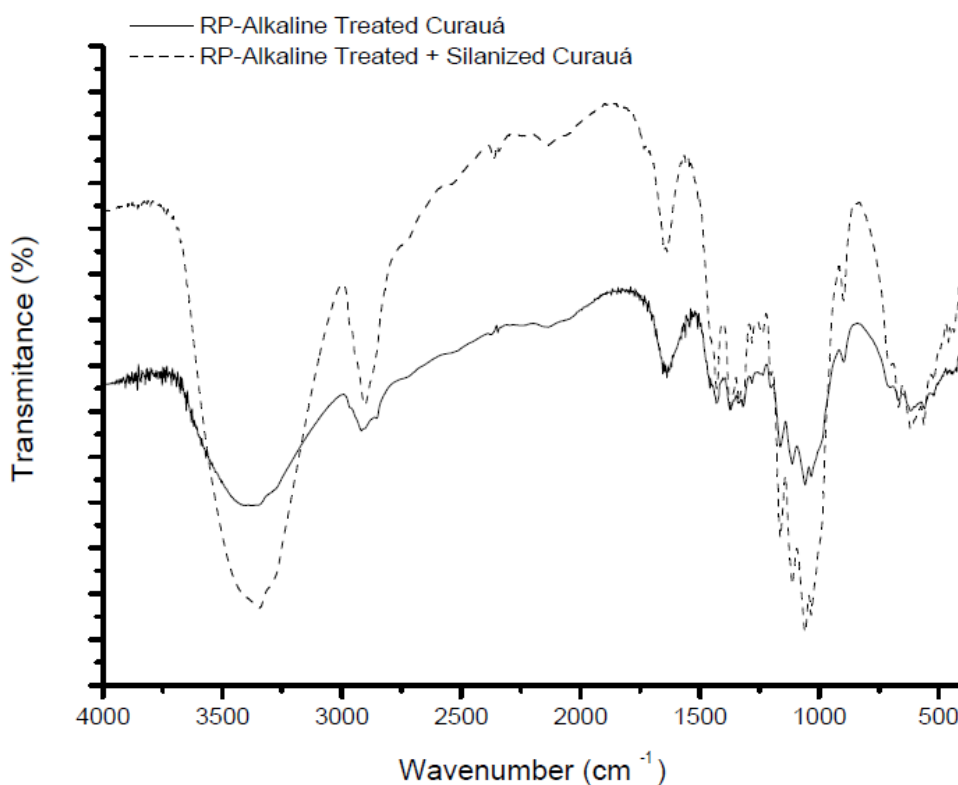


Figure 36: Spectra of curauá fibers treated with RP alkaline solutions and silane APTES

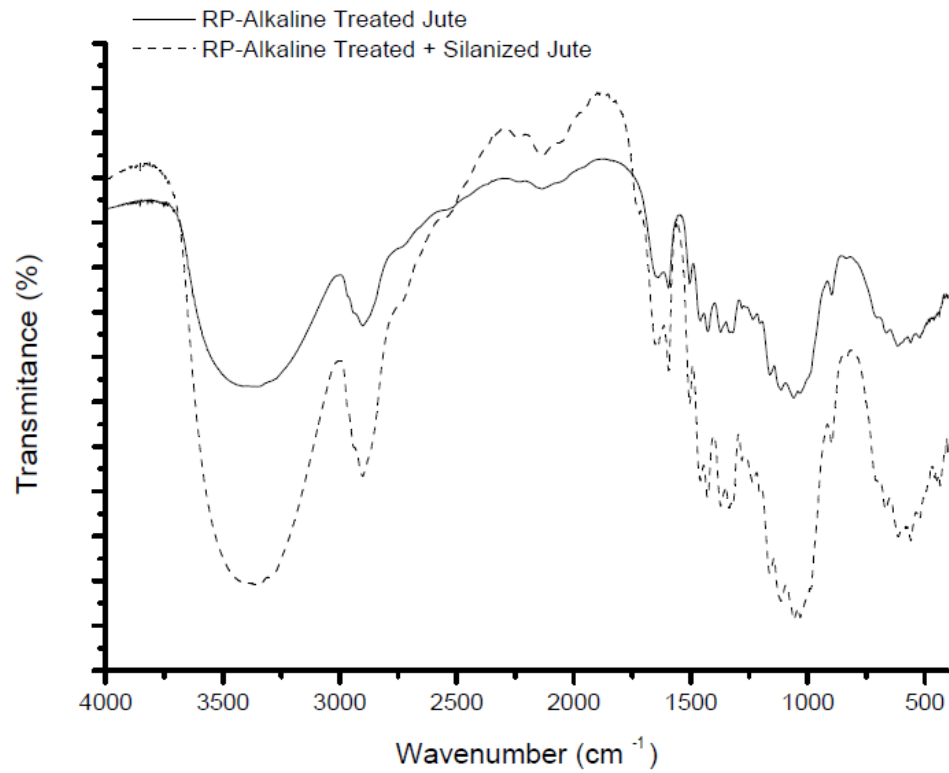


Figure 37: Spectra of jute fibers treated with RP alkaline solutions and silane APTES

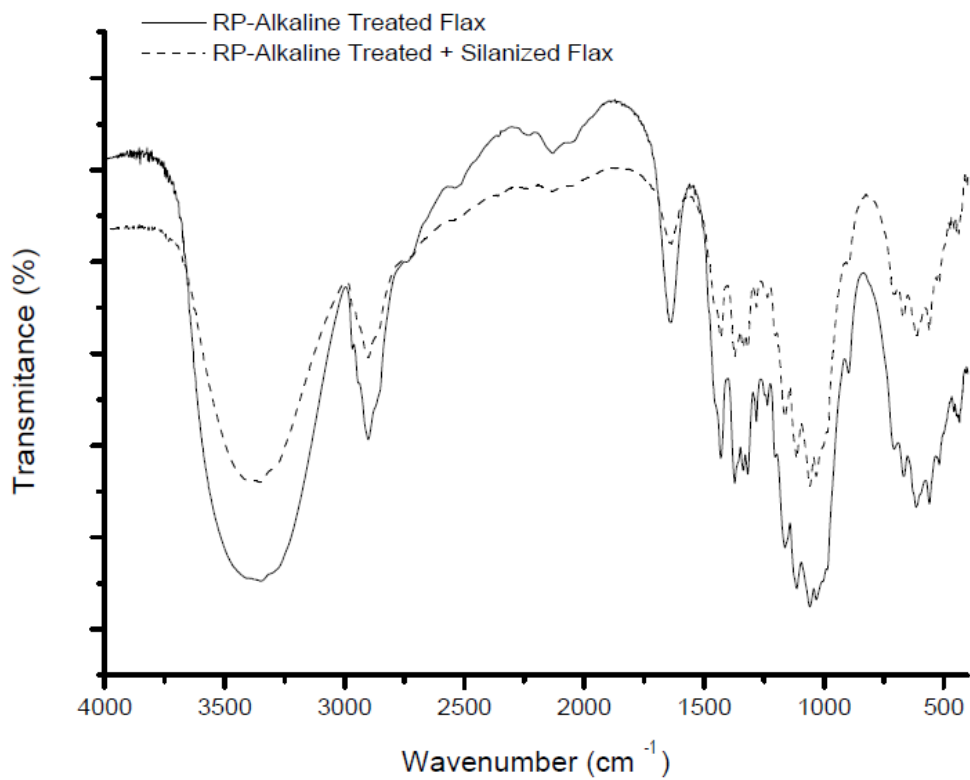


Figure 38: Spectra of flax fibers treated with RP alkaline solutions and silane APTES

5.2.3 XRD of RP alkaline-treated, acetylated and silanized fibers

Results of X-ray diffraction of untreated and treated natural fibers are shown in Table 15 and Figures 39 – 41. Comparing the numerical results of degree of crystallinity, no significant changes in this property are observed with acetylation or silanization of all natural fibers, compared with the ones that undergo only alkaline treatment. So, it can be assumed that, with exception of acetylated curauá, acetylation and silanization processes did not affect strongly the crystallinity of the fibers, just increasing their hydrophobicity.

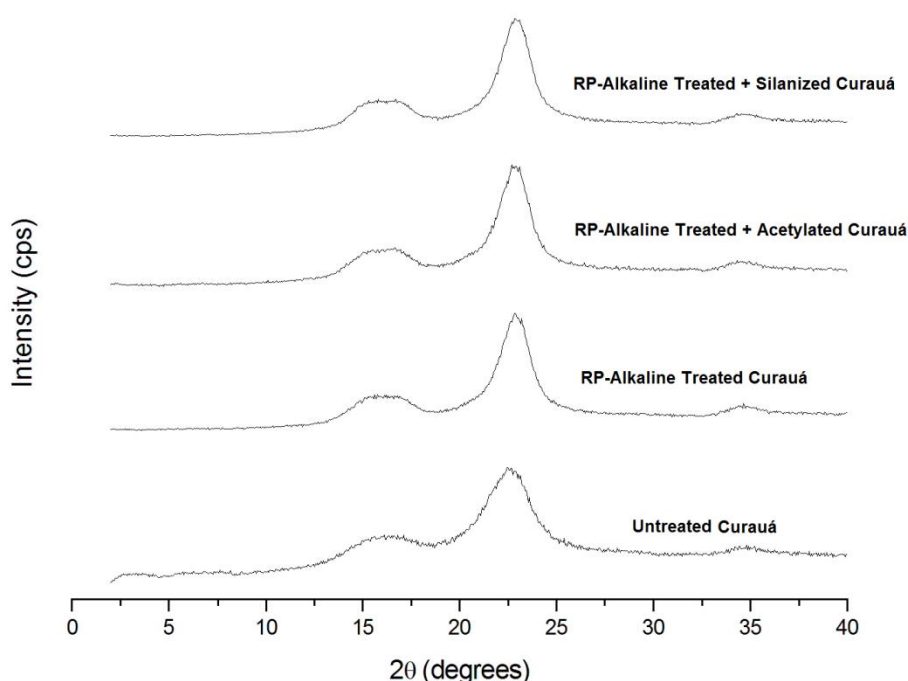


Figure 39 – Diffractograms of curauá fibers in nature and treated with RP alkaline solutions, acetic anhydride and silane APTES

According to the literature (RONG et al., 2001), it is expected a decrease of crystallinity with silanization of natural fibers. However, this behaviour is not observed in all RP-alkaline treated fibers. In general, reaction of silanes with hydroxyl groups occurs in three stages: hydrolysis, condensation and bond formation. This means that, in addition to the reaction of silanols with – OH groups of the fibers surface, formation of polysiloxane structures also occurs. A

large coupling of molecules can destroy the packing of cellulose chains by substituting its hydrogen bonds with $-\text{CH}_2\text{CH}_2\text{CN}$ characterized by decrystallization. As a certain extent of hydroxyl groups of fibers was already converted to $-\text{O}^- \text{Na}^+$ groups after mercerization process, it may explain why there is no change of degree of crystallinity.

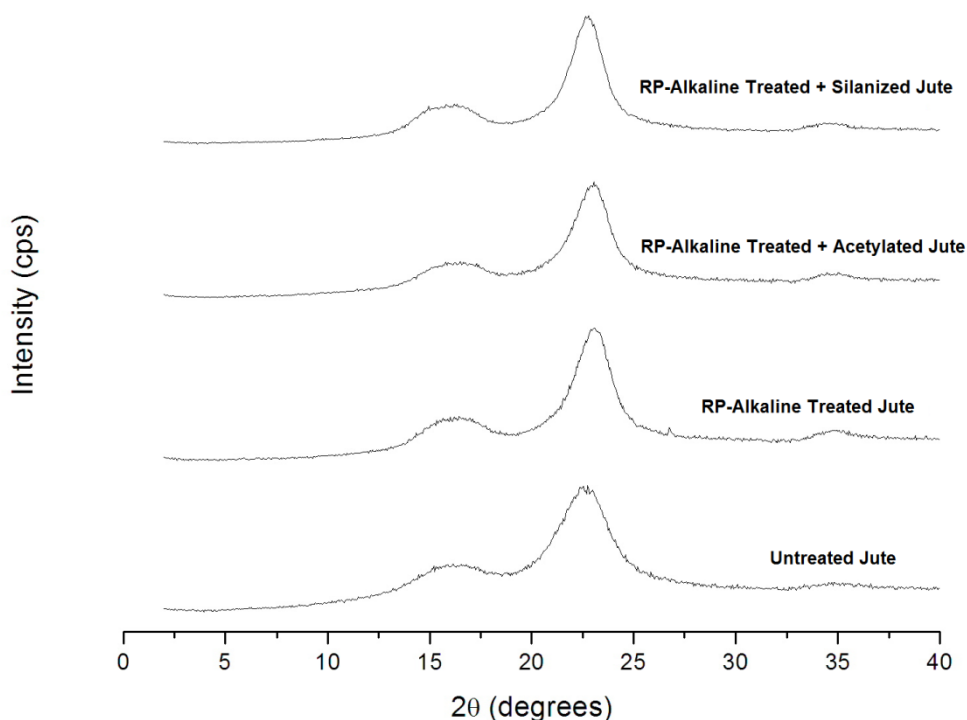


Figure 40 – Diffractograms of jute fibers in nature and treated with RP alkaline solutions, acetic anhydride and silane APTES

Although FTIR results show characteristic bands of acetylated fibers, no differences are observed in numerical results of I_c considering characteristic peaks. It is reported the presence of a peak at $2\theta = 8^\circ$, related to semicrystalline acetylated derivative cellulose (HUANG et al., 2014). As the modification was only in the fiber surface, this peak is not present in the diffractograms of the studied materials.

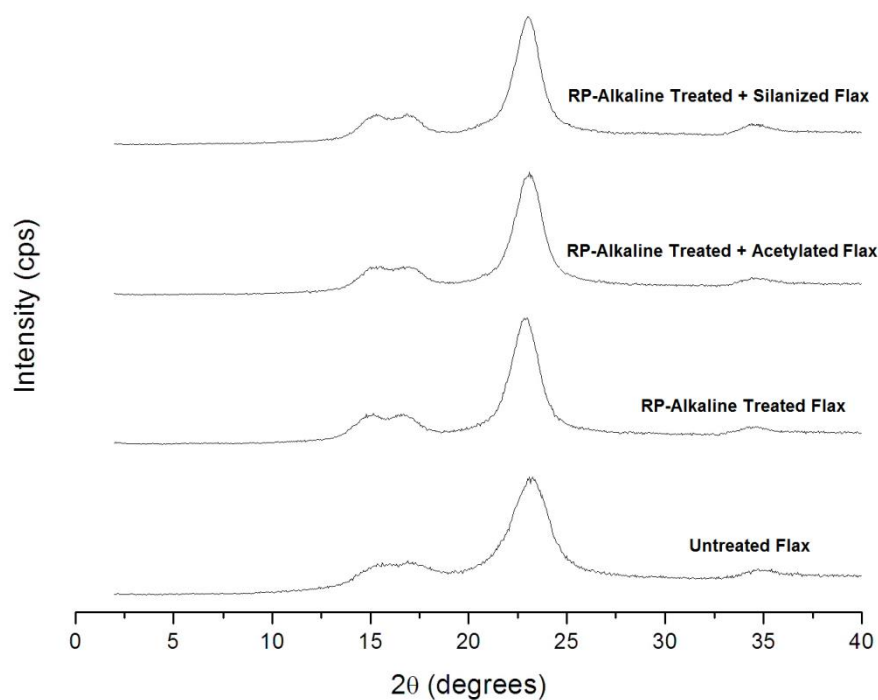


Figure 41 – Diffractograms of flax fibers in nature and treated with RP alkaline solutions, acetic anhydride and silane APTES

Table 15: Degree of crystallinity of untreated and treated natural fibers

| Sample/Fiber | Degree of crystallinity (%) | | |
|----------------------------------|-----------------------------|------|------|
| | Curauá | Jute | Flax |
| Untreated | 62 | 64 | 75 |
| RP-Alkaline Treated | 73 | 68 | 75 |
| RP-Alkaline Treated + Acetylated | 68 | 69 | 77 |
| RP-Alkaline Treated + Silanized | 71 | 70 | 77 |

5.2.4 TGA of RP alkaline-treated, acetylated and silanized fibers

Thermogravimetric analysis of all fibers before and after the treatments is presented in Figures 42 – 44 and Tables 16 – 18. In terms of thermodegradative events, acetylated and silanized mercerized fibers present similar behaviour to ones with only alkaline-treated and these events was already discussed in section 5.1.1 (Influence of successive room pressure alkaline treatments on natural fibers – thermogravimetric analysis).

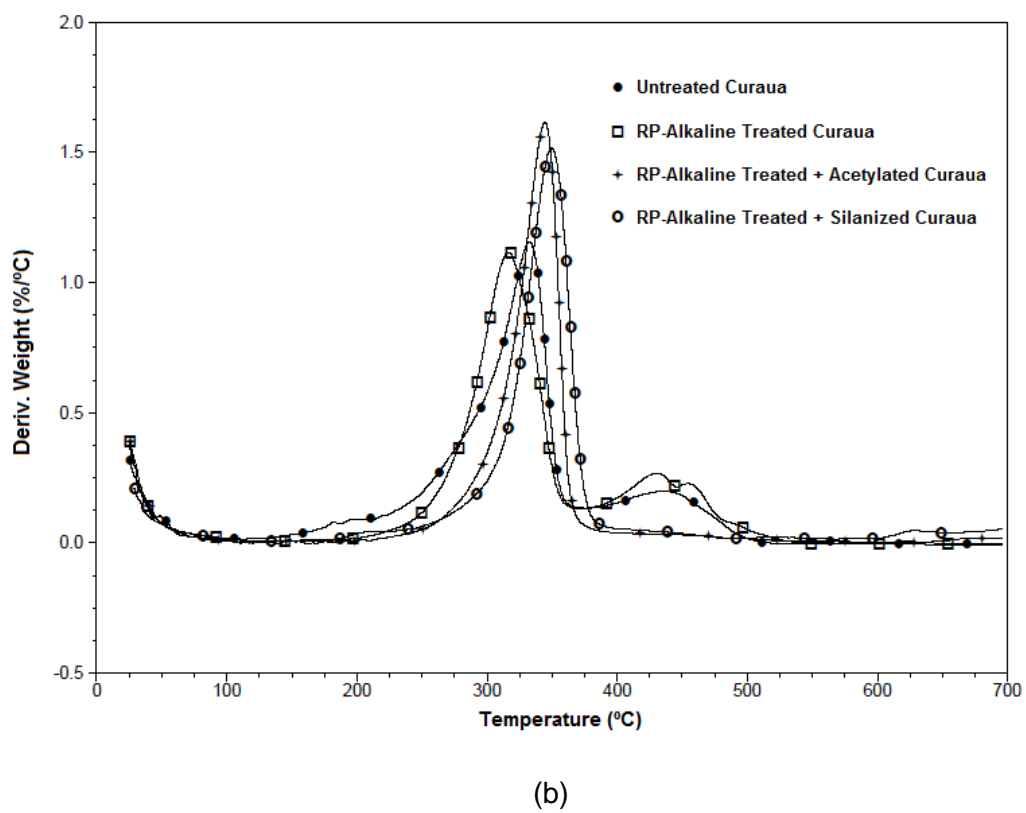
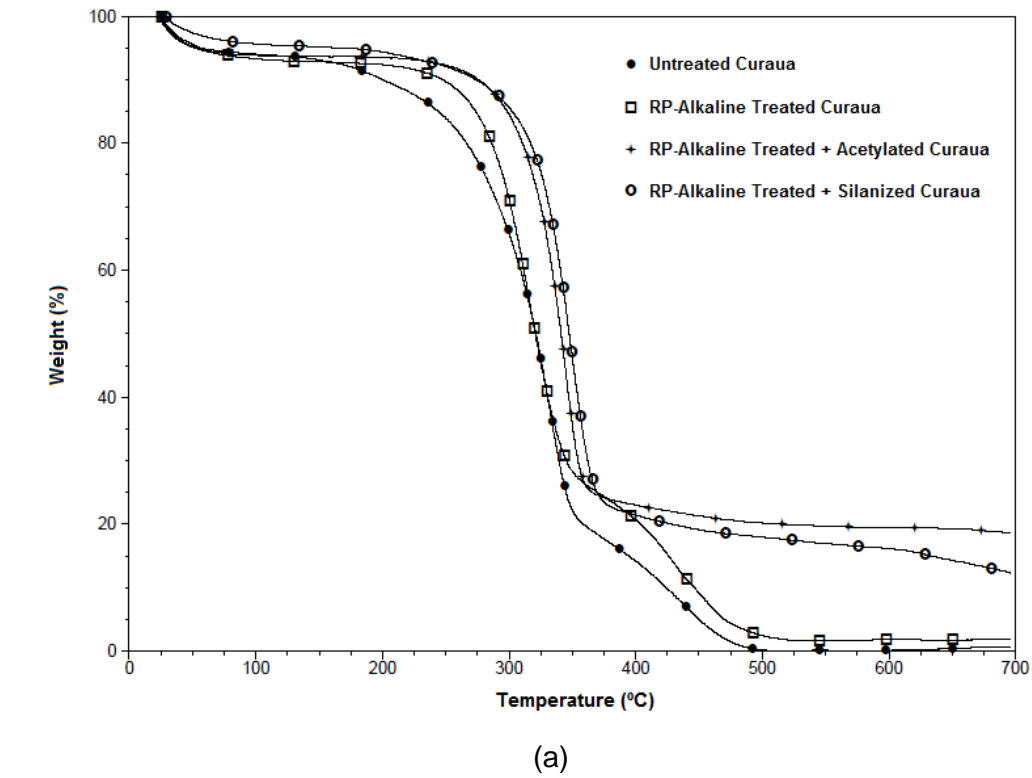


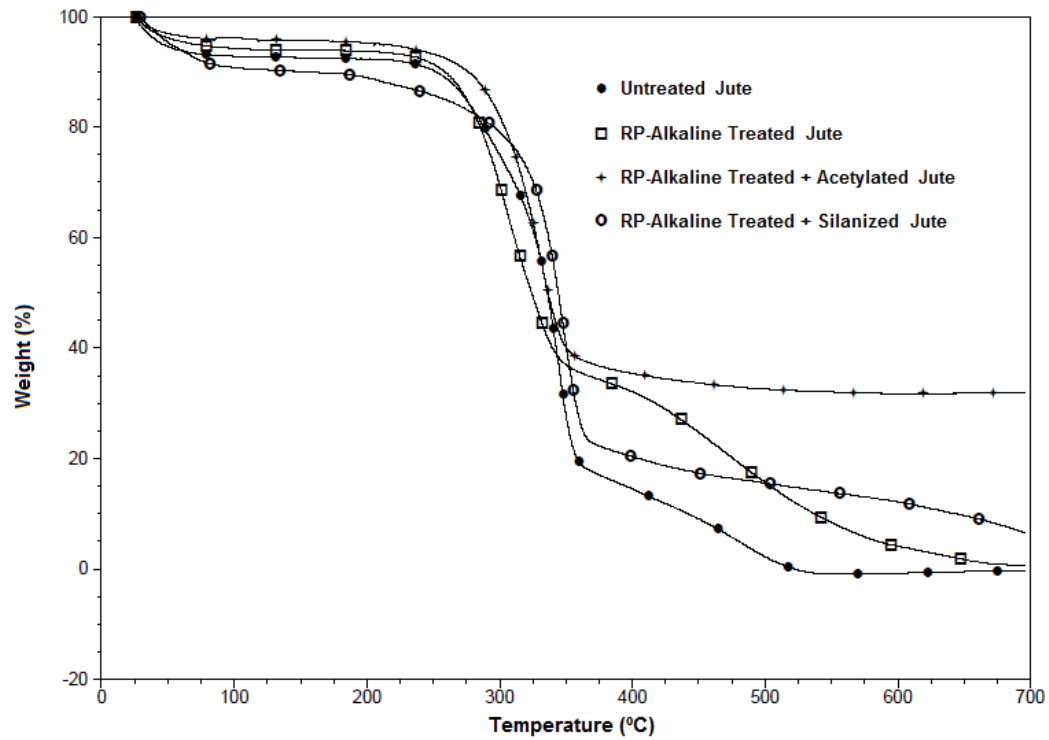
Figure 42 – TG (a) and DTG (b) patterns of curauá fibers in nature and treated with: RP alkaline solutions, acetic anhydride and silane APTES

Table 16 – Degradation temperatures of curauá fibers in nature and after chemical treatments

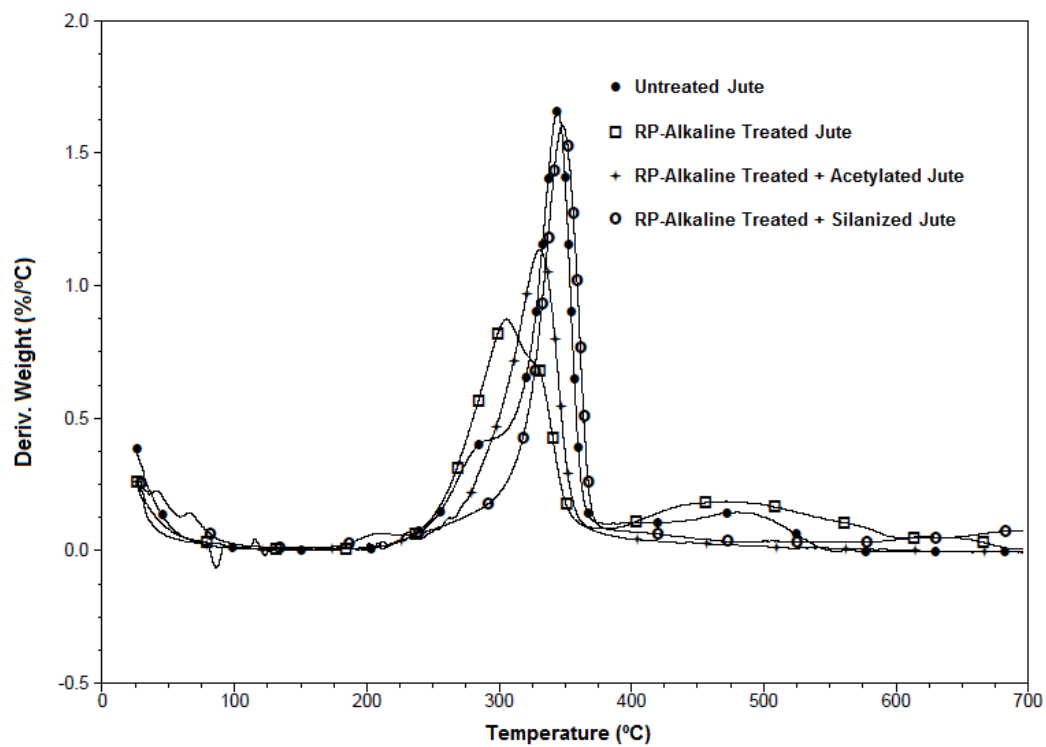
| Curauá | T_{0.05} (°C) | T_{max} (°C) | Loss at 100 °C (%) | Total loss (%) |
|----------------------------------|------------------------------|-----------------------------|---------------------------|-----------------------|
| Untreated | 217 | 333 // 439 | 5.8 | 99.2 |
| RP-Alkaline Treated | 263 | 316 // 430 // 458 | 6.7 | 98.1 |
| RP-Alkaline Treated + Acetylated | 285 | 344 | 6.2 | 81.3 |
| RP-Alkaline Treated + Silanized | 277 | 350 | 4.4 | 87.7 |

The objective of the post-treatments (acetylation and silanization) was only to increase the hydrophobicity of fibers. However, observing Figure 42 and Table 16, it can be seen that acetylation as well as silanization improved the thermal stability of RP – alkaline treated curauá fibers. This behaviour is remarkable for this fiber in terms of $T_{0.05}$ (which is the temperature of 5 wt. % mass loss after the initial loss of moisture), contrary to what was found to mercerized jute and flax. No significant change in $T_{0.05}$ was observed for them.

For curauá, these results can be correlated to the disappearance of peak at region between 420 – 500 °C in DTG (Figure 39b) in both acetylated and silanized fibers. This means that removing of lignin, in this case, can help curauá to increase its thermal stability, possibly creating crosslinking regions, leading to slight increase in $T_{0.05}$. The same event may also occur in treated jute and flax fibers. Finally, all post-treated natural fibers showed a higher char formation when compared to only RP-alkaline treated fibers.



(a)

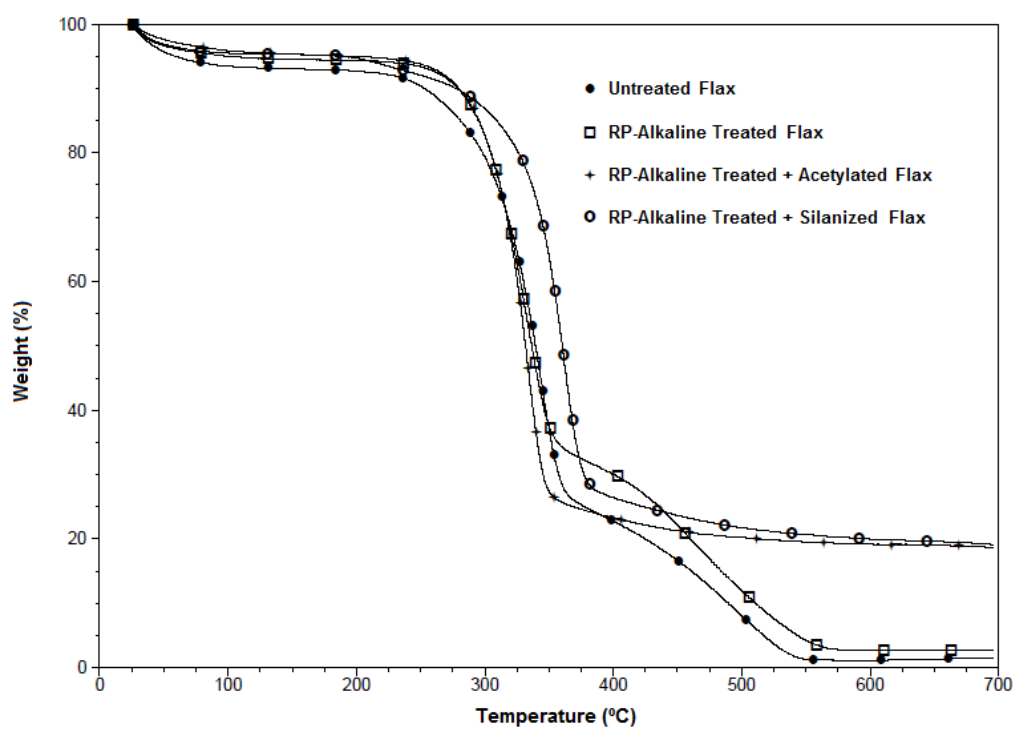


(b)

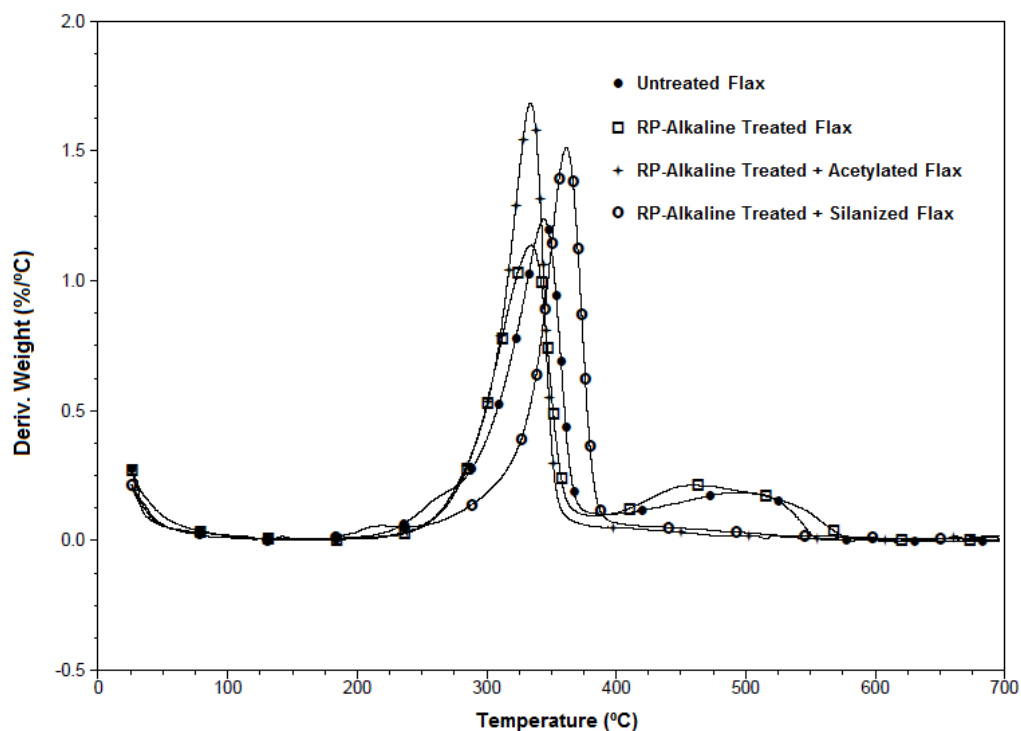
Figure 43 – TG (a) and DTG (b) patterns of jute fibers in nature and treated with: RP alkaline solutions, acetic anhydride and silane APTES

Table 17 - Degradation temperatures of jute fibers in nature and after chemical treatments

| Jute | T _{0.05} (°C) | T _{max} (°C) | Loss at 100 °C (%) | Total loss (%) |
|----------------------------------|------------------------|-----------------------|--------------------|----------------|
| Untreated | 267 | 344 | 7.2 | 100 |
| RP-Alkaline Treated | 263 | 306 | 5.8 | 99.0 |
| RP-Alkaline Treated + Acetylated | 273 | 331 | 3.9 | 67.9 |
| RP-Alkaline Treated + Silanized | 258 | 348 | 9.2 | 93.4 |



(a)



(b)

Figure 44 – TG (a) and DTG (b) patterns of flax fibers in nature and treated with: RP alkaline solutions, acetic anhydride and silane APTES

Table 18 – Degradation temperatures of flax fibers in nature and after chemical treatments

| Flax | $T_{0.05}$ (°C) | T_{max} (°C) | Loss at 100 °C (%) | Total loss (%) |
|----------------------------------|-----------------|----------------|--------------------|----------------|
| Untreated | 266 | 344 // 506 | 6.5 | 98.1 |
| RP-Alkaline Treated | 281 | 334 // 469 | 5.0 | 97.3 |
| RP-Alkaline Treated + Acetylated | 280 | 334 | 4.1 | 81.3 |
| RP-Alkaline Treated + Silanized | 276 | 362 | 4.5 | 80.7 |

It should be noted that the alkaline treatment is time-consuming (3 successive treatments, 1 hour each). For this reason, to decrease treatment time, high-pressure alkaline treatments on natural fibers were performed in autoclave and characterized by TGA and XRD, and analyzed in terms of thermal stability and crystallinity.

5.3 CHARACTERIZATION OF HIGH-PRESSURE ALKALINE TREATED FIBERS

5.3.1 X-Ray diffraction: analysis of crystallinity

For all three fibers studied, a sharp increase of crystallinity was observed at increased time of treatment, according to Table 19 and Figures 45 – 47. At only 15 minutes of treatment, there is a significant increasing in this property on all fibers when compared to untreated ones. Curauá and flax presented their maximum value of crystallinity at 45 minutes of treatment, while jute improved this property in 30 minutes.

Table 19: Degree of crystallinity of untreated and alkaline-treated natural fibers

| Sample/Fiber | Degree of crystallinity (%) | | |
|----------------------------------|-----------------------------|------|------|
| | Curauá | Jute | Flax |
| Untreated | 62 | 64 | 75 |
| HP-Alkaline Treated – 15 minutes | 70 | 72 | 80 |
| HP-Alkaline Treated – 30 minutes | 70 | 73 | 82 |
| HP-Alkaline Treated – 45 minutes | 75 | 74 | 81 |
| HP-Alkaline Treated – 60 minutes | 75 | 72 | 77 |

Comparing the maximum values reached with mercerization at room pressure carried out before, this process is more effective for removing low molar mass and, therefore, amorphous components of cellulose. For example, flax reached 80% of crystallinity index in 15 minutes of alkaline treatment at high pressure against 77% after 1h of alkaline treatment at room pressure. It is important to notice also that there is a significant difference in terms of temperature treatment. At high pressure, treatment was carried out at 120 °C, 50% more than the one performed at room pressure, 80 °C. A combination of pressure and heat should improve extraction of components of low molar mass and lignin.

As described previously in section 5.1.3, for all treated fibers (Figures 45 – 47), is also observed the three main peaks at $2\theta = 16^\circ$, 23° and 35° . They correspond to crystallographic planes (1 1 0), (0 0 2) and (0 2 3) or (0 0 4),

respectively, and characteristic for cellulose I. According to the literature (GUTIÉRREZ; DE PAOLI; FELISBERTI, 2012), chemical treatments on fibers performed do not change the cellulose structure, but the extraction of amorphous materials leads to an increase of crystallinity index.

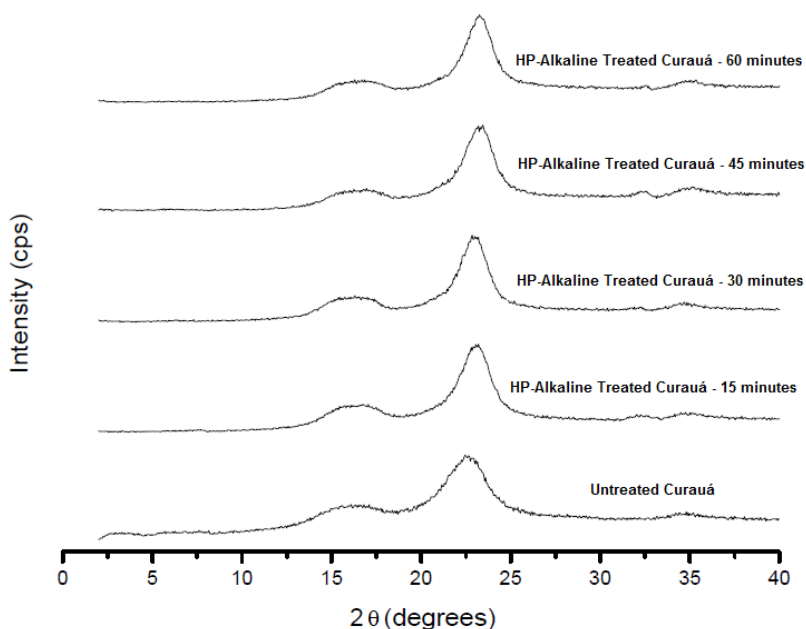


Figure 45 – Diffractograms of curauá fibers in nature and treated in autoclave with alkaline solution

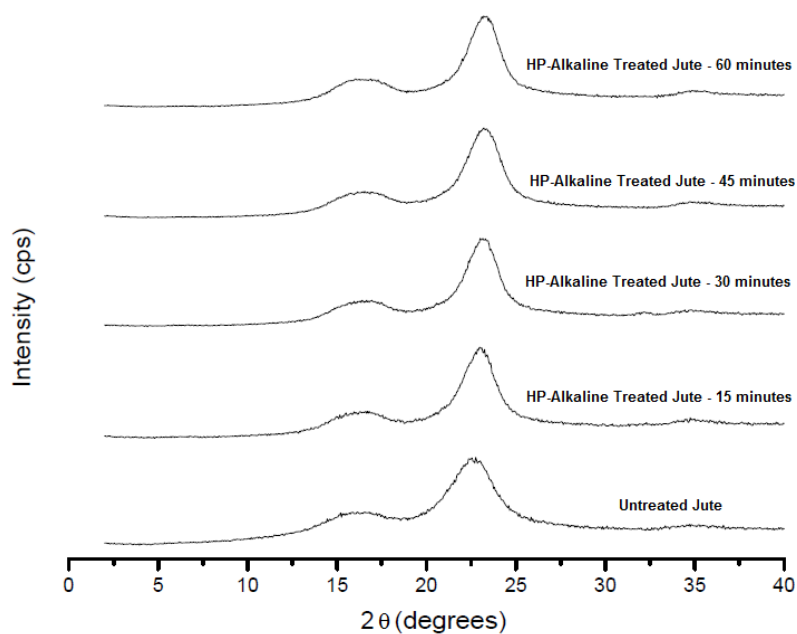


Figure 46 – Diffractograms of jute fibers in nature and treated in autoclave with alkaline solution

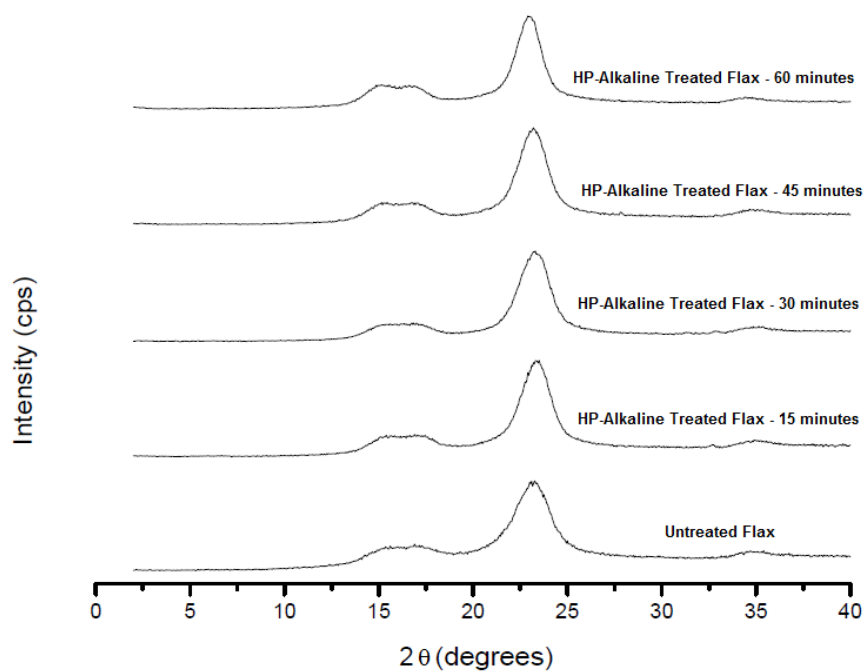
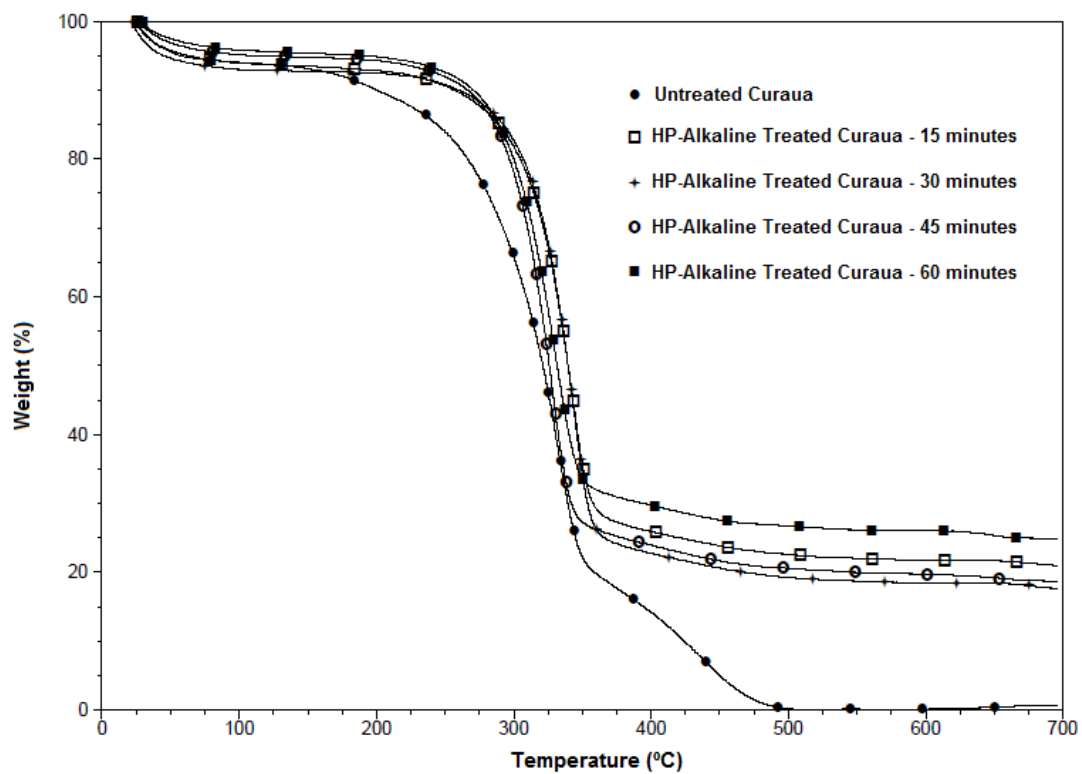


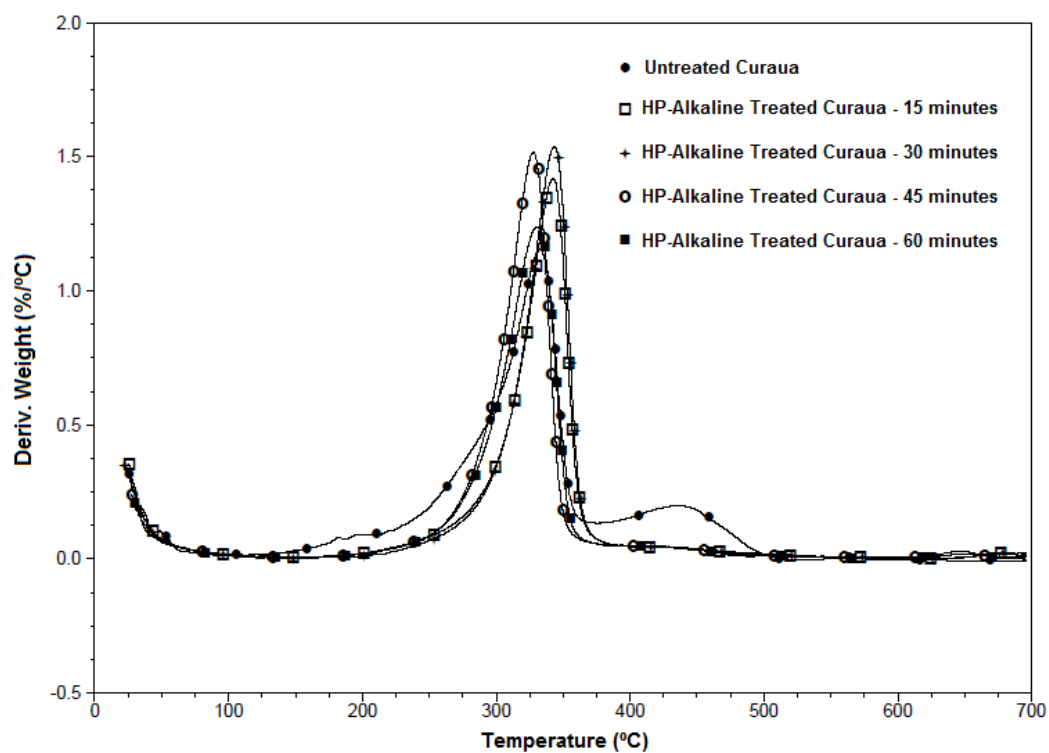
Figure 47 – Diffractograms of flax fibers in nature and treated in autoclave with alkaline solution

5.3.2 Thermal stability of high-pressure alkaline treated fibers

Confirming the XRD results, it is interesting to notice (Tables 20 – 22) that each fiber reacted of different way to the thermal decomposition. Curauá reached a maximum value of $T_{0.05}$ after 30 minutes of alkaline treatment (62 °C higher than the original fiber). On the other hand, thermal stability of flax reached higher results after 15 minutes of alkaline treatment (37 °C higher than the original fiber). Jute improved its thermal properties only after 1h treatment, with increasing of 18 °C in $T_{0.05}$ in comparison with raw materials. In terms of decomposition events of cellulose components, all HP-alkaline treated fibers keep the same behaviour when compared to mercerized fibers at room pressure (degradation in 3 stages).



(a)



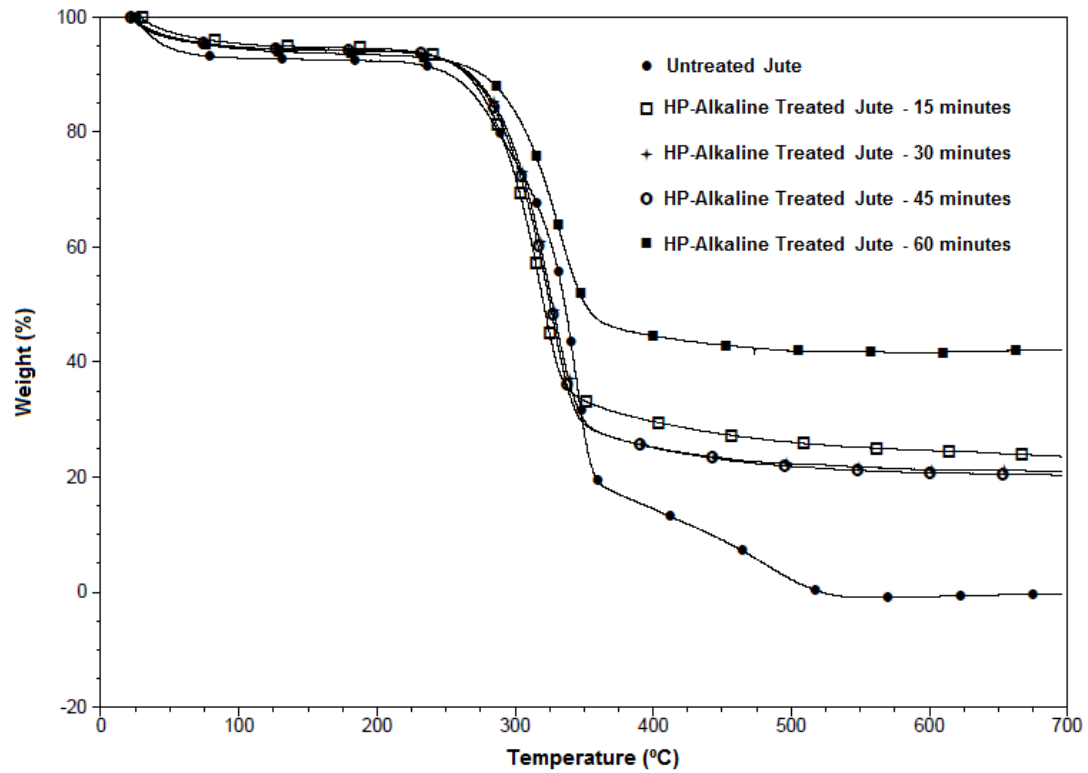
(b)

Figure 48 – TGA (a) and DTG (b) of curauá fibers in nature and treated in autoclave with alkaline solution

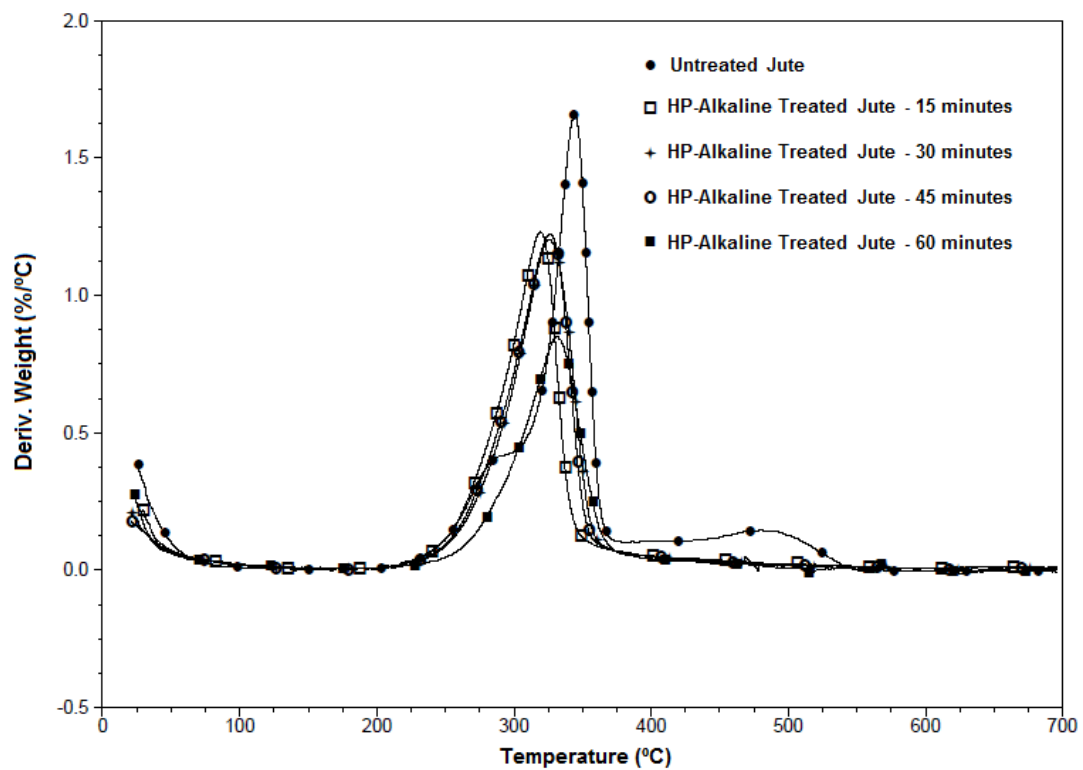
Table 20 – TGA results for curauá fibers in nature and treated in autoclave with alkaline solution

| Curauá | T _{0.05} (°C) | T _{max} (°C) | Loss at 100 °C (%) | Total loss (%) |
|----------------------------------|------------------------|-----------------------|--------------------|----------------|
| Untreated | 217 | 333 // 439 | 5.8 | 99.2 |
| HP-Alkaline Treated – 15 minutes | 273 | 342 | 6.1 | 78.9 |
| HP-Alkaline Treated – 30 minutes | 279 | 343 | 7.0 | 81.8 |
| HP-Alkaline Treated – 45 minutes | 270 | 327 | 4.9 | 81.1 |
| HP-Alkaline Treated – 60 minutes | 270 | 330 | 4.2 | 75.0 |

Moreover, the first derivative curves (DTG) of the fibers clearly show hemicelluloses and lignin removal by the disappearance of their correspondent curves shoulder (275 °C) for hemicelluloses and range between 420 – 500 °C for lignin) for all the fibers. By DTG, it can be observed an increase of T_{max} for flax and curauá fibers, after 15 and 30 minutes, respectively. Otherwise, it was noted a decrease of T_{max} for jute fibers in all time studied, compared to pure fiber. It confirms the previous results with room pressure treatments that the alkaline treatments on jute fibers are much less effective, contrary to curauá and flax.



(a)

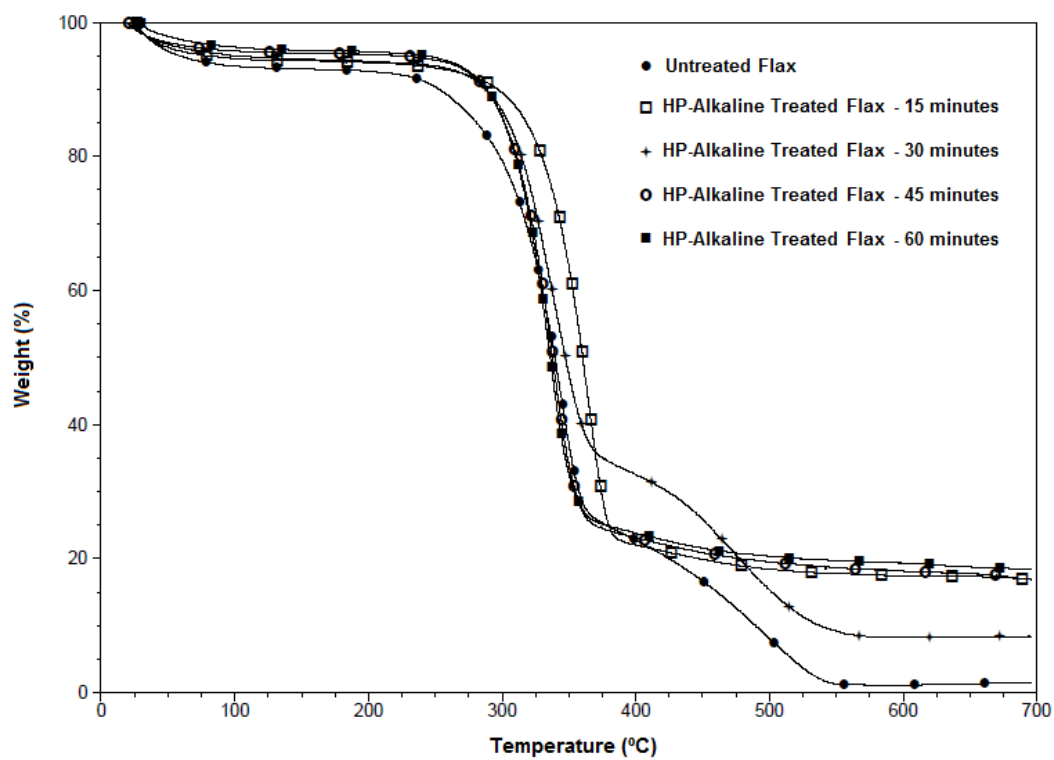


(b)

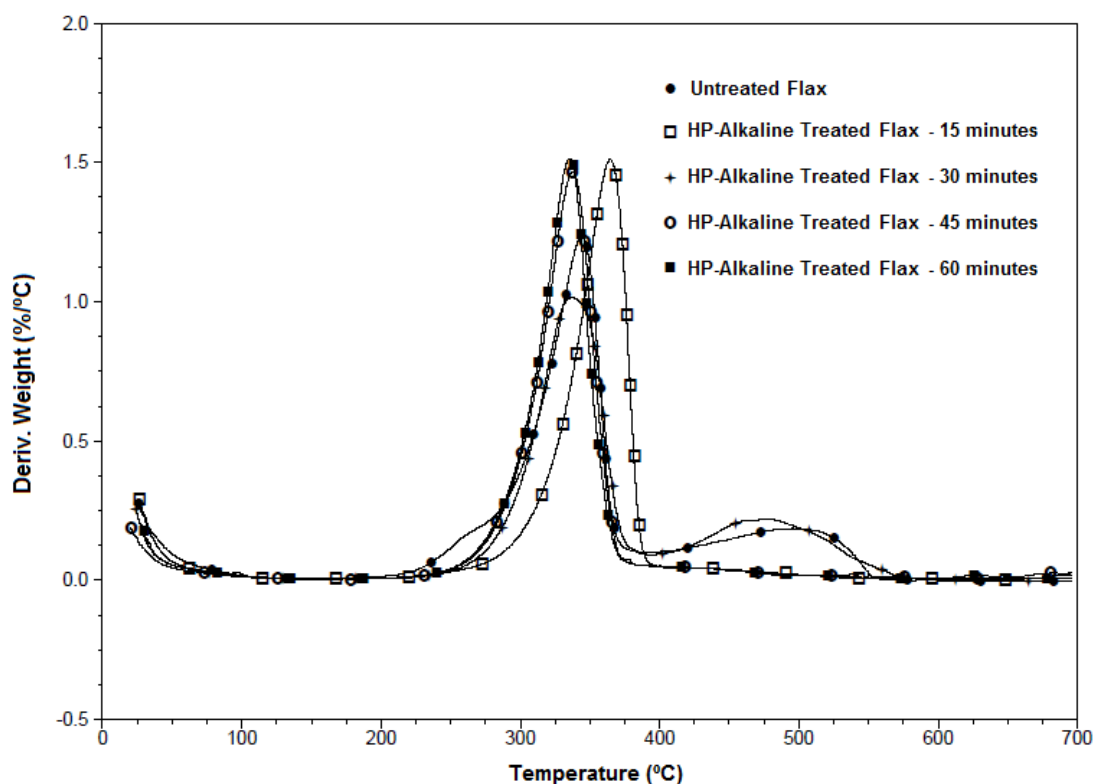
Figure 49 – TGA (a) and DTG (b) of jute fibers in nature and treated in autoclave with alkaline solution

Table 21 – TGA results for jute fibers in nature and treated in autoclave with alkaline solution

| Jute | T _{0.05} (°C) | T _{max} (°C) | Loss at 100 °C (%) | Total loss (%) |
|----------------------------------|------------------------|-----------------------|--------------------|----------------|
| Untreated | 267 | 344 | 7.2 | 100 |
| HP-Alkaline Treated – 15 minutes | 266 | 319 | 4.7 | 76.4 |
| HP-Alkaline Treated – 30 minutes | 272 | 326 | 5.4 | 79.1 |
| HP-Alkaline Treated – 45 minutes | 269 | 326 | 5.3 | 79.7 |
| HP-Alkaline Treated – 60 minutes | 284 | 331 | 5.6 | 57.9 |



(a)



(b)

Figure 50 – TGA (a) and DTG (b) of flax fibers in nature and treated in autoclave with alkaline solution

Table 22 – TGA resultd for flax fibers in nature and treated in autoclave with alkaline solution

| Flax | $T_{0.05}$ (°C) | T_{max} (°C) | Loss at 100 °C (%) | Total loss (%) |
|----------------------------------|-----------------|----------------|--------------------|----------------|
| Untreated | 266 | 344 // 506 | 6.5 | 98.1 |
| HP-Alkaline Treated – 15 minutes | 303 | 365 | 5.4 | 83.1 |
| HP-Alkaline Treated – 30 minutes | 292 | 337//478 | 5.0 | 91.6 |
| HP-Alkaline Treated – 45 minutes | 287 | 337 | 4.3 | 83.2 |
| HP-Alkaline Treated – 60 minutes | 286 | 335 | 3.7 | 81.6 |

Finally, considering all results in terms of thermal degradation, and the most important parameter, it can be concluded that alkaline treatments performed in high-pressure are more effective than the ones at room-pressure, bringing in a shorter treatment time a higher thermal resistance. Looking at the different responses of the three studied fibers (curauá, jute and flax) to the HP-alkaline

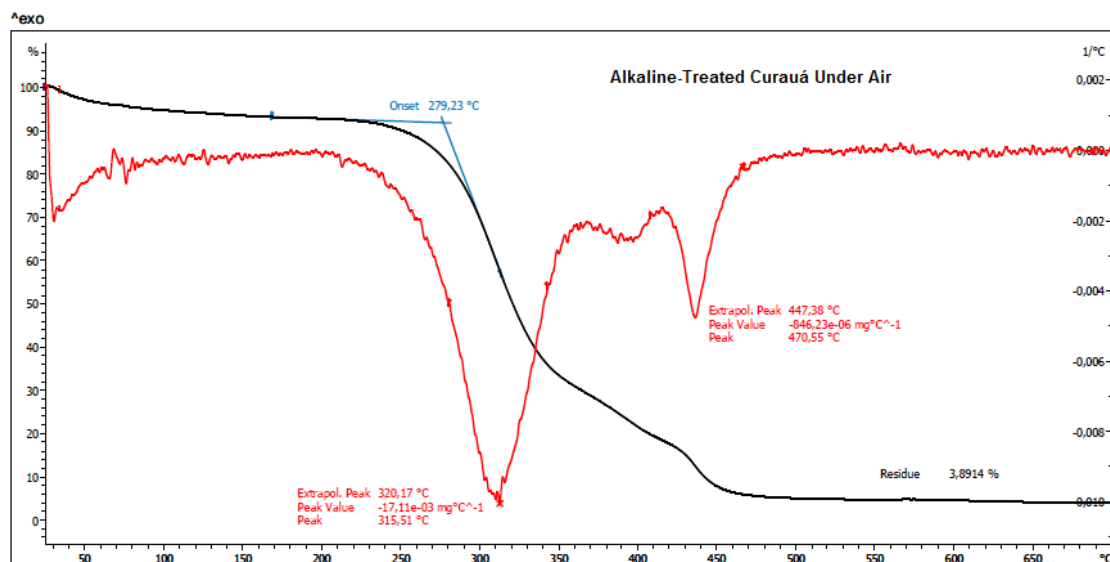
treatment, it was decided to fix 30 minutes of HP mercerization for all fibers before performing post-treatments and preparing composites using polyamide 6 and 6.6 as matrixes.

5.4 INFLUENCE OF GASEOUS ENVIRONMENT ON DEGRADATION AND PROPERTIES OF NATURAL FIBER FILLED POLYMER COMPOSITES

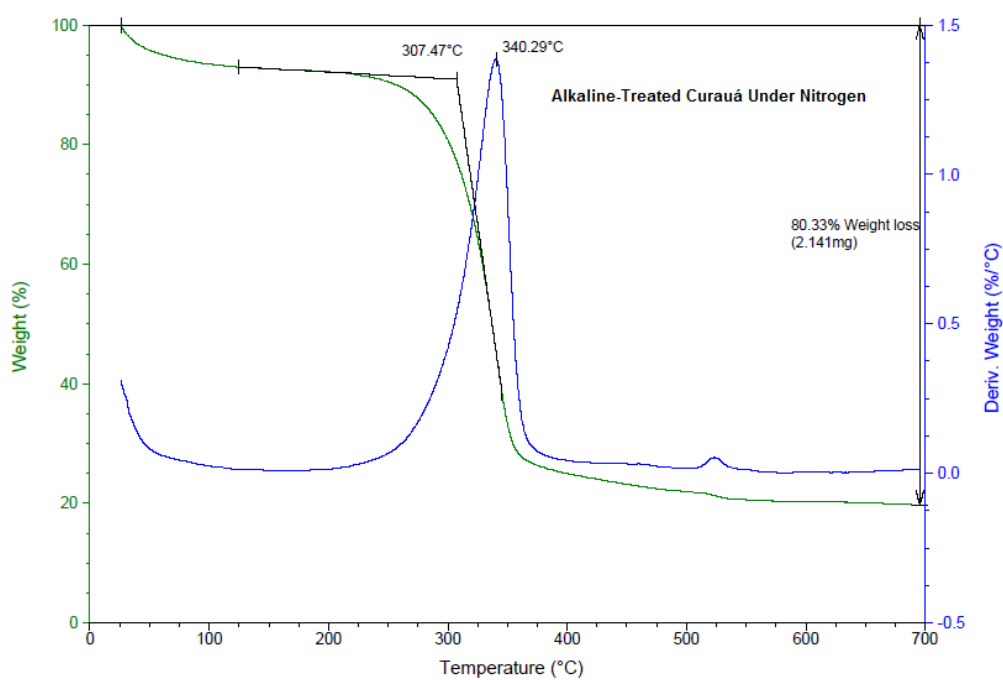
5.4.1 Thermostability of Fibers in Air and Nitrogen Studied by TGA

Results of thermal degradation of all treated fibers (curauá, jute and flax) under oxidative atmosphere and under nitrogen are shown in Tables 23 – 25 and some curves in Figures 51 – 53. As expected, decomposition in air occurs at lower temperatures than the ones under nitrogen. This behavior is more pronounced in treated curauá fibers. Decomposition under air, the ash content is significantly lower than found in degradation under nitrogen.

In general, when cellulose is heated, it occurs its dehydration by an endothermic process, as illustrated in Figures 51 – 53, leading to a compound called by some authors “dehydrocellulose” and generally takes place in a range between 200 – 280 °C. At 280 °C, a depolymerization reaction competes for the residual cellulose and product escapes as a tar. Levoglucosan (1,6-anhydro- β -D-glucopyranose) is an essential intermediate at this stage. Finally, decomposition of “dehydrocellulose” formed before occurs *via* one or several exothermic reactions forming gas and residual char (ARSENAU, 1971; KILZER, 1971; SOARES; CAMINO; LEVCHIK, 1995). At temperatures above 300 °C, cellulose is decomposed by an alternative pathway, providing a tarry pyrolyzate containing levoglucosan, other anhydroglucose compounds, randomly linked oligosaccharides and glucose decomposition products (SHAFIZADEH, 1982).



(a)



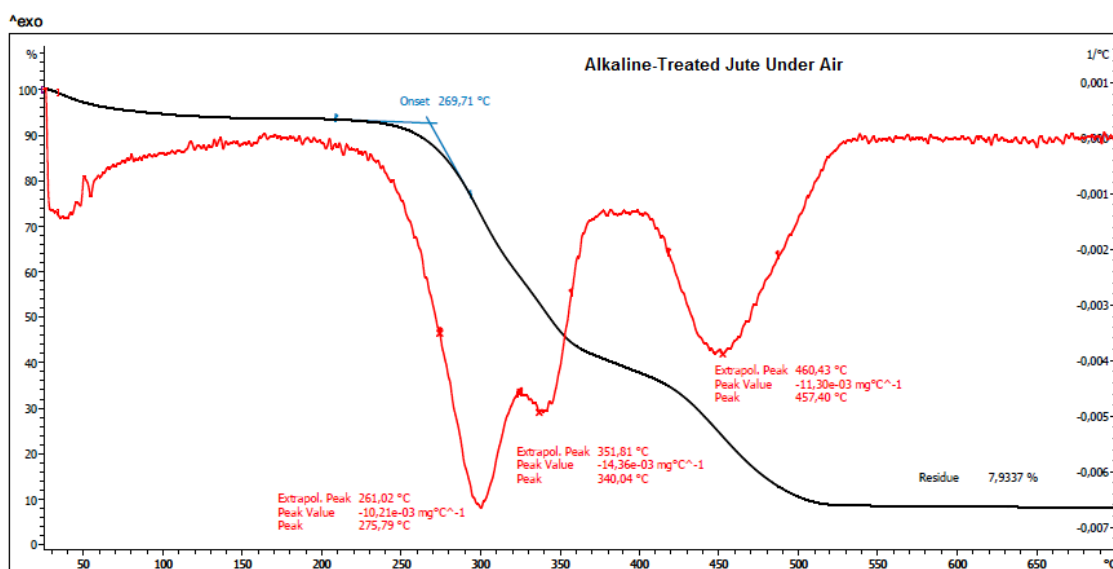
(b)

Figure 51: Thermal behaviour under (a) air and under (b) nitrogen of treated curauá fibers

Table 23: Decomposition under air and under nitrogen of treated curauá fibers

| Curauá | Nitrogen | | | Air | | | T _{0.05} (Nitrogen – Air) (°C) |
|-------------|------------------------|-----------------------|-------------|------------------------|-----------------------|-------------|--|
| | T _{0.05} (°C) | T _{max} (°C) | Residue (%) | T _{0.05} (°C) | T _{max} (°C) | Residue (%) | |
| Alk-treated | 273 | 340 | 19.7 | 251 | 320/447 | 3.9 | 22 |
| Acetylated | 282 | 340 | 16.1 | 260 | 310/401/449 | 2.3 | 22 |
| Silanized | 257 | 358 | 16.3 | 242 | 310/402 | 0 | 15 |

At high temperatures, degradation of cellulose is a first-order reaction. At lower temperatures, there is an initiation that is prolonged as temperature is lowered, since the first-order reaction is diminished. Pyrolysis takes place quickly at higher temperatures *via* transglycosylation reactions leading to anhydro sugars as the principal thermolysis products. These processes outshine the effect of oxygen, whereas at lower temperatures, oxygen plays a dominant role and oxidative degradation gradually occurs faster than under nitrogen. Moreover, it was found in literature (SHAFIZADEH; BRADBURY, 1979) that activation energy for cleavage of cellulosic bonds are higher in nitrogen (27 Kcal/mol) than under air (21 Kcal/mol). This data indicates that, at lower temperatures, a larger number of bonds are cleaved under oxidative atmosphere than in nitrogen.



(a)

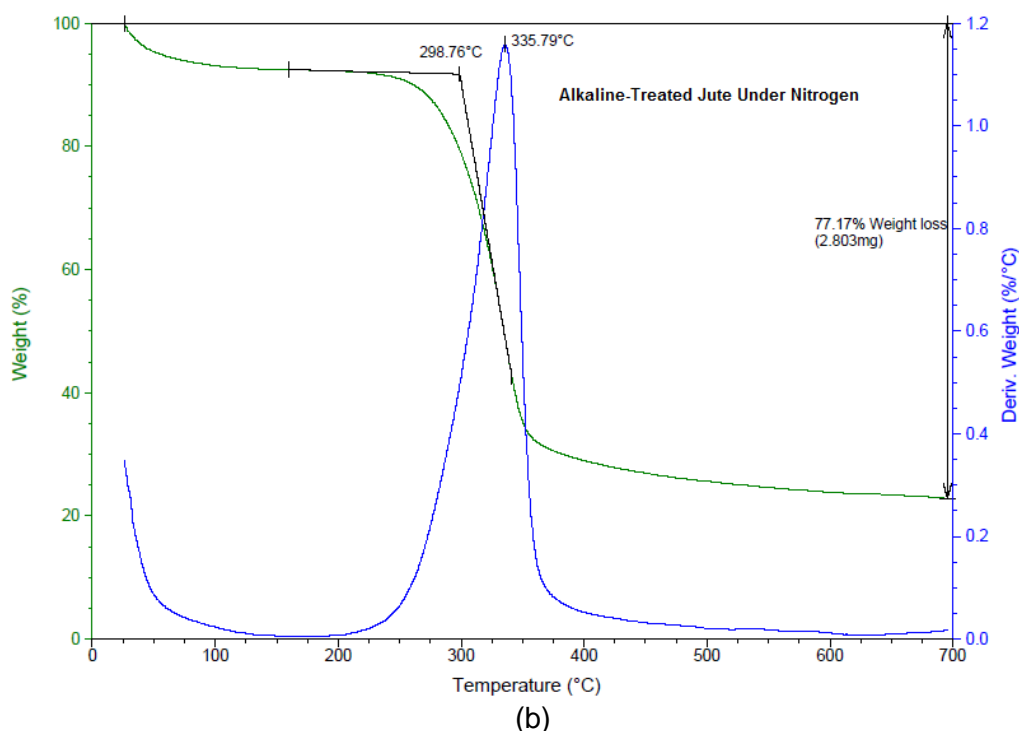


Figure 52: Thermal behaviour under (a) air and under (b) nitrogen of treated jute fibers

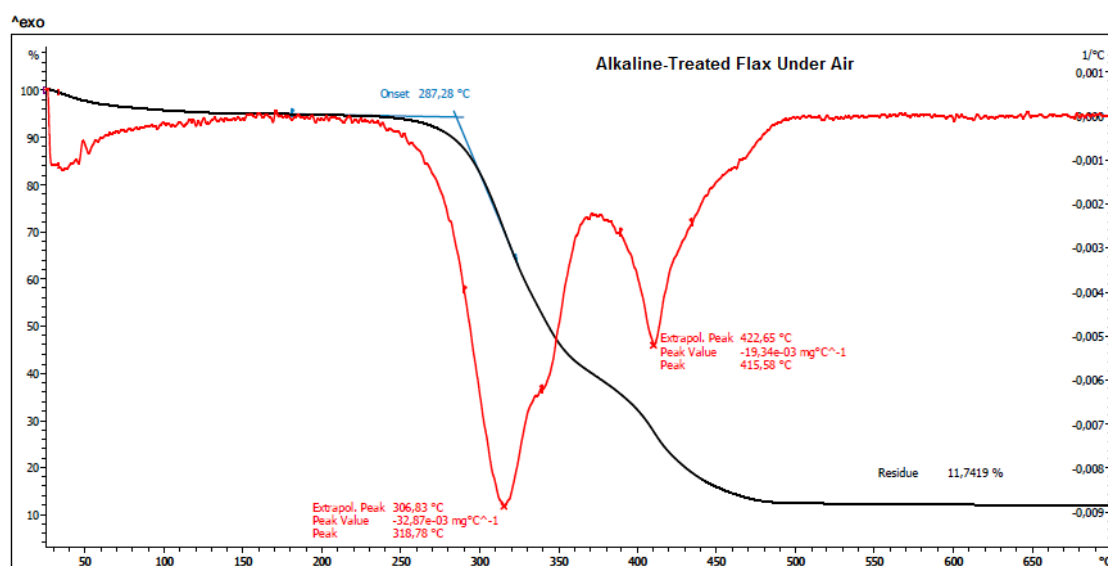
Table 24: Decomposition under air and under nitrogen of treated jute fibers

| Jute | Nitrogen | | | Air | | | $T_{0.05}$ (Nitrogen – Air) (°C) |
|--------------------|--------------------|-------------------|----------------|--------------------|----------------|----------------|-------------------------------------|
| | $T_{0.05}$ (°C) | T_{max} (°C) | Residue (%) | $T_{0.05}$ (°C) | T_{max} (°C) | Residue (%) | |
| Alk-treated | 275 | 336 | 22.8 | 262 | 276/340/457 | 7.9 | 13 |
| Acetylated | 280 | 341 | 20.9 | 267 | 312/434 | 2.1 | 13 |
| Silanized | 286 | 366 | 12.3 | 273 | 334/473 | 4.2 | 13 |

For almost all treated fibers, with exception of alkaline-treated jute, the T_{max} of main peaks in DTG is shifted to lower values in air, reflecting the oxidative degradation of cellulose, since under air the necessary energy to break cellulosic bonds is lower than under nitrogen. Moreover, under nitrogen, there is no maximum peaks at around 420 – 470 °C, characteristic of lignin degradation. Under oxidative atmosphere, in all treated fibers, it appear peaks in this temperature range, meaning that lignin is consumed and the remaining char is oxidised. So, the amount of char is lower in degradation under air than the one under nitrogen. It is important to remember that lignin is made of aromatic compounds that have numerous branches and is highly crosslinked. Thus, this

structure give high thermal stability to lignin and, consequently, decreases its degradation at inert atmosphere.

Finally, in a general overview, treated curauá fibers shows slightly higher values in difference of degradation in terms of $T_{0.05}$ (air x nitrogen) than other treated fibers. Degree of crystallinity of fibers could explain this difference. Even after 30 minutes of high-pressure alkaline treatments (Table 19), curauá fibers show less crystallinity than jute and flax. Therefore, less activation energy is required to break cellulosic glycosidic bonds, increasing the difference in degradations. Moreover, treated jute and flax showed similar differences, mainly alkaline-treated and alkaline-treated + acetylated fibers.



(a)

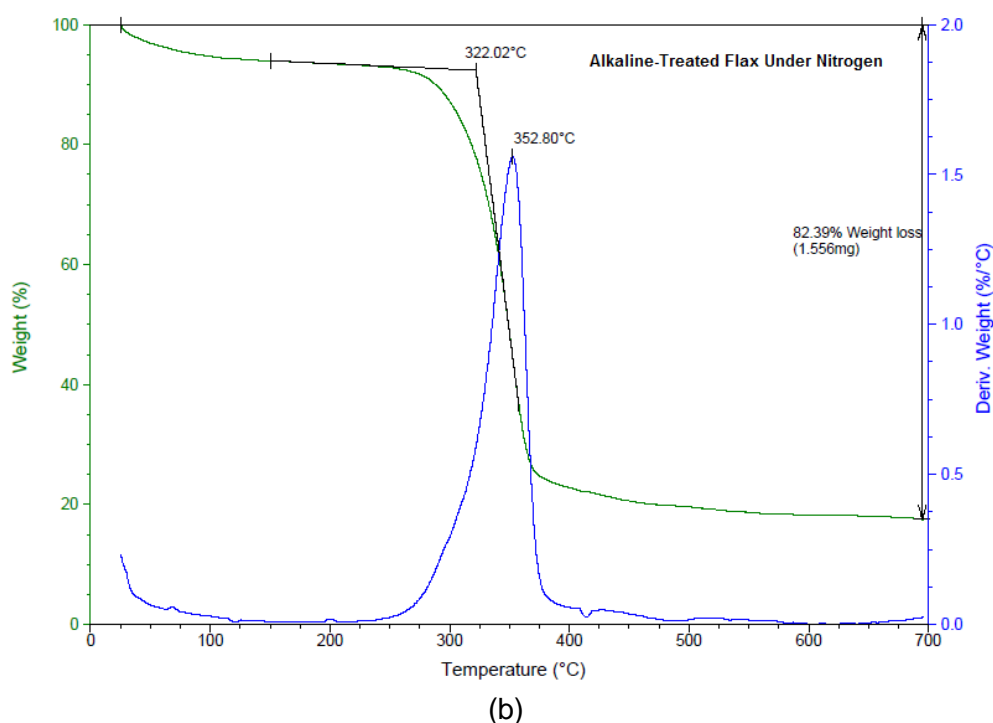


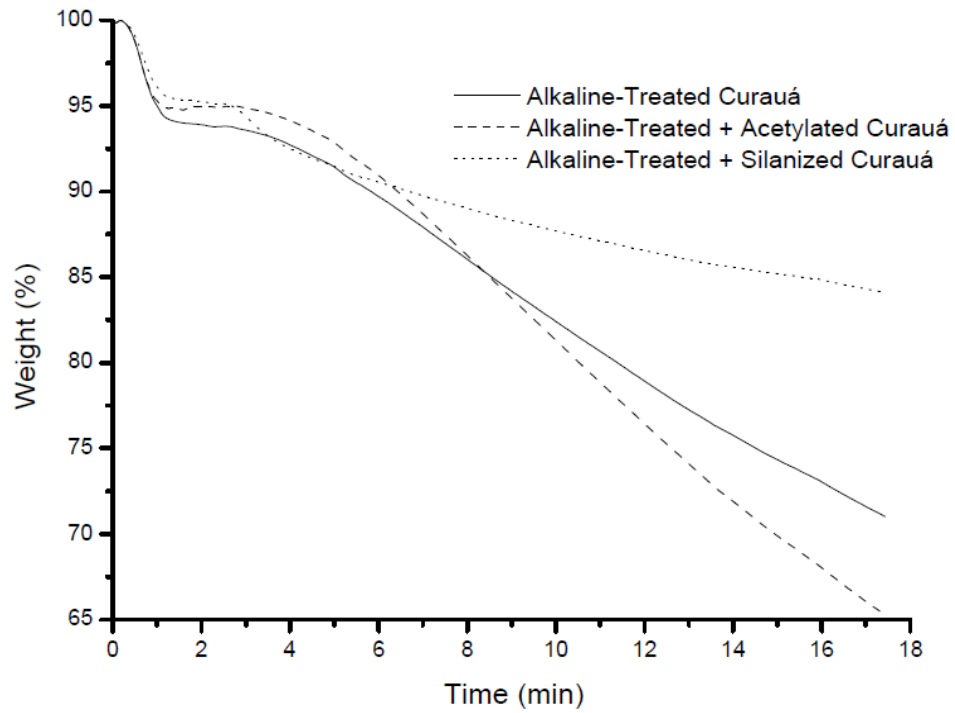
Figure 53: Thermal behaviour under (a) air and under (b) nitrogen of treated flax fibers

Table 25: Decomposition under air and under nitrogen of treated flax fibers

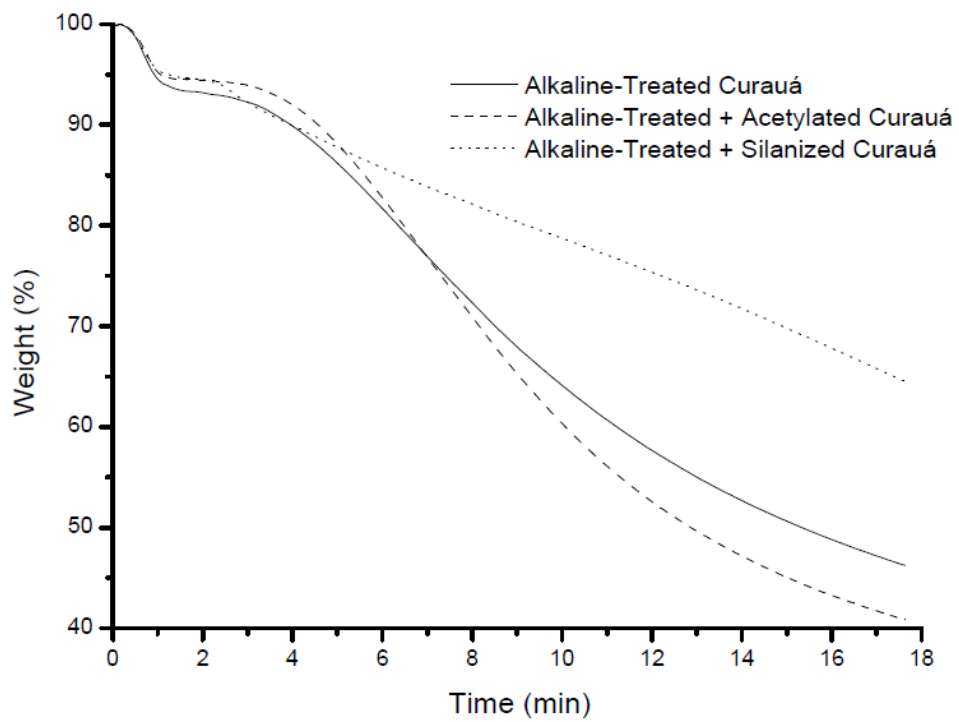
| Flax | Nitrogen | | | Air | | | $T_{0.05}$ (Nitrogen – Air) (°C) |
|--------------------|--------------------|-------------------|----------------|--------------------|---------------------|----------------|-------------------------------------|
| | $T_{0.05}$ (°C) | T_{max} (°C) | Residue (%) | $T_{0.05}$ (°C) | T_{max} (°C) | Residue (%) | |
| Alk-treated | 292 | 353 | 17.6 | 282 | 319/416 | 11.7 | 10 |
| Acetylated | 293 | 351 | 19.0 | 280 | 320/415 | 0 | 13 |
| Silanized | 237 | 231/355 | 23.0 | 241 | 214/322/457/ 480 | 5.7 | -4 |

5.4.2 Isothermal of treated fibers under air and under nitrogen

Isothermal behaviour of treated natural fibers can be seen in Tables 26 – 28 and Figures 54 – 59. Two temperatures were analyzed, 270 and 290 °C, in order to get an estimate of acceptable compounding times with high melting temperature matrices, as polyamide 6.6. In all isotherms, during the quick heating ramp (100 °C/min), all treated fibers showed a weight loss (5.0 to 7.0 wt.% approximately) and this can be attributed to moisture content of them. The amount of adsorbed water depends on the conditions of storage of fibers.



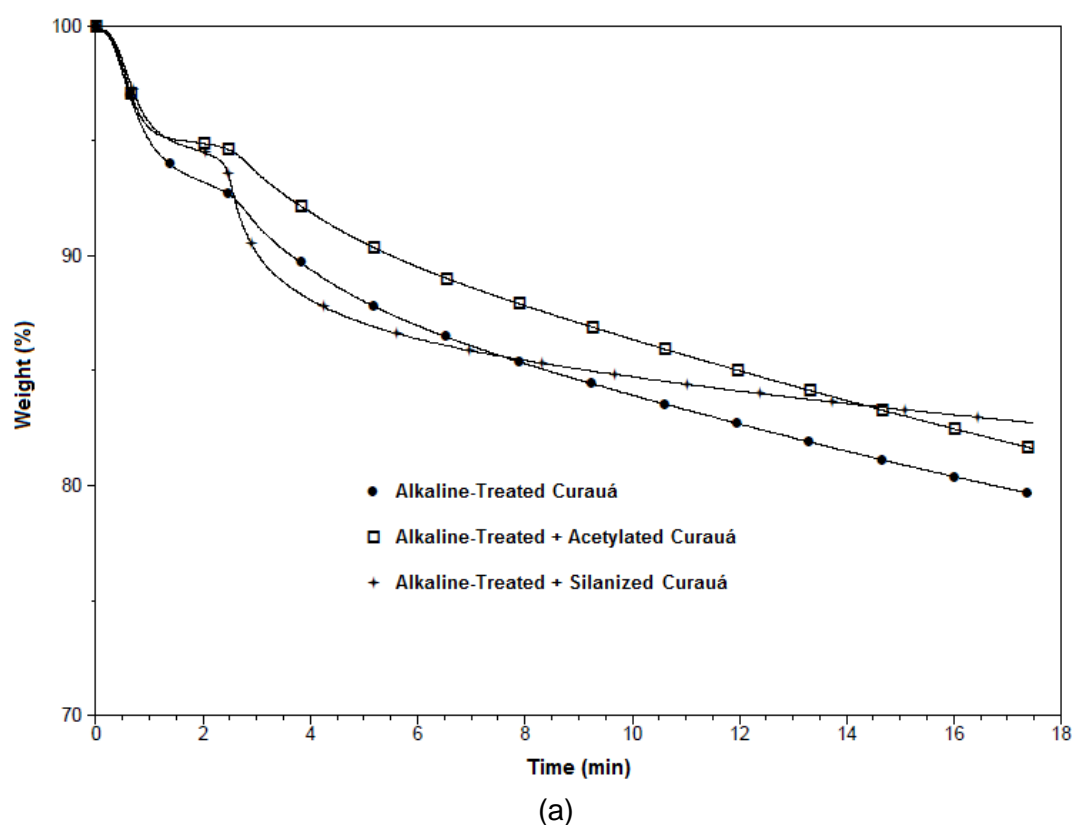
(a)

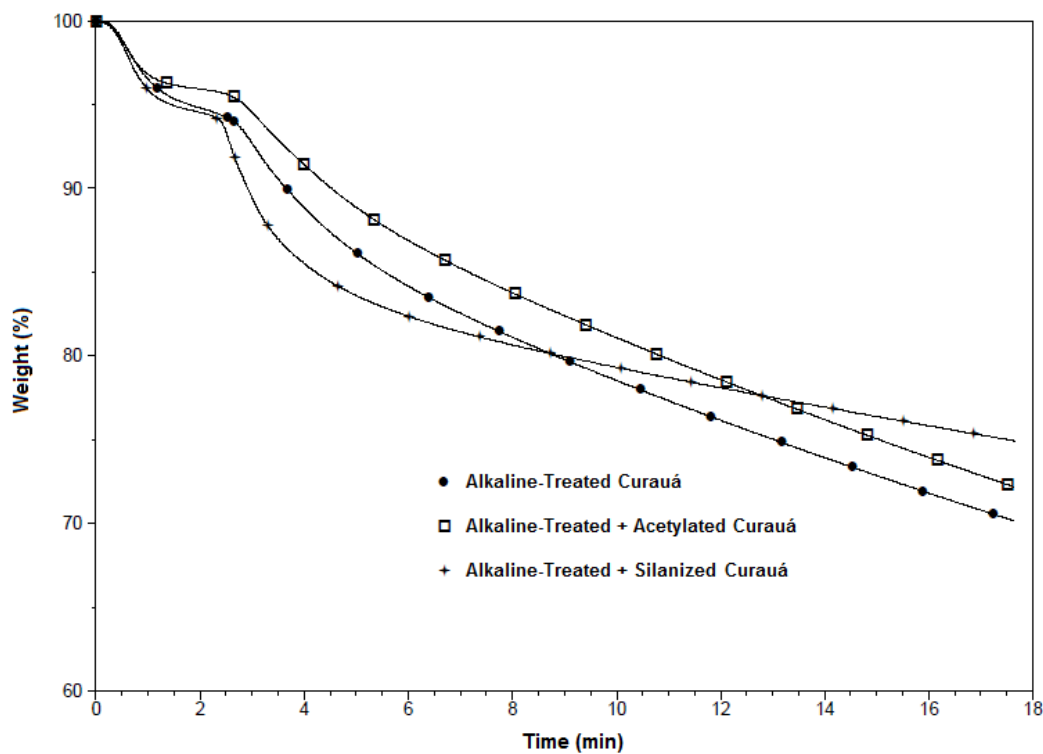


(b)

Figure 54: Isothermal decompositions under air of treated curauá fibers at (a) 270 °C and (b) 290 °C

Some events can be noted from these experiments: in all cases, increasing of isothermal temperature degradation leads to decreasing of final residues and, obviously, this event is more aggressive under oxidative environment mainly due to less activation energy required to break glycosidic bonds in air than under nitrogen, as already discussed. However, treated fibers respond to the degradation under air at different temperatures in different ways. Treated curauá fibers showed, in average, a range of 20 – 25% higher mass loss at 290 °C than at 270°C under air. Jute and flax presented similar differences (10 – 15 wt.% higher mass loss). Even less crystalline than flax, according to Table 19, jute has higher lignin content (12 wt.% vs. 2 wt.%) and part of it remains even after chemical treatments, as can be seen in DTG curve under air (Figure 52a). So, despite less crystalline than flax, lignin content can equalize this effect and, therefore, explain this similar difference. Less crystallinity compared with flax, as well as removal of hemicellulose (DTG curve in Figure 51a), compared to the jute fibers, can explain why curauá undergoes more aggressive degradation than the two others. Finally, all treated fibers showed approximately same behaviour in terms of difference of mass loss at different temperatures (10 – 15 wt. %).



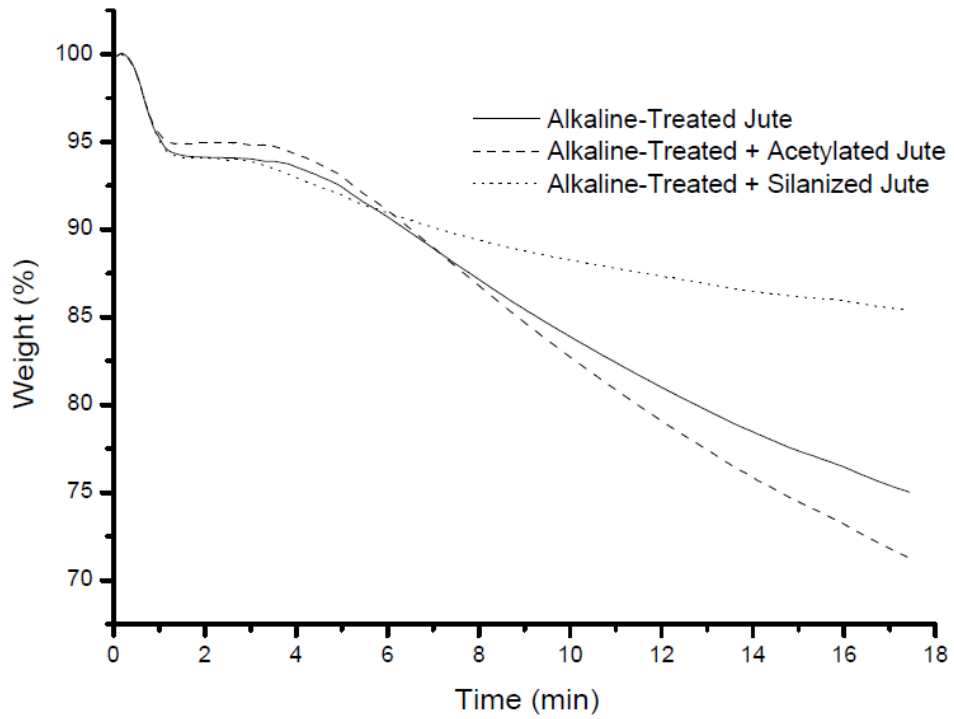


(b)

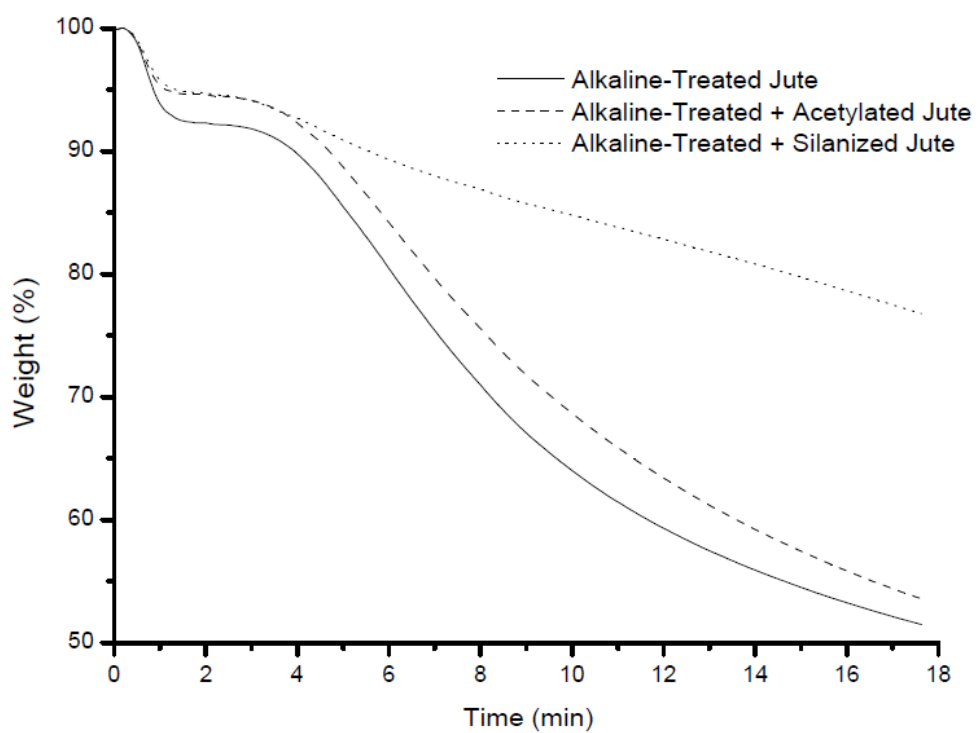
Figure 55: Isothermal decompositions under nitrogen of treated curauá fibers at (a) 270 °C and (b) 290 °C

Table 26: Isothermal decompositions of treated curaua fibers

| Temperature | | 270 °C | | 290 °C | |
|-------------------------------|------------|--------------------------|------------------------------|--------------------------|------------------------------|
| Curauá | Atmosphere | Degradation rate (%/min) | Residue after 18 minutes (%) | Degradation rate (%/min) | Residue after 18 minutes (%) |
| Alkaline-Treated | Air | 1.75 | 70 | 4.33 | 46 |
| | Nitrogen | 1.10 | 80 | 1.95 | 70 |
| Alkaline-Treated + Acetylated | Air | 2.45 | 66 | 5.73 | 40 |
| | Nitrogen | 1.03 | 81 | 1.90 | 72 |
| Alkaline-Treated + Silanized | Air | 0.73 | 86 | 1.78 | 64 |
| | Nitrogen | 0.75 | 83 | 1.22 | 75 |

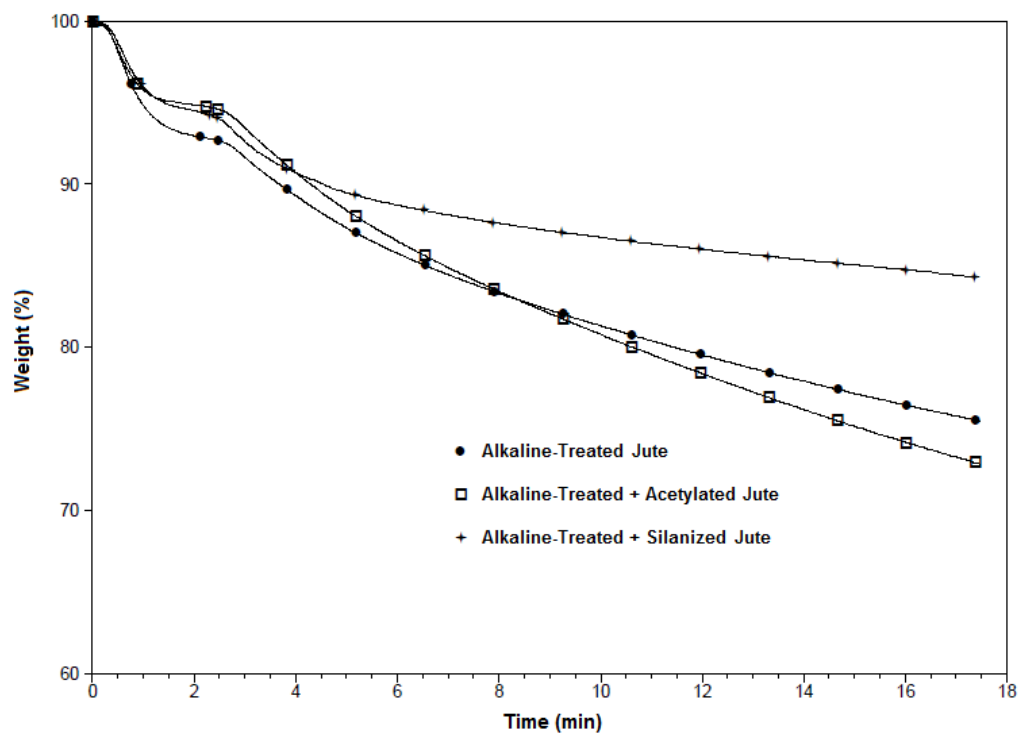


(a)

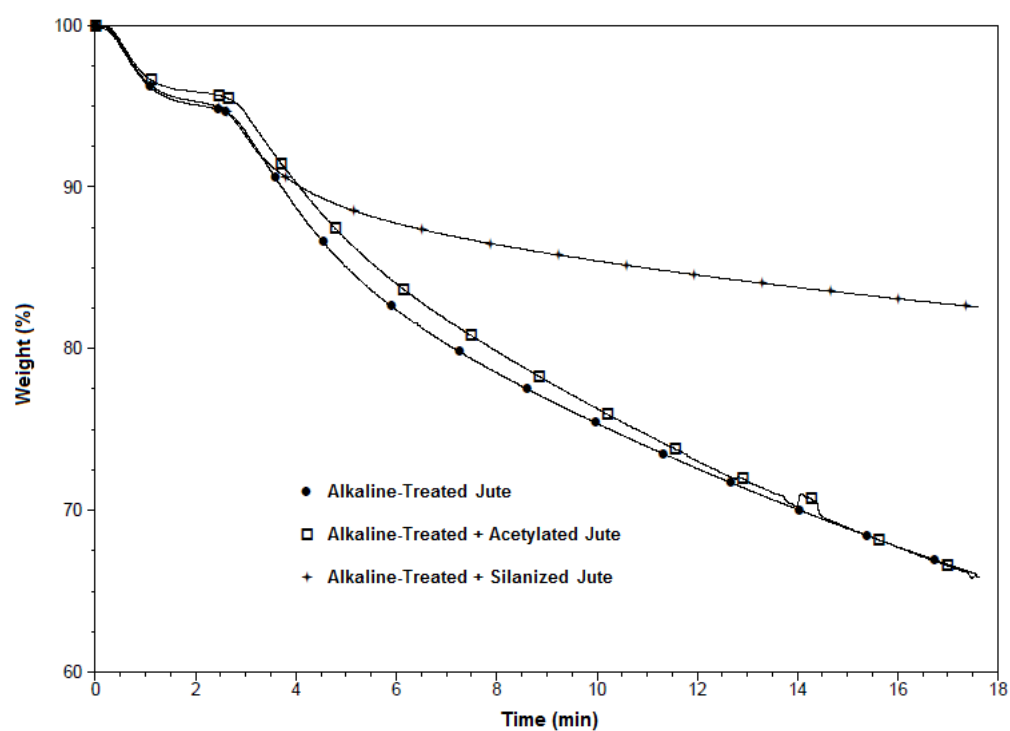


(b)

Figure 56: Isothermal decompositions under air of treated jute fibers at (a) 270 °C and (b) 290 °C



(a)

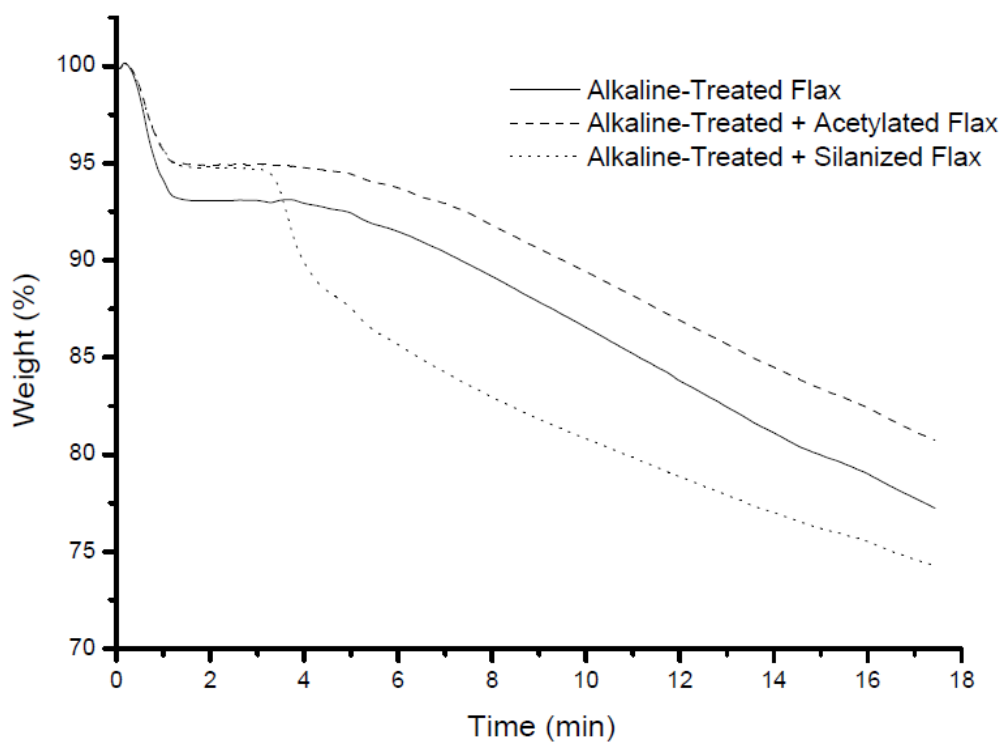


(b)

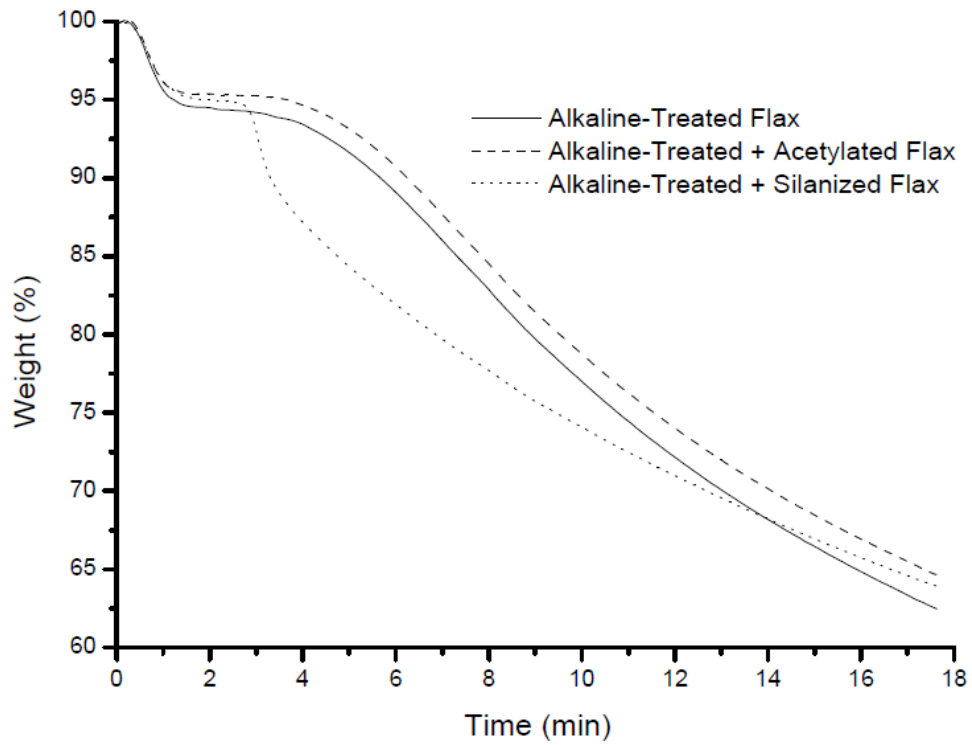
Figure 57: Isothermal decompositions under nitrogen of treated jute fibers at (a) 270 °C and (b) 290 °C

Table 27: Isothermal decompositions of treated jute fibers

| Temperature | | 270 °C | | 290 °C | |
|-------------------------------|------------|--------------------------|------------------------------|--------------------------|------------------------------|
| Jute | Atmosphere | Degradation rate (%/min) | Residue after 18 minutes (%) | Degradation rate (%/min) | Residue after 18 minutes (%) |
| Alkaline-Treated | Air | 1.60 | 75 | 4.73 | 52 |
| | Nitrogen | 1.80 | 76 | 2.22 | 66 |
| Alkaline-Treated + Acetylated | Air | 1.85 | 70 | 4.23 | 54 |
| | Nitrogen | 1.80 | 73 | 2.57 | 66 |
| Alkaline-Treated + Silanized | Air | 0.90 | 86 | 1.37 | 76 |
| | Nitrogen | 0.88 | 84 | 0.93 | 82 |

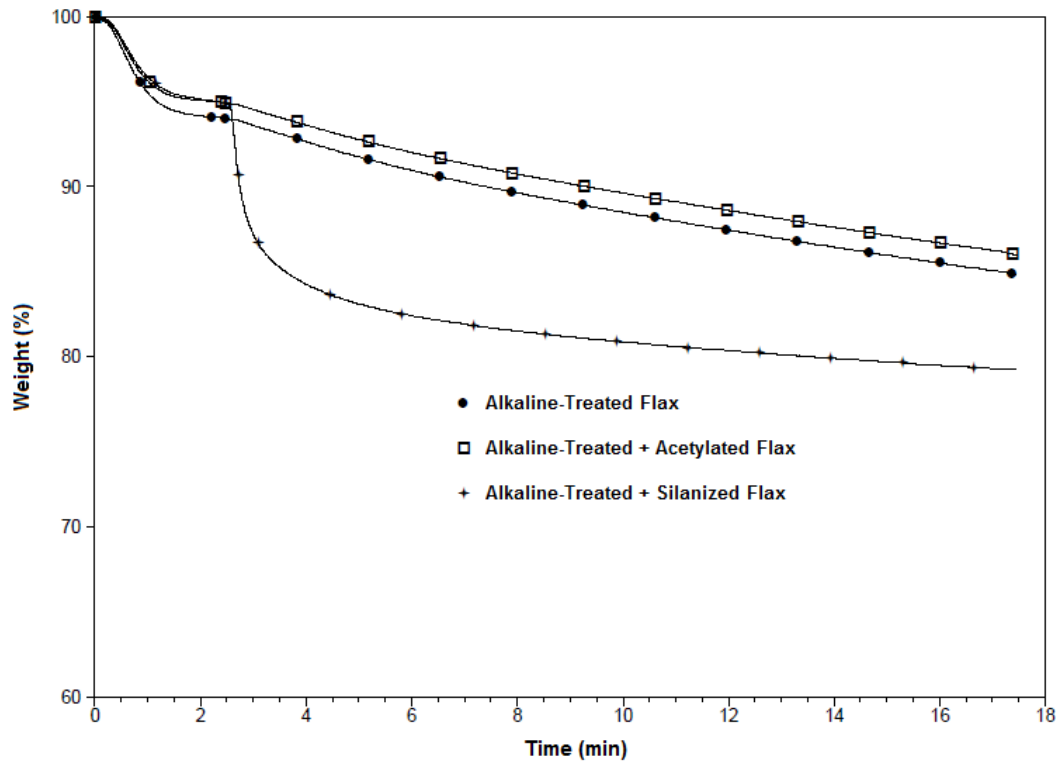


(a)

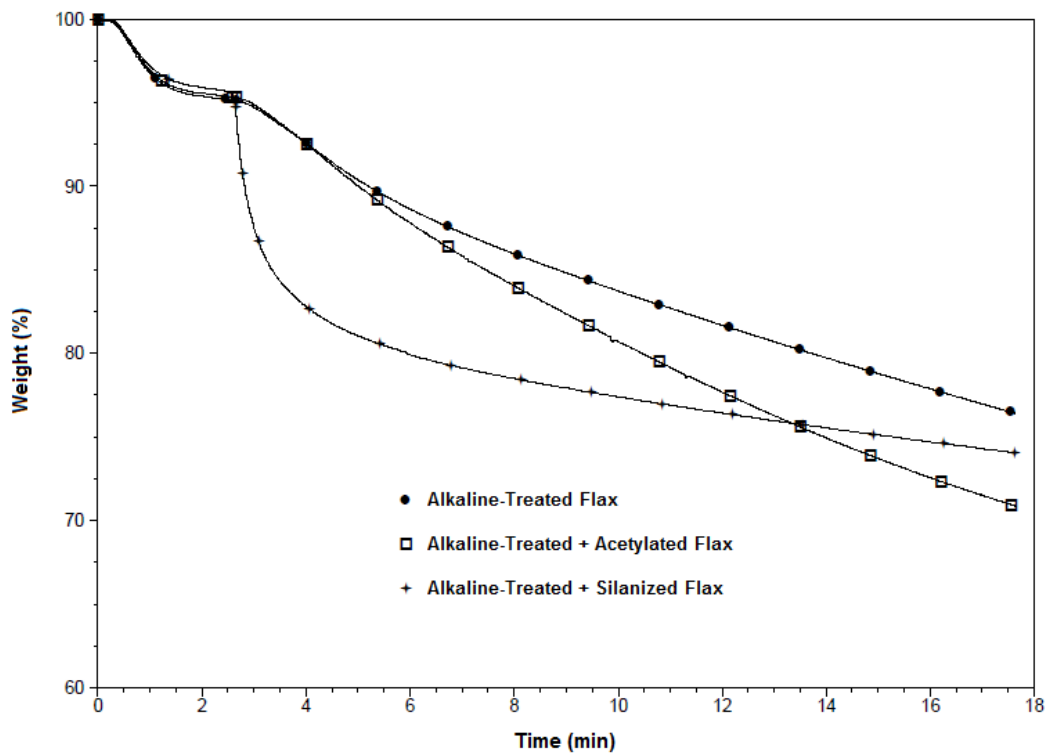


(b)

Figure 58: Isothermal decompositions under air of treated flax fibers at (a) 270 °C and (b) 290 °C



(a)



(b)

Figure 59: Isothermal decompositions under nitrogen of treated flax fibers at (a) 270 °C and (b) 290 °C

Table 28: Isothermal decompositions of treated flax fibers

| Temperature | | 270 °C | | 290 °C | |
|-------------------------------|------------|--------------------------|------------------------------|--------------------------|------------------------------|
| Flax | Atmosphere | Degradation rate (%/min) | Residue after 18 minutes (%) | Degradation rate (%/min) | Residue after 18 minutes (%) |
| Alkaline-Treated | Air | Air | 1.28 | 78 | 3.02 |
| | Nitrogen | Nitrogen | 0.75 | 85 | 1.62 |
| Alkaline-Treated + Acetylated | Air | Air | 1.08 | 82 | 2.97 |
| | Nitrogen | Nitrogen | 0.75 | 86 | 2.12 |
| Alkaline-Treated + Silanized | Air | Air | 1.20 | 76 | 1.97 |
| | Nitrogen | Nitrogen | 0.70 | 79 | 1.10 |

5.4.3 IR Spectroscopy of Degraded Fibers in Air and Nitrogen

Spectra of treated and post-treated curauá fibers, *in natura* and 5.0 wt.% degraded under different atmospheres (air and nitrogen) are shown in Figure 60 – 62. Observing the main band at approximately 900 cm^{-1} (stretch ring of glucose), it can be noted a slight decrease of intensity of this peak in air-degraded alkaline-treated curauá fibers, compared with undegraded and inert-degraded ones. It results from the exposure of fibers to oxidative environment.

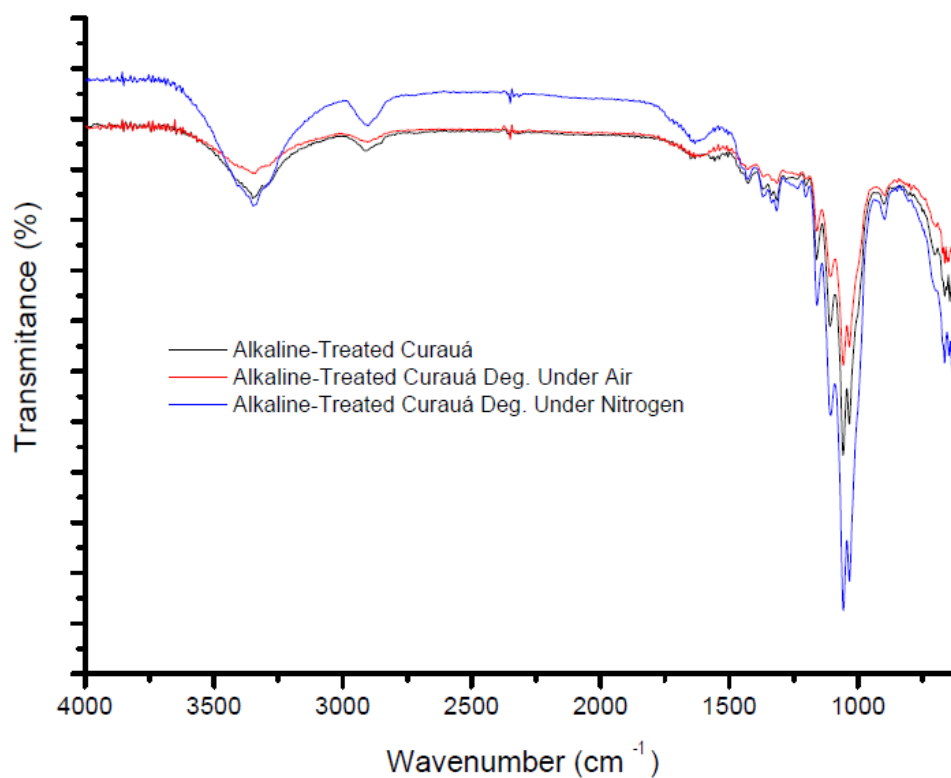


Figure 60: FTIR spectra of alkaline-treated curauá fibers *in natura* and degraded under different atmospheres

It is known that the activation energy necessary to break glycosidic bonds is lower under air than under nitrogen. For this reason, it is expected that degradation of natural fibers under air begins at lower temperatures. This behaviour is more pronounced for the following bands: 2900 cm⁻¹ (stretch C-H bond) and region between 1740 – 1630 cm⁻¹ (C=O stretching of lignin and O –H deformation due to water). This region presents the same behavior in alk-treated + silanized curauá fibers (Figure 60).

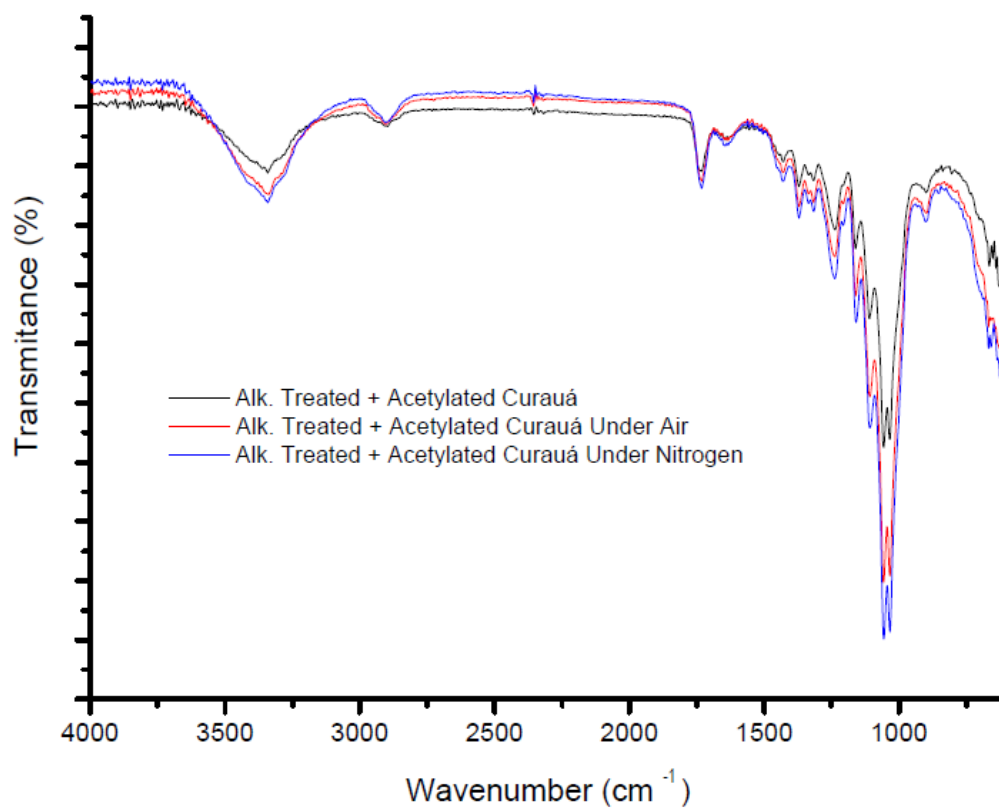


Figure 61: FTIR spectra of alkaline-treated + acetylated curauá fibers *in natura* and degraded under different atmospheres

No significant changes were observed in alkaline-treated + acetylated curauá spectra (Figure 61). Perhaps, its higher thermal resistance can reduce the difference in all spectra compared with alkaline-treated and alk-treated + silanized fibers.

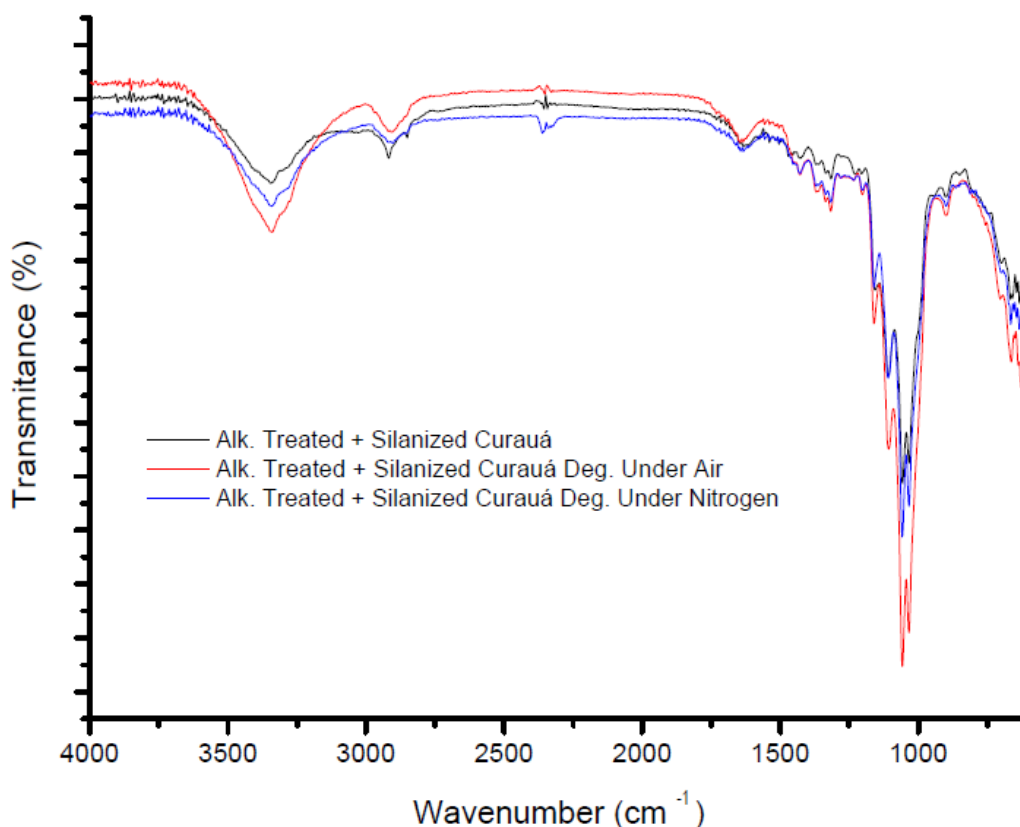


Figure 62: FTIR spectra of alkaline-treated + silanized curauá fibers *in natura* and degraded under different atmospheres

5.4.4 Surface Morphology of Degraded Fibers in Air and Nitrogen

SEM images of treated and post-treated curauá fibers, without heating and 5.0 wt.% degraded under different atmospheres (air and nitrogen) are shown in Figures 62 – 65. The images confirm results of FTIR performed previously. Damaged surfaces can be easily observed at fibers subjected to oxidative degradation and this behaviour is more easily noted in alkaline-treated curauá fibers. 5.0 wt.% degraded acetylated fibers does not show a significant damaging in their surfaces, even under oxidative degradation, assessing their higher thermal stability when compared with alkaline-treated and alk-treated + silanized fibers. It is also noticed that the degradation under nitrogen seems to allow the separation of fibers one from the others. It is possible that residues of amorphous fractions were preferentially degraded.

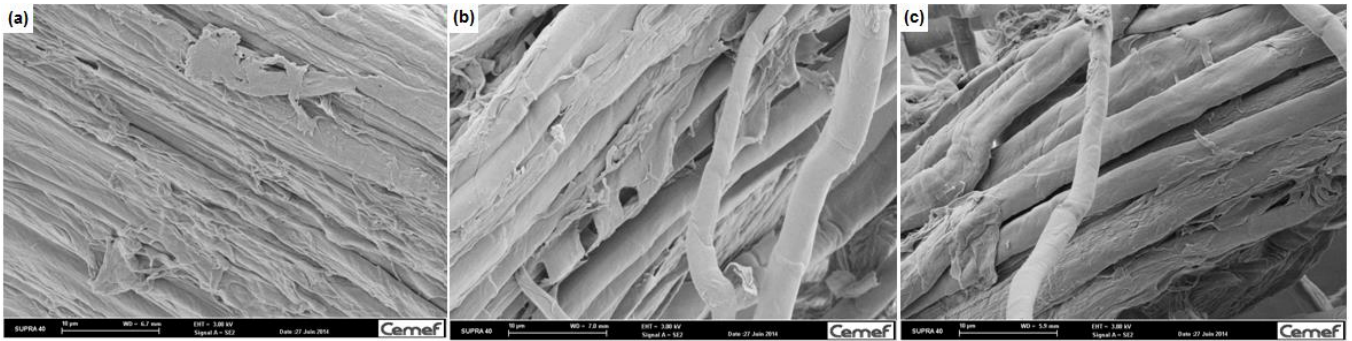


Figure 63: SEM images of alkaline-treated curauá fibers without heating (a) and 5 wt. % degraded under different atmospheres: air (b) and nitrogen (c)

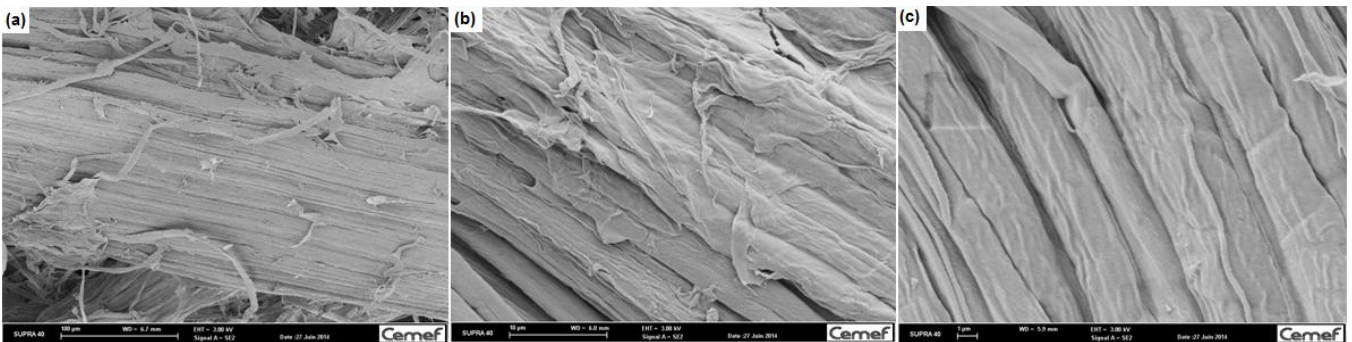


Figure 64: SEM images of alkaline-treated + acetylated curauá fibers without heating (a) and 5 wt. % degraded under different atmospheres: air (b) and nitrogen (c)

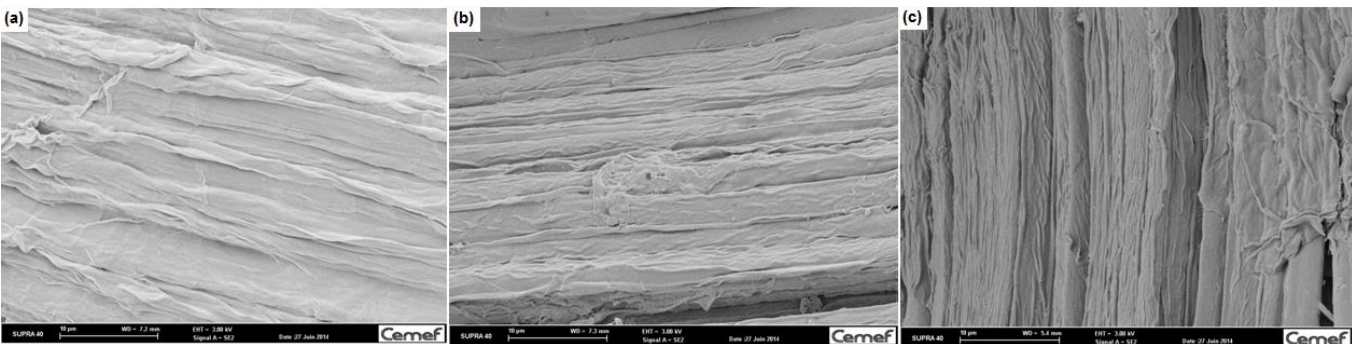


Figure 65: SEM images of alkaline-treated + silanized curauá fibers without heating (a) and 5 wt. % degraded under different atmospheres: air (b) and nitrogen (c)

5.5 STUDY OF PROCESSING CONDITIONS ON THE NATURAL FIBER FILLED POLYAMIDE 6 COMPOSITES

5.5.1 Evaluation of Degradation Risks of Composites

5.5.1.1 Analysis of composites color

Color results from an interaction between light, object and the viewer. It is usually described by three attributes or dimensions such as hue, saturation and lightness. A color space can be used to describe the range of visible colors. The CIE (*Commission Internationale de l'Eclairage* – International Commission on Illumination) developed more uniform color space called CIE L*a*b* (SHAMS-NATERI; MOHAJERANI, 2013).

Yellowness is defined as an attribute by which an object is judged to depart from a standard white towards yellow and is calculated by a given procedure from the colorimetric or spectrophotometric data which indicates the degree of deviation of the object color from the colorless or the standard white. A parameter b or b* defines the yellowness-blueness coordinate in certain color space. If this parameter is positive, there is more yellowness than blueness while if b or b* value is negative, more blueness is observed (SHAMS-NATERI; MOHAJERANI, 2013).

Another parameter called L can vary from 0 (black) to 100 (white) and can be considered for degradation analysis. Results of all colorimetry tests are presented in Tables 29 – 31, assuming polyamide 6 as standard. In a general overview, increasing the processing temperature decreases the L values, indicating the degradation of composites. Table 26 shows results of processed samples with pure celluloses. Comparing with pure polyamide, it can be noted a strong increase in darkness, by decrease of L factor, as well as increase of yellowness (parameter b) in all cases, mainly in Avicel processed at 270 °C (limit temperature of PA6 processing). This behavior becomes more pronounced in samples processed with curauá (Table 30 and 31), in which alkaline-treated + silanized curauá compounded at 240 °C reaches almost the

same values of Avicel processed at compounding limit temperature of polyamide 6.

Table 29: Colorimetry results of composites prepared with pure cellulose

| SAMPLE | L | a | b |
|-------------------------|-------------|-------------|------------|
| Polyamide 6 | 83.7 | -0.2 | 5.8 |
| PA 6 / Avicel – 230 °C | 46.7 | 12.4 | 24.9 |
| PA 6 / Avicel – 240 °C | 45.1 | 12.5 | 24.5 |
| PA 6 / Avicel – 270 °C | 28.7 | 2.8 | 3.3 |
| PA 6 / Cotton – 230 °C | 56.0 | 9.0 | 26.6 |
| PA 6 / Cotton – 240 °C | 46.4 | 11.3 | 23.8 |
| PA 6 / Lyocell – 230 °C | 45.7 | 13.6 | 22.6 |
| PA 6 / Lyocell – 240 °C | 39.3 | 13.1 | 15.9 |
| PA 6 / Viscose – 230 °C | 41.3 | 9.7 | 14.2 |
| PA 6 / Viscose – 240 °C | 38.8 | 8.4 | 12.6 |

Analyzing Table 29 and Table 30, there is a sensible decrease of yellowness and darkness with the increase of processing temperature. This can evidence a higher degradation susceptibility of the pure cellulose or surfaces of chemically treated fibers at higher compounding temperatures. However, even if colorimetry is a quick piece of information, it is needed more characterizations to confirm if fibers are degrading or not inside the polymeric matrix.

Table 30: Colorimetry results of composites prepared with treated curauá fibers

| SAMPLE | L | a | b |
|---|-------------|-------------|------------|
| Polyamide 6 | 83.7 | -0.2 | 5.8 |
| PA 6 / Alk-treated Curauá - 230 °C | 37.0 | 9.2 | 11.0 |
| PA 6 / Alk-treated + Acetylated Curauá - 230 °C | 35.1 | 8.9 | 9.5 |
| PA 6 / Alk-treated + Silanized Curauá - 230 °C | 38.9 | 8.0 | 7.0 |
| PA 6 / Alk-treated Curauá - 240 °C | 37.9 | 9.1 | 7.2 |
| PA 6 / Alk-treated + Acetylated Curauá - 240 °C | 33.5 | 7.7 | 7.5 |
| PA 6 / Alk-treated + Silanized Curauá - 240 °C | 38.3 | 6.2 | 6.1 |

It is interesting to note that lower values of yellowness is more strongly present in composites prepared with alkaline-treated + silanized curauá. And this result

can be directly related to its thermal behaviour. Even under oxidative and inert atmosphere, values of temperature at 5.0 wt.% of degradation is lower than the other chemically treated fibers. So, this behaviour is coherent with thermal results found before. Finally, reducing the processing time by more than half (8 to 3 min), for alkaline + acetylated curauá (curauá fiber with higher thermal stability) and pure cellulose, the colours of resulting composites became less dark, according to Table 31, suggesting that the fiber was not suffering so much damaging during the compounding by extrusion process caused by shearing into the machine.

Table 31: Colorimetry results of composites prepared under different processing times

| SAMPLE | L | a | b |
|--|-------------|-------------|------------|
| Polyamide 6 | 83.7 | -0.2 | 5.8 |
| PA 6 / Alk-treated + Acetylated Curauá - 240 °C – 8 min | 34.5 | 7.7 | 7.2 |
| PA 6 / Alk-treated + Acetylated Curauá - 240 °C – 3 min | 55.6 | 6.6 | 9.8 |
| PA 6 + Avicel – 240 °C - 8 min | 45.1 | 12.5 | 24.5 |
| PA 6 + Avicel – 240 °C - 3 min | 57.6 | 5.7 | 20.8 |

5.5.1.2 Analysis of molar mass of microcrystalline cellulose - viscosimetry

Viscosity experiments can only be performed on Avicel (pure cellulose) and not on chemically treated fibers because other cellulosic components, as lignin, are still present in chemically treated natural fibers. This method relies on the determination of intrinsic viscosities (or at least reduced viscosities) and can only be valid with one polymer present in the solvent. Values of degree of polymerisation of pure and cellulose extracted from composites are shown in Table 32. Short flow time of the solutions means low viscosity and, therefore, low degree of polymerization.

Table 32: Degree of polymerization of pure and processed Avicel cellulose

| Sample | Flow time (s) | Intrinsic viscosity (ml/g) | Degree of polymerization |
|----------------------------|---------------|----------------------------|--------------------------|
| Pure Avicel | 392 | 101 | 166 |
| Avicel Processed at 230 °C | 384 | 92 | 152 |
| Avicel Processed at 240 °C | 388 | 97 | 161 |
| Avicel Processed at 270 °C | 384 | 92 | 152 |

So, it is clear that no significant changing of molar mass is observed in extracted cellulose. This is coherent with the literature showing that pure cellulose like Avicel has a low degradation at temperature lower than 300°C. Results obtained in Cemef show that $T_{0.1}$ (10% mass loss) of Avicel is above 300°C. It means that the coupling of high compounding temperatures with other parameters as time and compounding speed into internal mixer did not degrade pure cellulose more than without compounding effects.

5.5.1.3 Identification of degradation products – IR spectra

Results of infra-red spectroscopy analysis of pure polyamide, alkaline-treated and alkaline-treated + acetylated fibers, as well as their composites compounded at 230 and 240 °C are shown in Figures 66 – 67. In all cases, spectra of composites in both processing temperatures, 230 and 240 °C are very similar to the ones of pure polyamide.

These events can confirm the viscosimetry results with Avicel cellulose extracted from the composite, in which the molar mass did not change for all studied temperatures (230, 240 and 270 °C). Another point that can be observed is a difference in a color composites which could be explained in terms of formation of chromophores.

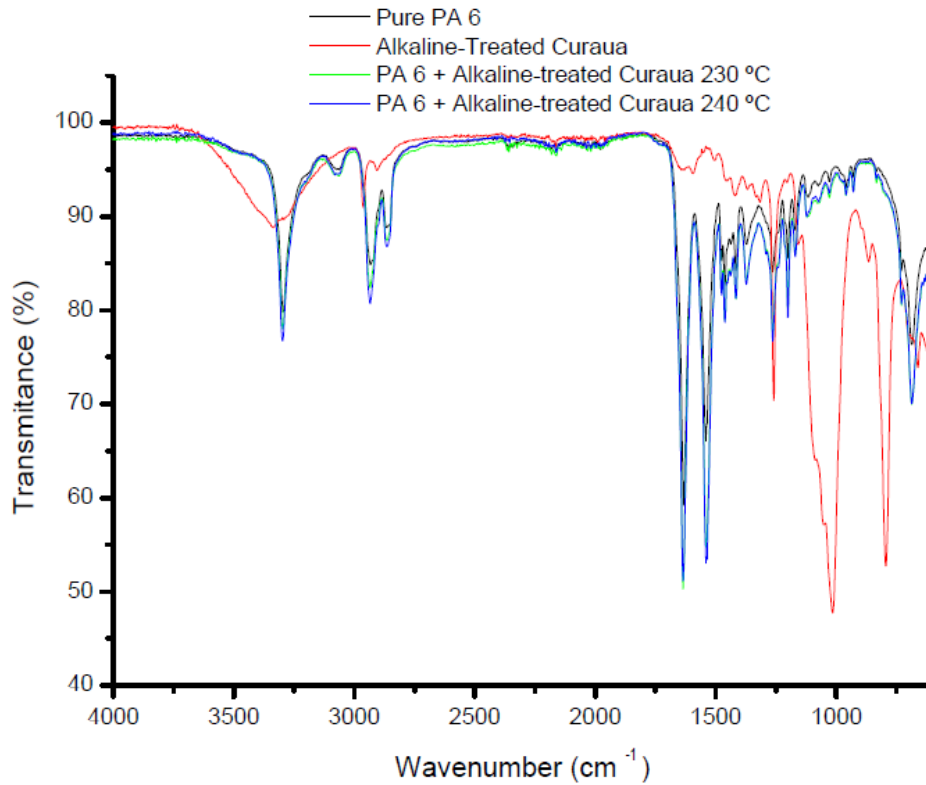


Figure 66: FTIR spectra of pure polyamide (PA 6), alkaline-treated curauá and their composites at 230 and 240 °C

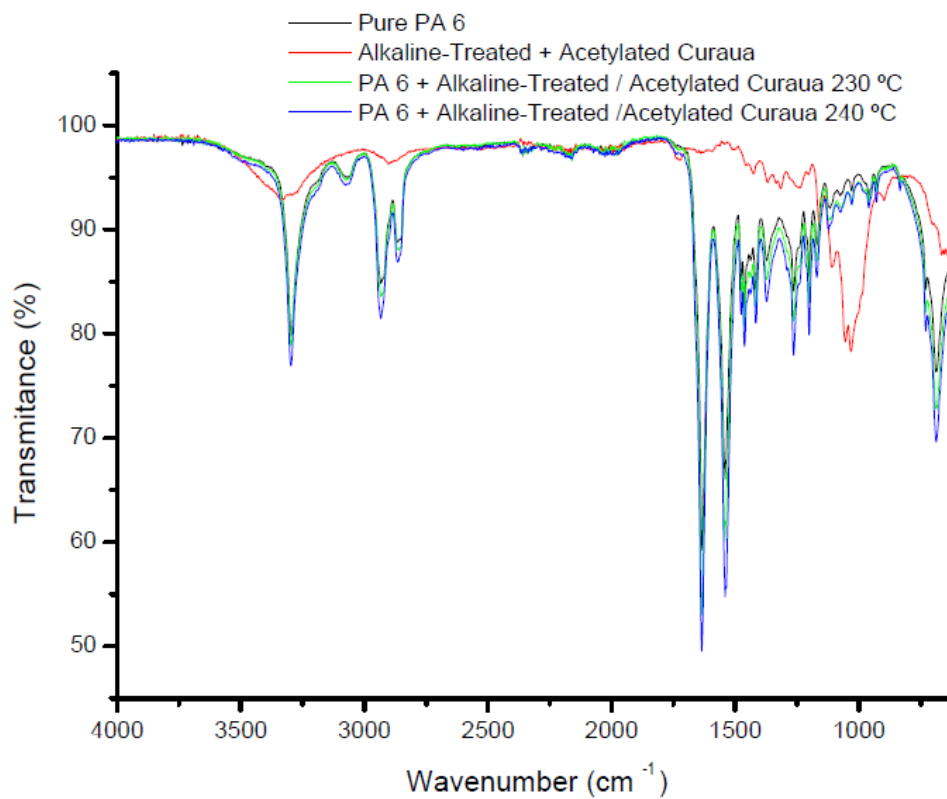


Figure 67: FTIR spectra of pure polyamide (PA 6), alkaline-treated + acetylated curauá and their composites at 230 and 240 °C

A closer view at band around 890 cm^{-1} (glucose ring stretching of natural fibers) in alkaline-treated and alkaline-treated + acetylated natural fibers, as well as their composites with PA 6, can be seen in Figures 68 – 69. This band is difficult to be observed in spectra of composites. However, it is not a warrant that degradation takes place onto the fibers. It is important to remember that composites were prepared with only 10 wt.% of natural fibers and, even in low amount, a slight difference in this band is observed when compared with pure polyamide (black spectra in both Figures) .

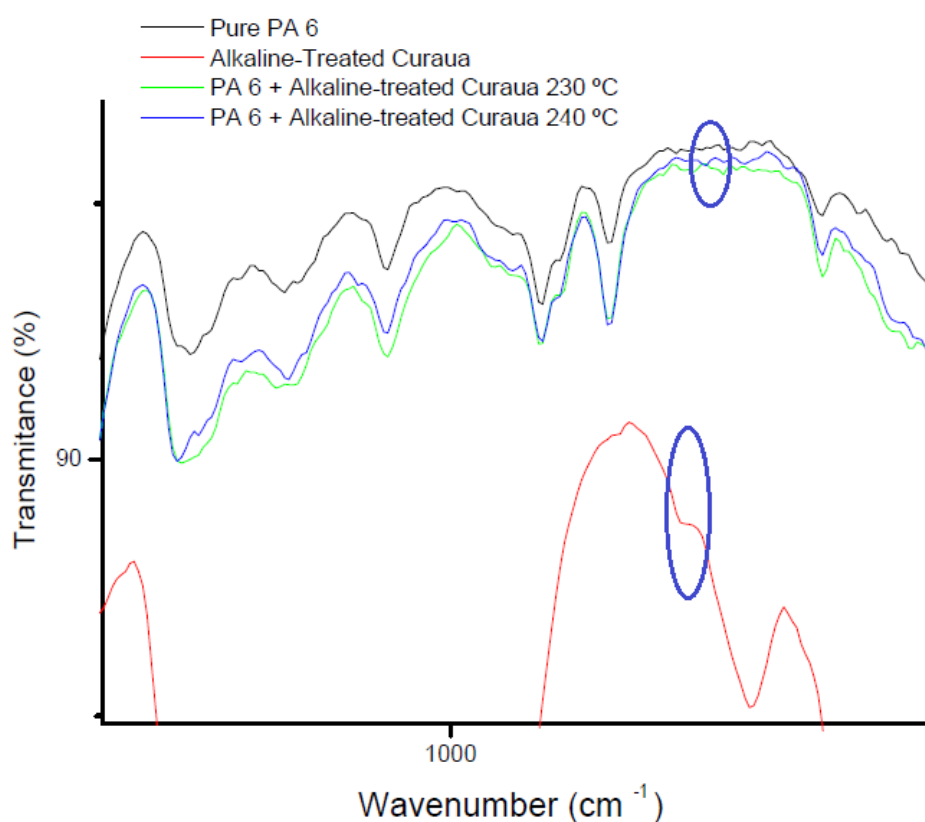


Figure 68: FTIR spectra in region at around 900 cm^{-1} of pure polyamide (PA 6), alkaline-treated curauá and their composites at 230 and 240 °C

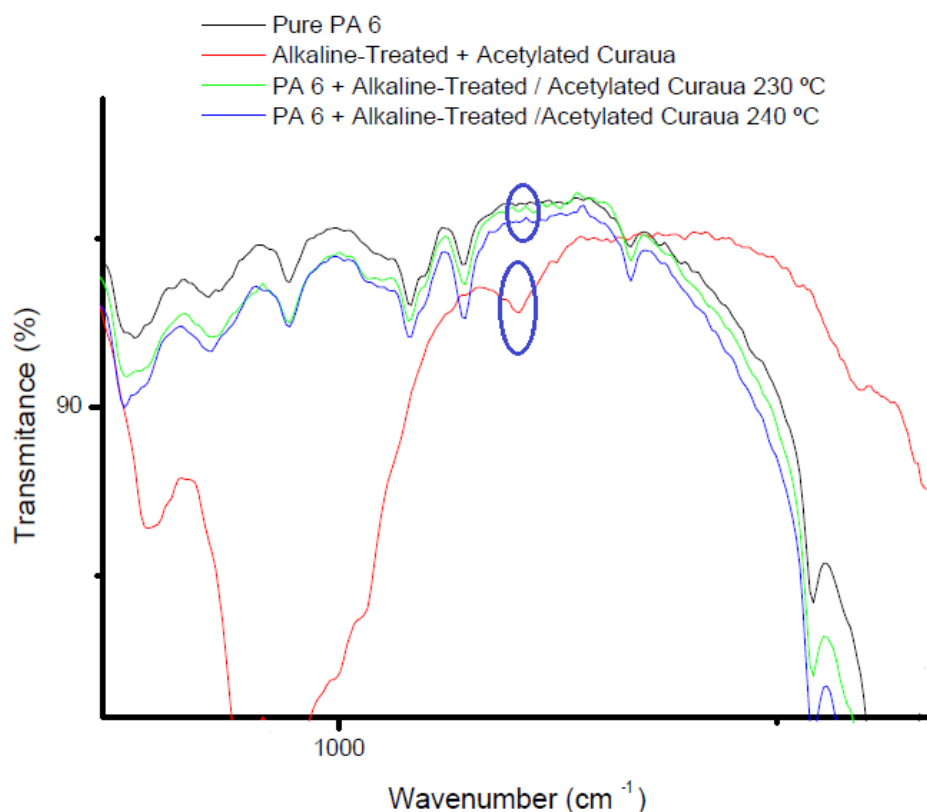


Figure 69: FTIR spectra in region at around 900 cm⁻¹ of pure polyamide (PA 6), alkaline-treated + acetylated curauá and their composites at 230 and 240 °C

5.5.2 Mechanical properties of composites: tensile testings

Results of tensile tests on moulded test bars are shown in Figures 70 – 72 and Table 33. In a general overview, it is observed an increase of elastic modulus when chemically treated natural fibers are mixed with pure polyamide. Several parameters must be considered such as the low percentage of treated fibers inserted in polyamide matrix (10 wt. %), the long compounding time (8 minutes) and long time needed to prepare test bars by compression moulding (10 minutes).

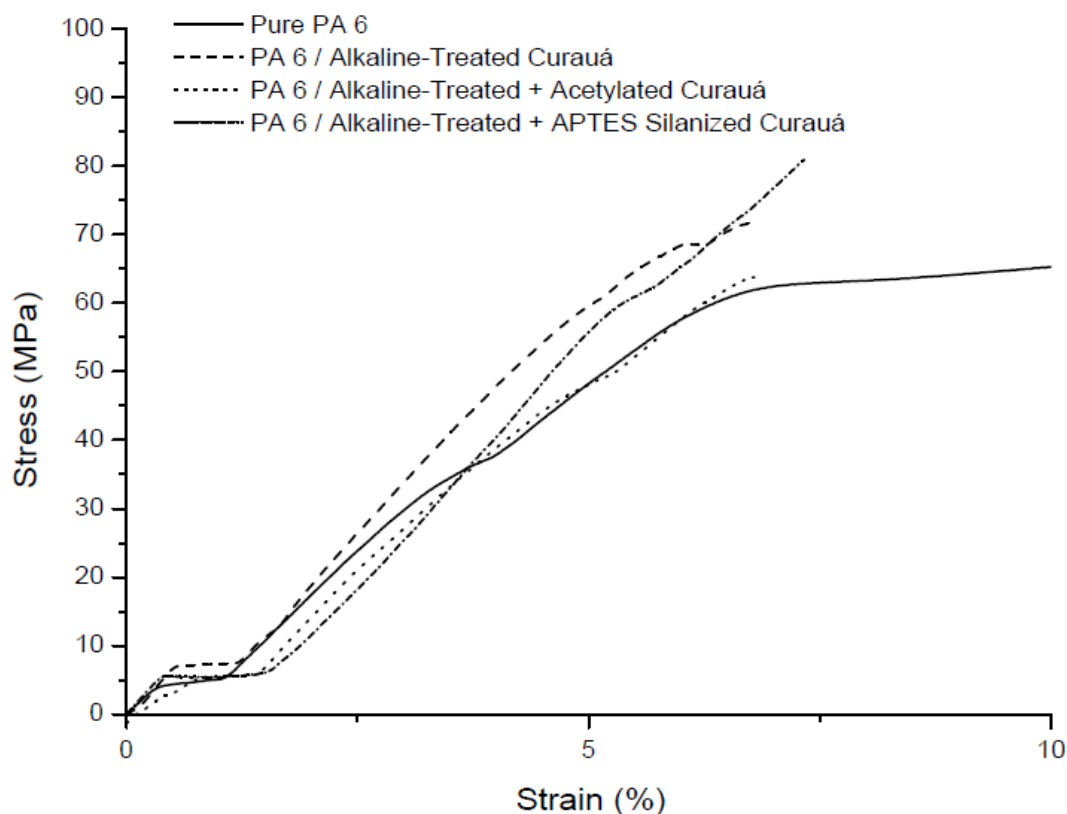


Figure 70: Stress versus strain curves of PA 6 – chemically treated curauá composites

It is noted, according to Table 33, that tensile strength of composites shows a visible improvement compared to pure resin. This means that the adhesion between the fillers and polyamide matrix is favourable. For example, for composites prepared with alkaline-treated curauá fibers, the enhancement of tensile strength is approximately 12%, so it denotes no weak bondings, which can be attributed to chemical treatment, as well as increasing of thermal stability of the fiber. All other fibers follow this behaviour. Moreover, it is also observed a significant improvement of elastic modulus in all composites. The enhancement of this parameter reaches 36 % with alkaline-treated curauá fibers and 40% to alkaline-treated flax fibers. In general, composites prepared with treated jute fibers showed minor enhancement of modulus, maybe due the lower thermal stability of their treated fibers compared to curauá and flax. The increase of modulus is explained by theory described by He and Jiang (1993), which states that a matrix zone around each particle is affected by stress concentration. Therefore, if the distance between particles is small enough, these zones join

together and form a percolation network, increasing the modulus. Finally, comparing the mechanical results of alkaline-treated composites with alkaline-treated acetylated or silanized fibers, it can be seen a decrease of values of tension and modulus. So, it can be concluded that, at least for polyamide 6 and inserting 10 wt. % of filler, there is no improvement of adhesion using these post-treatments. Only applying alkaline-treatment seems to be enough to prepare composites with better mechanical properties.

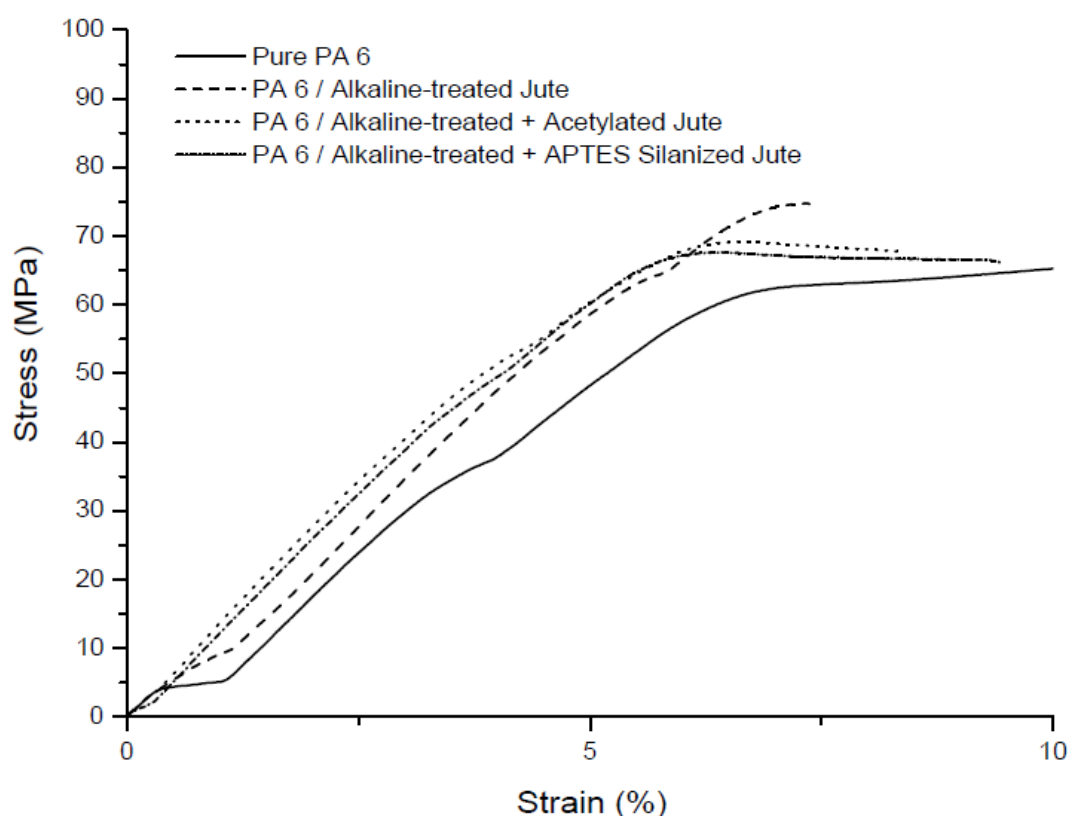


Figure 71: Stress versus strain curves of PA6 – chemically treated jute composites

Satisfactory improvement of interfacial bonding between the filler and matrix results in good stress propagation and improves mechanical parameters as tensile strength and elastic modulus, but fractures can arise inside the filler (since they are more fragile than the matrix) and these composites are more brittle than those in matrix polymer. Still analyzing Table 33 and stress-strain curves of composites prepared with chemically treated fibers in Figures 70 – 72, it was observed a decrease of strain at break for all composites and no

differences were observed in fibers with different chemical treatments. According to previous results found in literature using different matrices (UNAL, 2004; SANTOS et al., 2007), this behaviour was expected and can be attributed to immobilisation of the macromolecular chains of the polymeric matrix by the fibers and a possible orientation of the polymer matrix in this region, which increase the brittleness of the polymer.

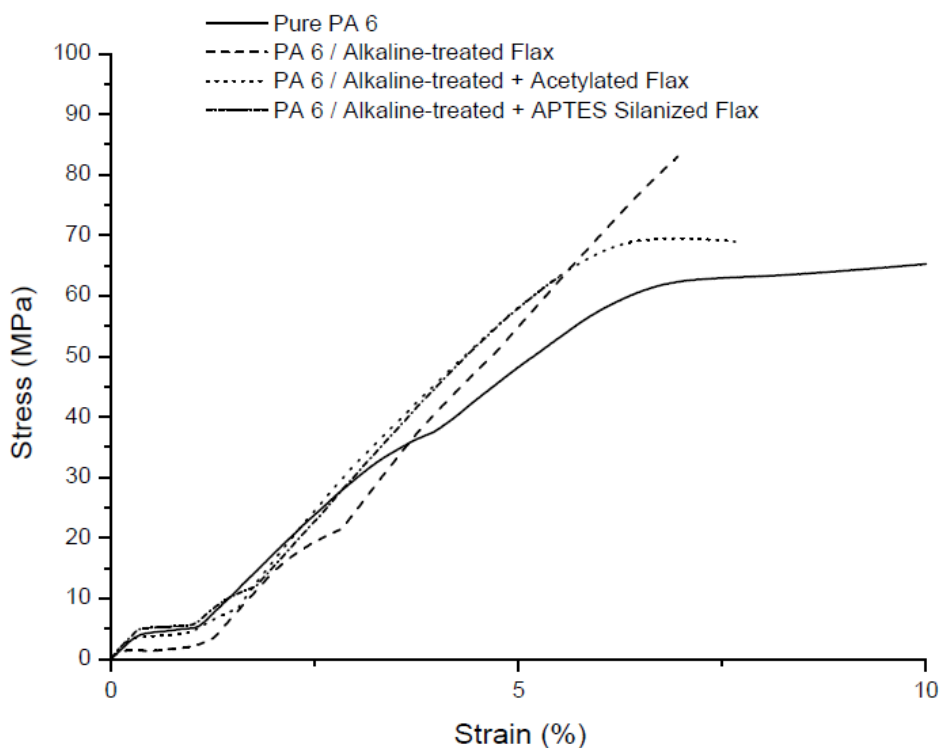


Figure 72: Stress versus strain curves of PA6 – chemically treated flax composites

Table 33: Mechanical properties of PA6 – curauá composites

| Sample | | Tensile Strength (MPa) | Strain (%) | Modulus (MPa) | Enhancement in Modulus (%) |
|---|--------|------------------------|------------|---------------|----------------------------|
| PA 6 | - | 54.3 ± 4.3 | 25.2 ± 1.1 | 1017 ± 90 | - |
| PA 6 / Alkaline-Treated Fibers | Curauá | 70.1 ± 4.1 | 6.4 ± 0.3 | 1568 ± 59 | 36 |
| | Jute | 67.1 ± 6.7 | 7.4 ± 0.3 | 1413 ± 114 | 17 |
| | Flax | 66.4 ± 5.3 | 7.0 ± 0.4 | 1606 ± 59 | 40 |
| PA 6 / Alkaline-Treated + Acetylated Fibers | Curauá | 64.3 ± 2.4 | 6.8 ± 0.2 | 1402 ± 65 | 21 |
| | Jute | 65.4 ± 4.2 | 7.2 ± 0.9 | 1317 ± 63 | 13 |
| | Flax | 68.7 ± 7.3 | 7.3 ± 0.4 | 1557 ± 72 | 34 |
| PA 6 / Alkaline-Treated + Silanized Fibers | Curauá | 73.4 ± 15.6 | 6.8 ± 1.2 | 1539 ± 121 | 28 |
| | Jute | 64.2 ± 1.7 | 8.0 ± 1.3 | 1350 ± 23 | 20 |
| | Flax | 54.4 ± 8.6 | 4.8 ± 0.6 | 1531 ± 101 | 29 |

5.5.3 Mechanical properties of composites based on PA 6 with different fillers and comparison with natural fibers

Aiming at selecting the best compounding time to prepare composites with different fiber contents and comparing with pure cellulose, glass fiber and neat curaua, composites were prepared fixing the processing temperature (240 °C), speed rotation of rotors (50 rpm) and fiber content (10 wt.%). Tensile testings according to ISO 527-2-1BA standard were performed after 2, 4, 6 and 10 -min compounding.

Looking to results presented in Table 34 and Figure 73, a significative increase in tensile strength, as well as elastic modulus, was observed when compounding time was doubled. This means that the adhesion between the fillers and polyamide matrix is favourable, as well as distribution of filler onto the PA 6 matrix and this can be seen in SEM results (next topic). When increasing the compounding time up to 6 minutes and 10 minutes, no significative change was observed.

Table 34: Mechanical properties of PA6 / Alkaline-Treated curauá composites at different compounding times

| Sample | Compounding time (min) | Tensile Strength (MPa) | Strain (%) | Modulus (MPa) |
|-------------------|------------------------|------------------------|------------|---------------|
| PA 6 + Alk-Curaua | 2 | 48.7 ± 2.4 | 14.5 ± 1.5 | 1033 ± 27 |
| | 4 | 56.6 ± 1.5 | 8.1 ± 1.2 | 1371 ± 64 |
| | 6 | 58.8 ± 1.5 | 10.5 ± 1.7 | 1256 ± 15 |
| | 10 | 59.4 ± 2.1 | 11.8 ± 1.6 | 1204 ± 29 |

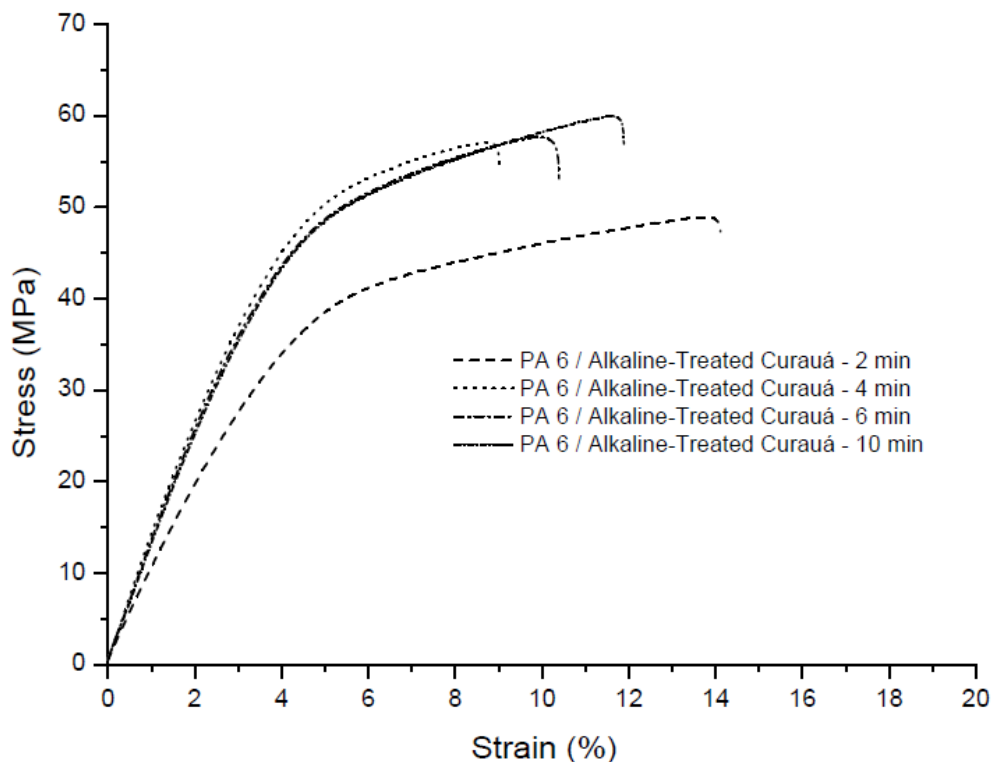


Figure 73 : Stress versus strain curves of PA6 / Alkaline-Treated curauá composites at different compounding times

5.5.4 – SEM images of PA 6/Alkaline-Treated Curaua fibers – influence of compounding time

Results of scanning electronical microscopy at 200x magnifications (200 μm) are shown in Figures 74 – 77. The micrographies confirm the elastic modulus' results, in which composites prepared at 4 minutes show that fibers are better dispersed into polyamide 6 matrix. It is important to observe also the higher amount of agglomerated fibers at the surface of other composites. It means worse distribution and, consequently, lower elastic modulus.

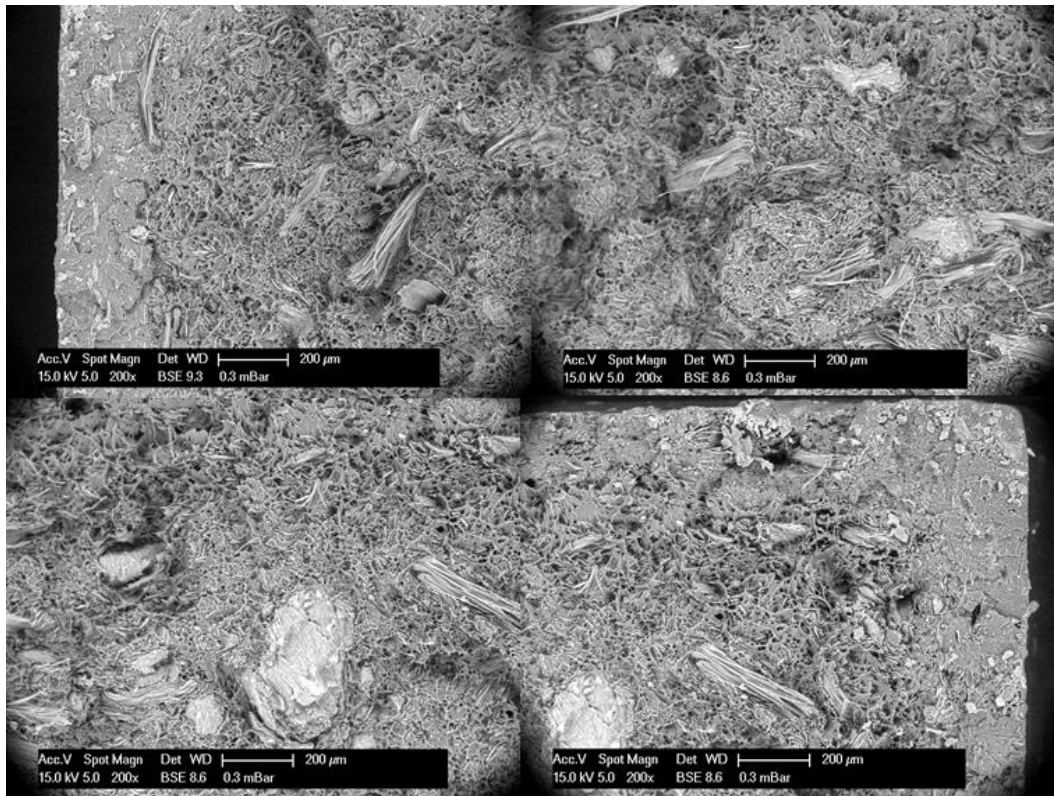


Figure 74: SEM micrographies (200x) of PA 6 composites with alkaline-treated curauá fibers compounded at 2 minutes

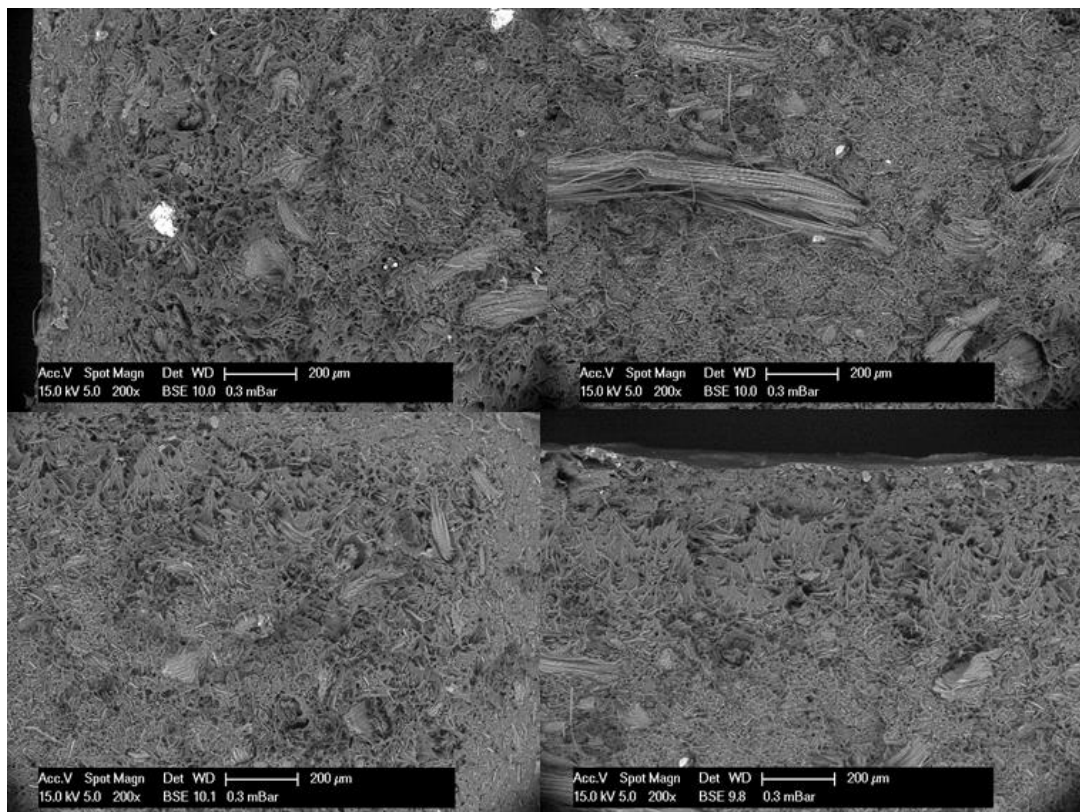


Figure 75: SEM micrographies (200x) of PA 6 composites with alkaline-treated curauá fibers compounded at 4 minutes

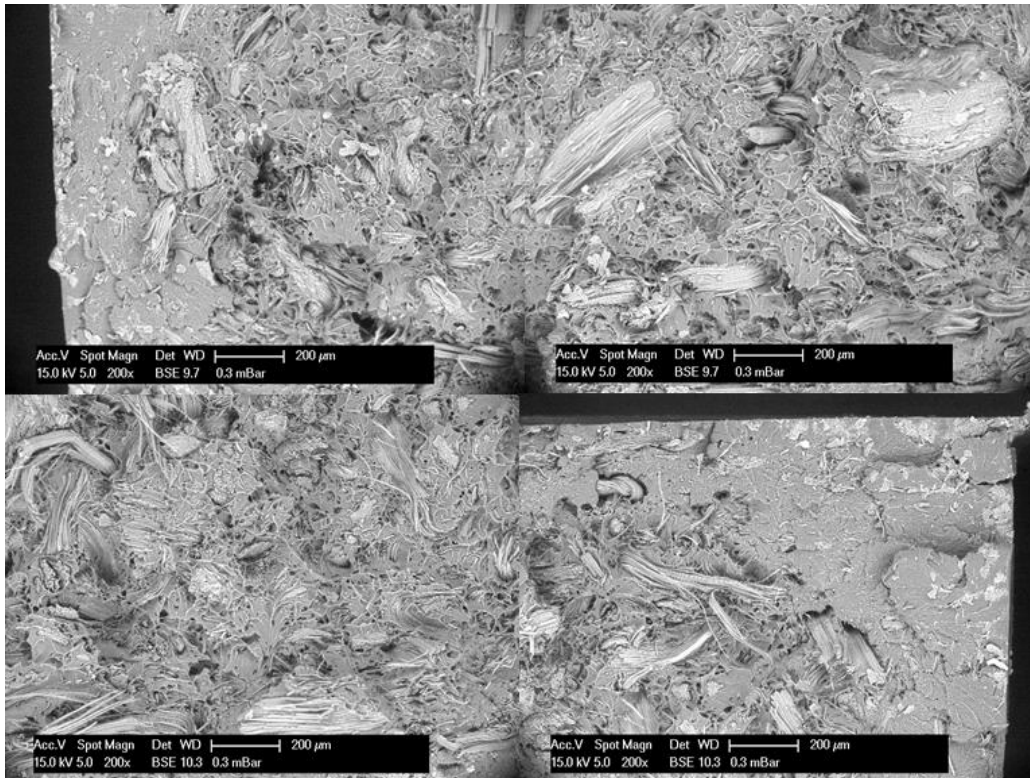


Figure 76: SEM micrographies (200x) of PA 6 composites with alkaline-treated curauá fibers compounded at 6 minutes

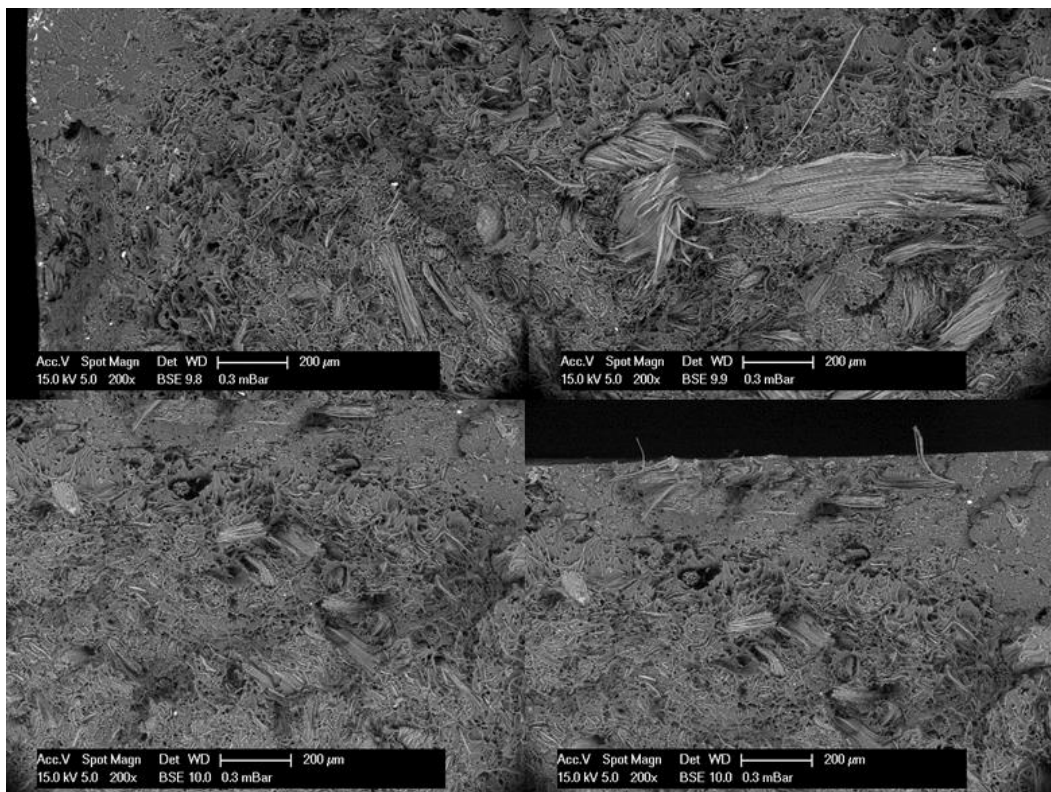


Figure 77: SEM micrographies (200x) of PA 6 composites with alkaline-treated curauá fibers compounded at 10 minutes

5.5.5 Mechanical properties of PA 6/ fibers – influence of fiber content

According to tensile test results given in Table 35 and Figure 78, alkaline treatments performed on curaua fibers are able to improve the tensile stress in composites with Polyamide 6, compared with the ones prepared with neat curaua fibers. This occurs due to the better adhesion between treated fibers with polyamide matrix. Increasing fiber content from 20 to 30 wt. %, tensile stress of PA 6 – alkaline curaua composite increases, while in composites prepared with untreated fibers, the value remains unchanged.

Table 35: Mechanical properties of composites prepared with natural fibers and pure cellulose at different fiber contents

| Composite | Fiber Content (wt.%) | Stress (MPa) | Strain (%) | Elastic Modulus (MPa) |
|--------------------------------|----------------------|--------------|------------|-----------------------|
| PA 6 | 0 | 45.8 ± 3.5 | > 100% | 751 ± 80 |
| PA 6 – Avicel | 20 | 52.7 ± 0.7 | 7.2 ± 1.2 | 1431 ± 16 |
| | 30 | 51.5 ± 0.9 | 4.5 ± 0.3 | 1719 ± 29 |
| PA 6 – Neat Curaua | 20 | 61.0 ± 2.2 | 5.0 ± 0.4 | 1921 ± 19 |
| | 30 | 58.7 ± 4.0 | 3.2 ± 0.4 | 2230 ± 31 |
| PA 6 – Alkaline-Treated Curaua | 20 | 74.0 ± 1.9 | 5.7 ± 0.3 | 1855 ± 45 |
| | 30 | 90.2 ± 1.7 | 5.3 ± 0.1 | 2259 ± 53 |

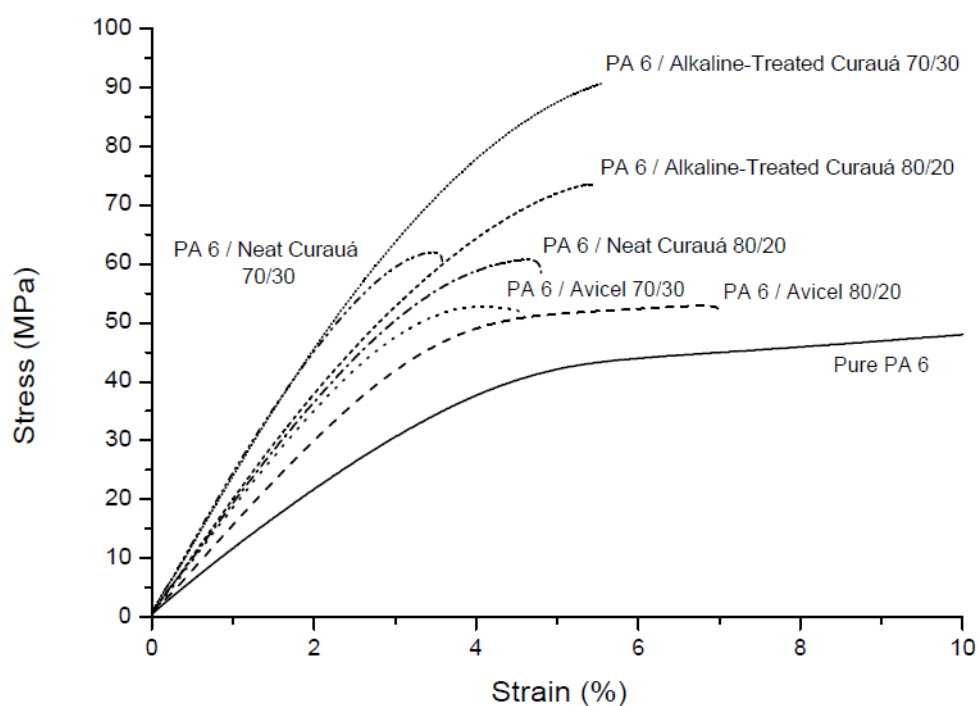


Figure 78: Stress versus strain curves of composites prepared with natural fibers and pure cellulose at different fiber contents

Comparing the values of elastic modulus, composites prepared with untreated and treated fibers shows similar results at 20 and 30 wt.%. In this case, the dispersion of fibers during compounding is the main parameter when elastic modulus should be considered. Improvement of elastic modulus of natural fibers compared to composites prepared with pure cellulose is also observed, as Avicell is not a reinforcing material.

SEM micrographies of all composites (Figures 79 – 84) confirm the results found in Table 35. It can be observed that alkaline-treated curauá is well bonded to polyamide 6 (Figures 79 and 80) and this is more pronounced when fiber content is 30 wt.%, considering the higher stress results in this case. It is also noted the presence of numerous voids and, consequently, low adhesion between neat fibers and polyamide 6 (Figures 81 and 82), resulting in lower mechanical properties. Finally, as expected, reinforcing effect can not be seen in composites with pure cellulose (Figures 83 and 84), as long as they does not have characteristic of fibers, showing lower Elastic Modulus and tensile stress than natural fibers.

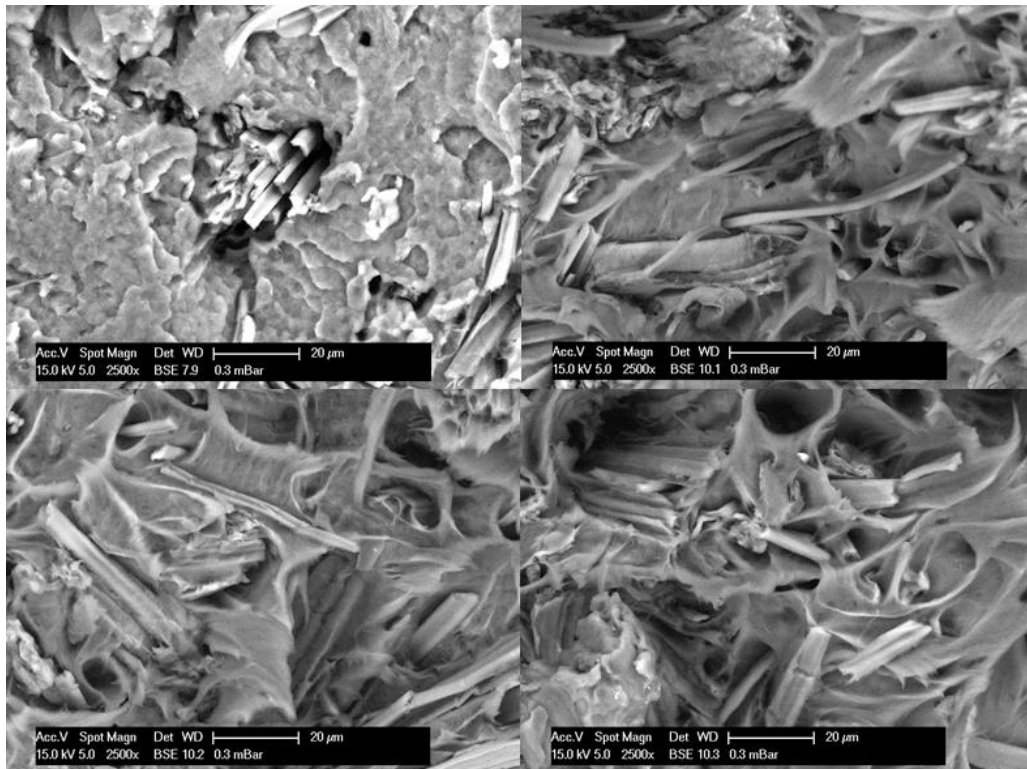


Figure 79: SEM micrographies (2500x) of 80/20 PA 6 composites with neat curauá fibers

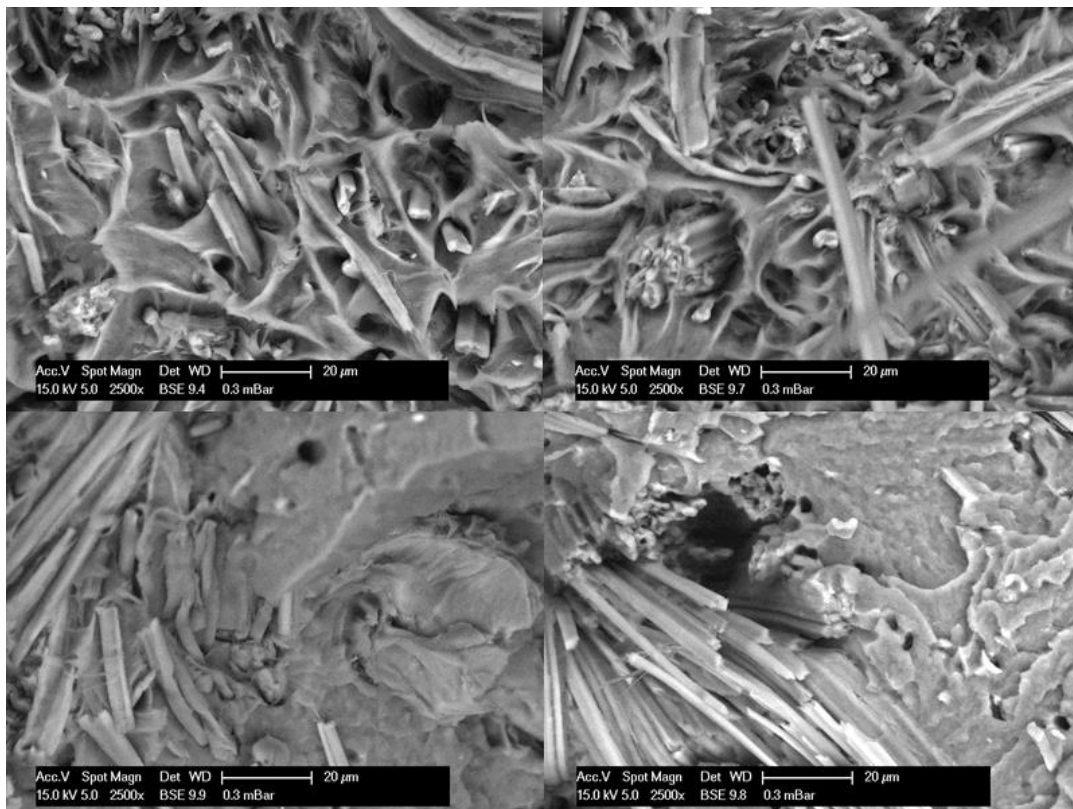


Figure 80: SEM micrographies (2500x) of 70/30 PA 6 composites with neat curauá fibers

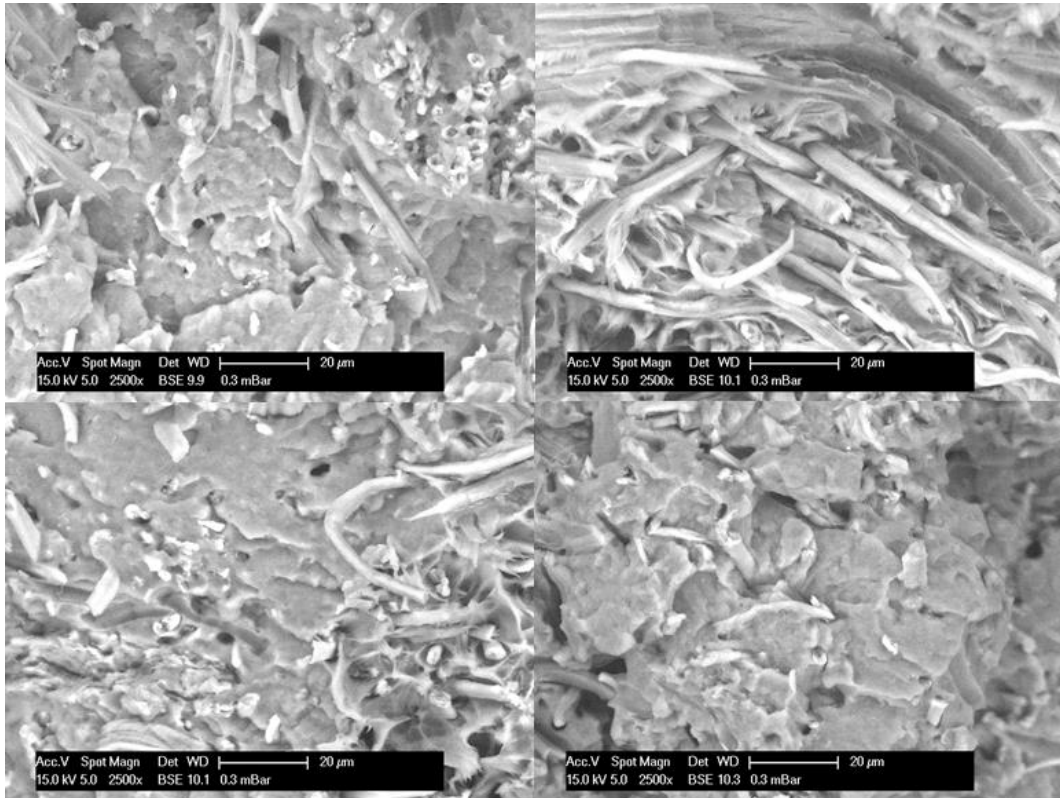


Figure 81: SEM micrographies (2500x) of 80/20 PA 6 composites with alkaline-treated curauá fibers

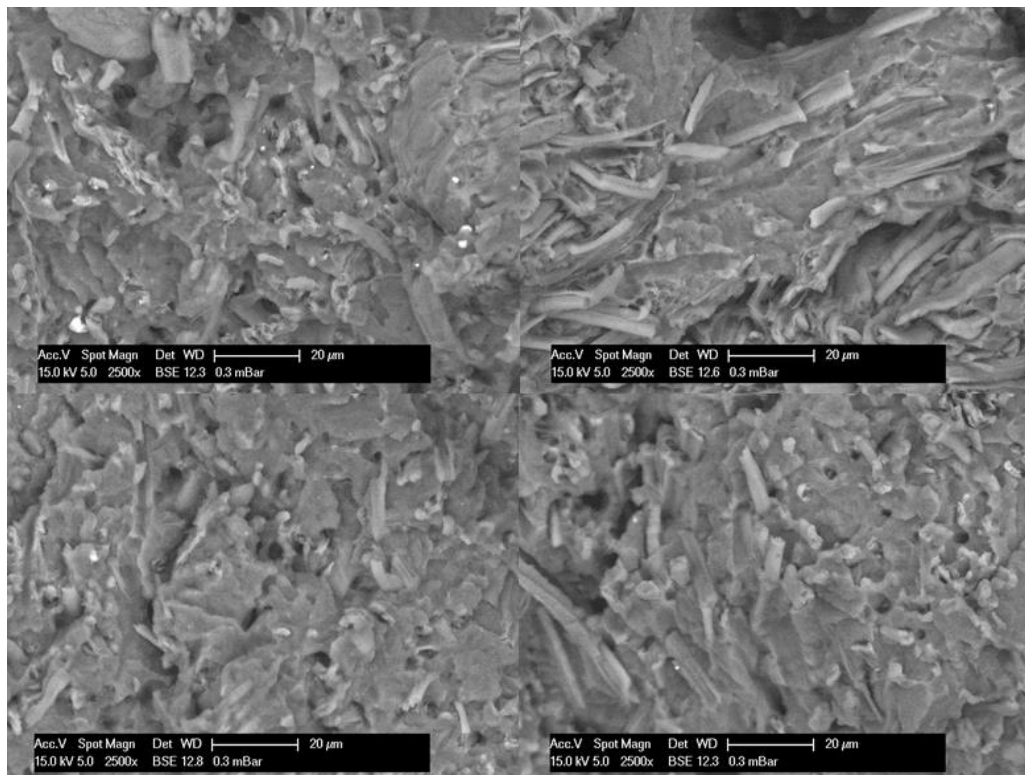


Figure 82: SEM micrographies (2500x) of 70/30 PA 6 composites with alkaline-treated curauá fibers

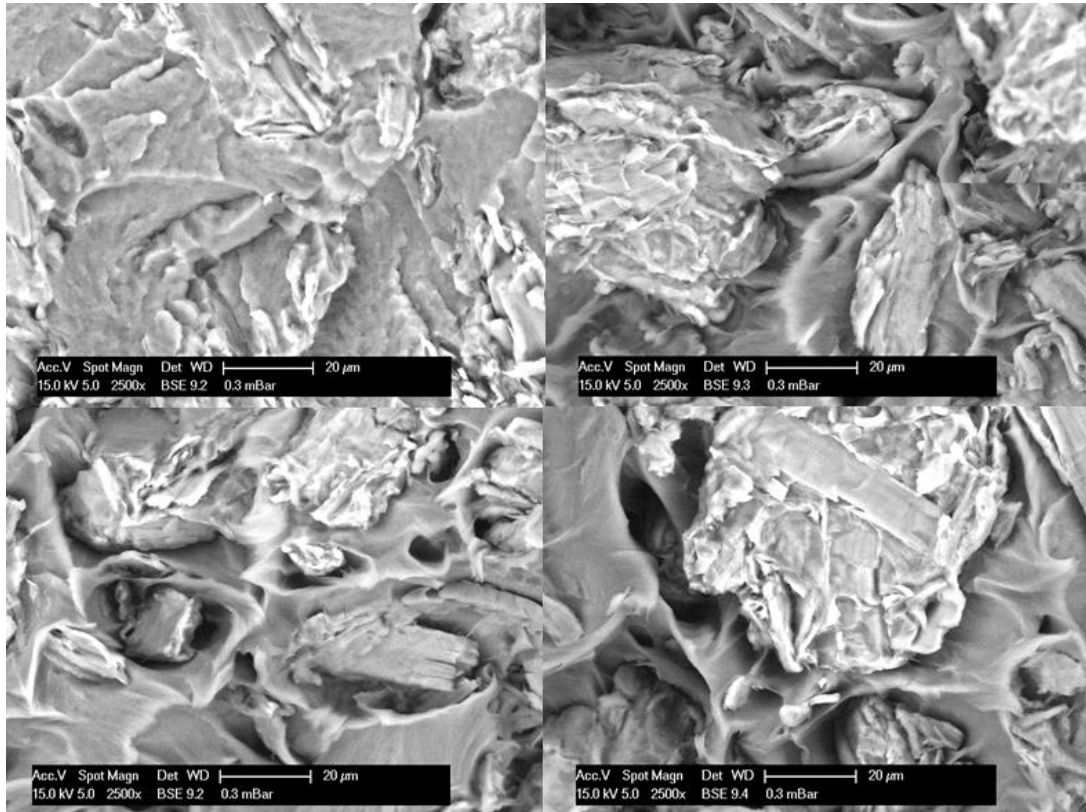


Figure 83: SEM micrographies (2500x) of 80/20 PA 6 composites with Avicel

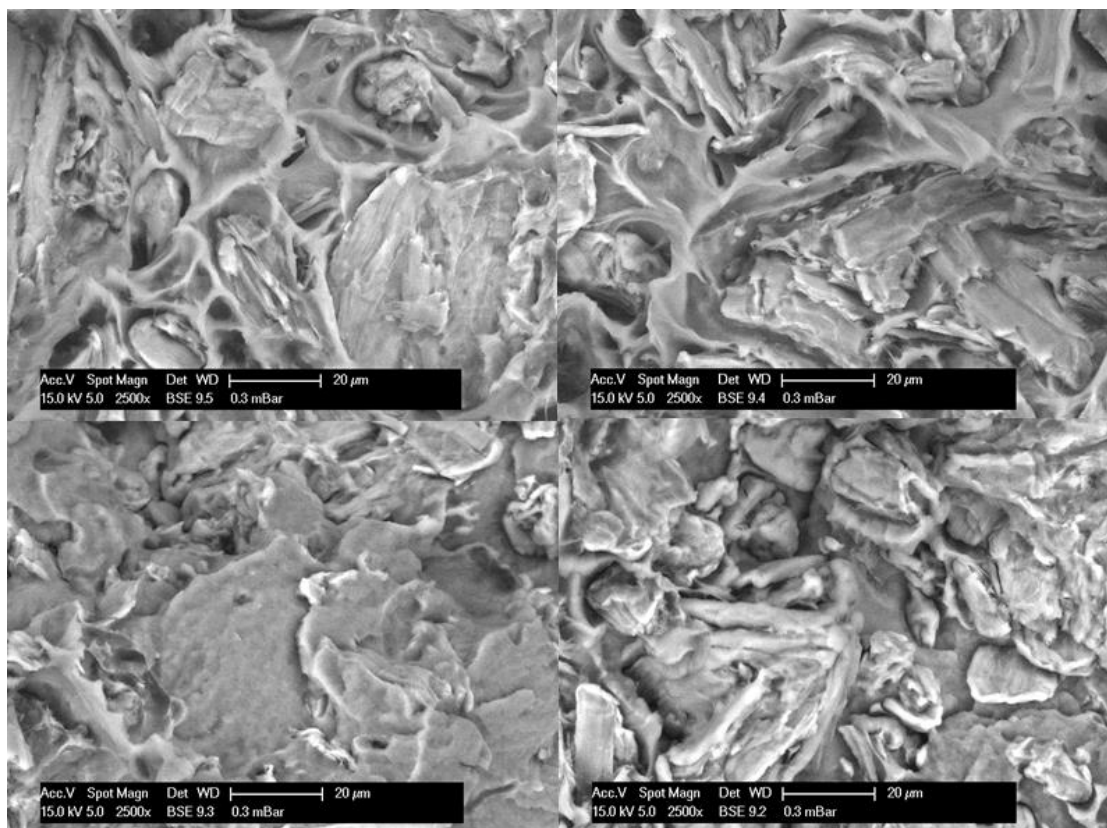


Figure 84: SEM micrographies (2500x) of 70/30 PA 6 composites with Avicel

5.6 COMPOUNDING PA 6.6 – NATURAL FIBERS

5.6.1 TGA of alkaline-treated curauá with different silanes

According to the previous results on thermal stability of treated natural fibers and looking for a higher improvement of the thermal stability of alkaline-treated fibers, as well as to enhance the adhesion between natural fibers and polyamide matrix, other silanes were employed to perform silanization in a way to diminish possible degradation effects during compounding which would decrease the mechanical properties of polyamide 6.6 composites. Silicon tetrachloride (SiCl_4), vinyl-trimethoxy silane (VTMS) and glycidyloxypropyl-trimethoxy silane (glycidyl) were chosen and applied to alkaline-treated curauá fibers. TGA ramps from room temperature up to 700 °C in a rate of 10 °C/min were performed to analyze the thermal behaviour. Results are shown in Table 36 and Figure 85. Glycidyloxypropyl-trimethoxy improved strongly the thermal stability of alkaline-treated curauá fibers, 60 °C higher than the silanized-alkaline treated fiber employed before (aminopropyl-trimethoxy silane) and any other post-treated fibers.

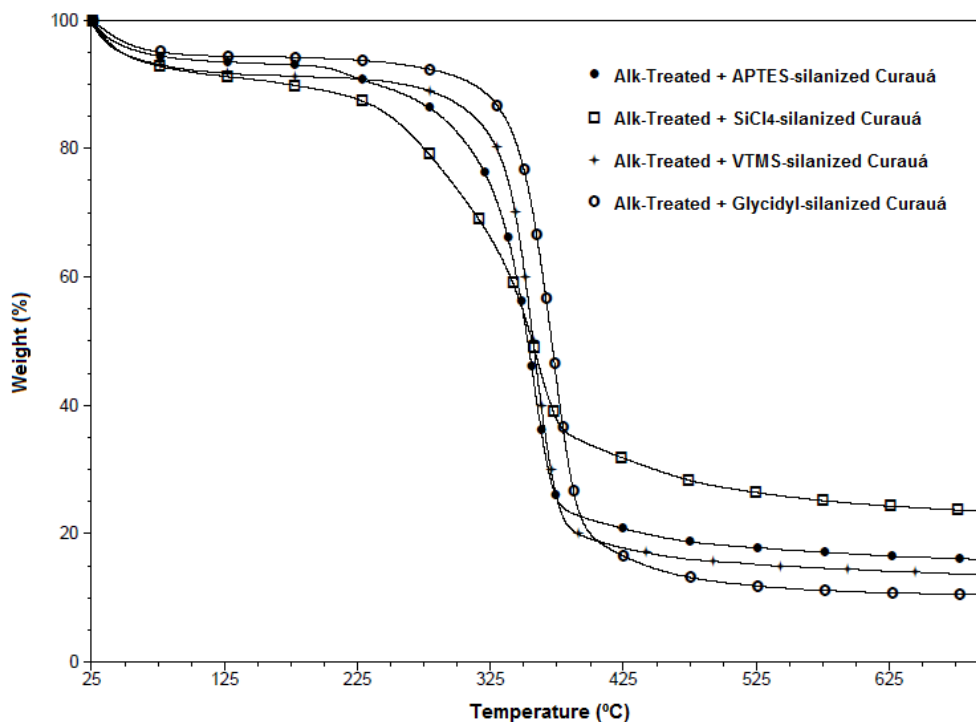


Figure 85: Thermal behaviour of silanized curauá fibers

Table 36: Thermal properties of silanized curauá fibers

| Silane treatments | Nitrogen | | | Residue (%) |
|-------------------|-----------------|------------------|----------------|-------------|
| | $T_{0.05}$ (°C) | T_{onset} (°C) | T_{max} (°C) | |
| APTES | 256 | 322 | 357 | 16.2 |
| $SiCl_4$ | 227 | 306 | 360 | 24.0 |
| VTMS | 303 | 333 | 357 | 13.6 |
| Glycidyl | 315 | 344 | 373 | 10.6 |

These results showed above encouraged us to apply this silane on post-treatment of high-pressure alkaline-treated jute and flax. TGA curves for these two fibers in heating mode are shown in Figure 86 and Table 37. Curauá and flax have of $T_{0.05}$, higher than 300 °C. Residues content at the end of heating are also similar. For jute, the thermal properties are not as good as the two others, keeping the same tendency of lower thermal stability than curauá and flax observed in previous results at different treatments. So, analyzing these results and comparing to those found before, it was decided to prepare composites with polyamide 6.6 using alkaline-treated + glycidyl-silanized fibers.

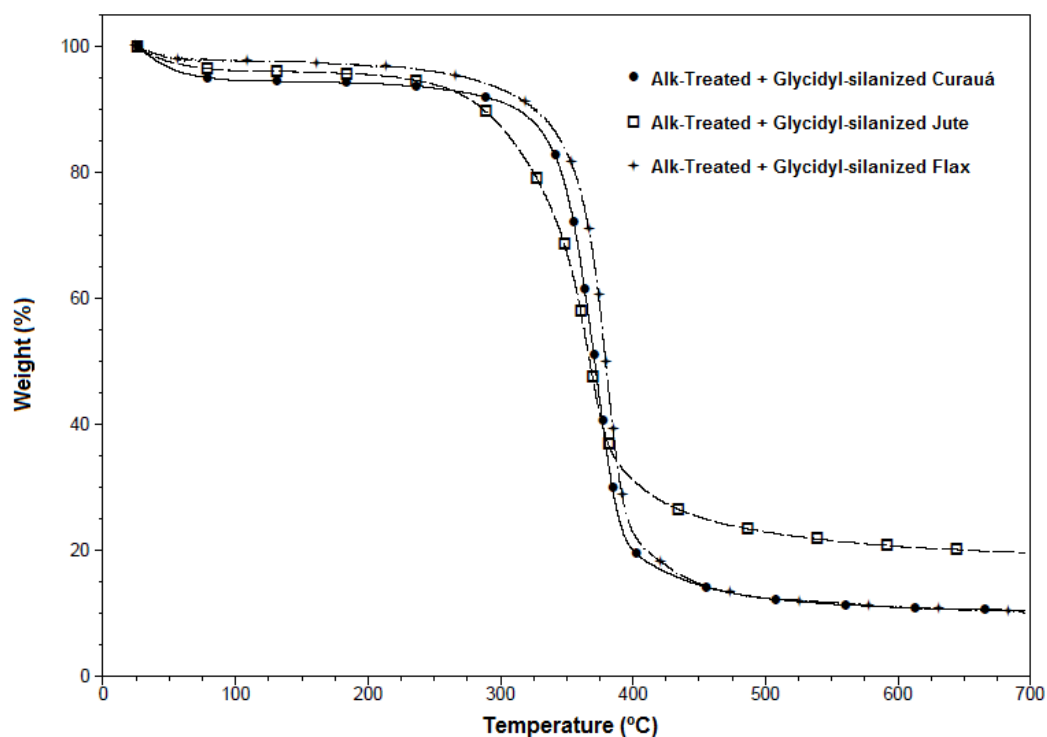
**Figure 86:** TGA curves of alkaline-treated + glycidyl-silanized curauá, jute and flax

Table 37: Thermal properties of Glycidyl-silanized fibers (under nitrogen)

| Gly-Silane treatments | Nitrogen | | | Residue (%) |
|-----------------------|------------------------|-------------------------|-----------------------|-------------|
| | T _{0.05} (°C) | T _{onset} (°C) | T _{max} (°C) | |
| Curauá | 315 | 344 | 373 | 10.6 |
| Jute | 282 | 329 | 366 | 19.6 |
| Flax | 309 | 356 | 380 | 10.1 |

5.6.2 Mechanical properties of PA 6/ fibers – influence of fiber silanization

Initially, composites with PA 6 and fibers were prepared to evaluate the performance of different fibers in the composite. Table 38 and Figure 87 show the mechanical behaviour of composites prepared with neat and alkaline-treated + glycidyl-silanized natural fibers, fixing the fibers content in 30 wt.%. In a general overview, PA 6/ treated curauá is the composite with the best mechanical properties. Composites with treated curauá and jute shows significative enhancement of mechanical properties when compared with untreated ones. It means that there is a good adhesion between treated fibers and the polyamide matrix.

Table 38: Mechanical properties of composites prepared with neat and alkaline-treated + silanized fibers at 30 wt.% fiber content

| Composite | Fiber | Stress (MPa) | Strain (%) | Elastic Modulus (MPa) |
|---------------|-------------------------------|--------------|------------|-----------------------|
| PA 6 | - | 45.8 ± 3.5 | > 100% | 751 ± 80 |
| PA 6 – Curauá | Neat | 58.7 ± 4.0 | 3.2 ± 0.4 | 2230 ± 31 |
| | Alk. Treated + Gly. Silanized | 89.6 ± 2.7 | 5.3 ± 0.2 | 2328 ± 73 |
| PA 6 – Jute | Neat | 71.3 ± 2.2 | 3.8 ± 0.4 | 2337 ± 13 |
| | Alk. Treated + Gly. Silanized | 83.6 ± 1.8 | 5.6 ± 0.3 | 2208 ± 10 |
| PA 6 – Flax | Neat | 83.4 ± 1.1 | 5.4 ± 0.05 | 2345 ± 32 |
| | Alk. Treated + Gly. Silanized | 83.4 ± 0.6 | 6.0 ± 0.2 | 2256 ± 38 |

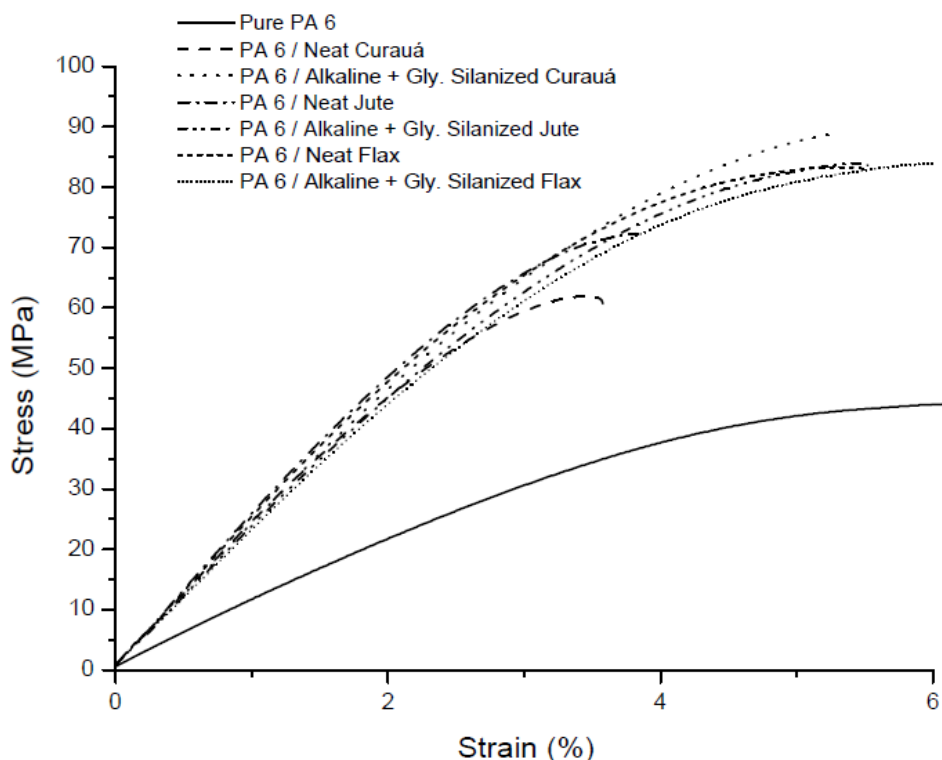


Figure 87 : Stress versus strain curves of composites prepared with neat and alkaline-treated + gly. silanized fibers at 30 wt.% fiber content

Unlike to what was expected, composites with treated flax fibers did not show any mechanical improvement compared to mixtures with neat flax. Finally, concerning the composites with curauá, it is important to observe the similarity of mechanical properties between composites with silanized fibers and ones with only alkaline treatment (Table 39 and Figure 88). Probably, it means that silanization did not affect the adhesion between alkaline-treated curauá and polyamide 6 matrix, only increasing the thermal stability of this fiber, allowing processing with polyamide 6.6 with low risk of degradation, as it will be performed afterwards.

Table 39: Mechanical properties of composites prepared with neat, alkaline-treated and alkaline-treated + silanized curauá at 30 wt.% fiber content

| Composite | Fiber | Stress (MPa) | Strain (%) | Elastic Modulus (MPa) |
|---------------|--------------------------|--------------|------------|-----------------------|
| PA 6 | - | 45.8 ± 3.5 | > 100% | 751 ± 80 |
| PA 6 – Curauá | Neat | 58.7 ± 4.0 | 3.2 ± 0.4 | 2230 ± 31 |
| | Alk. Treated | 90.2 ± 1.7 | 5.3 ± 0.1 | 2259 ± 53 |
| | Alk. Treated + Silanized | 89.6 ± 2.7 | 5.3 ± 0.2 | 2328 ± 73 |

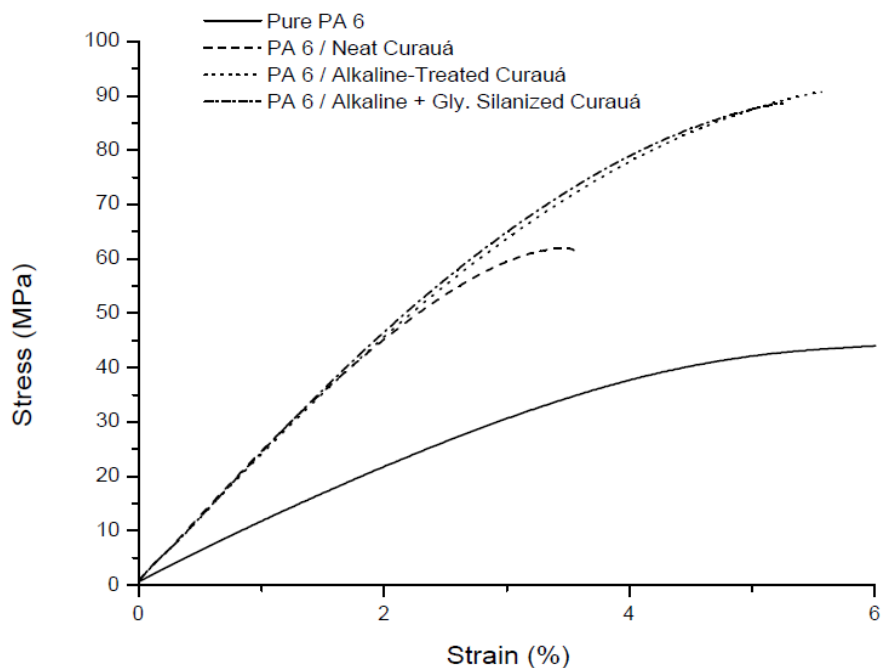


Figure 88: Stress versus strain curves of composites prepared with neat, alkaline-treated and alkaline-treated + silanized curauá at 30 wt.% fiber content

After this set of experiments, composites of PA 6.6 and fibers were prepared using a salt and plasticized to investigate the decrease of melting temperature of PA 6.6 and to allow the processing with natural fibers.

5.6.3 Decreasing melting temperature of polyamide 6.6 - Influence of plasticizers

Three parameters were chosen to perform experimental design with plasticizers (LiCl and NBBSA), according to described in methodology (chapter 4, section 4.5.2.1): viscosity (detected during extrusion compounding in Haake Minilab), melting temperature by differential scanning calorimetry and elastic modulus, characterized by dynamic mechanical analysis, DMA.

5.6.3.1 DSC of different extruded formulations of polyamide 6.6

Table 40 shows the DSC results of neat polyamide 6.6 and with plasticizers. It can be seen on the DSC curve of neat polyamide 6.6 (Figure 89) that there is a

shoulder at lower temperatures, explained by the presence of two crystalline structures (alpha and gamma) present in polyamide 6.6. Melting peaks of PA 6.6 are narrow, meaning that most crystals presents at the polyamide 6.6 structure are well organized and large.

Table 40: Crystallization temperature, melting temperature and crystallinity of neat PA 6.6 and with plasticizers

| | Formulations | T_c (°C) | T_m (°C) | X_c (%) |
|---|--|---------------------------|---------------------------|--------------------------|
| 1 | PA 6.6 | 233 | 262 | 29.5 |
| 2 | PA 6.6 + 5.0 wt.% LiCl | 202 | 241 | 19.1 |
| 3 | PA 6.6 + 5.0 wt.% BBSA | 213 | 246 | 21.1 |
| 4 | PA 6.6 + 5.0 wt.% LiCl + 5.0 wt.% BBSA | 213 | 247 | 31.5 |
| 5 | PA 6.6 + 2.5 wt.% LiCl + 2.5 wt.% BBSA | 219 | 251 | 23.2 |
| 6 | PA 6.6 + 2.5 wt.% LiCl + 2.5 wt.% BBSA | 214 | 248 | 21.5 |
| 7 | PA 6.6 + 2.5 wt.% LiCl + 2.5 wt.% BBSA | 210 | 244 | 27.0 |

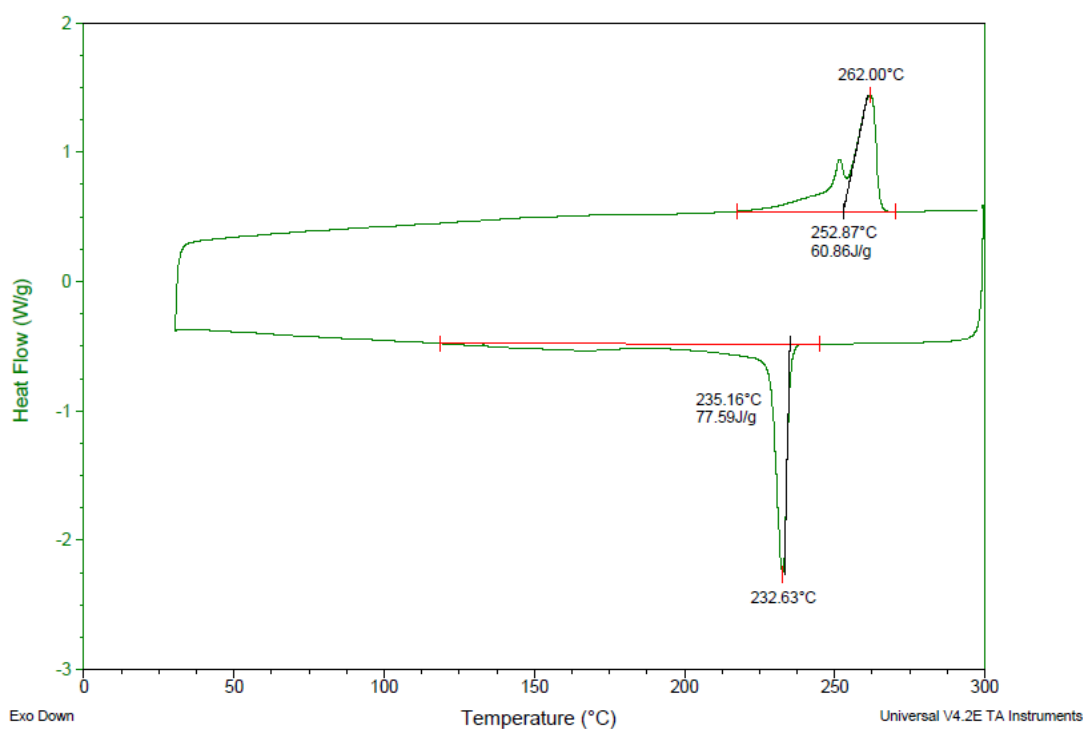


Figure 89: DSC curve of pure PA 6.6

The decrease of T_m observed in PA 6.6 with the addition of only BBSA can be related to the plasticizer act as a “liquid impurity”, preventing formation of certain crystals. (Figure 90). The same behavior is observed to samples with only LiCl (Figure 91) because of the formation of ionic interactions between the polyamide molecules and the halide salt due to elimination of the polyamide hydrogen bonding. And, finally, the combination of LiCl and BBSA (Figure 92) shows the elimination of low thermal stability crystals and result in lower melting temperatures, which can be an advantage for processing of PA 6.6 with natural fibers).

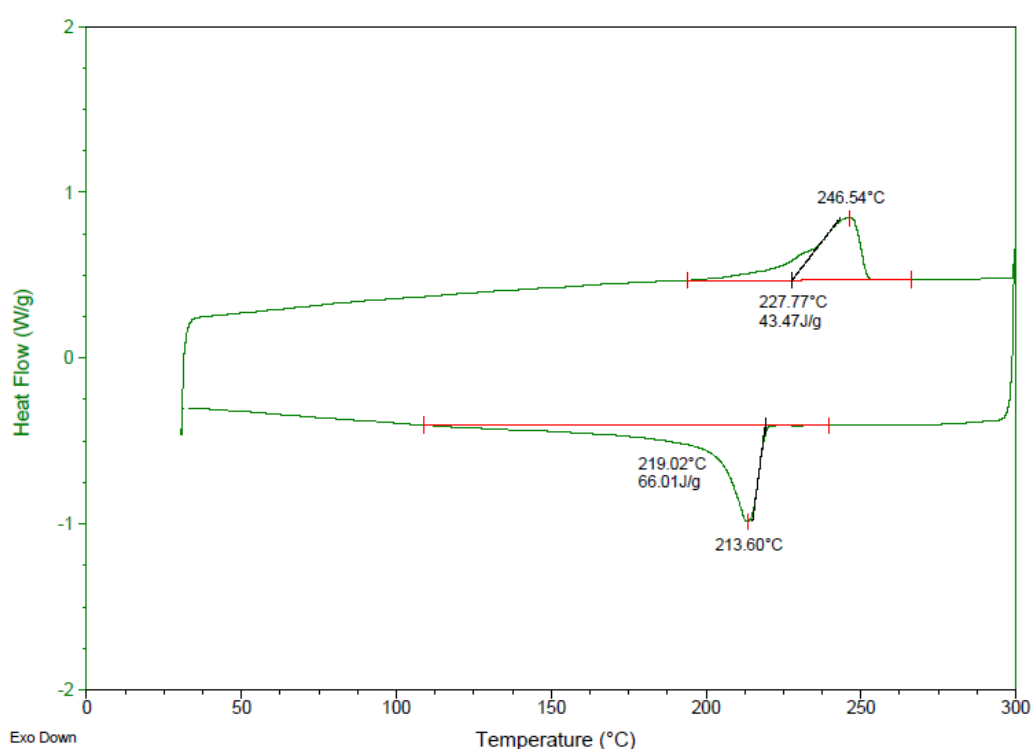


Figure 90: DSC of PA 6.6 + 5.0 wt.% BBSA

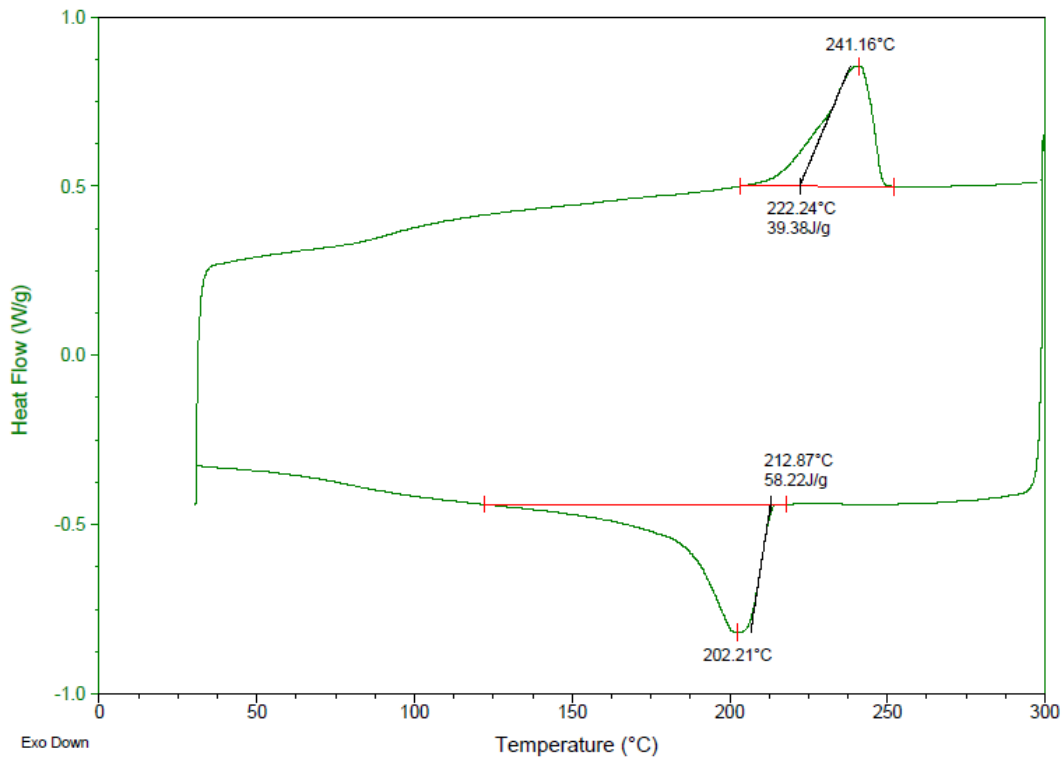


Figure 91: DSC curve of PA 6.6 + 5.0 wt.% LiCl

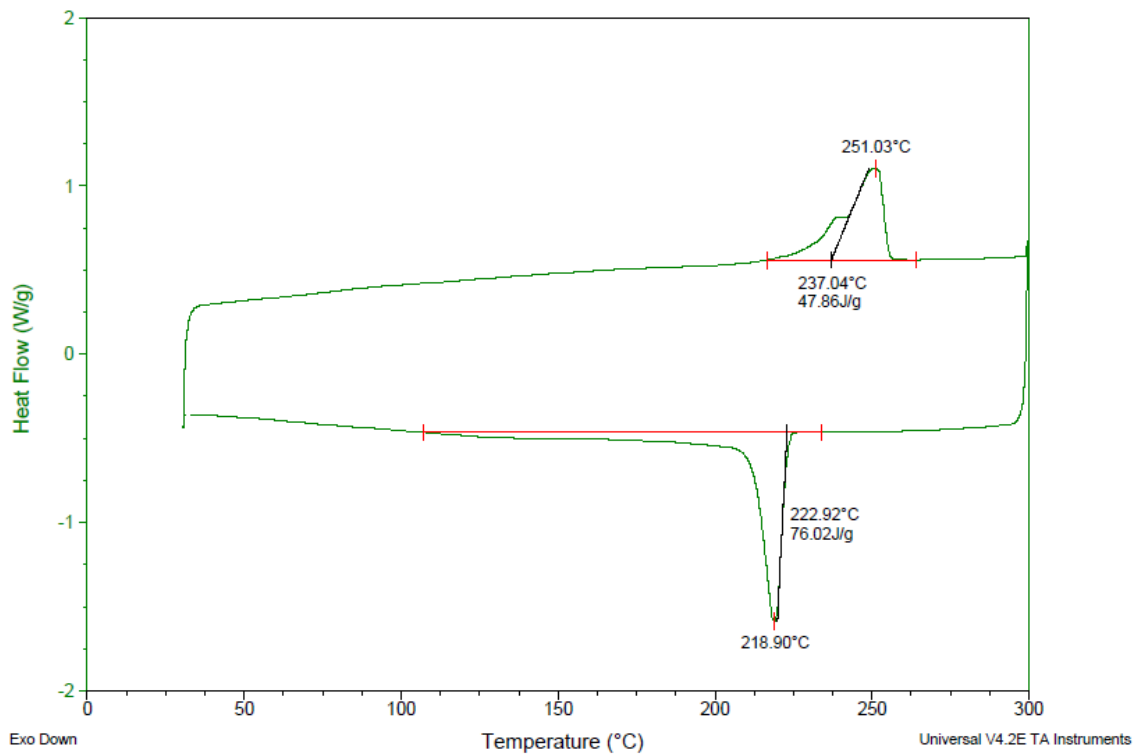


Figure 92: DSC curve of PA 6.6 + 2.5 wt.% LiCl + 2.5 wt.% BBSA (sample 5)

5.6.3.2 DMTA of different extruded formulations of polyamide 6.6

The main results of DMA experiments with the PA 6.6 formulations are found in Table 41. The increase of viscosity for all samples with at least 2.5 wt.% of LiCl is the consequence of the formation of a “pseudo-crosslinked structure” (AMINTOWLIEH; SARDASHTI; SIMON, 2012) observed with the addition of this salt. The increase of $\tan \delta$ (damping factor) for all samples when compared to pure PA 6.6 means less rigid material with good impact properties. As expected, T_g of samples with LiCl increased because of the effect of this “pseudo-crosslinked” structure. The reduction of T_g of PA 6.6 with BBSA in comparison with pure PA 6.6 can be explained in terms of increasing of free volume between the polymer chains and increasing of molecular mobility.

Table 41: DMA analysis and viscosity of neat PA 6.6 and with plasticizers

| Formulations | | E' (GPa) at 0 °C | Tan δ | Tg at E'' (°C) | Viscosity (Pa.s) |
|--------------|--|------------------|--------------|----------------|------------------|
| 1 | PA 6.6 | 4.04 | 0.1003 | 71 | 3.3 |
| 2 | PA 6.6 + 5.0 wt.% LiCl | 3.55 | 0.2642 | 109 | 7.5 |
| 3 | PA 6.6 + 5.0 wt.% BBSA | 3.38 | 0.1405 | 67 | 3.3 |
| 4 | PA 6.6 + 5.0 wt.% LiCl + 5.0 wt.% BBSA | 4.25 | 0.2361 | 100 | 5.6 |
| 5 | PA 6.6 + 2.5 wt.% LiCl + 2.5 wt.% BBSA | 4.96 | 0.1590 | 49 | 5.0 |
| 6 | PA 6.6 + 2.5 wt.% LiCl + 2.5 wt.% BBSA | 4.89 | 0.1905 | 34 | 5.9 |
| 7 | PA 6.6 + 2.5 wt.% LiCl + 2.5 wt.% BBSA | 4.99 | 0.1842 | 7.1 | 6.4 |

5.6.3.3 Experimental Design

The best conditions of processing PA 66 with natural fibers can be chosen from the thermal and mechanical parameters presented in Table 42.

Table 42: Elastic modulus, melting temperature and viscosity of samples

| Formulations | | E' (MPa) | T _m (°C) | Viscosity (Pa.s) |
|--------------|--------------------------------------|----------|---------------------|------------------|
| 1 | PA 6.6 | 4.04 | 262 | 3.3 |
| 2 | PA 6.6 + 5.0 wt.% LiCl | 3.55 | 241 | 7.5 |
| 3 | PA 6.6 + 5.0 wt.% BBSA | 3.38 | 246 | 3.3 |
| 4 | PA 6.6 + 5.0 wt.% LiCl + 5.0 wt.% | 4.25 | 247 | 5.6 |
| 5 | PA 6.6 + 2.5 wt.% LiCl + 2.5 wt.% | 4.96 | 251 | 5.0 |
| 6 | PA 6.6 + 2.5 wt.% LiCl + 2.5 wt.% | 4.89 | 248 | 5.9 |
| 7 | PA 6.6 + 2.5 wt.% LiCl + 2.5 wt.% | 4.99 | 244 | 7.1 |

According to the Pareto charts (Figures 93 to 95), it can be noted that the only significant parameter is the melting temperature. And, according to this parameter (Figure 95), combined effect of both LiCl/BBSA is more decisive to influence T_m than each component separately. As values of elastic modulus of components at the central point (samples 5, 6 and 7 of Table 20) are significantly higher than the others, it can be concluded that the best formulation when using natural fibers is PA 6.6 with 2.5% of LiCl and 2.5% of BBSA. Moreover, it is feasible to compound this formulation at 260 °C, according to preliminary experiments in Haake Minilab.

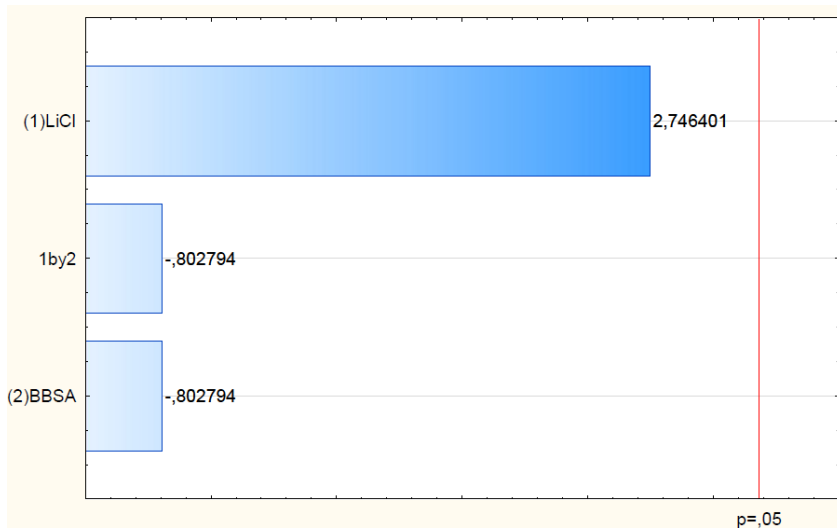


Figure 93: Pareto chart of modified polyamide 6.6 – influence of viscosity

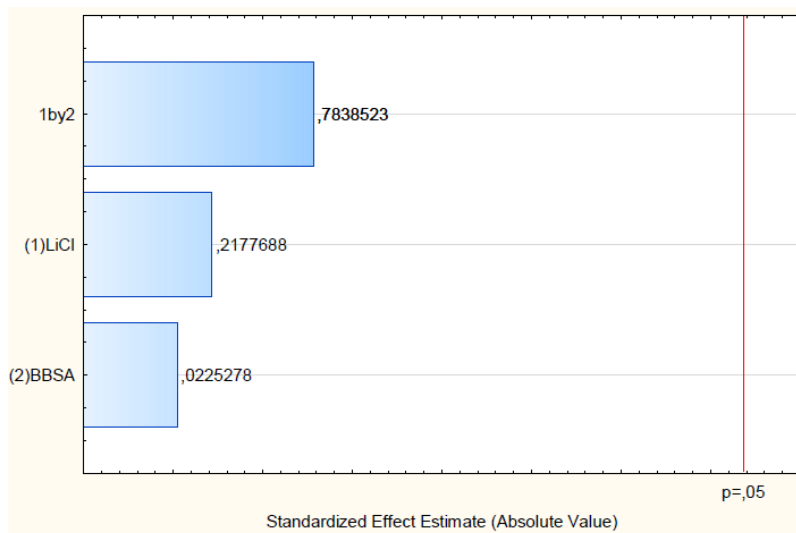


Figure 94: Pareto chart of modified polyamide 6.6 – influence of elastic modulus

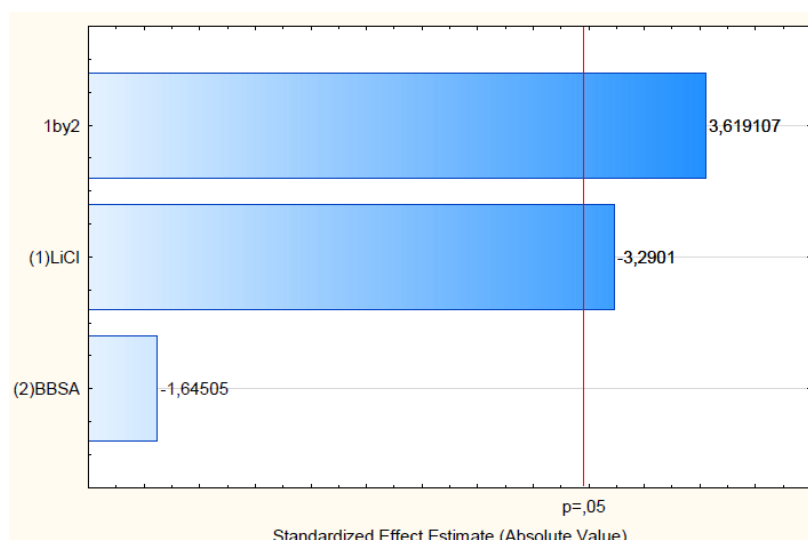


Figure 95: Pareto chart of modified polyamide 6.6 – influence of melting temperature

5.6.4 FTIR and DSC of compounded PA 6.6/ silanized curauá composites

FTIR analysis was performed on composites of alkaline-treated + glycidyl-silanized curauá / polyamide 6.6 with and without plasticizers processed at 260 and 280 °C, respectively, showing similar results to pure polyamide. Figure 96 shows the spectra of pure PA 6.6, PA 6.6/ alkaline-treated + glycidyl-silanized curauá without plasticizer and PA 6.6/ alkaline-treated + glycidyl-silanized curauá with plasticizer. It can be observed some characteristic polyamide bands as: N – H stretching vibration at 3317 cm^{-1} ; C – H stretching vibration at 2939 cm^{-1} ; C=O stretching vibration (amide I) at 1645 cm^{-1} and C – N stretching and CO – N – H bending modes (amide II) at 1554 cm^{-1} (DU; GEORGE, 2007). Observing closely the region between 1200 – 900 cm^{-1} (Figure 97), characteristic glucose ring stretching at 897 cm^{-1} , is clearly appearing, showing the insertion of fiber onto polymer.

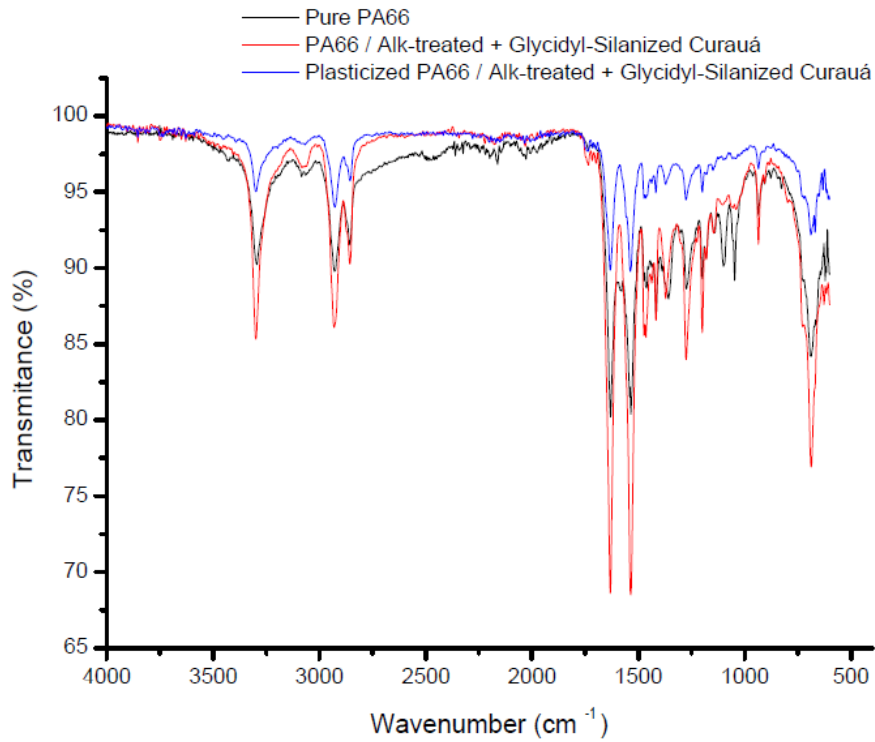


Figure 96: FTIR spectra of PA 6.6/ alkaline-treated + glycidyl-silanized curauá composites

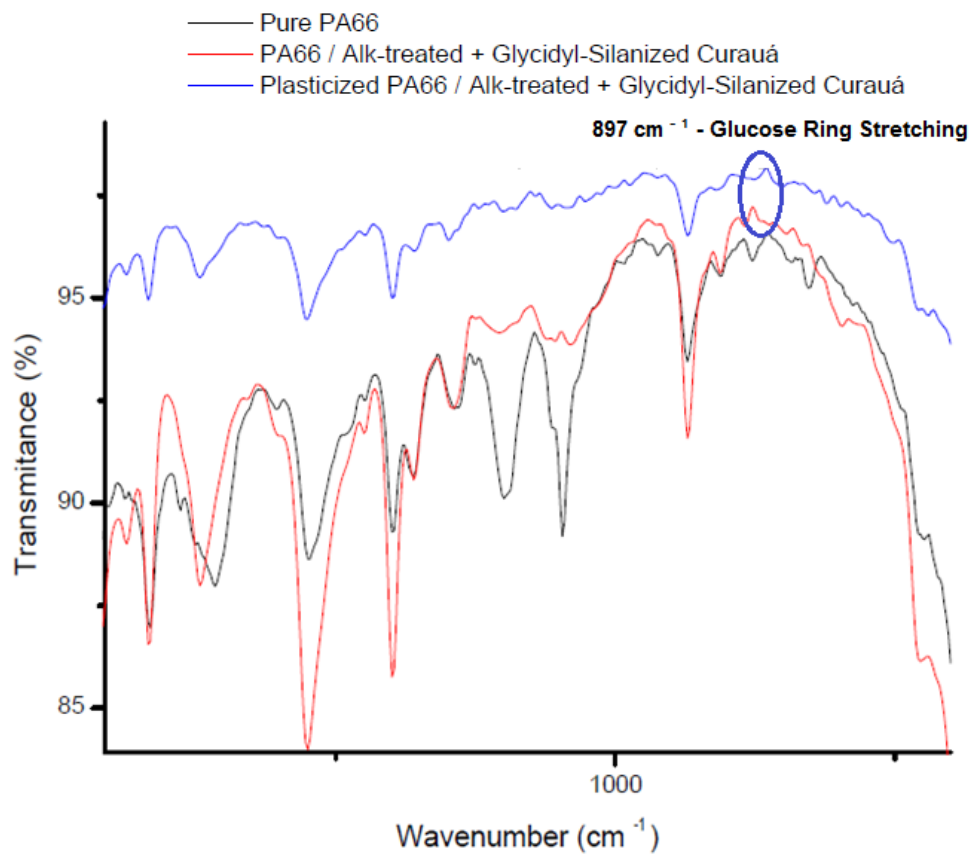
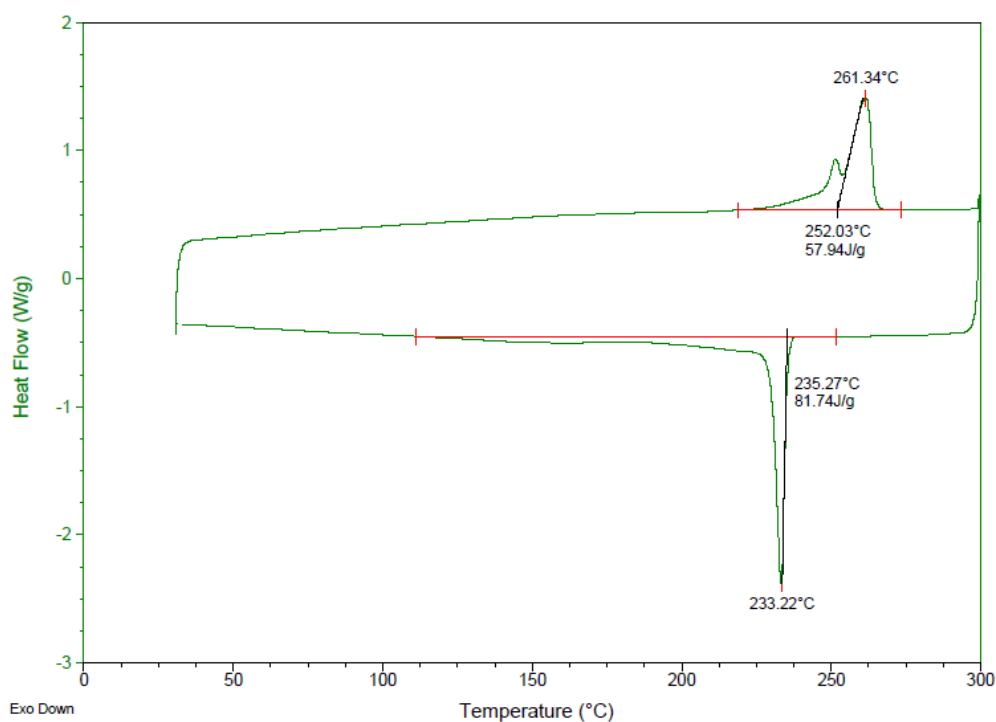
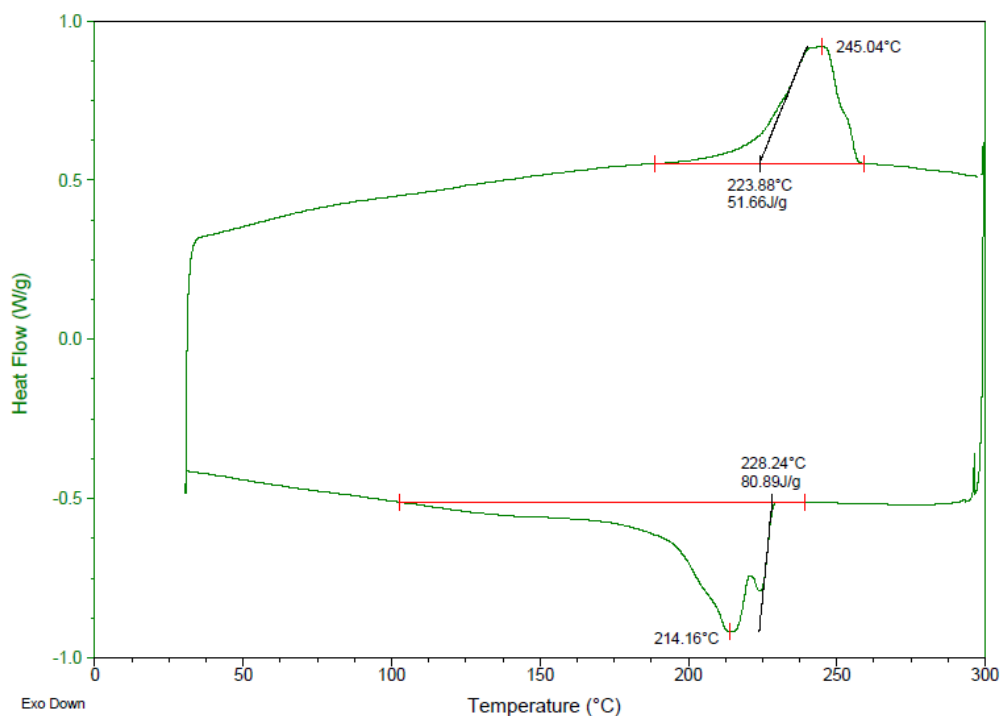


Figure 97: A zoom to FTIR spectra of PA 6.6/ alkaline-treated + glycidyl-silanized curauá composites

In the same way, differences between the composites with and without plasticizers were similar in DSC analysis. Table 43 and Figure 98 show the results of formulations prepared with alkaline-treated + glycidyl-silanized curauá. Melting temperature of composites with plasticizers as well as degree of crystallinity showed a significant decrease when compared to samples without plasticizer and neat PA6.6. Probably, insertion of salt and plasticizer caused a disarrangement of crystals organization, as evidenced by the enlargement of melting peak, leading to the reduction of degree of crystallinity.



(a)



(b)

Figure 98: DSC curves of composites PA 6.6 / alkaline-treated + glycidyl-silanized curauá composites (a) without plasticizers; (b) with plasticizers

Table 43: Crystallization, melting temperature and degree of crystallinity of PA 6.6 / alkaline-treated + glycidyl-silanized curauá composites, without and with (noted (p)) plasticizer

| Formulations | T_c (°C) | T_m (°C) | X_c (%) |
|--|------------|------------|-----------|
| PA 6.6 | 233 | 262 | 29.5 |
| PA6.6 / alkaline-treated + glycidyl-silanized curauá | 233 | 261 | 28.1 |
| PA 6.6 (p)* / alkaline-treated + glycidyl-silanized curauá | 228 | 245 | 25.0 |

*plasticized with 2.5 wt.% of LiCl/BBSA

5.6.5 Mechanical properties: tension testings of PA 6.6 / natural fibers

Table 44 and Figures 99 – 101 show the results of mechanical properties of composites prepared with untreated and alkaline treated + silanized fibers (curauá, jute and flax), fixing the fiber content at 10 wt. %. As expected, it is

observed an increasing of elastic modulus due to insertion of fibers. Moreover, a strong decrease of strain at break is also observed due to the fact that the filler has a very low strain at break.

Table 44: Mechanical properties of composites prepared with neat PA 6.6 (without plasticizers) and alkaline-treated + gly.silanized fibers at 10 wt.% fiber content. (composites compounded at 280 °C)

| Composite | Fiber | Plasticizer | Stress (MPa) | Strain (%) | Elastic Modulus (MPa) |
|-----------------|--------------------------|-------------|--------------|------------|-----------------------|
| PA 6.6 | - | No | 60,5 ± 0.6 | >100 | 713 ± 14 |
| | | Yes | 69.3 ± 2.5 | 31.7 ± 14 | 826 ± 28 |
| PA 6.6 – Curauá | Neat | No | 50.9 ± 3.3 | 8.5 ± 0.4 | 925 ± 58 |
| | | Yes | 49.8 ± 2.3 | 7.4 ± 0,1 | 906 ± 15 |
| | Alk. Treated + Silanized | No | 58,0 ± 1.8 | 9.8 ± 0.4 | 889 ± 20 |
| | | Yes | 64.6 ± 1.4 | 9.4 ± 0.3 | 934 ± 48 |
| PA 6.6 – Jute | Neat | No | 49.6 ± 2.7 | 7.7 ± 0.4 | 855 ± 49 |
| | | Yes | 50.4 ± 3,9 | 7.6 ± 0.4 | 923 ± 52 |
| | Alk. Treated + Silanized | No | 55.7 ± 2.3 | 8.9 ± 0.4 | 840 ± 45 |
| | | Yes | 56.0 ± 3.0 | 8.3 ± 0.4 | 928 ± 49 |
| PA 6.6 – Flax | Neat | No | 66.7 ± 2.5 | 11.8 ± 1.0 | 919 ± 40 |
| | | Yes | 64.2 ± 3.4 | 9.4 ± 0.5 | 933 ± 46 |
| | Alk. Treated + Silanized | No | 66.8 ± 2.8 | 11.6 ± 1.3 | 886 ± 36 |
| | | Yes | 67.7 ± 2.0 | 11.0 ± 0.3 | 874 ± 56 |

However, the only improvement of tensile stress, related to enhancement of mechanical properties of neat PA 6.6, is seen in composites with flax fibers. Composites prepared with treated jute and curauá fibers show higher tensile stress than their respective composites with neat fibers, but only the composite with treated curauá is able to show similar mechanical properties compared to pure resin. Moreover, when treated curauá is compounded with plasticized polyamide, it is observed a slight increase of tensile stress compared to pure resin.

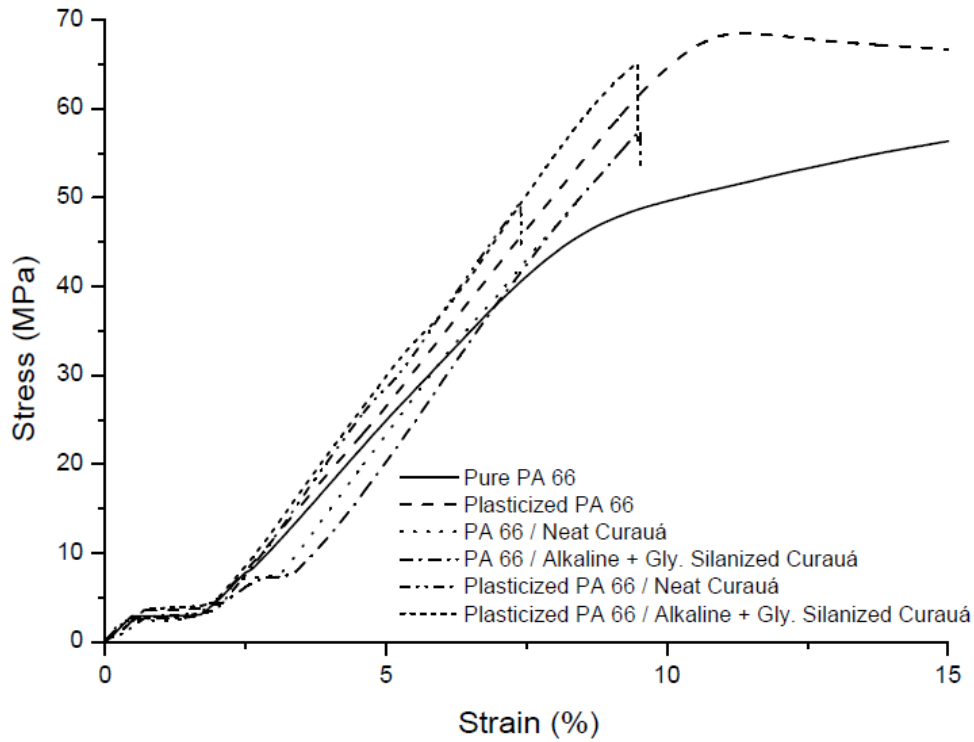


Figure 99: Stress versus strain curves of PA 6.6 / curauá composites 90/10

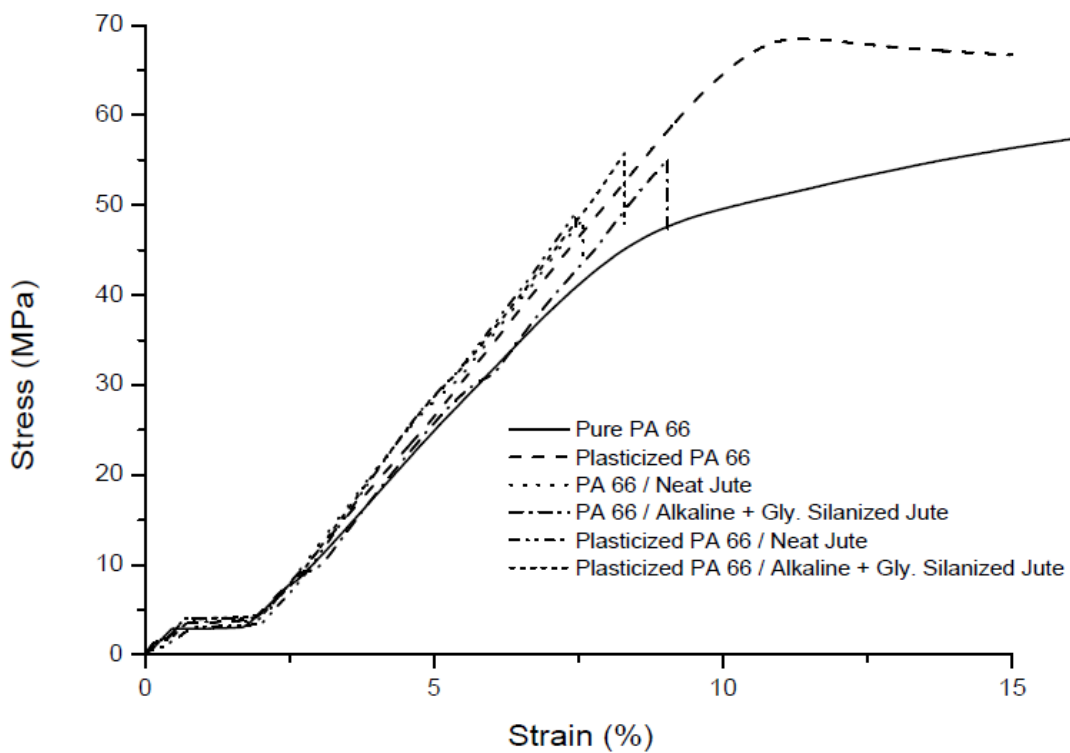


Figure 100: Stress versus strain curves of PA 6.6 / jute composites 90/10

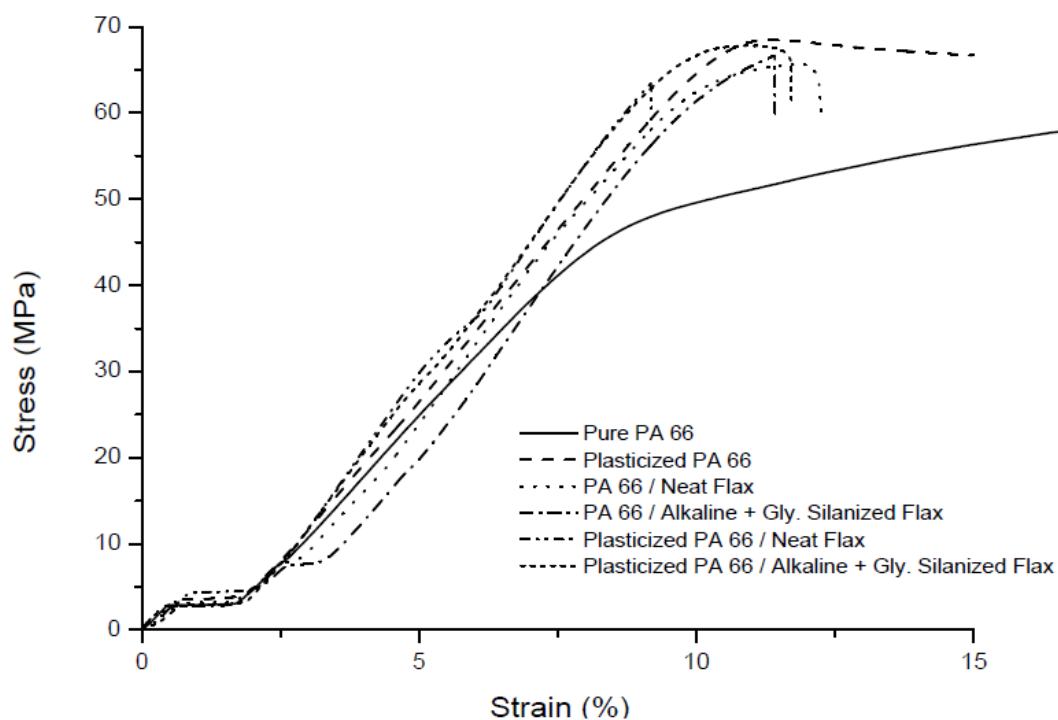


Figure 101: Stress versus strain curves of PA 6.6 / flax composites 90/10

For the next set of composite, the effect of curauá content on mechanical and thermal properties of plasticized PA 66 / curauá fiber composites, will be studied employing 20 and 30 wt. % of neat and treated fiber in polyamide matrix.

5.6.6 Mechanical properties: impact resistance of PA 6.6 / natural fibers

Results of impact resistance (resilience) are shown in Table 45 and Figure 102. All composites have divided completely in two separate pieces, with no substantial plastic deformation. Use of the combination NBBSA + lithium salt led to decrease of resilience of PA 66 due to pseudo-crosslinking effect caused by lithium salt, increasing its rigidity.

Table 45: Impact properties of composites prepared with neat PA 6.6 (without plasticizers) and alkaline-treated + silanized fibers at 10 wt.% fiber content.

| Composite | Fiber | Plasticizer | Resilience (KJ/m ²) |
|----------------|--------------------------|-------------|---------------------------------|
| PA66 | - | No | 4.26 ± 0.02 |
| | | Yes | 2.66 ± 0.36 |
| PA 66 – Curauá | Neat | No | - |
| | | Yes | 2.22 ± 0,56 |
| | Alk. Treated + Silanized | No | 3,09 ± 0,62 |
| | | Yes | 2.30 ± 0.25 |
| PA 66 – Jute | Neat | No | - |
| | | Yes | 1,85 ± 0,19 |
| | Alk. Treated + Silanized | No | 2,10 ± 0,44 |
| | | Yes | 1.43 ± 0.17 |
| PA 66 – Flax | Neat | No | - |
| | | Yes | 2.64 ± 0.29 |
| | Alk. Treated + Silanized | No | 2,92 ± 0,60 |
| | | Yes | 2.45 ± 0.03 |

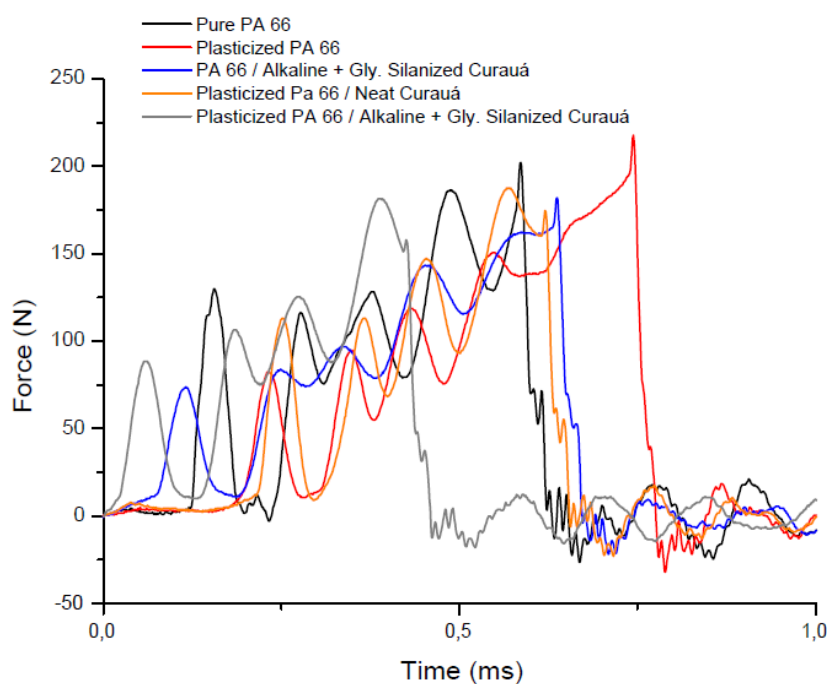


Figure 102: Impact curves of PA 6.6 / curauá fibers composites 90/10

In a general overview, insertion of natural fibers lead to a decrease of impact resistance when compared to neat polyamide 66. These results are coherent with tension results, where an increase of elastic modulus is observed for composites due to the presence of fibers. For composites with plasticized polyamide, the values of resilience are similar to the one found in neat polyamide with NBBSA + LiCl, despite its higher elastic modulus. Finally, no

tests were conducted with composites prepared using untreated fibers and neat polyamide without plasticizer. It was not possible to inject test bars of these composites because, at 280 °C, after melting, there was a strong releasing of gas probably due to the degradation of fiber at higher temperatures. As for impact test bars the amount of material necessary to prepare one test bar is significantly higher than that to prepare tension test bars, one of the components of Haake mini-injection machine was pulled out due to overflow of melted material, becoming impossible to inject the impact test bars.

5.6.7 Mechanical properties: tension testings of plasticized PA 6.6 / curauá fibers - influence of fiber content

Aiming at investigating the improvement (or not) of mechanical properties of PA 66 / natural fibers composites, different content of neat and alkaline + silanized curauá fibers were mixed with plasticized polyamide 66 and results can be observed in Table 46 and Figure 103. It should be mentioned that, during the moulding of test bars, higher treated fiber content lead to longer time to melt the composite and to inject it, from 2 minutes (composites with 10 wt.% of alkaline + silanized fibers) up to 6 minutes (composites with 30 wt.% of alkaline + silanized fibers), which drove the decomposition of the fibers.

Table 46: Tension properties of composites prepared with neat PA 6.6 (without plasticizers) and alkaline-treated + silanized fibers at 20 and 30 wt.% fiber content. (composites compounded at 280 °C)

| Composite | Fiber Content (wt.%) | Curauá Fiber | Stress (MPa) | Strain (%) | Elastic Modulus (MPa) |
|-----------------|----------------------|--------------------------|--------------|------------|-----------------------|
| PA 6.6 | - | - | 60,5 ± 0,6 | >100 | 713 ± 14 |
| PA 6.6 – Curauá | 10 | Neat | 49.8 ± 2,3 | 7.4 ± 0,1 | 906 ± 15 |
| | | Alk. Treated + Silanized | 64.6 ± 1.4 | 9.4 ± 0.3 | 934 ± 48 |
| | 20 | Neat | 40.3 ± 4.1 | 7.6 ± 0.4 | 826 ± 33 |
| | | Alk. Treated + Silanized | 51.3 ± 1.0 | 8.8 ± 0.1 | 905 ± 41 |
| | 30 | Neat | 32.0 ± 2.2 | 6.3 ± 0.4 | 884 ± 72 |
| | | Alk. Treated + Silanized | 39.4 ± 1.7 | 7.1 ± 0.4 | 935 ± 55 |

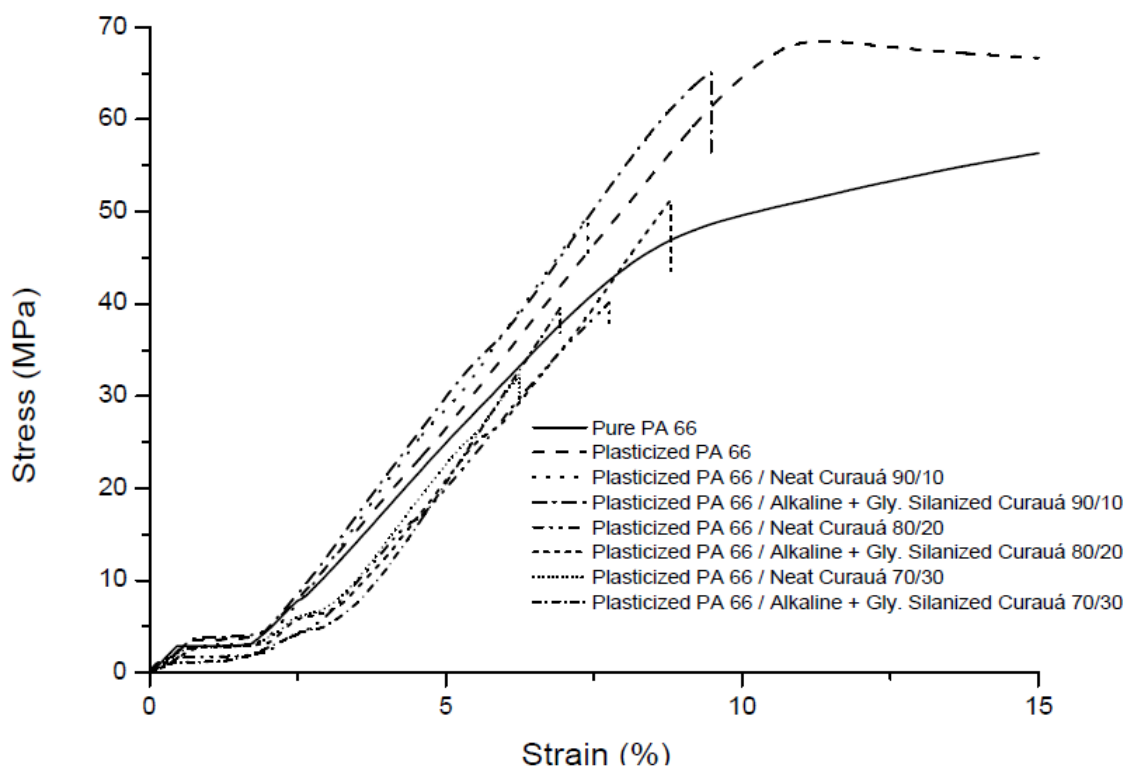


Figure 103: Stress versus strain curves of plasticized PA 6.6 / curauá fibers at different fiber content

By increasing the fiber content, there was no significant change in elastic modulus. In each composite with different fiber content, tensile stress properties are higher in composites with chemically modified fibers and it could be probably explained by a better dispersion between fiber and matrix, as well as a less degradation extension that takes place on treated fibers. However, mechanical properties tends to decrease with increasing of curauá content and this behavior can be attributed to degradation of fibers as time to prepare test bars is longer for composites with higher curauá content. So, to obtain composites with improved mechanical properties, the extrusion parameters needed to prepare the parts must be optimized.

We can compare these results to the ones obtained when studying the thermal resistance of fibers, as given in Table 36. Table 36 shows that the thermal resistance, measured for example as the loss of 5% of matter is much higher than 315°C, which should be enough for using PA66. However, the rate of degradation is here the key parameter. Degradation kinetics is fast. As shown in

Figure 36, it is already more than 1%/min at 190°C. Degradation being a thermally activated phenomenon, we can expect that at temperatures higher than 250°C, mass loss will be several % per min. Keeping high temperatures for 8-10 min will then lead to damages which are strongly decreasing the mechanical properties of the fibers and could inject in the matrix degradation products which will also change its properties.

5.6.8 SEM analysis of PA 6.6 / curauá fibers composites

Images of fractured surfaces of PA 6.6 / curauá fibers in a 90/10 fixed proportion can be observed in Figures 104 and 105. They confirm results of tension and impact testings in which plasticized PA 66 / alkaline + silanized fibers showed better mechanical properties. Composites with treated curauá fibers and plasticized polyamide (compounded at lower temperature, 260 °C) seem to present better distribution of fibers (Figure 104d), more interaction points between fiber and matrix and, consequently, less pull out regions (Figure 105d). It is also easily noted presence of fiber agglomerates and poor adhesion between neat curauá fibers and polyamide 66 and, mainly for plasticized PA 66 / neat curauá fibers (Figures 104a and 105a).

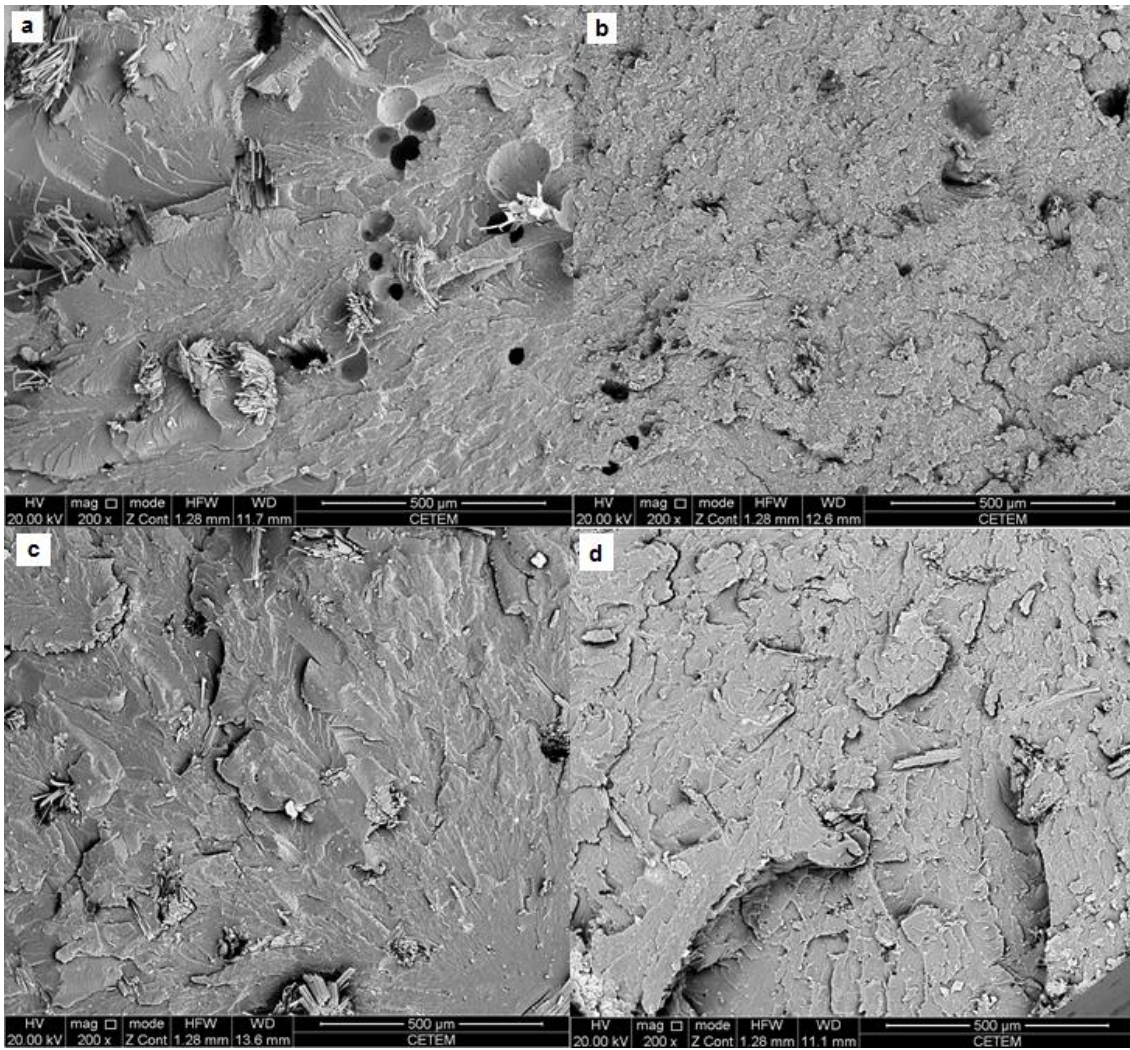


Figure 104: SEM micrographies (200x) of 90/10 : (a) PA 66 / neat curauá ; (b) PA 66 / alkaline + silanized curauá ; (c) plasticized PA 66 / neat curauá ; (d) plasticized PA 66 / alkaline + silanized curauá

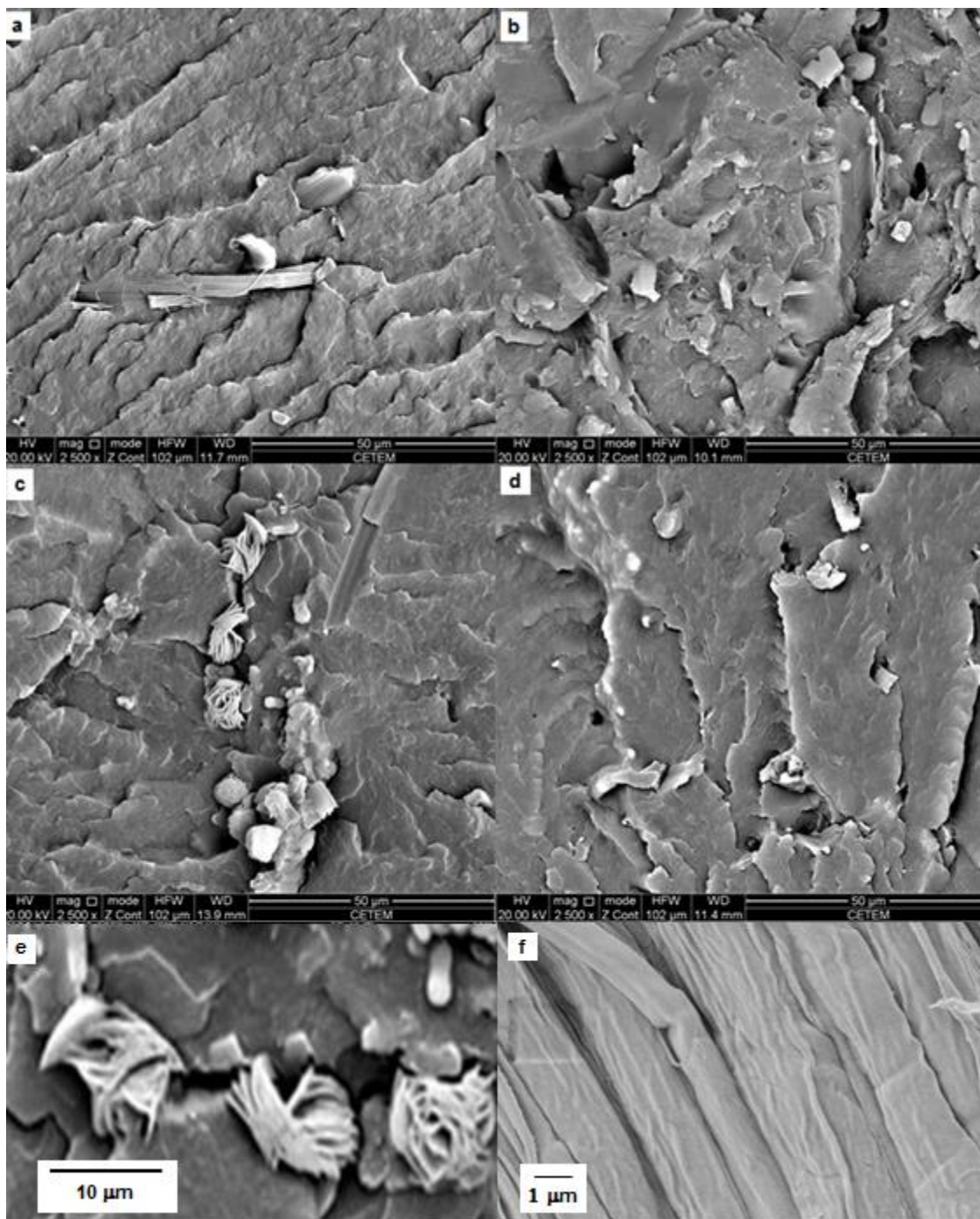


Figure 105: SEM micrographies (2500x) of 90/10 : (a) PA 66 / neat curauá ; (b) PA 66 / alkaline + silanized curauá ; (c) plasticized PA 66 / neat curauá ; (d) plasticized PA 66 / alkaline + silanized curauá; (e) enlargement of photo c (size of the sub-fibers about 0.5 µm); (f) degraded curauá fibers, Figure 62 c

Figure 105c and its enlargement 105e show that under the strong shear and temperature conditions suffered by the fibers, the packed sub-fibers of less than 0.5 micron diameter which are composing the macro-curauá fibers are fully

separated. This is compatible with the observations made on Figure 64 that curauá sub-fibers are better individualized when some thermal degradation occurs (Figures 105f and 64). The fact that the diameter of the sub-fibers seen after a simple heat treatment (Figure 64) have a larger diameter than the ones observed after processing is intriguing.

Increasing content of curauá fiber in plasticized composite leads to decreasing of mechanical properties, as could be seen in Table 46 despite of what, in Figure 106 and mainly in Figure 107, it can be observed that some adhesion points still remain in composites with 20 and 30 wt. % of alkaline + silanized curauá. On the other hand, when fibers are inserted in PA 66 matrix, agglomerates of fibers are clearly noted, according to Figures 106d, 106f and Figures 107d, 107f, showing that possibly the chosen parameters to perform compounding of composites did not contribute well to good dispersion of fibers. This means that other processing extrusion parameters must be employed to improve dispersion of fibers, such as type of screw, mixing elements, extrusion force, etc.

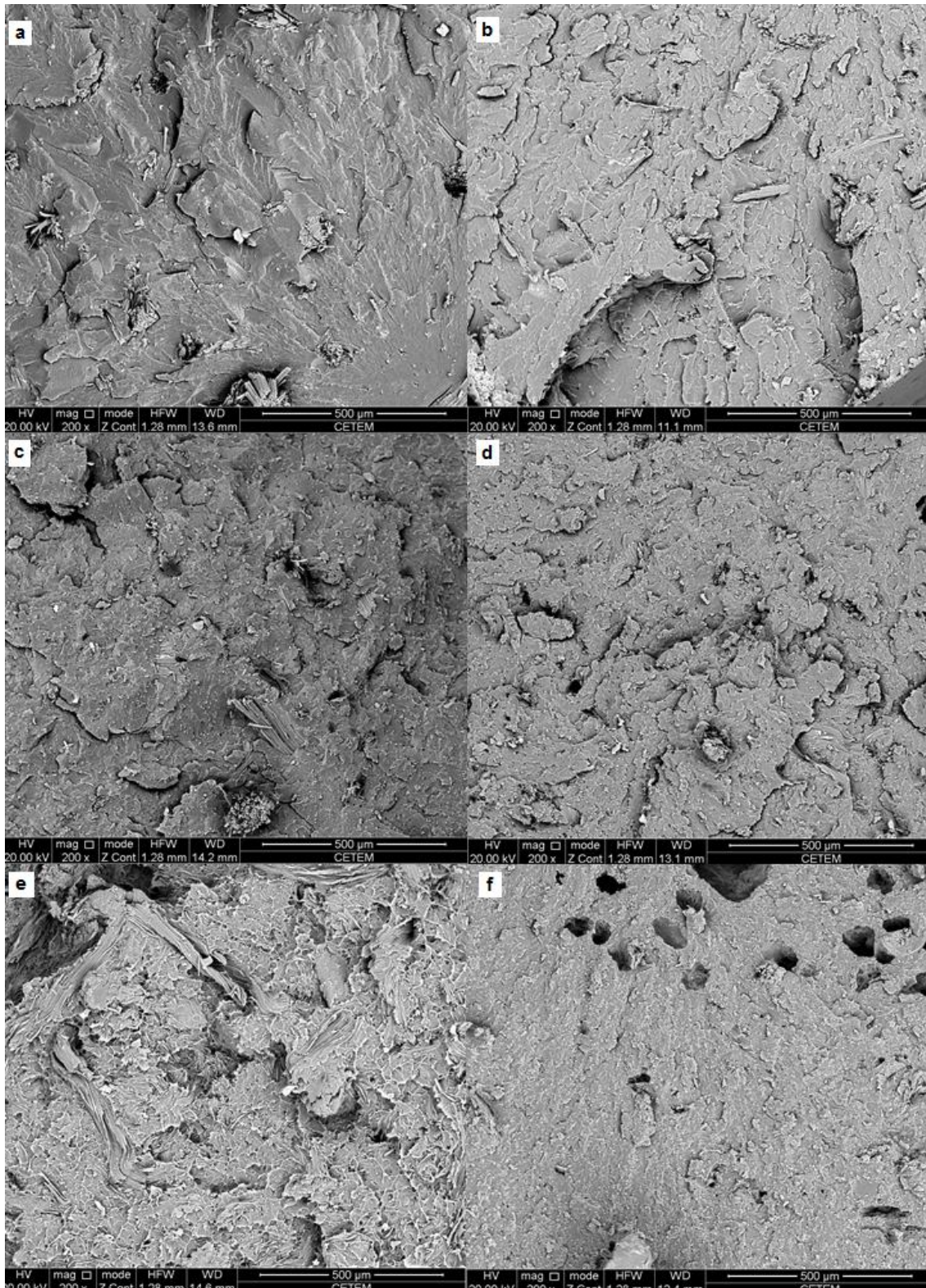


Figure 106: SEM micrographies (200x) of plasticized: (a) PA 66 / neat curauá 90/10 ; (b) PA 66 / alkaline + silanized curauá 90/10 ; (c) PA 66 / neat curauá 80/20; (d) PA 66 / alkaline + silanized curauá 80/20; (e) PA 66 / neat curauá 70/30; (f) PA 66 / alkaline + silanized curauá 70/30

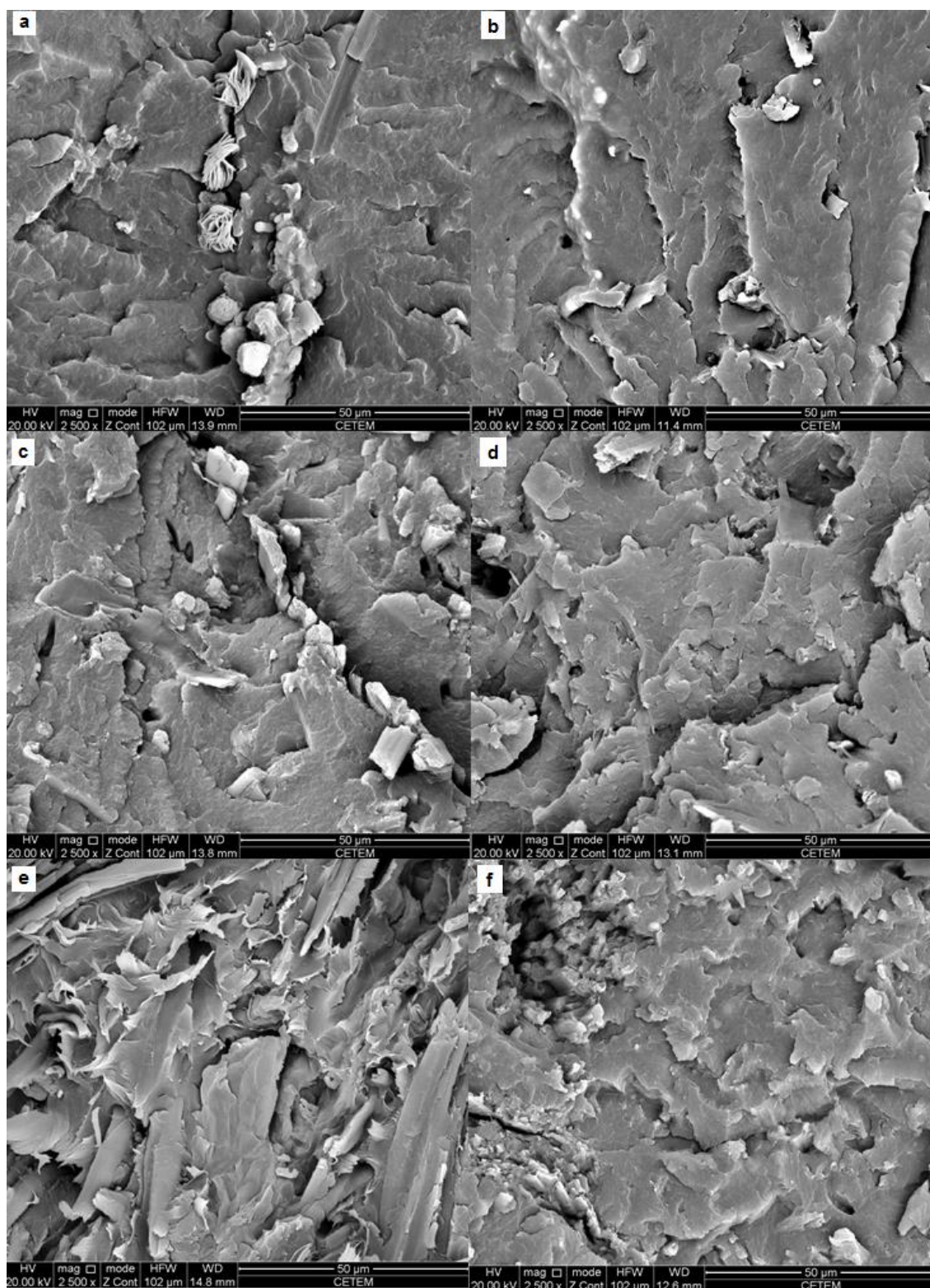


Figure 107: SEM micrographies (2500x) of plasticized: (a) PA 66 / neat curauá 90/10 ; (b) PA 66 / alkaline + silanized curauá 90/10 ; (c) PA 66 / neat curauá 80/20; (d) PA 66 / alkaline + silanized curauá 80/20; (e) PA 66 / neat curauá 70/30; (f) PA 66 / alkaline + silanized curauá 70/30

5.6.9 Thermal behaviour of PA 6.6 / curauá fibers composites

According to Figures 108 – 110, related to TGA and DTG curves of PA 6.6 / curauá fibers composites, some events can be noted during their thermal decompositions. The first, at around 300 °C, is due to degradation of fibers. The second, starting close to 350 °C, is attributed to polyamide 66. However, in case of composites with plasticized polyamide, a third event can be observed, immediately after 400 °C, and it is believed that this can be related to the presence of pseudo-crosslinking of polyamide segments caused by the presence of lithium chloride, increasing their thermal degradation temperature.

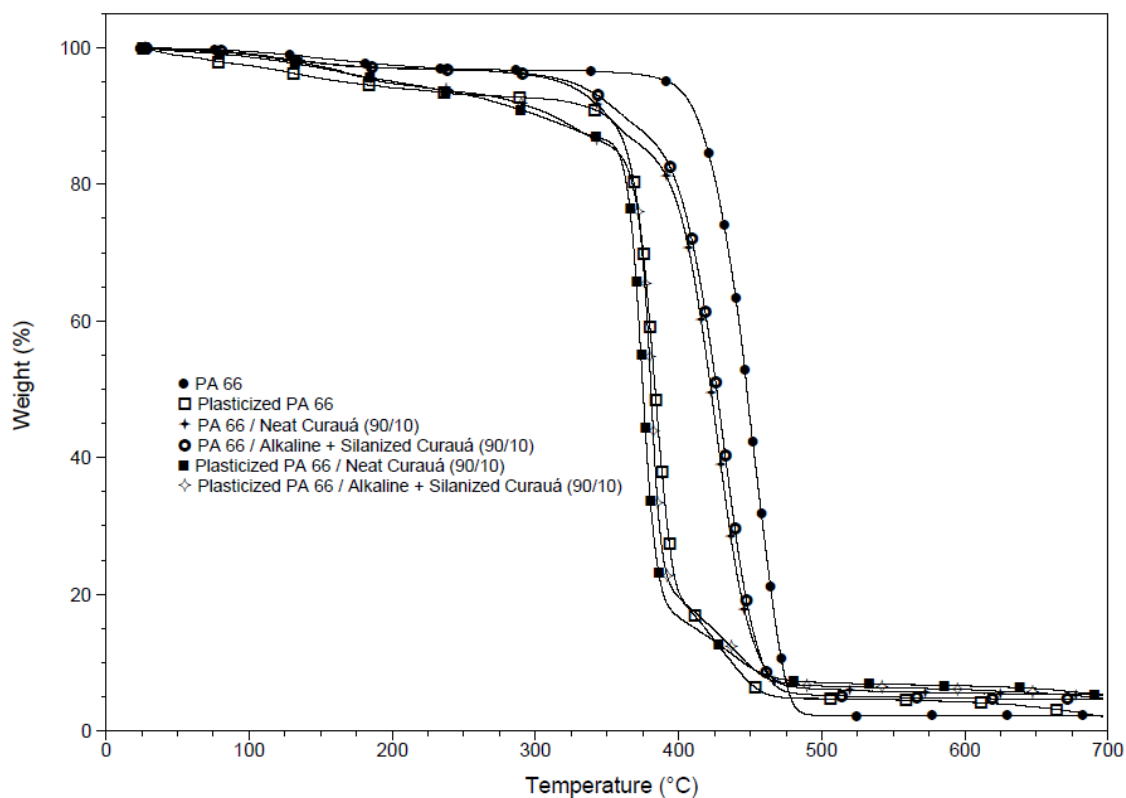


Figure 108: TGA curves of all 90/10 PA 66 / curauá composites

Analyzing the DTG curve of Figure 109, specifically the region of cellulosic degradation, it is perfectly noted, in the range between 300 and 370 °C, more intense degradation peak of composite with neat curauá than that with alkaline + silanized fiber. This is due to the pyrolysis of not only cellulose, but also other components, as hemicelluloses and lignin, since the chemical treatment of natural fibers removed their low molar mass components. However, in Figure 110, these peaks almost disappear completely. Probably some interaction between the plasticizer NBBSA and cellulose is taking place, protecting the fiber against any degradation.

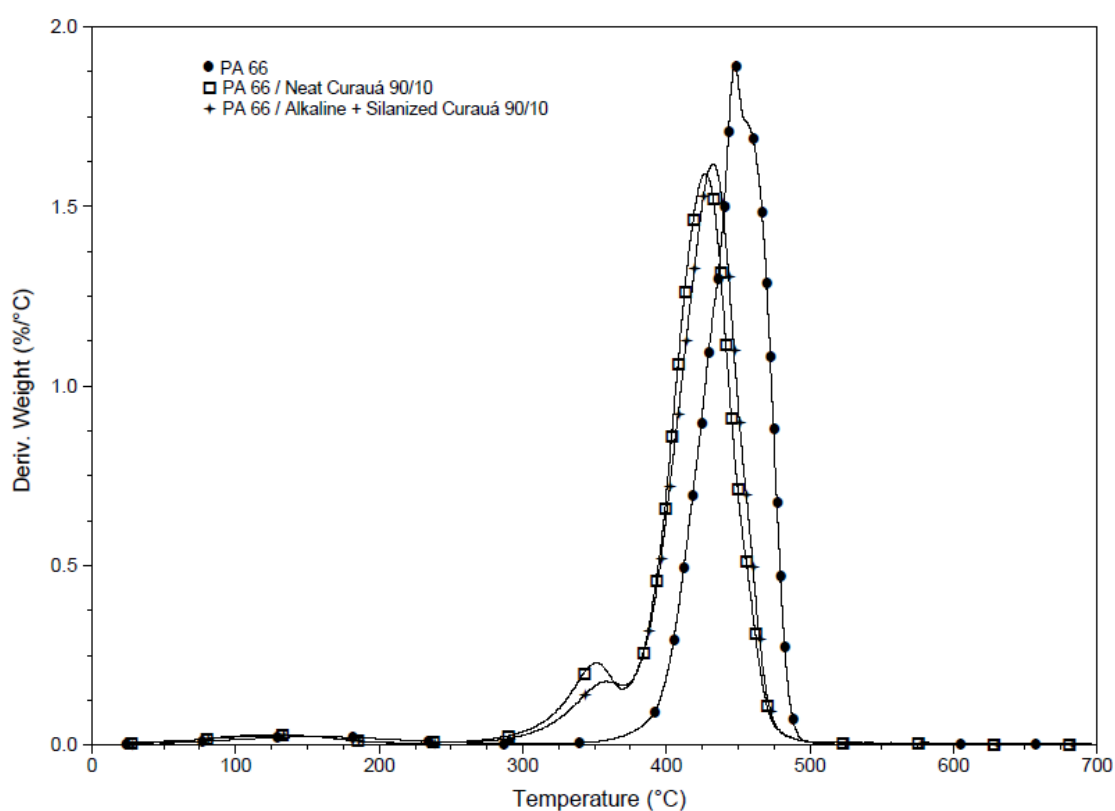


Figure 109: DTG curves of 90/10 PA 66 / curauá composites

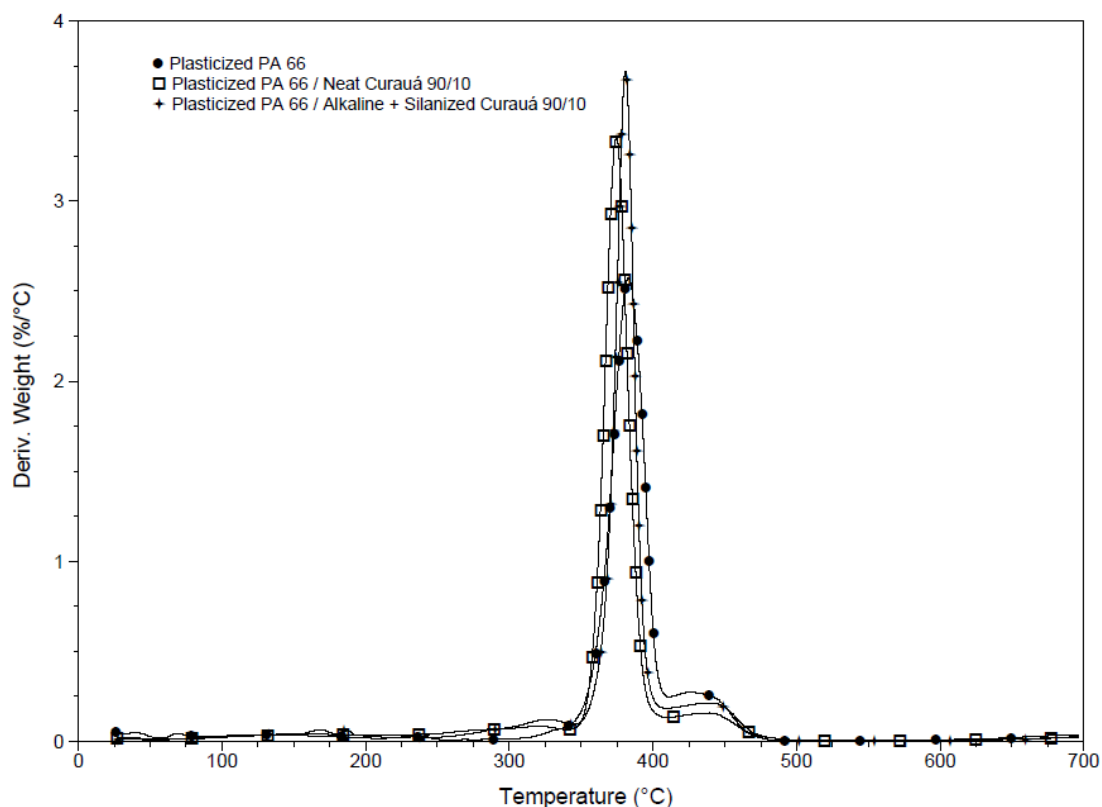


Figure 110: DTG curves of 90/10 plasticized PA 66 / curauá composites

Table 47: Thermal degradation of PA 66 and composites with curauá fibers at 90/10 proportion

| Sample | T _{0.05} (°C) | T _{max} (°C) | Total loss (%) |
|---|------------------------|-----------------------|----------------|
| PA 66 | 408 | 447 | 97.7 |
| PA 66 / Neat Curauá 90/10 | 342 | 352 / 427 | 94.7 |
| PA 66 / Alkaline + Silanized Curauá 90/10 | 351 | 358 / 432 | 95.4 |
| Plasticized PA 66 | 358 | 383 / 425 | 97.8 |
| Plasticized PA 66 / Neat Curauá 90/10 | 300 | 374 / 440 | 94.6 |
| Plasticized PA 66 / Alkaline + Silanized Curauá 90/10 | 315 | 380 / 438 | 95.0 |

Analyzing Table 48 and Figure 111, it is notorious that, increasing fiber content, the first degradation event becomes more evident. Decreasing of T_{0.05} degradation temperature is also observed, showing that the plasticized polyamide with 30 wt.% of curauá fiber resulted in poorer thermal properties compared to the others. Therefore, it can be concluded that using only 10 wt. % of alkaline + silanized curauá on plasticized polyamide can maintain the mechanical properties of pure polyamide, as well as show better thermal

properties than the composites with higher fiber content. In the composites with higher fiber contents, it is noticed low fiber dispersion since SEM micrographs show agglomeration of fibers, which results in lower thermal stability.

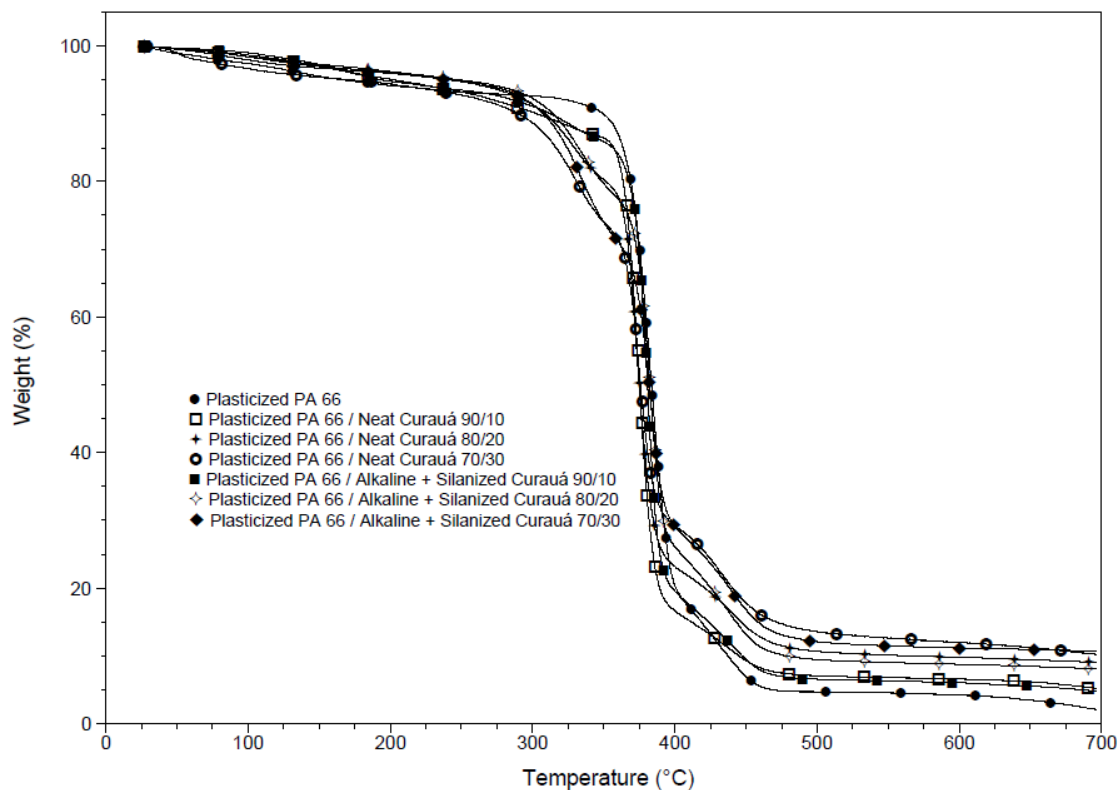


Figure 111: Thermal degradation of plasticized PA 66 and composites with curauá fibers at 90/10, 80/20 and 70/30 proportions

Table 48: Thermal degradation of plasticized PA 66 and composites with curauá fibers at 90/10, 80/20 and 70/30 proportions

| Sample | T _{0.05} (°C) | T _{max} (°C) | Total loss (%) |
|---|------------------------|-----------------------|----------------|
| Plasticized PA 66 | 358 | 383 / 425 | 97.8 |
| Plasticized PA 66 / Neat Curauá 90/10 | 300 | 374 / 440 | 94.6 |
| Plasticized PA 66 / Alkaline + Silanized Curauá 90/10 | 315 | 380 / 438 | 95.0 |
| Plasticized PA 66 / Neat Curauá 80/20 | 298 | 328 / 373 / 439 | 91.0 |
| Plasticized PA 66 / Alkaline + Silanized Curauá 80/20 | 305 | 334 / 382 / 437 | 91.9 |
| Plasticized PA 66 / Neat Curauá 70/30 | 292 | 330 / 375 / 431 | 89.7 |
| Plasticized PA 66 / Alkaline + Silanized Curauá 70/30 | 299 | 335 / 383 / 440 | 89.2 |

6 CONCLUSIONS

This study put in light the difficulties which can be found when willing to process natural fibers at temperatures which are close or above their degradation temperature. The aim of this work was to explore some paths for trying to avoid these detrimental degradation effects.

We can draw the following conclusions of our work:

- Alkaline treatments with NaOH are capable to remove low-molar fractions cellulosic components of the fibers, leading to increase of crystallinity and thermal stability;
- In composites based on polypropylene, a strong increase of elastic modulus are observed using only 10 wt.% of alkaline-treated curauá as filler;
- Acetylation and silanization processes did not change strongly crystallinity and, in some cases, increase the thermal stability of the fibers;
- Alkaline treatments performed in high-pressure are more effective than those at room-pressure, bringing in a short time higher thermal resistance;
- For all treated fibers, decomposition in air occurs at lower temperatures than the ones under nitrogen due to oxidation mechanisms;
- Although viscosimetry results show that there is no degradation on the pure cellulose component of fibers, colorimetry results as well as FTIR, evidence a degradation of treated curaua fibers on PA 6 matrix;
- Utilization of alkaline treated fibers are enough to improve mechanical properties of polyamide 6 matrix. In terms of Elastic Modulus and Tensile

Stress, no differences were observed in composites with alkaline-treated fibers acetylated or silanized;

- Better adhesion between alkaline-treated fibers and PA-6 was observed at 30 wt.% of fiber content, as shown by SEM;
- Fiber degradation is not enough to promote a decrease of the mechanical properties of composites with PA 6;
- Experimental design showed that combination of 2.5 wt. % of LiCl and 2.5 wt. % of NBBSA can reduce the melting temperature of PA 6.6 and, consequently, decrease the processing temperature of this polymer and, at same time, increase its elastic modulus;
- When natural fibers are inserted in polyamide 6.6 at 90/10 wt.% proportion, it was observed an slight increase of elastic modulus and, when plasticizer is in the composite formulation, it is noted an enhancement of tensile stress compared to pure resin, for example, in composite with alkaline + silanized curauá;
- Finally, there is a decrease of mechanical properties when fiber content is 20 and 30 wt.% in plasticized PA 6.6 matrix. This can be attributed to insufficient dispersion of fibers as well as thermal degradation.

7 – PERSPECTIVES

To avoid agglomeration of fibers and thermal degradation in composite processing, the two major problems faced in this work, and classically found in all the literature, we can suggest the following ways.

Avoiding agglomeration is the less difficult task since it can be solved by a combination of fiber incorporation in the extruder with the proper tools and design of the screw. Already, in industry, compounds with up to 40% plant fibers can be successfully prepared. However, the incorporation step is still a matter of research, requiring more understanding of the physical processes at stake.

Avoiding degradation of fibers is a very difficult, if not impossible task. Two ways, tried here, are of course to either use matrices processable below 200°C (which seems to be a sort of upper limit) or decrease the melting temperature of the matrix with additives. This last method is usually associated with a decrease of mechanical properties. Another way is to try increasing the thermal stability of the fibers. Among the methods tested during this work, some were indeed able to increase the thermal stability, but in a way which was not enough to allow processing at temperatures around 240°C. The main problem is not the resistance at these temperatures measured by TGA for example, but the very fast degradation kinetics.

This last point opens a possible way for processing at high temperatures. Taking a combination of a matrix where melting temperature is slightly decreased with treatments which are increasing thermal resistance of fibers, it might be worth working on a processing design which would minimize the exposure at temperatures above 220°C, keeping it below 2 min while ensuring still a good dispersion. This would include a specific design of the mixing screw with a direct coupling to injection, avoiding the re-melting.

REFERENCES

AGRAWAL, R.; SAXENA, N.S.; SHARMA, K.B.; THOMAS, S.; SREEKALA, M.S. Activation energy and crystallization kinetics of untreated and treated oil palm fibre reinforced phenol formaldehyde composites. **Materials Science and Engineering A**, [S.I.], v. 277, n. 1-2, p. 77–82, Jan. 2000. DOI:10.1016/S0921-5093(99)00556-0

AMINTOWLIEH, Y.; SARDASHTI, A.; SIMON, L.C. Polyamide 6 – wheat straw composites: Effects of additives on physical and mechanical properties of the composite. **Polymer Composites**, [S.I.], v. 33, n. 6, p. 976-984, jun. 2012. DOI: 10.1002/pc.22228

ARAÚJO, J.R. ; ADAMO, C.B. ; DE PAOLI, MARCO – A. Conductive composites of polyamide-6 with polyaniline coated vegetal fiber. **Chemical Engineering Journal**, [S.I.], v.174, p.425-431, Aug. 2011. DOI:10.1016/j.cej.2011.08.050

ARCAYA, P.A.; RETEGI, A.; ARBELAIZ, A.; KENNY, J.M; MONDRAGON, I. Mechanical properties of natural fibers/polyamides composites. **Polymer Composites**, [S.I.], v. 30, n. 3, p. 257–264, Mar. 2009. DOI: 10.1002/pc.20558

ARSENAU, D.F. Competitive reactions in the thermal decomposition of cellulose. **Canadian Journal of Chemistry**, [S.I.], v. 49, n. 4, p. 632-638, 1971. DOI: 10.1139/v71-101

BLEDZKI, A. K.; GASSAN, J. Composites reinforced with cellulose based fibres. **Progress in Polymer Science**, [S.I.], v. 24, n. 2, p. 221–274, May. 1999. DOI:10.1016/S0079-6700(98)00018-5

BOGOEVA-GACEVA, G.; AVELLA, M.; MALINCONICO, M.; BUZAROVSKA, A.; GROZDANOV, A.; GENTILE, G.; ENRICO, M.E. Natural fiber eco-composites. **Polymer Composites**, [S.I.],v. 28, n. 1, p. 98-107, Feb. 2007. DOI: 10.1002/pc.20270

BOS, H. **The potential of flax fibres as reinforcement for composite materials**. 2004. 193 p. Ph.D. Thesis – Technische Universteit Eindhoven, Eindhoven, The Netherlands, 2004. Available in <alexandria.tue.nl/extra2/200411364.pdf >. Access on 12 Feb., 2010

BROSIUS, D. Natural fiber composites slowly take root. **Composites Technology**, 2006. Available in <www.compositesworld.com/articles/natural-fiber-composites-slowly-take-root>. Access on 19 Jan., 2010.

CAPART, R.; KHEZAMI, L.; BURNHAM, A.K. Assessment of various kinetic models for the pyrolysis of a microgranular cellulose. **Thermochimica Acta**, [S.I.], v.417, p.79–89, mar. 2004. DOI:10.1016/j.tca.2004.01.029

CHAUHAN, S.; KARMARKAR, A.; AGGARWAL, P. Damping behavior of wood filled polypropylene composites. **Journal of Applied Polymer Science**, [S.I.], v. 114, n. 4, p. 2421-2426, 2009. DOI: 10.1002/app.30718

CHOW, W.S.; ISHAK, Z.A.M. Mechanical, morphological and rheological properties of polyamide 6/ organo-montmorillonite nanocomposites. **Express Polymer Letters**, [S.I.], v.1, n.2, p.77-83, Dec.2006. DOI: 10.3144/expresspolymlett.2007.14

CLEMONS, C. Wood-plastic composites in the United States: the interfacing of two industries. **Forest Products Journal**, v. 52, n. 6, p. 10-18, Jun. 2002. Available in < <http://connection.ebscohost.com/c/articles/6938095/wood-plastic-composites-united-states-interfacing-two-industries> >. Access on 24 Mar., 2010

COUTINHO, F.M.B.; COSTA, T.H.S.; CARVALHO, D.L. Polypropylene–wood fiber composites: Effect of treatment and mixing conditions on mechanical properties. **Journal of Applied Polymer Science**, [S.I.], v. 65, n. 6, p. 1227-1235, Aug. 1997. DOI: 10.1002/(SICI)1097-4628(19970808)65:6<1227::AID-APP18>3.0.CO;2-Q

CULLER, S.R.; ISHIDA, H.; KOENIG, J.L. The silane interphase of composites: effects of process conditions on γ -aminopropyltriethoxysilane. **Polymer Composites**, [S.I.], v. 7, n. 4, p. 231-238, Aug. 1986. DOI: 10.1002/pc.750070406

DU, Y.; GEORGE, S.M. Molecular layer deposition of nylon 66 films examined using in situ FTIR spectroscopy. **The Journal of Physical Chemistry C**, [S.I.], v. 111, n. 24, p. 8509-8517, May 2007. DOI: 10.1021/jp067041n

EICHHORN, S.J.; BAILLIE, C.A.; ZAFEIROPOULOS, N.; MWAIKAMBO, L.Y.; ANSELL, M.P.; DUFRESNE, A.; ENTWHISTLE, K.M.; HERRERA-FRANCO, P.J.; ESCAMILLA, G. C.; GROOM, L.; HUGUES, M.; HILL, C.; RIALS, T.G.; WILD, P.M. Review: current international research into cellulose fibres and composites. **Journal of Materials Science**, [S.I.], v. 36, n. 9, p. 2107-2131, May. 2001. DOI: 10.1023/A:1017512029696

EKLUND, T.; BRICHTER, L.; BÄCHAM, J.; ROSENHOLM, J. Thermogravimetric analysis of γ -aminopropyl-trimethoxysilane adsorbed on silica support. **Journal of Thermal Analysis and Calorimetry**, [S.I.], v. 58, p. 67-76, Oct. 1999. DOI: 10.1023/A:1010195620272

ETAATI, A.; PATHER, S.; FANG, Z.; WANG, H. The study of fibre/matrix bond strength in short hemp polypropylene composites from dynamic mechanical analysis. **Composites: Part B**, [S.I.], v. 62, p. 19-28, Feb. 2014. DOI:10.1016/j.compositesb.2014.02.011

FRISK, H.; SCHWENDEMANN, D. Compounding wood fibers with plastics. *Kunststoffe Plast Europe*, v. 4, p. 76 – 80, 2004. Available in <<https://www.kunststoffe.de/en/journal/archive/article/injection-moulding-compounding-wood-fibres-with-plastics-583684.html>>. Access on 24 Mar., 2010

GARCIA-JALDON, C.; DUPEYRE, D.; VIGNON, M.R. Fibres from semi-retted hemp bundles by steam explosion treatment. **Biomass and Bioenergy**, [S.l.], v. 14, n. 3, p. 251–260, Mar. 1998. DOI:10.1016/S0961-9534(97)10039-3

GEHM, R. **Plastics on the outside**. Automotive Engineering International, p. 46, aug. 2006. Available in <https://www.recyclingtoday.com/Article.aspx?article_id=20469> Access in: 20 Oct. 2010.

GHATGE, N.D.; KHISTI, R.S. Performance of new silane coupling agents along with phenolic no-bake binder for sand core. **Journal of Polymer Materials**, [S.l.], v. 6, p. 145–149, 1989.

GONZALEZ, L.; RODRIGUEZ, A.; DE BENITO, J.L.; MARCOS-FERNANDEZ, A. Applications of an azide sulfonyl silane as elastomer crosslinking and coupling agent. **Journal of Applied Polymer Science**, [S.l.], v. 63, n. 10, p. 1353-1359, Mar. 1997. DOI: 10.1002/(SICI)1097-4628(19970307)63:10<1353::AID-APP15>3.0.CO;2-5

GOWDA, T. M. Some mechanical properties of untreated jute fabric-reinforced polyester composites. **Composites Part A: Applied Science and Manufacturing**, [S.l.], v. 30, n. 3, p. 277–284, Mar. 1999. DOI:10.1016/S1359-835X(98)00157-2

GRAFOVA, I.; KEMELL, M.; LUNZ, J.N.; MARQUES, M.F.V.; GRAFOV, A.; LESKELÄ, M. “Curauá fibre microimaging, atomic layer deposition of metal oxide films, and obtaining of thin wall nanotubes”, in: 11st Brazilian Congress of Polymers, São Paulo, BR, 16 – 20 Oct. 2011.

GUTIÉRREZ, M.C.; DE PAOLI, M.A., FELISBERTI, M.I. Biocomposites based in cellulose acetate and short curauá fibres: Effect of plasticizers and chemical treatments of the fibers. **Composites: Part A**, [S.l.], v. 43, n. 8, p. 1338-1346, Aug. 2012. DOI: 10.1016/j.compositesa.2012.03.006

HE, D.; JIANG, B. The elastic modulus of filled polymer composites. **Journal of Applied Polymer Science**, [S.l.], v. 49, n. 4, p. 617-621, Jul. 1993. DOI: 10.1002/app.1993.070490408

HILL, A.S.C.; ABDUL KHALIL, H.P.S.; HALE, M.D. A study of the potential of acetylation to improve the properties of plant fibers. **Industrial Crops and Products**, [S.l.], v. 8, n. 1, p. 53-63, Mar. 1998. DOI:10.1016/S0926-6690(97)10012-7

HOUBERY, J.; HOUSTON, D. Natural-fiber-reinforced composites in automotive applications. **Journal of the Minerals, Metals and Materials Society**, [S.l.], v. 58, n. 11, p. 80-86, Nov. 2006. DOI: 10.1007/s11837-006-0234-2

HUANG, K.; ZHANG, K.; ZHANG, G.; JIANG, X.; HUANG, D. Acetylation modification of rice straw fiber and its thermal properties. **Cellulose Chemistry and Technology**, v. 48, n. 3-4, p. 199-207, 2014. Available in < <http://www.cellulosechemtechnol.ro/pdf/CCT3-4%282014%29/p.199-207.pdf> >. Access on 17 Aug., 2011

HUJURI, U.; CHATTOPADHAY, S.K.; UPPALURI, R.; GHOSHAL, A.K. Effect of maleic anhydride grafted polypropylene on the mechanical and morphological properties of chemically modified short-pineapple-leaf-fiber-reinforced polypropylene composites. **Journal of Applied Polymer Science**, [S.I.], v. 107, n. 3, p. 1507-1516, Feb. 2008. DOI: 10.1002/app.27156

JACOB, M.; THOMAS, S.; VARUGHESE, K.T. Mechanical properties of sisal/oil palm hybrid fiber reinforced natural rubber composites. **Composites Science and Technology**, [S.I.], v. 64, n. 7-8, p. 955-965, Jun. 2004. DOI:10.1016/S0266-3538(03)00261-6

JÄHN, A.; SCHRÖDER, M.W.; FÜTING, M.; SCHENZEL, K.; DIEPENBROCK, W. Characterization of alkali treated flax fibres by means of FT Raman spectroscopy and environmental scanning electron microscopy. **Spectrochimica Acta Part A: Molecular and Biomolecular Spectroscopy**, [S.I.], v. 58, n. 10, p. 2271-2279, Aug. 2002. DOI:10.1016/S1386-1425(01)00697-7

JAWAID, M.; ABDUL KHALIL, H.P.S.; HASSAN, A.; DUNGANI, R.; HADIYANE, A. Effect of jute fibre loading on tensile and dynamic mechanical properties of oil palm epoxy composites. **Composites: Part B**, [S.I.], v. 45, n. 1, p. 619-624, 2013. DOI:10.1016/j.compositesb.2012.04.068

JOHN, M.J.; ANANDJIWALA, R.D. Chemical modification of flax reinforced polypropylene composites. **Composites Part A: Applied Science and Manufacturing**, [S.I.], v. 40, n. 4, p. 442-448, 2009. DOI:10.1016/j.compositesa.2009.01.007

JOHN, M.J.; ANANDJIWALA, R.D. Recent developments in chemical modification and characterization of natural-fiber reinforced composites. **Polymer Composites**, [S.I.], v. 29, n. 2, p. 187-207, Feb. 2008. DOI: 10.1002/pc.20461

KALIA, S.; KAITH, B.S.; KAUR, I. Pretreatments of natural fibers and their application as reinforcing material in polymer composites: a review. **Polymer Engineering & Science**, [S.I.], v. 49, n. 7, p. 1253-1272, Jul. 2009. DOI: 10.1002/pen.21328

KILZER, F.J. Thermal degradation of cellulose. In **High polymers** (Bikales, N. M. and Segal, L. eds.), Interscience, New York, p. 1015-1031, 1971.

KIM, S.H.; KIM, S.; KIM, J.H.; YANG, S.H. Thermal properties of bio-flour-filled polyolefin composites with different compatibilizing agent type and content.

Thermochimica Acta, [S.I.], v. 451, p. 181-188, Oct. 2006.
DOI:10.1016/j.tca.2006.09.013

KIM, U.J.; EOM, S.H.; WADA, M. Thermal decomposition of native cellulose: influence of crystallite size. **Polymer Degradation and Stability**, [S.I.], v. 95, p. 778-781, May. 2010. DOI:10.1016/j.polymdegradstab.2010.02.009

KLATA, E.; BORYSIK, S.; VAN DER VELDE, K.; GARBARCZYK, J.; KRUCINSKA, I. Crystallinity of polyamide-6 matrix in glass fibre/polyamide-6 composites manufactured from hybrid yarns. **Fibriles & Textiles in Eastern Europe**, v. 12, n. 3, p. 64-68, Jul.- Oct. 2004. . Available in < http://www.fibtex.lodz.pl/47_16_64.pdf >. Access on 2 Nov., 2011

LEÃO, A. L.. Fibra de curauá: uma alternativa na produção de termoplásticos reforçados. **Plástico Industrial**, v. 3, n. 31, p. 214–229, 2001.

LE MOIGNE, M.L. **Mecanismos de gonflement et de dissolution des fibres de cellulose**. Ph.D. Thesis (thèse de doctorat) Ecole Nationale Supérieure des Mines de Paris, France, p. 10-14, Jan. 2009.

LE ROUXEL, O.; CAVALIER, D.M.; LIEPMAN, A.H.; KEEGSTRA, K. Biosynthesis of plant cell wall polysaccharides – a complex process. **Current Opinion in Plant Biology**, [S.I.], v.9, p. 621 - 625, Oct. 2006.
DOI:10.1016/j.pbi.2006.09.009

MARSH, G. Next step for the automotive materials. **Materials Today**, [S.I.], v. 6, n. 4, p. 36-43, Apr. 2003. DOI:10.1016/S1369-7021(03)00429-2

MISHRA, S.; MISRA, M.; TRIPATHY, S.S.; NAYAK, S.K.; MOHANTY, A.K. Graft copolymerization of acrylonitrile on chemically modified sisal fibers. **Macromolecular Materials and Engineering**, [S.I.], v. 286, n. 2, p. 107-113, Feb. 2001. DOI: 10.1002/1439-2054(20010201)286:2<107::AID-MAME107>3.0.CO;2-0

MISHRA, S.; MISRA, M.; TRIPATHY, S.S.; NAYAK, S.K.; MOHANTY, A.K. The influence of chemical surface modification on the performance of sisal-polyester biocomposites. **Polymer Composites**, [S.I.], v. 23, n. 2, p. 164-170, Apr. 2002. DOI: 10.1002/pc.10422

MISHRA, S.; MOHANTY, A.K.; DRZAL, L.T.; MISRA, M.; HINRICHSEN, G. A review of pineapple leaf fibers, sisal fibers and their biocomposites. **Macromolecular Materials and Engineering**, [S.I.], v. 289, n. 11, p. 955-974, Nov. 2004. DOI: 10.1002/mame.200400132

MISHRA, S.; MOHANTY, A.K.; DRZAL, L.T.; MISRA, M.; PARIJA, S.; NAYAK, S.K.; TRIPATHY, S.S. Studies on mechanical performance of biofibre/glass reinforced polyester hybrid composites. **Composites Science and Technology**, [S.I.], v. 63, n. 10, p. 1377-1385, Aug. 2003. DOI:10.1016/S0266-3538(03)00084-8

MOHANTY, A. K. Biofibres biodegradable polymers and biocomposites: an overview. **Macromolecular Materials and Engineering**, [S.I.], v. 276/277, n. 1, p. 1–24, Mar. 2000. DOI: 10.1002/(SICI)1439-2054(20000301)276:1<1::AID-MAME1>3.0.CO;2-W

MOHANTY, A.K.; MISRA, S.; DRZAL, L.T. Surface modifications of natural fibers and performance of the resulting biocomposites: an overview. **Composites Interface**, [S.I.], v. 8, n. 5, p. 313-343, Oct. 2001. DOI: 10.1163/156855401753255422

MORÁN, J. I.; ALVAREZ, V. A.; CYRAS, V. P.; VÁZQUEZ, A. Extraction of cellulose and preparation of nanocelulose from sisal fibers. **Cellulose**, [S.I.], v. 15, n. 1, p. 149-159, 2008. DOI: 10.1007/s10570-007-9145-9

MORRISON III, W.H.; ARCHIBALD, D.D.; SHARMA, H.S.S.; AKIN, D.E. Chemical and physical characterization of water and dew-retted flax fibers. **Industrial Crops and Products**, [S.I.], v. 12, n. 1, p. 39-46, Jun. 2000. DOI:10.1016/S0926-6690(99)00044-8

MOTHÉ, C. G.; ARAÚJO, C. R. (2004). Caracterização térmica e mecânica de compósitos de poliuretano com fibras de curauá. **Polímeros: Ciência e Tecnologia**, v. 14, n. 4, p. 274–278, Aug. 2004. Available in < <http://www.scielo.br/pdf/po/v14n4/22073.pdf> >. Access on 17 Jun., 2012

MWAIKAMBO, L.Y.; ANSELL, M.P. The effect of chemical treatment on the properties of hemp, sisal, jute and kapok fibres for composite reinforcement. **Macromolecular Materials and Engineering**, [S.I.], v. 272, n. 1, p. 108-116, dec. 1999. DOI: 10.1002/(SICI)1522-9505(19991201)272:1<108::AID-APMC108>3.0.CO;2-9

NAIR, K.C.M; THOMAS, S.; GROENINCKX. Thermal and dynamic mechanical analysis of polystyrene composites reinforced with short sisal fibres. **Composites Science and Technology**, [S.I.], v. 61, n. 16, p. 2519-2529, Dec. 2001. DOI:10.1016/S0266-3538(01)00170-1

NETRAVALI, A.N.; CHABBA, S.; Composites get greener. **Materials Today**, [S.I.], v. 6, n. 4, p. 22-29, Apr. 2003. DOI:10.1016/S1369-7021(03)00427-9

NICKEL, J.; RIEDEL, U. Activities in biocomposites. **Materials Today**, [S.I.], v. 6, n. 4, p. 44-48, Apr. 2003. DOI:10.1016/S1369-7021(03)00430-9

OLARU, N.; OLARU, L.; VASILE, V.; ANDER, P. Surface modified cellulose obtained by acetylation without solvents of bleached and unbleached kraft pulps. **Polimery**. v. 56, n. 11-12, p. 834-840, Mar. 2011. Available in < www.ichp.pl/attach.php?id=1201 >. Access on 1 Jul., 2014

PARK, J.M.; KIM, P.G.; JANG, J.H.; WANG, Z.; HWANG, B.S.; DEVRIES, K.L. Interfacial evaluation and durability of modified jute fibers/polypropylene composites using micromechanical test and acoustic emission. **Composites**

Part B: Engineering, [S.I.], v. 39, n. 6, p. 1042–1061, Sep. 2008.
DOI:10.1016/j.compositesb.2007.11.004

PAUL, A.; JOSEPH, K.; THOMAS, S. Effect of surface treatments on the electrical properties of low-density polyethylene composites reinforced with short sisal fibers. **Composites Science and Technology**, [S.I.], v. 57, n. 1, p. 67-79, 1997. DOI:10.1016/S0266-3538(96)00109-1

PEIJS, T. Composites for recyclability. **Materials Today**, [S.I.], v. 6, n. 4, p. 30-35, Apr. 2003. DOI: 10.1016/S1369-7021(03)00428-0

POLETTI, M.; ZATTERA, A.J.; FORTE, M.M.C.; SANTANA, R.M.C. Thermal decomposition of wood: influence of wood components and cellulose crystallite size. **Bioresource Technology**, [S.I.], v.109, p. 148-153, Nov. 2011.
DOI:10.1016/j.biortech.2011.11.122

RAJESH, A.; KOZLOWSKI, R. Proceedings of international conference on textiles for sustainable developments. In: FAO/ESCORENA, Port Elizabeth, South Africa, 23-27 Oct, 2005. CD-ROM.

RANA, A.K.; BASAK, R.K.; MITRA, B.C.; LAWATHER, M.; BANERJEE, A.N. Studies of acetylation of jute using simplified procedure and its characterization. **Journal of Applied Polymer Science**, [S.I.], v. 64, n. 8, p. 1517-1523, May. 1997. DOI: 10.1002/(SICI)1097-4628(19970523)64:8<1517::AID-APP9>3.0.CO;2-K

RAY, D.; SARKAR, B.K.; RANA, A.K.; BOSE, N.R. Effect of alkali treated jute fibres on composites properties. **Bulletin of Materials Science**, [S.I.], v. 24, n. 2, p. 129-135, Apr. 2001. DOI: 10.1007/BF02710089

RIPPERT, P.; PUYAUBERT, J.; GRISOLLET, D.; DERRIER, L.; MATRINGE, M. Tyrosine and phenylalanine are synthesized within the plastids in *Arabidopsis*. **Plant Physiology**, [S.I.], v.149, p. 1251–1260, Mar. 2009. DOI: 10.1104/pp.108.130070

ROMANZINI, D.; ORNAGHI H,L.; ALICO, SC.; ZATTERA, A.J. Influence of fiber hybridization on the dynamic mechanical properties of glass/ramie fiber-reinforced polyester composites. **Journal of Reinforced Plastic Composites**, [S.I.], v. 31, n. 23, p. 1652-1661, 2012. DOI:10.1177/0731684412459982

RONG, M.Z.; ZHANG, M.Q.; LIU, Y.; YANG, G.C.; ZENG, H.M. The effect of fiber treatment on the mechanical properties of unidirectional sisal-reinforced epoxy composites. **Composites Science and Technology**, [S.I.], v. 61, n. 10, p. 1437-1447, Aug. 2001. DOI:10.1016/S0266-3538(01)00046-X

ROSA, M.F.; MEDEIROS, E.S.; MALMONGE, J.A.; GREGORSKI, K.S.; WOOD, D.F.; MATTOSO, L.H.C.; GLENN, C.; ORTS, W.J.; IMAM SH. Cellulose nanowhiskers from coconut husk fibers: Effect of preparation conditions on their thermal and morphological behaviour. **Carbohydrate**

Polymers, [S.I.], v. 81, n. 1, p. 83-92, May. 2010.
DOI:10.1016/j.carbpol.2010.01.059

SAMIR, M.Y.A.S.A.; ALOIN, F.; DUFRESNE, A. Review of recent research into cellulosic whiskers, their properties and their application in nanocomposite field. **Biomacromolecules**, [S.I.], v. 6, n. 2, p. 612-626, Dec. 2004.
DOI: 10.1021/bm0493685

SANTOS, P.A.; SPINACÉ, M.A.S.; FERMOSELLI, K.K.G.; DE PAOLI, M.A. Polyamide-6/vegetal fiber composite prepared by extrusion and injection molding. **Composites Part A: Applied Science and Manufacturing**, [S.I.], v. 38, n. 12, p. 2404 – 2411, Dec. 2007. DOI:10.1016/j.compositesa.2007.08.011

SCHUH, T.G. **Renewable Materials for Automotive Applications**. Available in <www.ienica.net/fibresseminar/schuh.pdf> Access in: 20 Oct. 2010.

SHAFIZADEH, F. Introduction to pyrolysis of biomass. **Journal of Analytical and Applied Pyrolysis**, [S.I.], v. 3, n. 4, p. 283-305, 1982. DOI:10.1016/0165-2370(82)80017-X

SHAFIZADEH, F.; BRADBURY, A.G.W. Thermal degradation of cellulose in air and nitrogen at low temperatures. **Journal of Applied Polymer Science**, [S.I.], v. 23, n. 5, p. 1431-1442, 1979. DOI: 10.1002/app.1979.070230513

SHAMS-NATERI, A.; MOHAJERANI, M. Evaluation of cotton fibers stickness by colorimetric method. **Progress in Color, Colorants and Coatings**, v. 6, p. 9-15, 2013. Available in <<http://en.journals.sid.ir/ViewPaper.aspx?ID=300806>>. Access on 10 Jul., 2014

SHEN, D.K.; GU, S. The mechanism of thermal decomposition of cellulose and its main products. **Bioresource Technology**, [S.I.], v.100, p. 6496, Jul. 2009. DOI:10.1016/j.biortech.2009.06.095

SILVA, H.S.P. **Development of polymeric composites with curauá fibers and hybrids with glass fibers**. 2010. 72 p. Master's Dissertation – University of Rio Grande do Sul, Rio Grande do Sul, Brazil, 2010.

SILVA, R.V.; AQUINO, E.M.F. Curauá Fiber: A New Alternative to Polymeric Composites. **Journal of Reinforced Plastics and Composites**, [S.I.], v. 27, n. 1, p. 1-10, Feb. 2007. DOI:10.1177/0731684407079496

SOARES, S.; CAMINO, G.; LEVCHIK, S. Comparative study of the thermal decomposition of pure cellulose and pulp paper. **Polymer Degradation and Stability**, [S.I.], v. 49, n. 2, p. 275-283, 1995. DOI:10.1016/0141-3910(95)87009-1

SPINACÉ, M.A.S.; FERMOSELLI, K.K.G.; DE PAOLI, M.A. Effect of coupling agent in composites of post-consumed PP reinforced with curauá fiber. In: Proceedings of the polymer processing symposium – Americas Regional Meeting. Florianopolis; 2004. P. 48 – 9.

SREEKALA, M.S.; KUMARAN, M.G.; JOSEPH, S.; JACOB, M.; THOMAS, S. Oil palm fiber reinforced phenol formaldehyde composites: influence of fiber surface modifications on the mechanical performance. **Applied Composite Materials**, [S.I.], v. 7, p. 295-329, 2000. DOI:10.1023/A:1026534006291

SREEKALA, M.S.; THOMAS, S. Effect of fibre surface modification on water-sorption characteristics of oil palm fibres. **Composites Science and Technology**, [S.I.], v. 63, n. 6, p. 861-869, May. 2003. DOI:10.1016/S0266-3538(02)00270-1

TAJ, S.; MUNAWAR, M.A.; KHAN, S. Natural fiber-reinforced polymer composites. **The Proceedings of the Pakistan Academy of Sciences**, v. 44, n.2, p. 129 – 144, 2007.

TAJVIDI, M.; FEIZMAND, M. Effect of cellulose fiber reinforcement on the temperature dependent mechanical performance of nylon 6. **Journal of Reinforced Plastics and Composites**, [S.I.], v. 28, n. 2, p. 2781-2790, 2009. DOI: 10.1177/0731684408093875

TRINDADE, W.G.; HOAREAU, W.; MEGIATTO, J.D.; RAZERA, I.A.T.; CASTELLAN, A.; FROLLINI, E. Thermoset phenolic matrices reinforced with unmodified and modified surface-grafted furfuryl alcohol sugar cane bagasse and curauá fibers: properties of fibers and composites. **Biomacromolecules**, [S.I.], v.6, p. 2485-2496, Jul. 2005. DOI: 10.1021/bm058006+

TSERKI, V.; ZAFEIROPOULOS, N.E.; SIMON, F.; PANAYIOTOU, C. A study of the effect of acetylation and propionylation surface treatments on natural fibres. **Composites: Part A**, [S.I.], v.36, p. 1110-1118, Jan. 2005. DOI:10.1016/j.compositesa.2005.01.004

UNAL, H. Morphology and mechanical properties of composites based on polyamide 6 and mineral additives. **Materials & Design**, [S.I.], v. 25, n. 6, p. 483-487, Jan. 2004. DOI:10.1016/j.matdes.2004.01.007

VALADEZ-GONZALEZ, A.; CERVANTES-UC, J.M.; OLAYO, R.; HERRERA-FRANCO, P.J. Effect of fiber surface treatment on the fiber–matrix bond strength of natural fiber reinforced composites. **Composites Part B: Engineering**, [S.I.], v. 30, n. 3, p. 309-320, Apr. 1999. DOI:10.1016/S1359-8368(98)00054-7

VAN DER WEYENBERG, I.; IVENS, J.; DE COSTER, A.; KINO, B.; BAETENS, E.; VEPOES, I. Influence of processing and chemical treatment of flax fibres on their composites. **Composites Science and Technology**, [S.I.], v. 63, n. 9, p. 1241-1246, Jul. 2003. DOI:10.1016/S0266-3538(03)00093-9

VANHOLME, R.; DEMEDTS, B.; MORREEL, K.; RALPH, J.; BOERJAN, W. Lignin biosynthesis and structure. **Plant Physiology**, [S.I.], v.153, p.895, Jul. 2010. DOI: 10.1104/pp.110.155119

WADA, M.; HORI, R.; KIM, U.J.; SASAKI, S. X-ray diffraction study on the thermal expansion behavior of cellulose I β and its high-temperature phase. **Polymer Degradation and Stability**, [S.I.], v. 95, n. 8, p. 1330 – 1334, Aug. 2010. DOI:10.1016/j.polymdegradstab.2010.01.034

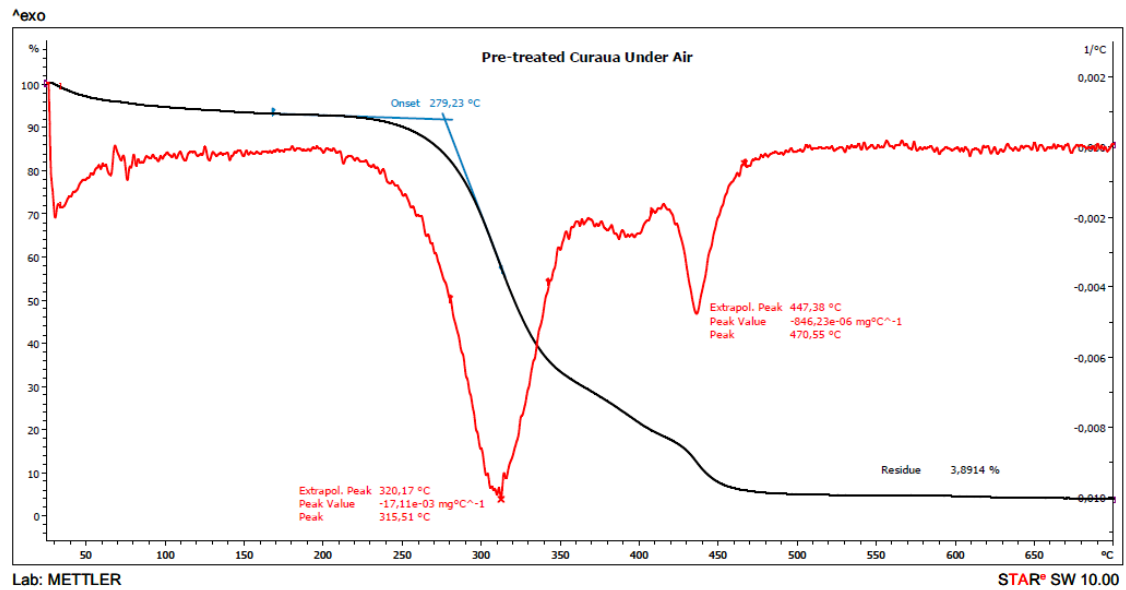
WEYENBERG, I.V.; TRUONG, B.; VANGRIMDE, B.; VERPOEST, I. Improving the properties of UD flax fibre reinforced composites by applying an alkaline fibre treatment. **Composites Part A: Applied Science and Manufacturing**, [S.I.], v. 37, n. 9, p. 1368 – 1376, Sep. 2006. DOI:10.1016/j.compositesa.2005.08.016

XIE, Y.; HILL, C.A.S.; XIAO, Z.; MILITZ, H.; MAI, C. Silane coupling agents used for natural fiber/polymer composites: A review. **Composites: Part A**, [S.I.], v. 41, p. 806-819, Mar. 2010. DOI:10.1016/j.compositesa.2010.03.005

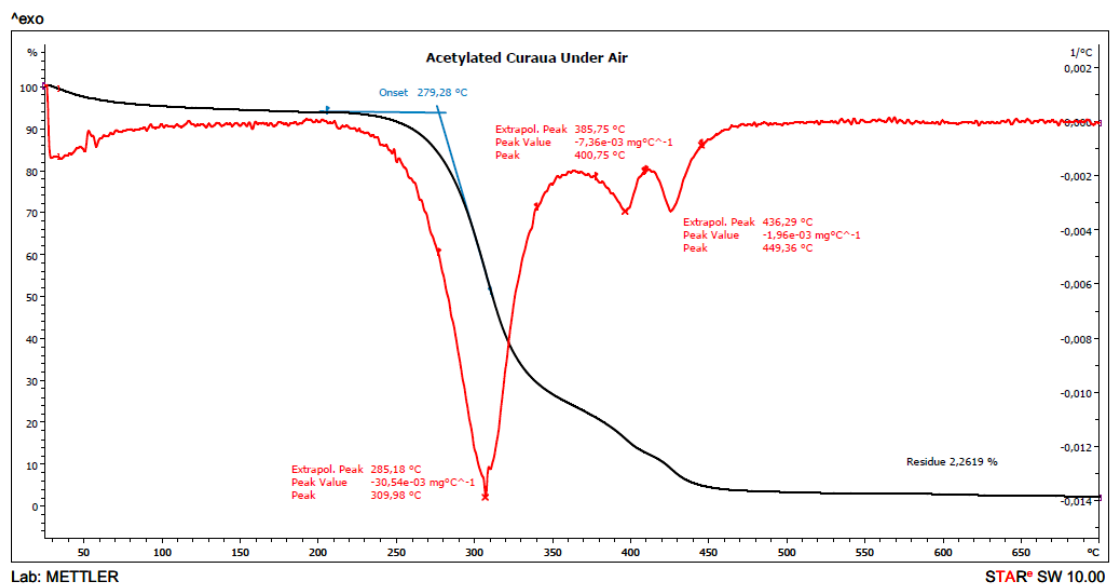
XU, X. **Cellulose fiber reinforced nylon 6 or nylon 66 composites**. Ph.D. Thesis, Georgia Institute of Technology, USA, p. 72-74, Dec. 2008. Available in <<https://smartech.gatech.edu/handle/1853/26487?show=full>>. Access on 8 May., 2013

APPENDIX A – TGA CURVES OF NATURAL FIBERS

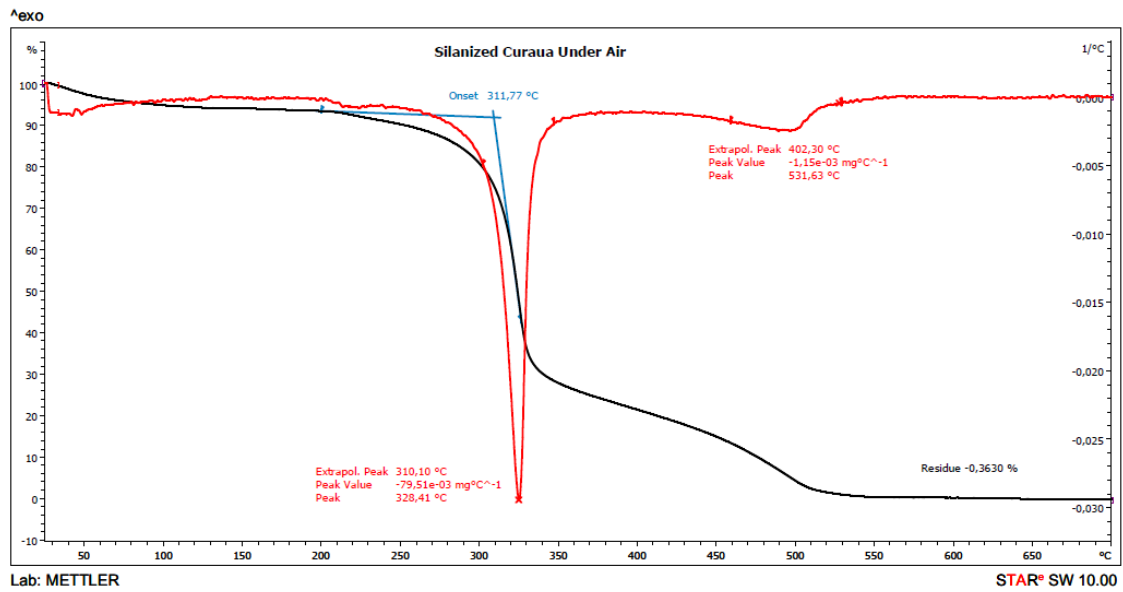
TGA curve of HP-alkaline treated curauá under air



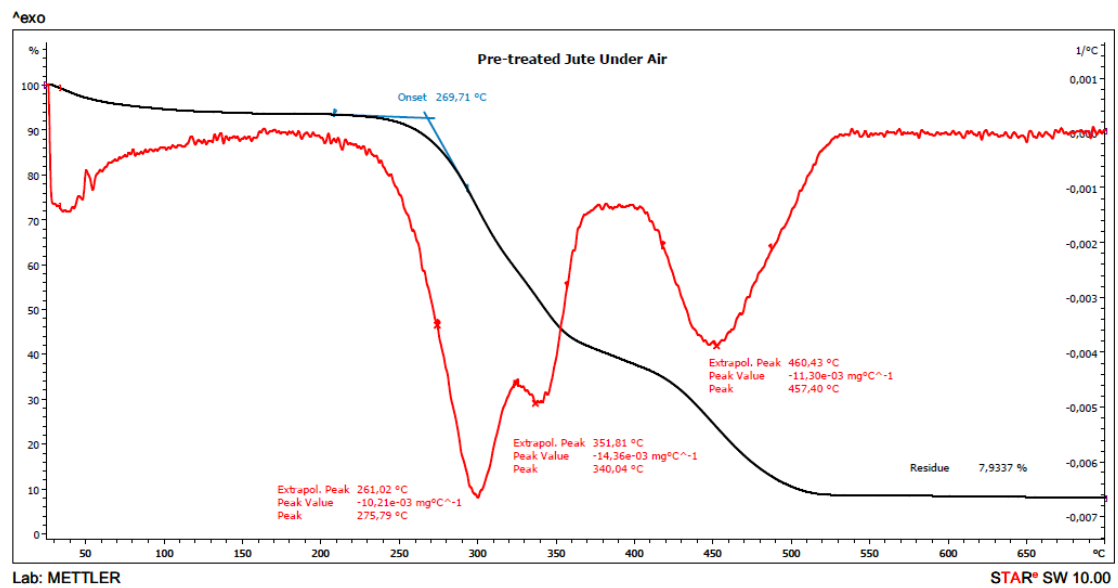
TGA curve of HP-alkaline treated + acetylated curauá under air



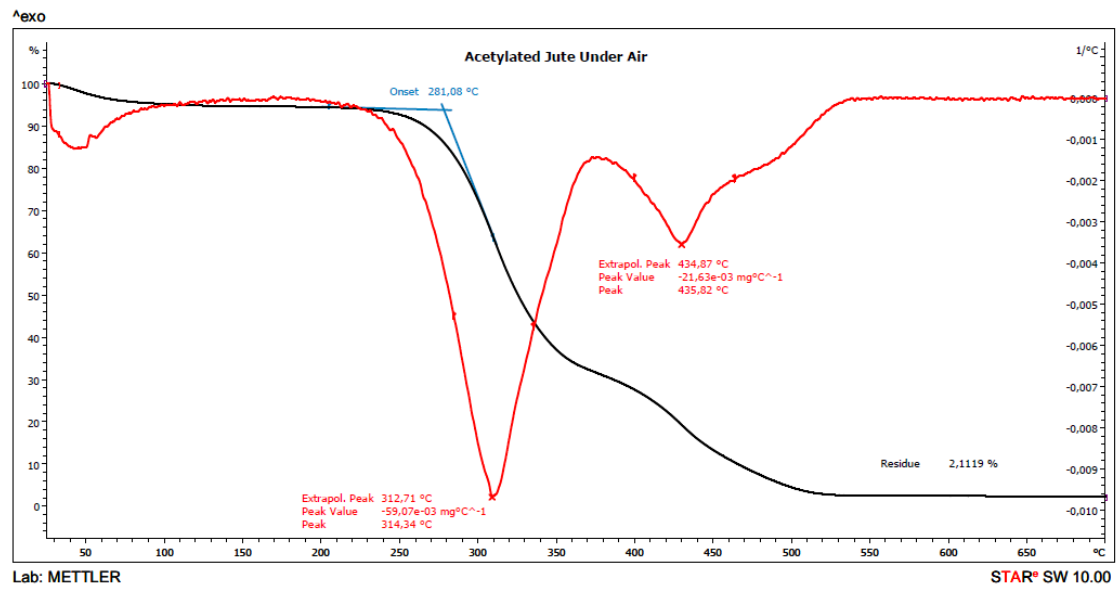
TGA curve of HP-alkaline treated + silanized curauá under air



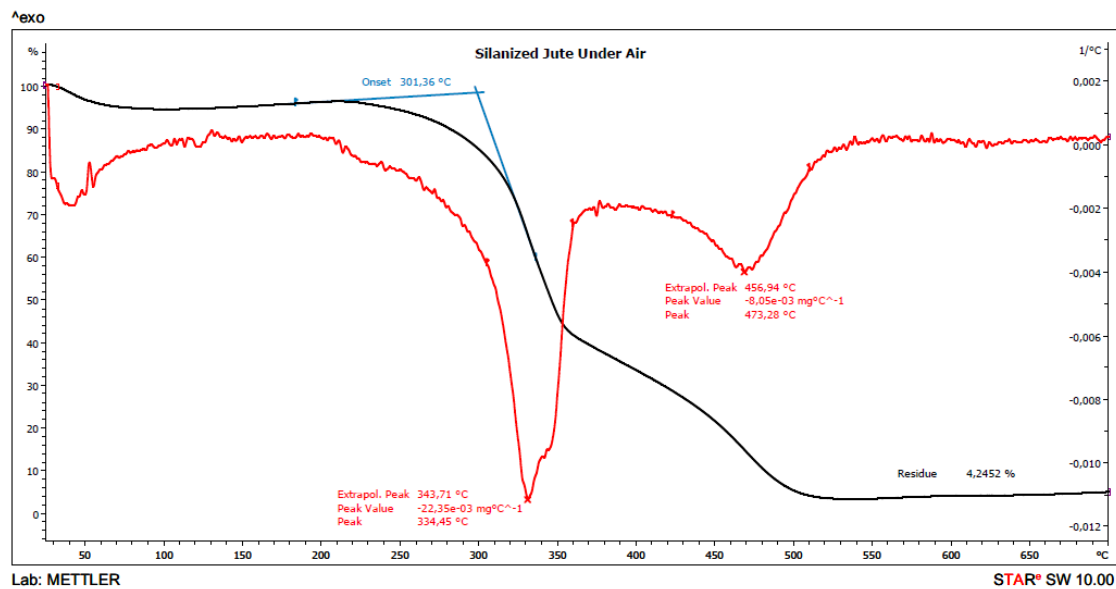
TGA curve of HP-alkaline treated jute under air



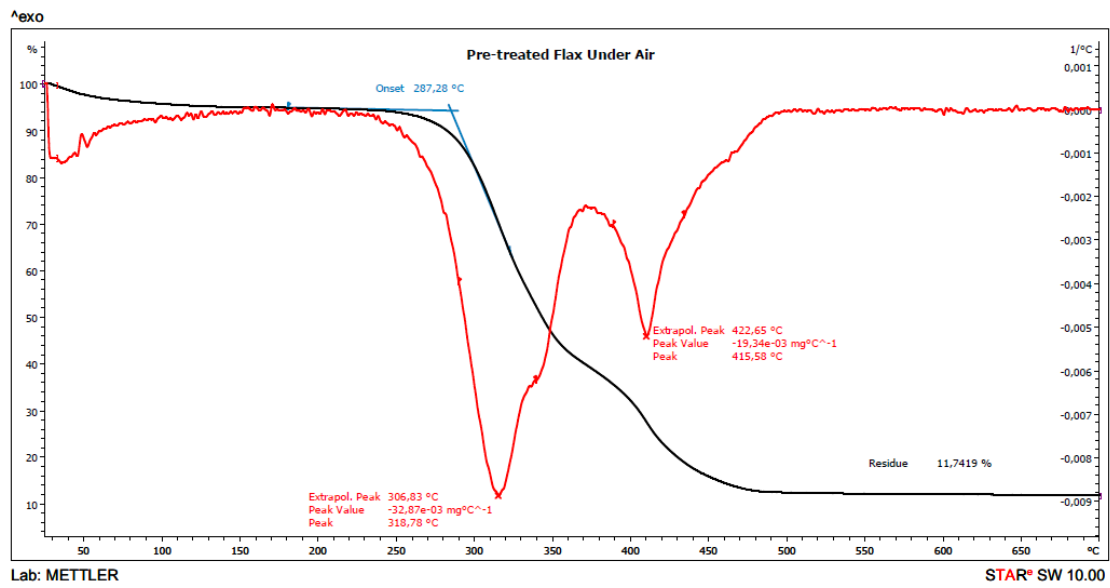
TGA curve of HP-alkaline treated + acetylated jute under air



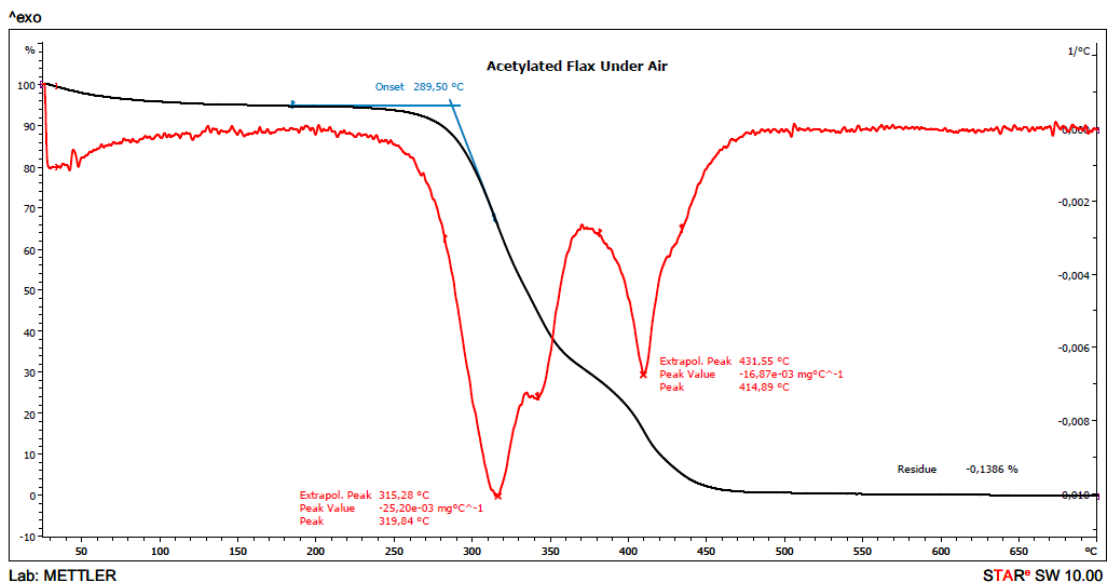
TGA curve of HP-alkaline treated + silanized jute under air



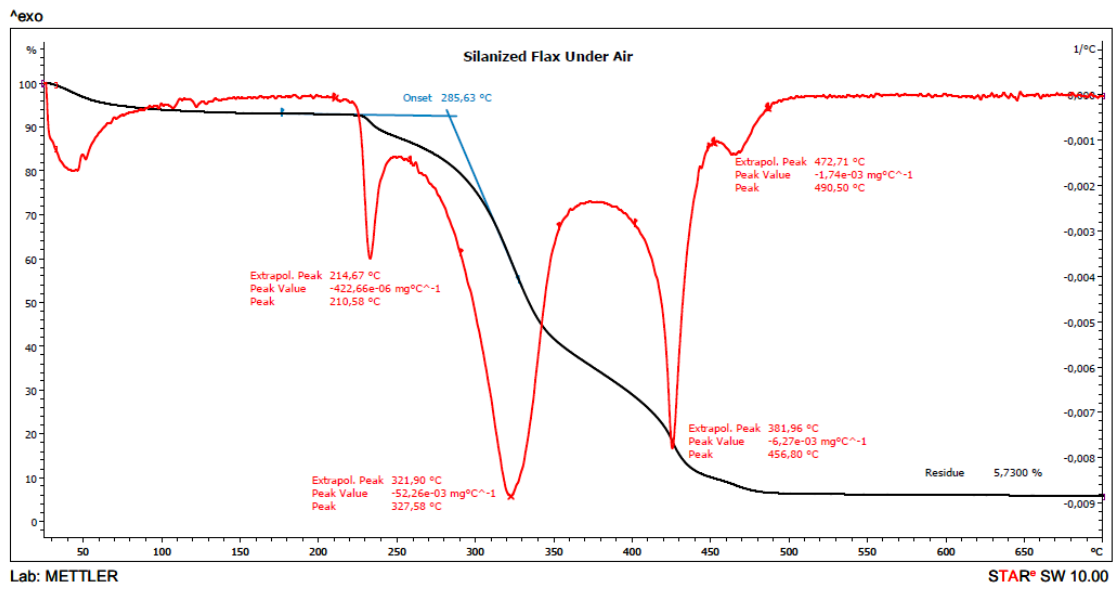
TGA curve of HP-alkaline treated flax under air



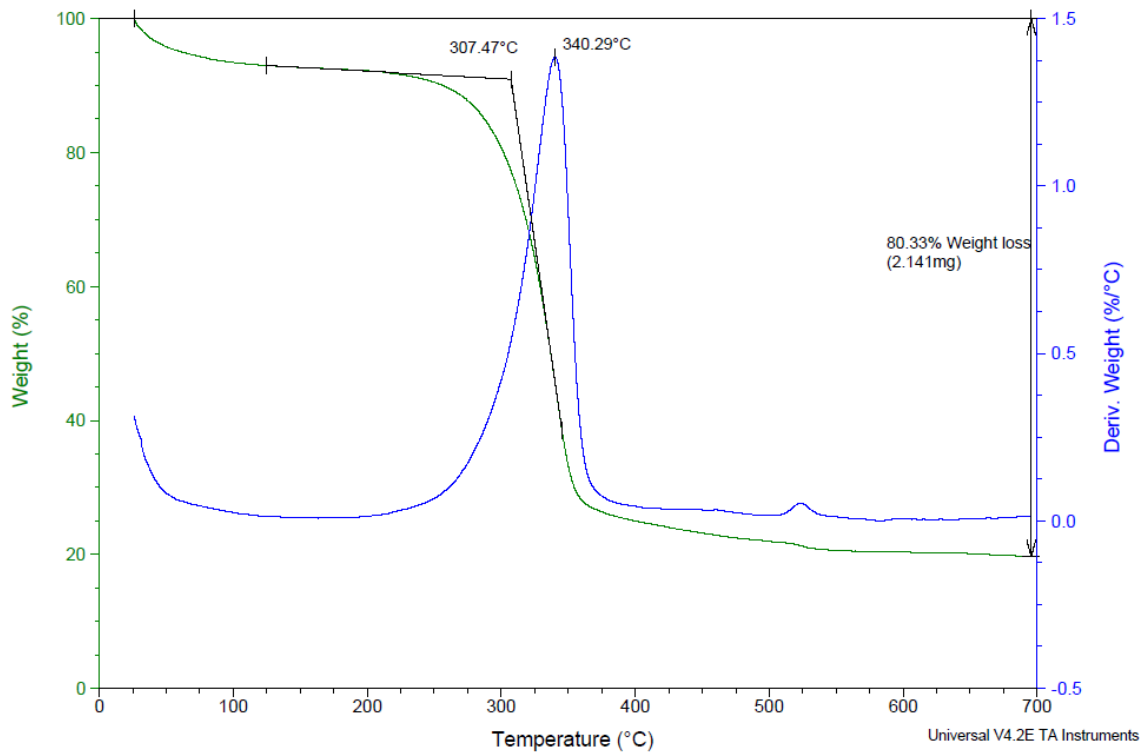
TGA curve of HP-alkaline treated + acetylated flax under air



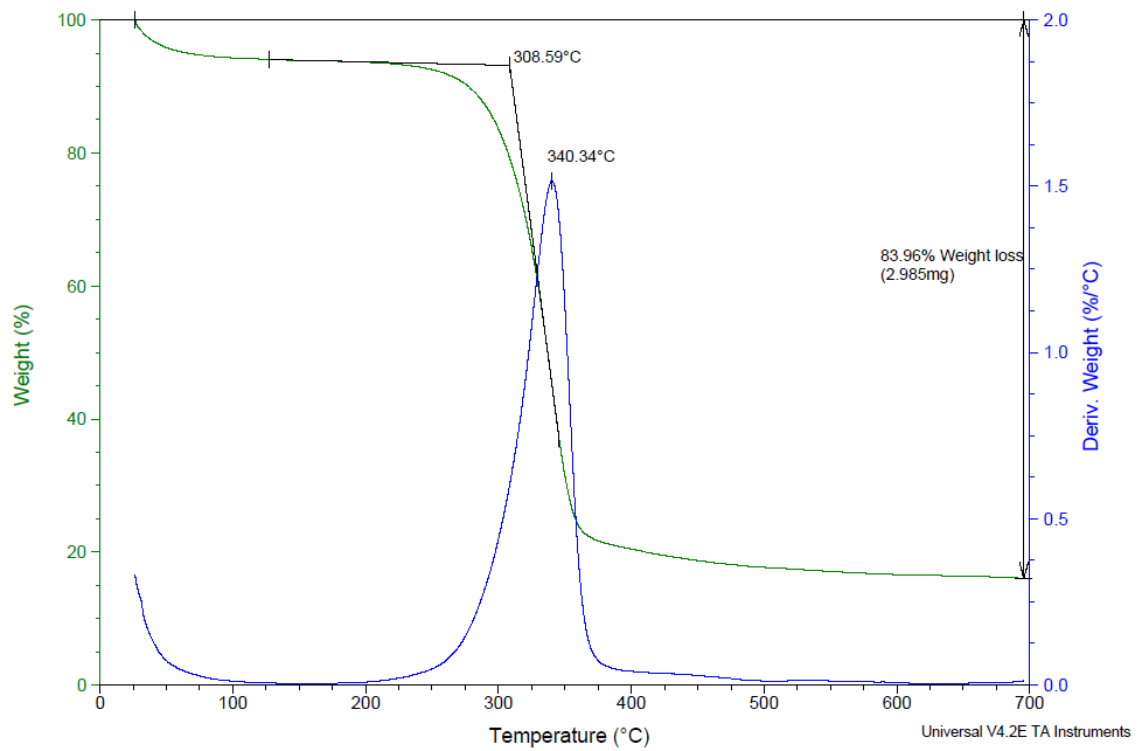
TGA curve of HP-alkaline treated + silanized flax under air



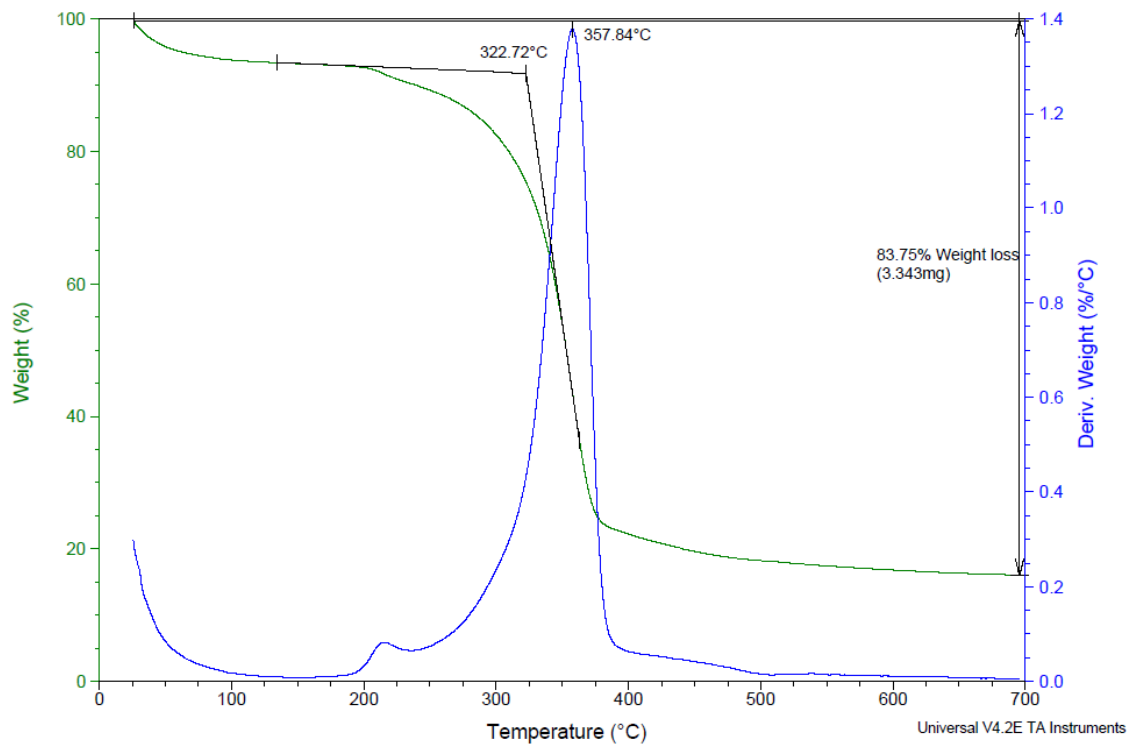
TGA curve of HP-alkaline treated curauá under nitrogen



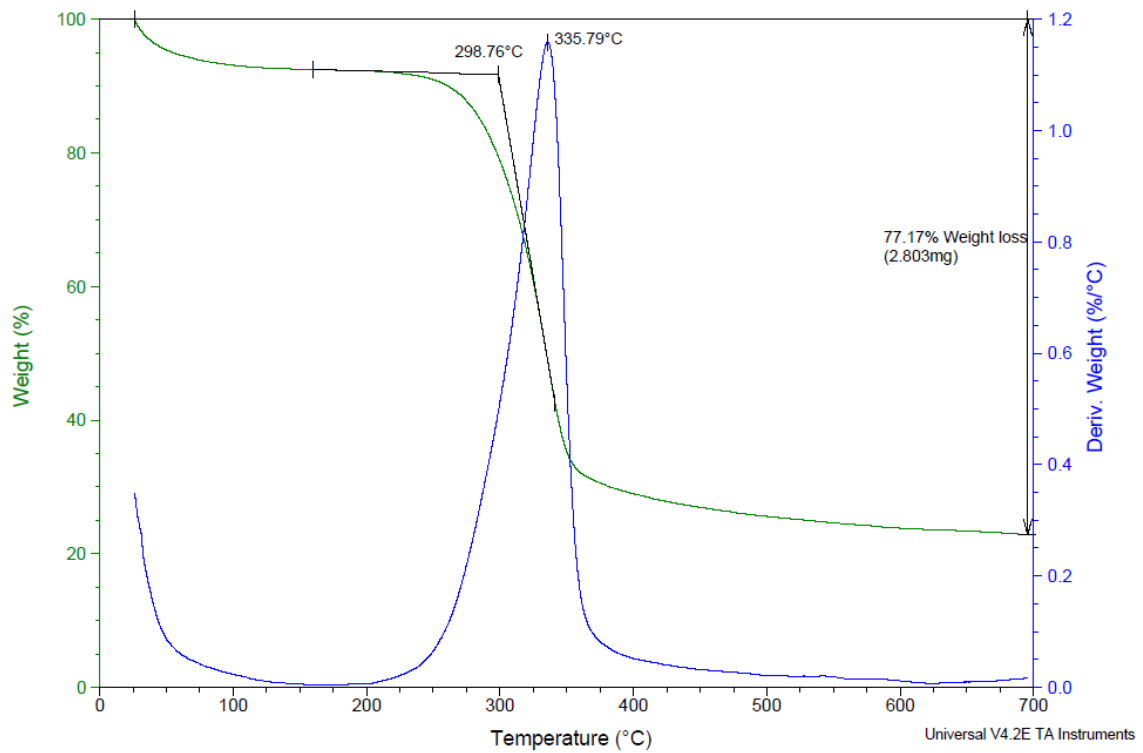
TGA curve of HP-alkaline treated + acetylated curauá under nitrogen



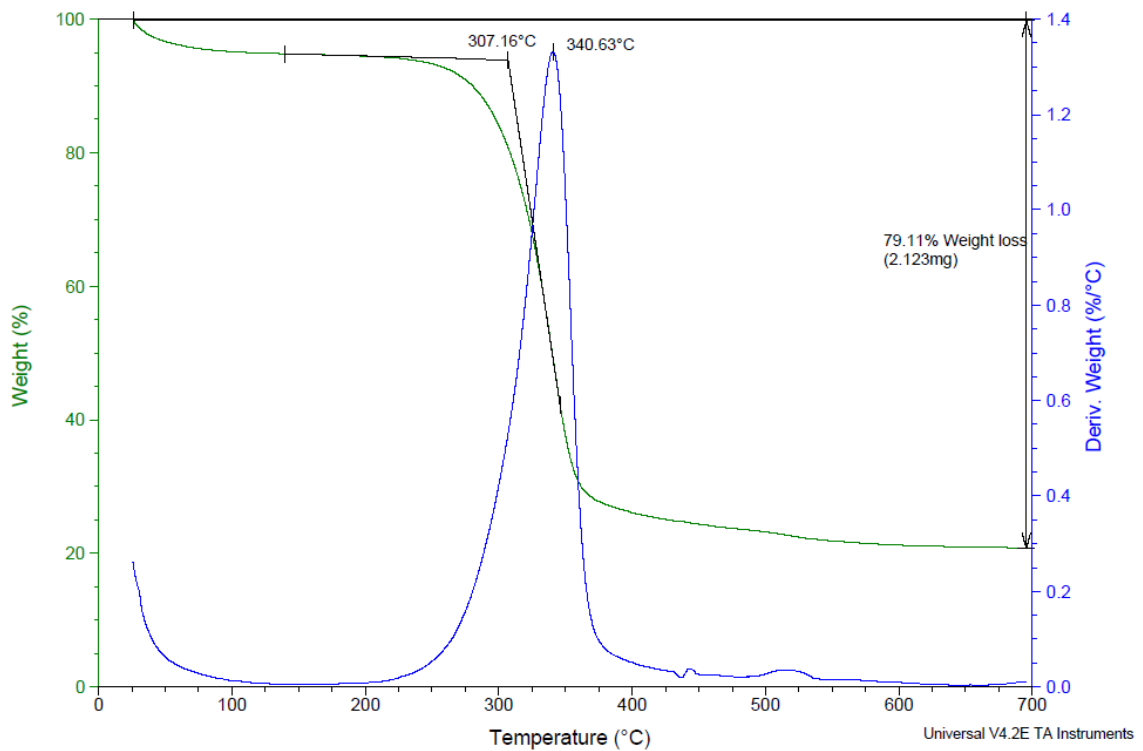
TGA curve of HP-alkaline treated + silanized curauá under nitrogen



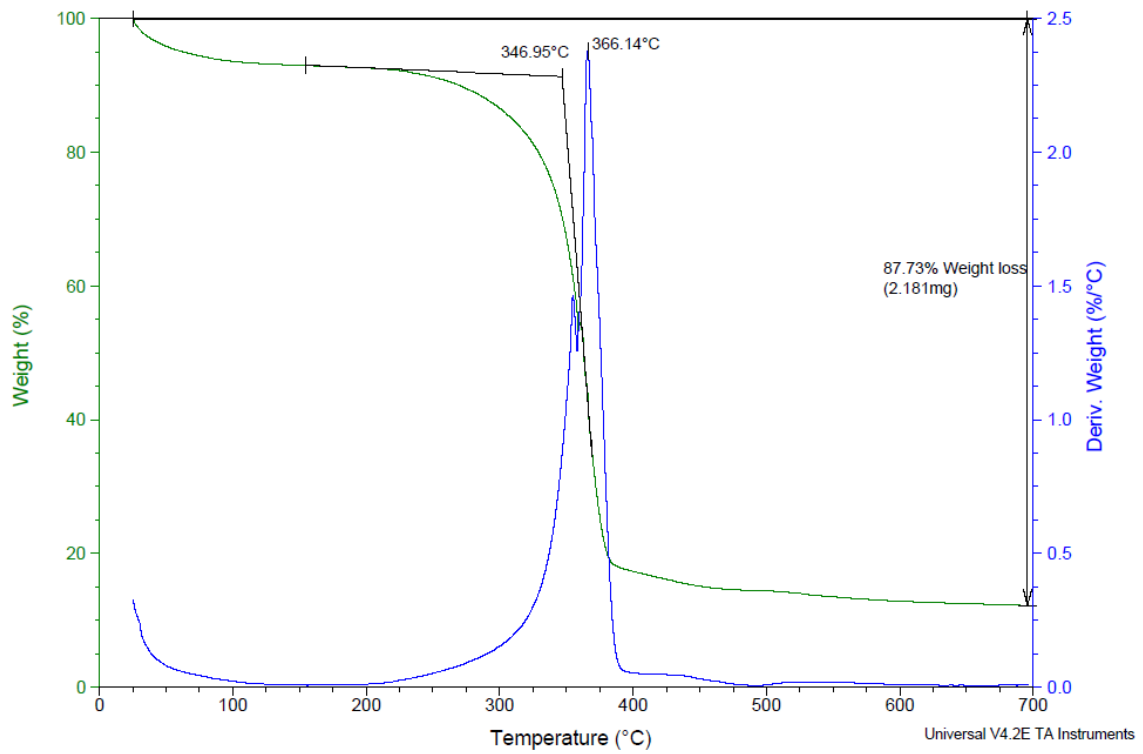
TGA curve of HP-alkaline treated jute under nitrogen



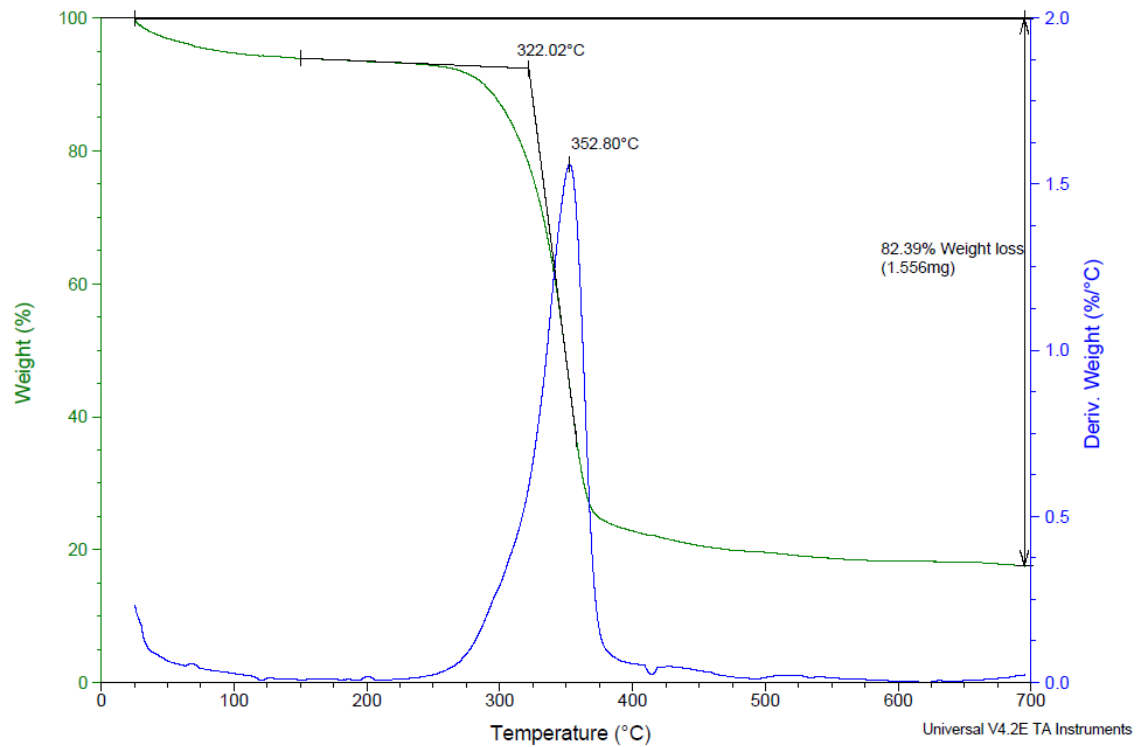
TGA curve of HP-alkaline treated + acetylated jute under nitrogen



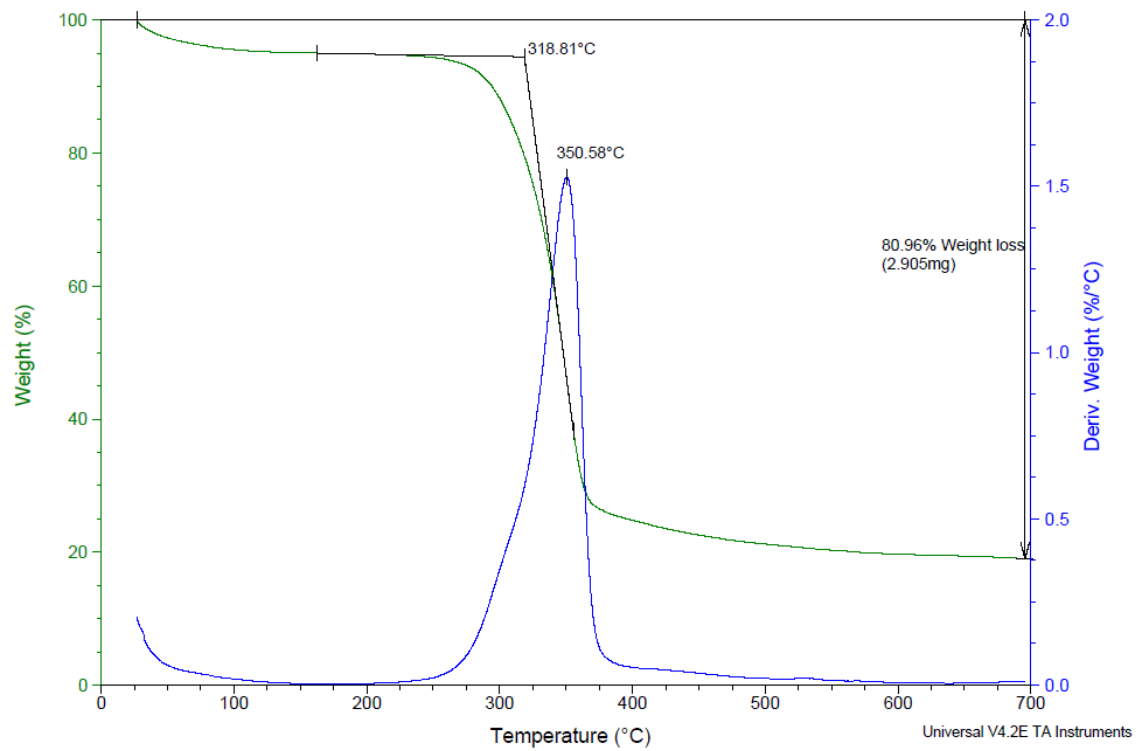
TGA curve of HP-alkaline treated + silanized jute under nitrogen



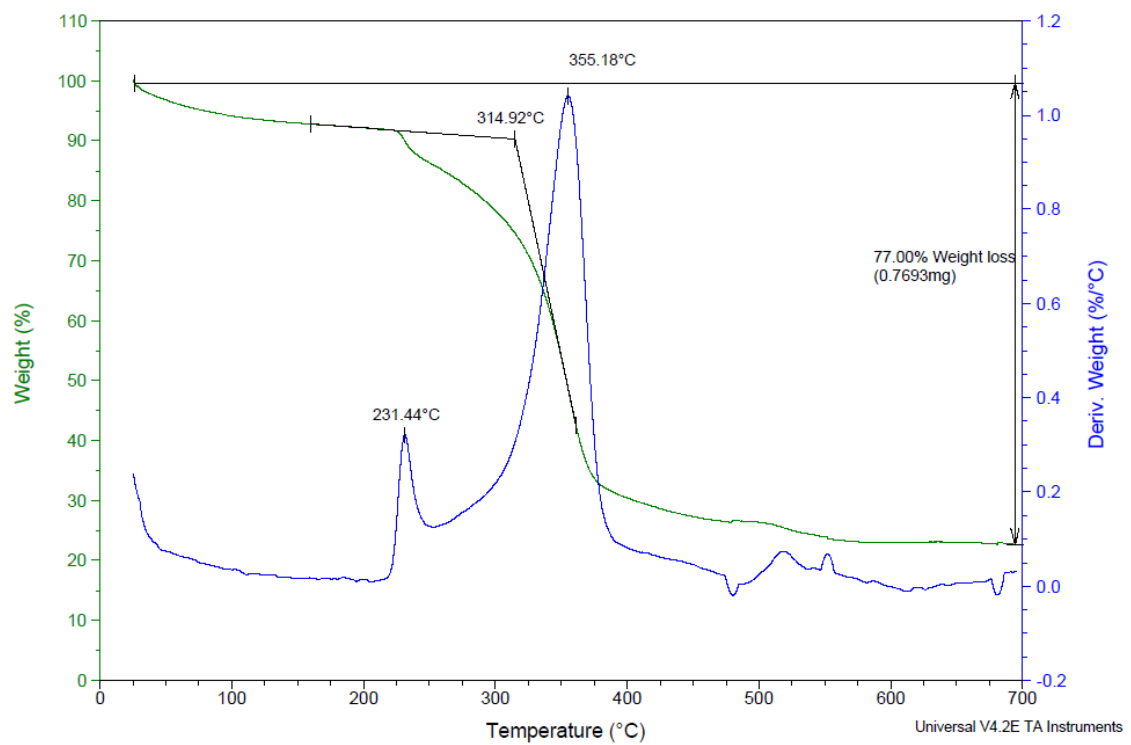
TGA curve of HP-alkaline treated flax under nitrogen



TGA curve of HP-alkaline treated + acetylated jute under nitrogen

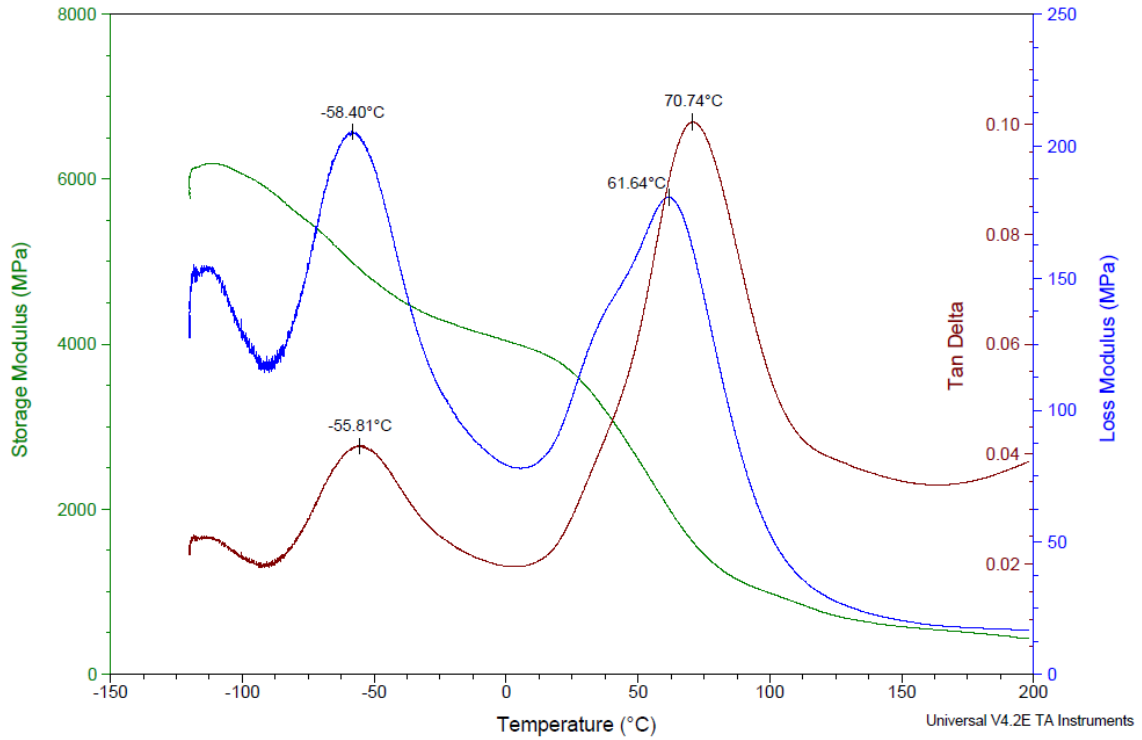


TGA curve of HP-alkaline treated + silanized flax under nitrogen

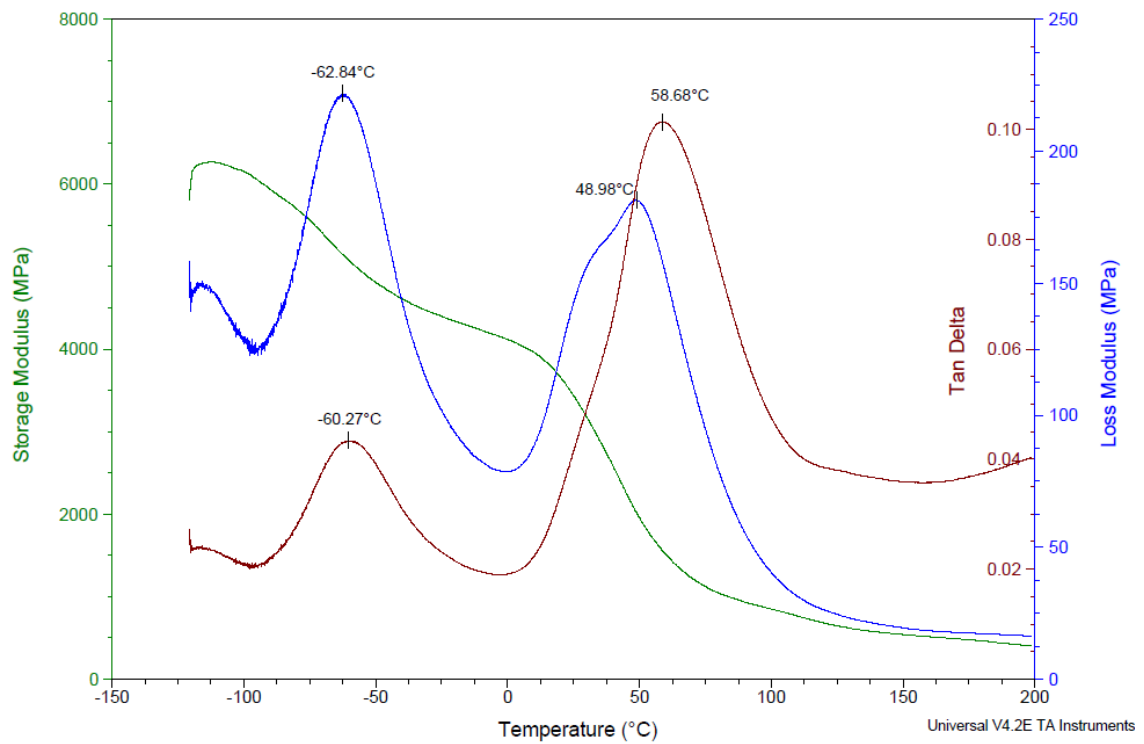


APPENDIX B – DMA CURVES OF NEAT PA 66 AND WITH DIFFERENT FORMULATIONS

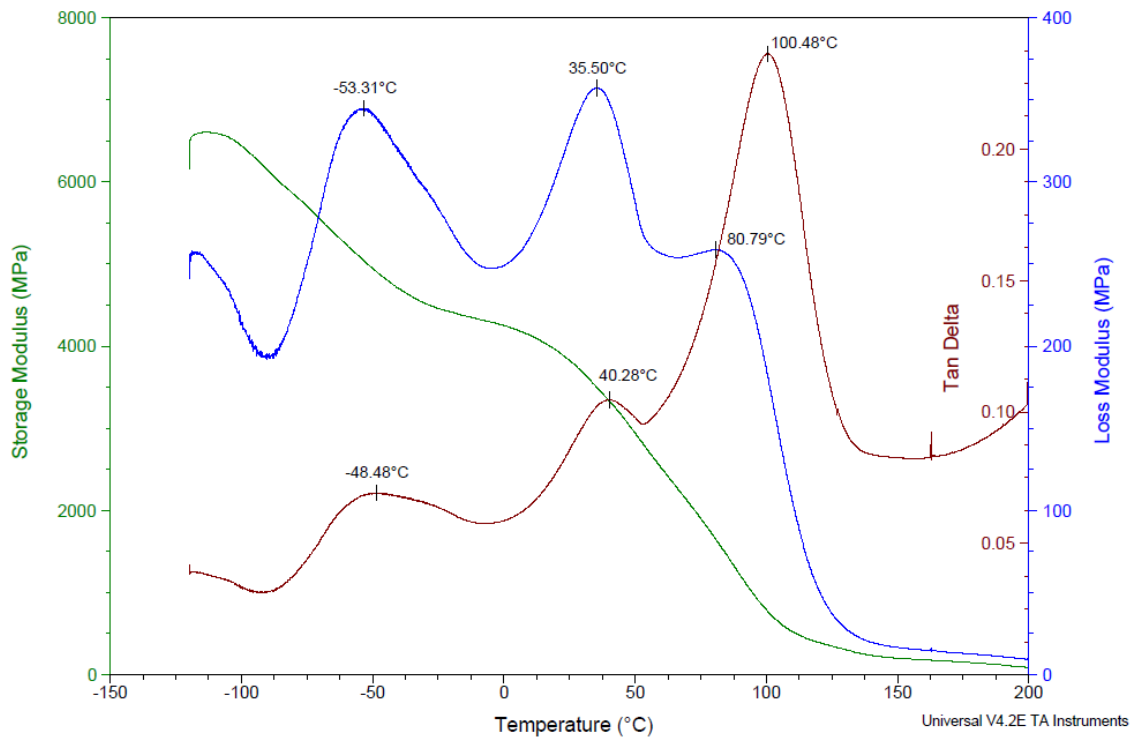
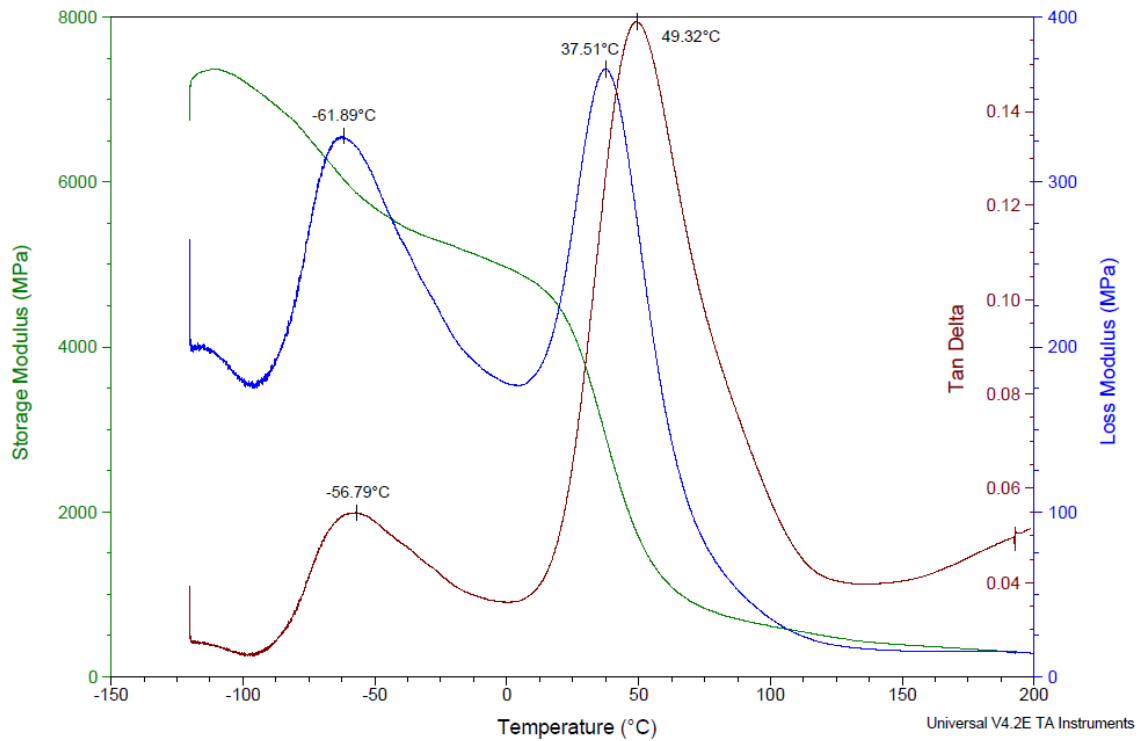
DMA curves of neat PA 66

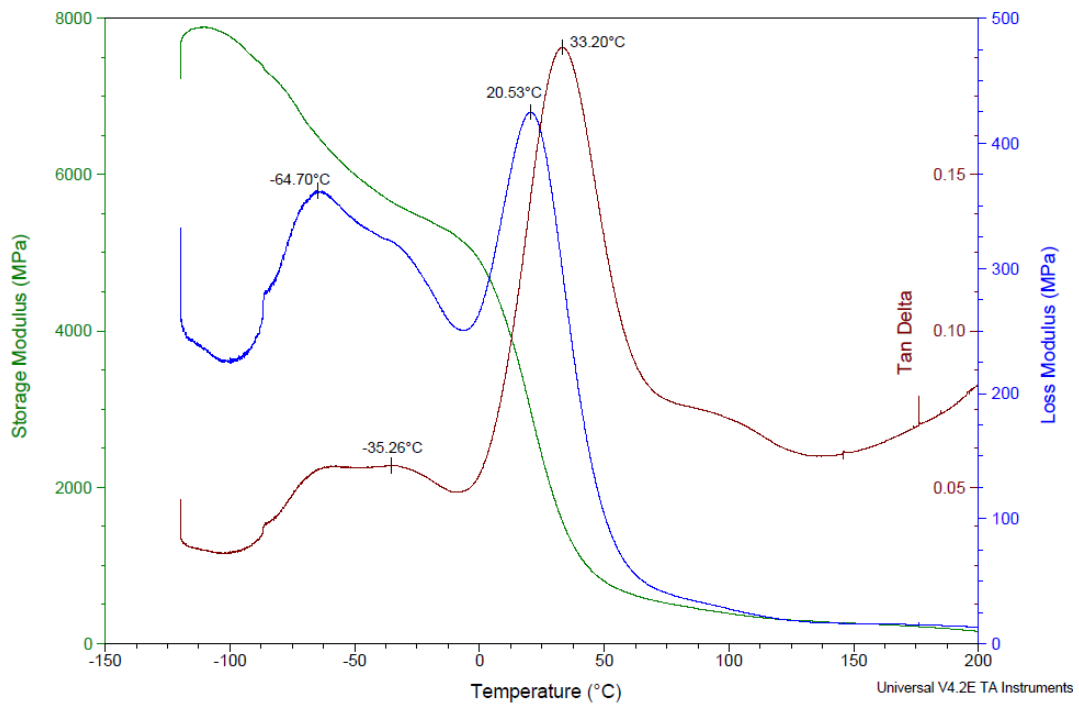
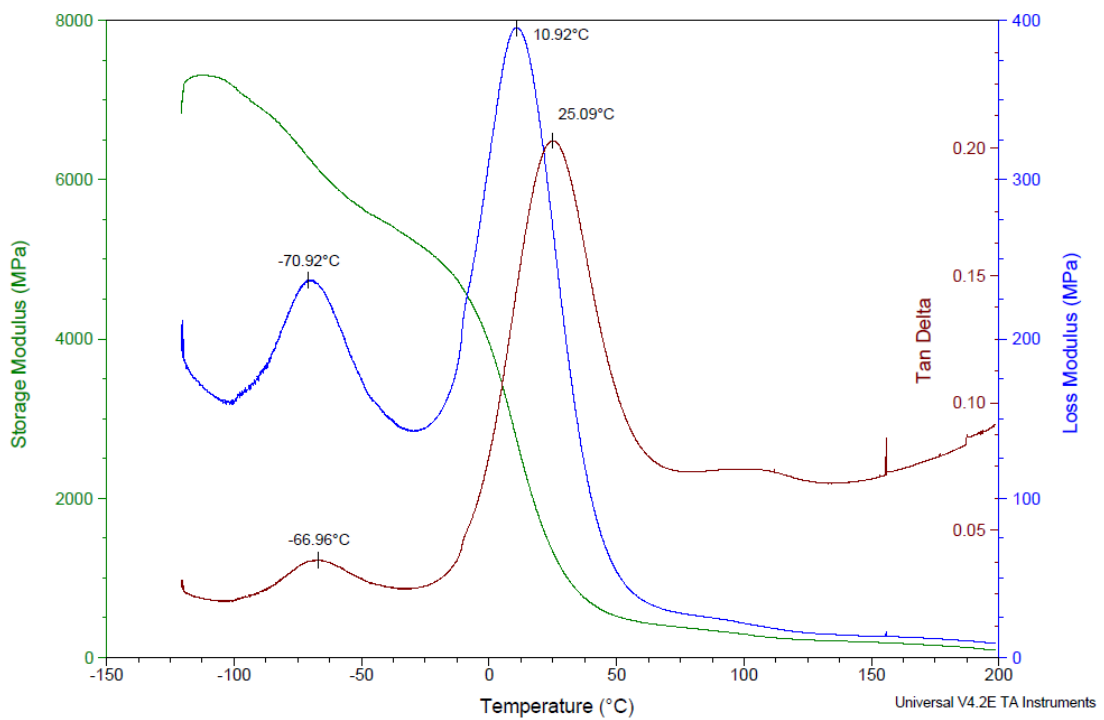


DMA curves of PA 66 + 5.0 wt. % of LiCl



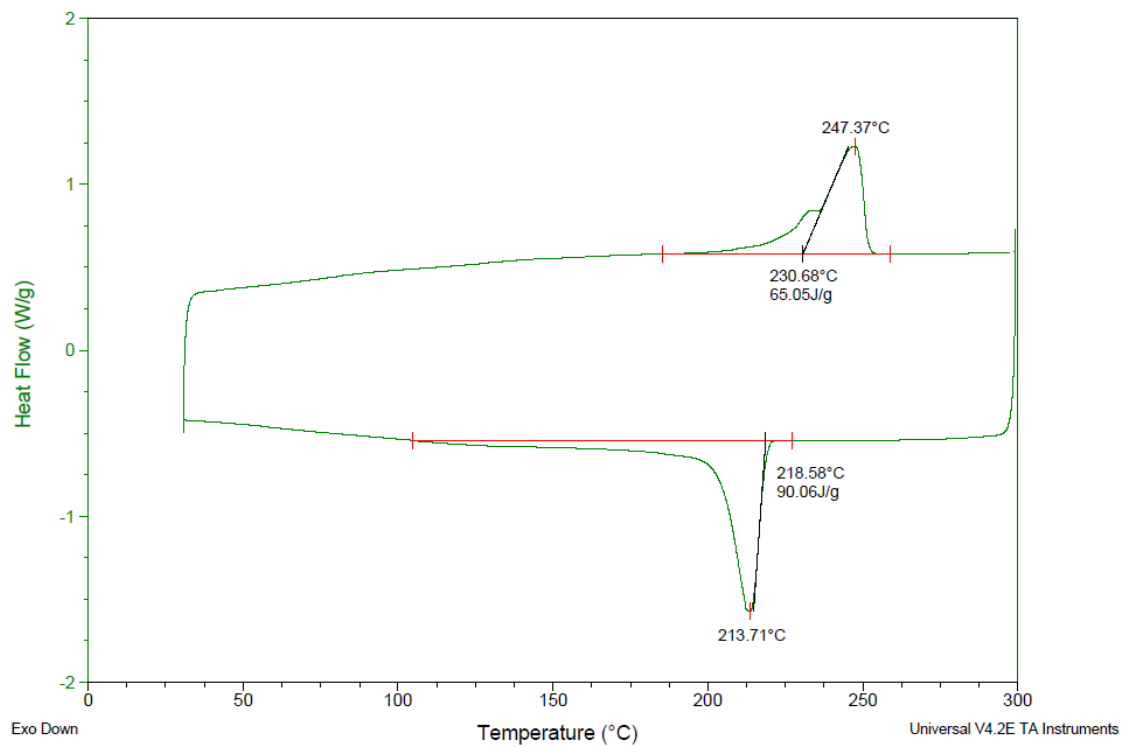
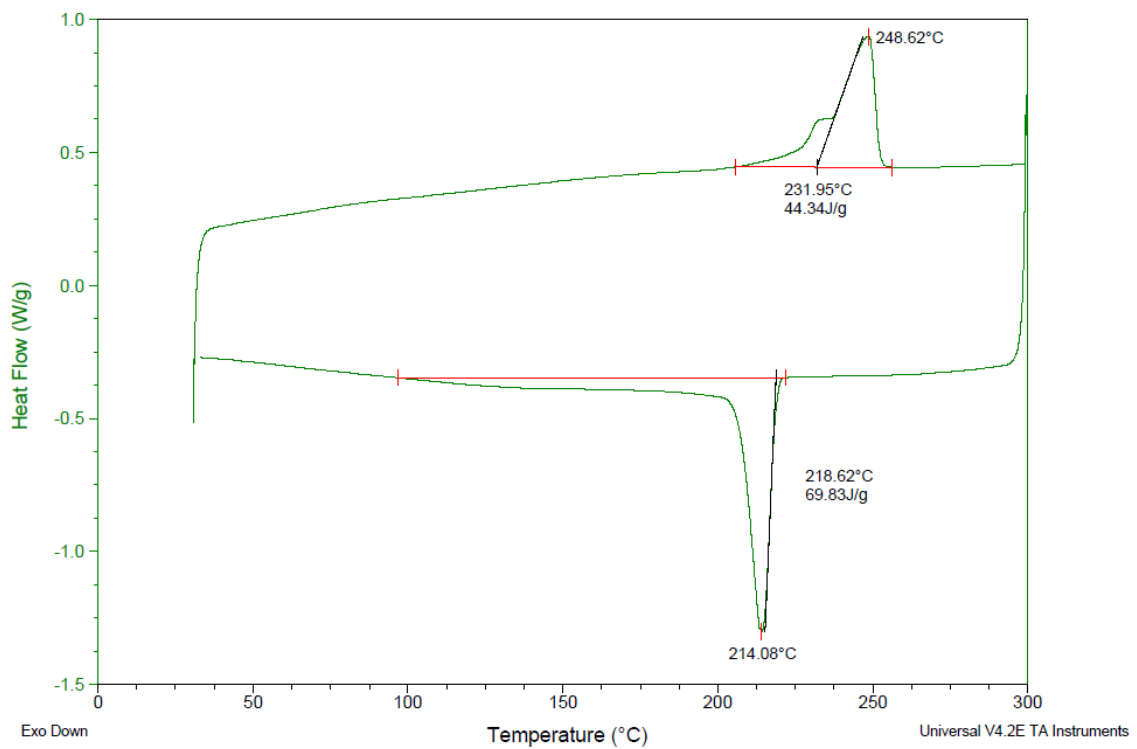
DMA curves of PA 66 + 5.0 wt. % of LiCl + 5.0 wt. % of NBBSA

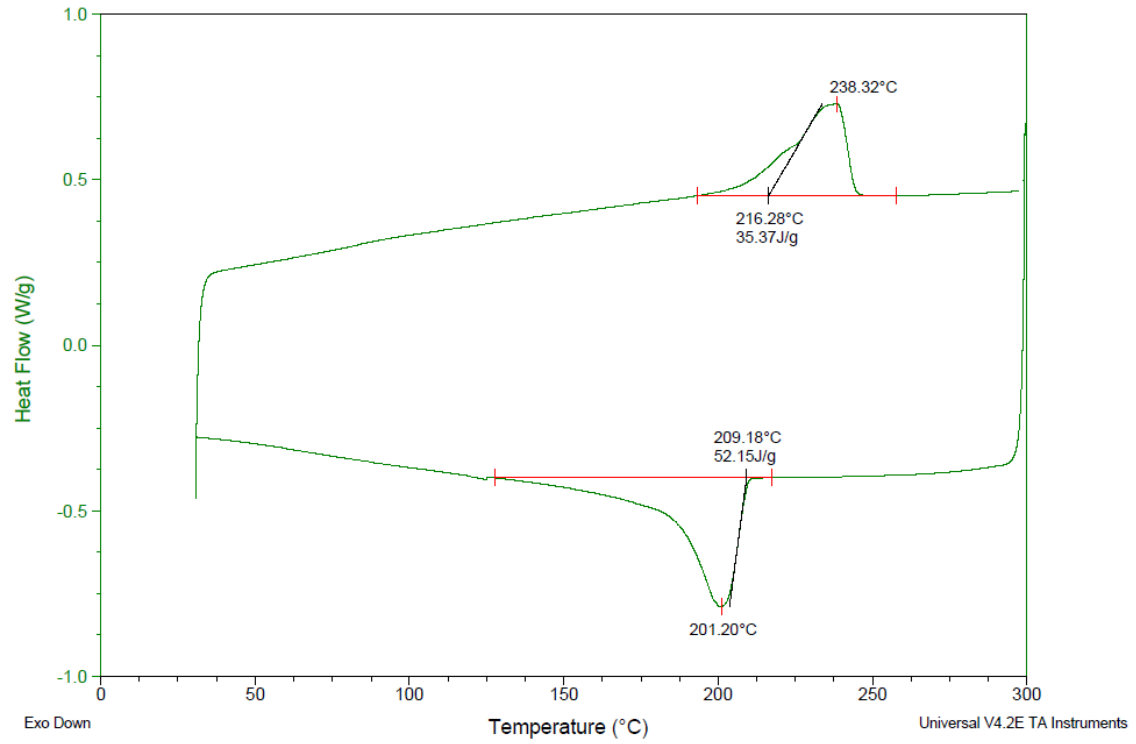
DMA curves of PA 66 + 2.5 wt. % of LiCl + 2.5 wt. % of NBBSA – 1st replication

DMA curves of PA 66 + 2.5 wt. % of LiCl + 2.5 wt. % of NBBSA – 2nd replicationDMA curves of PA 66 + 2.5 wt. % of LiCl + 2.5 wt. % of NBBSA – 3rd replication

APPENDIX C – DSC CURVES PA 66 WITH DIFFERENT FORMULATIONS

DSC curves of PA 66 + 5.0 wt. % of LiCl + 5.0 wt. % of NBBSA

DSC curves of PA 66 + 2.5 wt. % of LiCl + 2.5 wt. % of NBBSA – 2nd replication

DSC curves of PA 66 + 2.5 wt. % of LiCl + 2.5 wt. % of NBBSA – 3rd replication

APPENDIX D – PUBLICATIONS GENERATED FROM THIS WORK

Publication:

MARQUES, M.F.V.; MELO, R.P.; ARAUJO, R.S.; LUNZ, J.N.; AND AGUIAR, V.O. Improvement of mechanical properties of natural fiber–polypropylene composites using successive alkaline treatments, **Journal of Applied Polymer Science**, v. 132, n. 12, Mar, 2015, DOI: 10.1002/app.41710

Presentation in a International Conference:

MELO, R.P.; MARQUES, M.F.V.; NAVARD, P; FROMONTEIL, D. "Thermal behavior and degradation studies of treated natural fibers and microcrystalline cellulose in composites with polyamide 6". The 3rd International Polysaccharide Conference EPNOE 2013 "Polysaccharides and polysaccharide-derived products, from basic science to applications", Nice, 22-26 october 2013;

Patent:

R. de MELO, M. MARQUES, P. NAVARD, N. PENEDO et D. FROMONTEIL "PROCÉDÉ DE PRÉPARATION DE FIBRES VÉGÉTALES POUR UN MATÉRIAU COMPOSITE CONTENANT UNE MATRICE EN POLYMÈRE Corresponding to FRANCE Priority Document No. 1362955 filed on 19.12.2013.

Développement de polyamide composites avec des fibres naturelles pour les applications automobiles

RÉSUMÉ : L'objectif de cette thèse est de préparer les composites de polyamide avec des fibres naturelles, capables de résister à des températures élevées. Curauá, jute et lin sont des fibres utilisées. Alcalin-treatment a été effectué en utilisant un poids de 5,0.% de solution d'hydroxyde de sodium. Deux techniques de traitement à des environnements différents ont été comparés: à la pression ambiante et haute pression. Amélioration des propriétés thermiques des fibres naturelles a été observée dans les deux cas par analyse thermogravimétrique (TGA) et, il a été décidé de fixer 30 minutes de haute pression mercerisage pour tous fibres avant d'effectuer des post-traitements (acétylation et silanisation) et la préparation de composites utilisant polyamide 6 et 6.6 comme matrices. On a utilisé des teneurs en fibres à la fois dans la matrice de polyamide (10, 20 et 30 en poids.%). Par testings de tension et observations au MEB, on a montré une amélioration des propriétés mécaniques des PA 6/ curauá fibres traités au la proportion 70/30. Pour réduire la température de traitement de PA 6.6, une combinaison de 2,5 en poids. % de LiCl et 2,5 en poids. % de N-butyl benzène sulfonamide (NBBSA) a été définie par conception expérimentale et il a été ajouté au polyamide 6.6 pur. En outre, on a trouvé la plus grande des propriétés mécaniques des composites préparés avec matrice de polyamide et 10 % en poids de fibres alcaline-traitées + silanisées sur polyamide plastifié 6,6. Il était possible de préparer des composites en utilisant comme matrice PA 6.6 à plus forte teneur en fibres allant jusqu'à 30 en poids. %, sans endommager de fibres.

Mots clés : polyamide, composites, fibres

Development of polyamide composites with natural fibers for automotive applications

ABSTRACT: The objective of this PhD Thesis is to prepare composites of polyamide with natural fibers, able to withstand high temperatures. Curauá, jute and flax were the fibers used. Alkaline-treatment was conducted using a 5.0 wt.% of sodium hydroxide solution. Two treatment techniques at different environments were compared: at room pressure and high. Improvement of thermal properties of natural fibers was observed in both cases by thermogravimetric analysis (TGA) and, it was decided to fix 30 minutes of high pressure mercerization for all fibers before performing post-treatments (acetylation and silanization) and preparing composites using polyamide 6 and 6.6 as matrixes. It was employed different fiber contents in both polyamide matrix (10, 20 and 30 wt. %). By tension testings and SEM observations, it was shown improvement of mechanical properties of PA 6 / treated curauá fibers at 70/30 proportion. To reduce the processing temperature of PA 6.6, a combination of 2.5 wt. % of LiCl and 2.5 wt. % of N-butyl benzene sulphonamide (NBBSA) was defined through experimental design and it was added to pure polyamide 6.6. Moreover, it was found that the highest mechanical properties for composites prepared with polyamide 6.6 matrix was those using 10 wt. % of alkaline-treated + silanized fibers on plasticized polyamide 6.6. It was possible to prepare composites using PA 6.6 as matrix with higher fiber content up to 30 wt. % without damaging of fibers.

Keywords : polyamide, composites, fibers